



Durham E-Theses

Preparation and study of magnetic fluids

Mason, Neil

How to cite:

Mason, Neil (1986) *Preparation and study of magnetic fluids*, Durham theses, Durham University.
Available at Durham E-Theses Online: <http://etheses.dur.ac.uk/6862/>

Use policy

The full-text may be used and/or reproduced, and given to third parties in any format or medium, without prior permission or charge, for personal research or study, educational, or not-for-profit purposes provided that:

- a full bibliographic reference is made to the original source
- a [link](#) is made to the metadata record in Durham E-Theses
- the full-text is not changed in any way

The full-text must not be sold in any format or medium without the formal permission of the copyright holders.

Please consult the [full Durham E-Theses policy](#) for further details.

PREPARATION AND STUDY OF MAGNETIC FLUIDS

Neil Mason, B.Sc. (Dunelm)

The copyright of this thesis rests with the author.
No quotation from it should be published without
his prior written consent and information derived
from it should be acknowledged.

Thesis submitted to the University of Durham
in candidature for the Degree of
Doctor of Philosophy
November 1986



23. APR. 1987

To my Mother, Father and Sister Helen
for their support over many years

"I have yet to see any problem,
however complicated, which, when
you look at in the right way,
did not become more complicated".

P. Anderson 1969.

DECLARATION

The work described in this thesis was carried out in the University of Durham between October 1983 and September 1986. This work has not been submitted either completely or in part, for a degree in this or any other University and is the original work of the author except where acknowledged by reference.

Some aspects of this work have already been published, accepted for publication and submitted for publication.

1. "An Iron-Cobalt 'Alloy' Magnetic Fluid".
D.B. Lambrick, N. Mason, N.J. Harris, G.J. Russell, S.R. Hoon and M. Kilner, IEEE Trans. Magn., 1985, 21, 1891.
2. "Preparation and Properties of Ni-Fe Magnetic Fluids"
D.B. Lambrick, N. Mason, S.R. Hoon and M. Kilner, To be published in J. Magn. Mag. Mat., 1986.
3. "A New Technique for the Preparation of Metallic Magnetic Fluids from Metal Atoms"
M. Kilner, N. Mason, D.B. Lambrick, P.D. Hooker and P.L. Timms, submitted to J. Chem. Soc. Chem. Comm., 1986.

ACKNOWLEDGEMENTS

I wish to thank Dr. M. Kilner for his supervision and encouragement throughout this project. I also thank my industrial supervisor Dr. J. Schofield for his guidance during my work at I.C.I. Organics Division (Blackley).

As the reader will become aware, the research into magnetic fluids reported is of an interdisciplinary nature, and has relied upon contributions from several sources. The success of the project was particularly dependent on a close working relationship with colleagues from the Physics Department. In this respect I thank Dr. B.K. Tanner for overseeing the physics side of the project, and Dr. S.R. Hoon (now at Manchester Polytechnic) for many useful discussions. Special thanks and acknowledgements go to my fellow researcher David Lambrick for the dedication and skill applied to the magnetic analysis essential for this project.

I am grateful to Dr. G.J. Russell (Applied Physics Department) for electron diffraction patterns for the "FeCo" and "Ni₃Fe" systems. Sincere thanks go to Dr. G. Beamson (now with I.C.I.) for his help and co-operation in recording EXAFS spectra.

I also thank our collaborators from Bristol University, namely Paul Hooker and Dr. P.L. Timms for the preparation of a cobalt fluid by metal evaporation.

I would like to express my gratitude to the Zoology

department for allowing me the use of the electron microscope. Special thanks go to Mrs. A.C. Richardson for training me in the required skills.

EDX data collected at other institutions are referred to in the relevant sections of this thesis. Finally, I thank Margaret Chipchase for typing this manuscript.

I am indebted to the SERC and I.C.I. for financial support.

ABSTRACT

A study of the preparation and characterization of hydrocarbon based metal particle magnetic fluids (ferrofluids) is reported. Bimetallic alloy particle magnetic fluids with the particle compositions: FeCo, Co₃Fe and Ni₃Fe have been prepared by the thermal decomposition of the organometallic complexes: $[(\pi\text{-C}_5\text{H}_5)\text{Fe}(\text{CO})_2\text{Co}(\text{CO})_4]$, $\text{HFeCo}_3(\text{CO})_{12}$ and $[(\pi\text{-C}_5\text{H}_5)_2\text{Ni}_2\text{Fe}(\text{CO})_5]$ respectively. In all cases the magnetic fluids were superparamagnetic at room temperature, containing particles with diameters in the 5-8nm range. In the FeCo and Ni₃Fe systems electron diffraction revealed alloy particles with ordered "superlattice" structures. In these iron alloy systems, the iron content of the particles is less than that of the organometallic starting material, due to chemical reaction.

A cobalt magnetic fluid prepared in collaboration with Bristol University by the evaporation of cobalt metal has been examined and compared to cobalt fluids prepared from the decomposition of $\text{Co}_2(\text{CO})_8$. Characterization indicated no significant differences between fluids prepared using the two contrasting techniques.

The surfactant Sarkosyl-0 is completely converted to a cobalt carboxylate derivative during the preparation of cobalt magnetic fluids from $\text{Co}_2(\text{CO})_8$. This result, determined by IR spectroscopy implies both surface active

and "free" solution Sarkosyl-0 are in the form of a cobalt complex. The atmospheric oxidation of the metallic cobalt particles in these systems has been observed by EXAFS spectroscopy.

Preparation of iron particle magnetic fluids has proven difficult. Particles believed to consist of iron-carbon alloy are produced during thermolysis of $\text{Fe}(\text{CO})_5$. Decomposition of organometallic compounds was concluded to be an unsatisfactory method of producing iron magnetic fluids.

In general nickel magnetic fluids were also difficult to prepare. However, large (13-27nm) regularly shaped nickel particles were obtained on decomposition of $[\pi\text{-C}_5\text{H}_5\text{Ni}(\text{CO})]_2$.

CONTENTS

Page

Abbreviations and Symbols i

CHAPTER 1 : MAGNETIC FLUIDS

1.1	Introduction	1
1.2	Definition	1
1.3	Historical Development	2
1.4	Components of a Magnetic Fluid	3
1.5	Magnetism	5
1.5.1	Electronic and Atomic Magnetic Moments	5
1.5.2	Magnetism in Bulk Materials	8
1.6	Magnetic Properties of Magnetic Fluids	12
1.6.1	Single Domain Particles	12
1.6.2	Variation of Coercivity with Particle Size	14
1.6.3	Superparamagnetism	15
1.6.4	Physical and Magnetic Particle Diameters and the Non-magnetic "Dead" layer	18
1.6.5	Determination of Particle Size Distributions from Magnetization Curves	19
1.6.6	Magnetic Relaxation	21
1.7	Ferrofluid Stability	22
1.7.1	Internal Stability - Interparticle Forces	23
(i)	London Type - Van der Waals Forces	23
(ii)	Magnetic Dipole-Dipole Attraction	24
(iii)	Steric Repulsion	26
(iv)	Enthalpic Repulsion	28
(v)	Electrostatic Repulsion	28
(vi)	Net Potential Energy Curves	29

1.7.2	Stability in External Fields	31
	(i) Sedimentation in the Gravitational Field	31
	(ii) Stability in a Magnetic Field Gradient	31
1.8	The Properties of Magnetic Fluids	33
1.8.1	Mechanical Properties	33
1.8.2	Electrical Properties	34
1.8.3	Thermal Properties	34
1.8.4	Rheological Properties	34
1.9	Applications of Magnetic Fluids	35
1.10	Metal Particles in Other Areas of Chemistry	38
1.10.1	Heterogeneous Catalysis	38
1.10.2	Metal Slurries	39
1.10.3	Metal Atom Condensation	40

CHAPTER 2 : A REVIEW OF MAGNETIC FLUID PREPARATIONS

	Introduction	42
2.1	Non-metallic Fluids	42
2.1.1	Size Reduction - Ball Milling	42
	(i) Substitution of Carrier Liquid	44
	(ii) Substitution of Surfactant	44
	(iii) Magnetic Fluids via Milling of a Non-magnetic Precursor	45
2.1.2	Chemical Precipitation from Aqueous Solution	46
2.2	Metallic Magnetic Fluids	50
2.2.1	Evaporation Techniques	50
2.2.2	Electrodeposition-Liquid Metal Based Systems	52
2.2.3	Preparation of Fine Metal Particles by Chemical Reduction	54

2.2.4	The Organometallic Route	54
	(i) Cobalt Magnetic Fluids	55
	(ii) Iron Magnetic Fluids	57
	(iii) Nickel Magnetic Fluids	58
2.2.5	Spark Erosion	59
<u>TER 3 : ORGANOMETALLIC STARTING MATERIALS AND THE</u>		
<u>DECOMPOSITION PROCESS</u>		
	roduction	60
	Transition Metal Complexes with Carbonyl and/or Cyclopentadienyl Ligands	61
3.1.1	Bonding and Structure	61
3.1.2	Preparation	63
	Metal Particle Formation by the Thermal Decomposition of Metal Carbonyls in the Presence of Surfactants in Hydrocarbon Solution	64
3.2.1	Mechanism of Iron Pentacarbonyl Thermal Decomposition in the Presence of Polymeric Surfactants	65
3.2.2	Mechanism of Dicobalt Octacarbonyl Thermal Decomposition in a Toluene Solution of Surfactant	67
<u>TER 4 : GENERAL EXPERIMENTAL TECHNIQUES AND INSTRUMENTATION</u>		
	General Experimental Techniques	71
4.1.1	General Handling Techniques	71
4.1.2	Nitrogen Supply	71
4.1.3	Glove Box	71
4.1.4	Solvents	72
4.1.5	Starting Materials	72
	(i) Organometallics	72
	(ii) Surfactants	72
4.1.6	Infra-red Spectroscopy	73
4.1.7	Analytical Methods	73

4.2	Instrumentation	73
4.2.1	Electron Microscopy	73
4.2.2	Electron Diffraction	74
4.2.3	EDX	75
4.2.4	The Automated Electro-optic Image Size Analyser (Particle Size Analysis)	76
4.2.5	The Vibrating Sample Magnetometer	77
4.2.6	EXAFS Spectroscopy	78

CHAPTER 5 : SOME STUDIES OF COBALT MAGNETIC FLUIDS

	Introduction	80
5.1	Comparison of Cobalt Magnetic Fluids Prepared by the Carbonyl Route and the Metal Atom Technique	80
5.1.1	Fluid Preparation	80
	(i) Via Thermal Decomposition of Dicobalt Octacarbonyl	80
	(ii) Using Metal Atom Techniques	81
5.1.2	Particle Size Analysis	82
5.1.3	Magnetization Curves	83
5.1.4	Electron Diffraction	84
5.1.5	A Qualitative Kinetic Study of the Decomposition Process	84
5.1.6	Discussion and Conclusions	86
5.2	An EXAFS Spectroscopic Study of Cobalt Magnetic Fluids	89
5.2.1	Introduction	89
5.2.2	Spectra	89
5.2.3	Supporting Magnetic Data	91
5.2.4	Discussion	92

5.3	Infra-red Spectroscopic Study of Cobalt Magnetic Fluids	93
5.3.1	Introduction	93
5.3.2	Experimental	94
	(i) Systems Examined	94
	(ii) Technique	94
5.3.3	Results and Discussion	94
	(i) Sarkosyl-O	94
	(ii) Manoxol-OT	99
5.3.4	Conclusion	99

CHAPTER 6 : IRON-COBALT ALLOY MAGNETIC FLUIDS

	Introduction	100
6.1	Iron-Cobalt Magnetic Fluids from [$(\pi\text{-C}_5\text{H}_5)\text{Fe}(\text{CO})_2\text{Co}(\text{CO})_4$]	101
6.1.1	Fluid Preparation	101
	(i) Preparation of [$(\pi\text{-C}_5\text{H}_5)\text{Fe}(\text{CO})_2\text{Co}(\text{CO})_4$]	101
	(ii) Magnetic Fluid Preparation	102
6.1.2	Transmission Electron Microscopy	103
6.1.3	Particle Structure and Composition	104
	(i) Electron Diffraction	104
	(ii) EDX Spectroscopy	105
6.1.4	Magnetic Data	106
6.2	Magnetic Fluids from $\text{HFeCo}_3(\text{CO})_{12}$	107
6.2.1	Preparations	108
	(i) Preparation of $\text{HFeCo}_3(\text{CO})_{12}$	108
	(ii) Ferrofluid Preparation	108
6.2.2	TEM Analysis	109
6.2.3	Composition and Structure	110
	(i) Electron Diffraction	110
	(ii) Local Area EDX Spectroscopy	110

6.2.4	Magnetic Measurements	114
6.2.5	Kinetics of $\text{HFeCo}_3(\text{CO})_{12}$ Decomposition	115
6.3	Other Work	117
6.3.1	Attempted Thermal Decomposition of $\text{PNP}^+\text{FeCo}(\text{CO})_8^-$	117
6.3.2	Simultaneous Thermal Decomposition of Single Metal Carbonyls	118
6.4	Discussion and Conclusion	118

CHAPTER 7 : NICKEL-IRON MAGNETIC FLUIDS

	Introduction	121
7.1	Fluid Preparation	121
7.2	Particle Size Analysis	124
7.3	Particle Structure and Composition	124
7.3.1	Electron Diffraction	124
7.3.2	EDX Spectroscopy	126
7.4	Magnetic Data	127
7.5	Attempted Infra-red Spectroscopic Study of the Decomposition Process	128
7.6	Conclusion	129

CHAPTER 8 : NICKEL AND IRON MAGNETIC FLUIDS

	Introduction	131
8.1	Nickel Fine Particle Systems	132
8.1.1	Preparative Studies	132
	(i) η^5 -dicyclopentadienylnickel(II)	132
	(ii) $[\text{Me}_4\text{N}^+]_2[\text{Ni}_5(\text{CO})_{12}]^-$	133
	(iii) Cyclopentadienylnickelcarbonyl dimer	134
8.1.2	Electron Microscopy	135
8.1.3	Magnetization Curve	137
8.1.4	Particle Composition and Structure	137
8.1.5	Conclusion	139

8.2	Preparative Studies of Iron Ferrofluids	143
8.2.1	Cyclopentadienyliron dicarbonyl Dimer	144
8.2.2	The Simple Carbonyls	145
	(i) Diiron Nonacarbonyl	145
	(ii) Studies of Triiron Dodecarbonyl	145
	(a) Preparations	145
	(b) EXAFS Spectra and Discussion	148
	(iii) Studies of Iron Pentacarbonyl	149
	(a) Preparations	150
	(b) Analysis of Fluids 8.2.6 and 8.2.7 and Discussion	151
8.2.3	Iron Dicarbonyl Dinitrosyl	154
8.2.4	Conclusion	156

CHAPTER 9 : CONCLUSIONS AND FUTURE WORK

9.1	Conclusions	158
9.2	Future Work	163
	9.2.1 Existing Problems	163
	9.2.2 Extension of Present Work	164

<u>APPENDIX</u>	RESEARCH COLLOQUIA, SEMINARS, LECTURES, MEETINGS AND CONFERENCES	166
-----------------	---	-----

REFERENCES		177
------------	--	-----

ABBREVIATIONS AND SYMBOLS

bcc	body centred cubic
fcc	face centred cubic
hcp	hexagonal close packed
SEM	Scanning Electron Microscopy
TEM	Transmission Electron Microscopy
EDX	Energy Dispersive Analysis of X-rays.
EXAFS	Extended X-ray Absorption Fine Structure
T.H.F.	Tetrahydrofuran
PNP	Bis(triphenylphosphoranyl-idene) ammonium.
M_b^∞	Saturation magnetization per unit volume of bulk material.
M_{ff}	Ferrofluid magnetization per unit volume.
M_{ff}^∞	Ferrofluid saturation magnetization per unit volume.
σ_{ff}	Ferrofluid magnetization per unit mass.
σ_{ff}^∞	Ferrofluid saturation magnetization per unit mass.
ϵ_v	Volume packing fraction
ϵ_m	Mass packing fraction
B_o	Magnetic Field in Teslas.
\bar{d}_p	Mean physical particle diameter.
\bar{d}_v	Median magnetic particle diameter (volume median)
\bar{d}_m	Mean magnetic particle diameter (number mean)
$\bar{\nu}$	Frequency in cm^{-1}
ρ	Density

CHAPTER 1

MAGNETIC FLUIDS

1.1 Introduction

In the last 20 years the amount of published work on magnetic fluids has expanded dramatically¹ and the subject is now recognized as a separate research area. Literature on the subject covers a wide spectrum of interests, ranging from the highly theoretical at one extreme to medical applications at the other. Simply to understand the concept of magnetic fluids, we must draw upon a variety of normally separate disciplines. This introductory chapter gives a brief background to this relatively novel area.

1.2 Definition

Ferromagnetism is a property associated only with the solid state, and although ferromagnetism in the liquid state is theoretically feasible, it has not been observed.² Magnetic fluids should not be confused with ferromagnetic liquids. Magnetic fluids (or ferrofluids) are a class of magnetic material consisting of a colloidal suspension of single domain ferro- or ferri- magnetic particles dispersed in a liquid carrier and stabilized by a surfactant. Figure 1.1 shows the three components of a ferrofluid schematically; the nature of these components is discussed



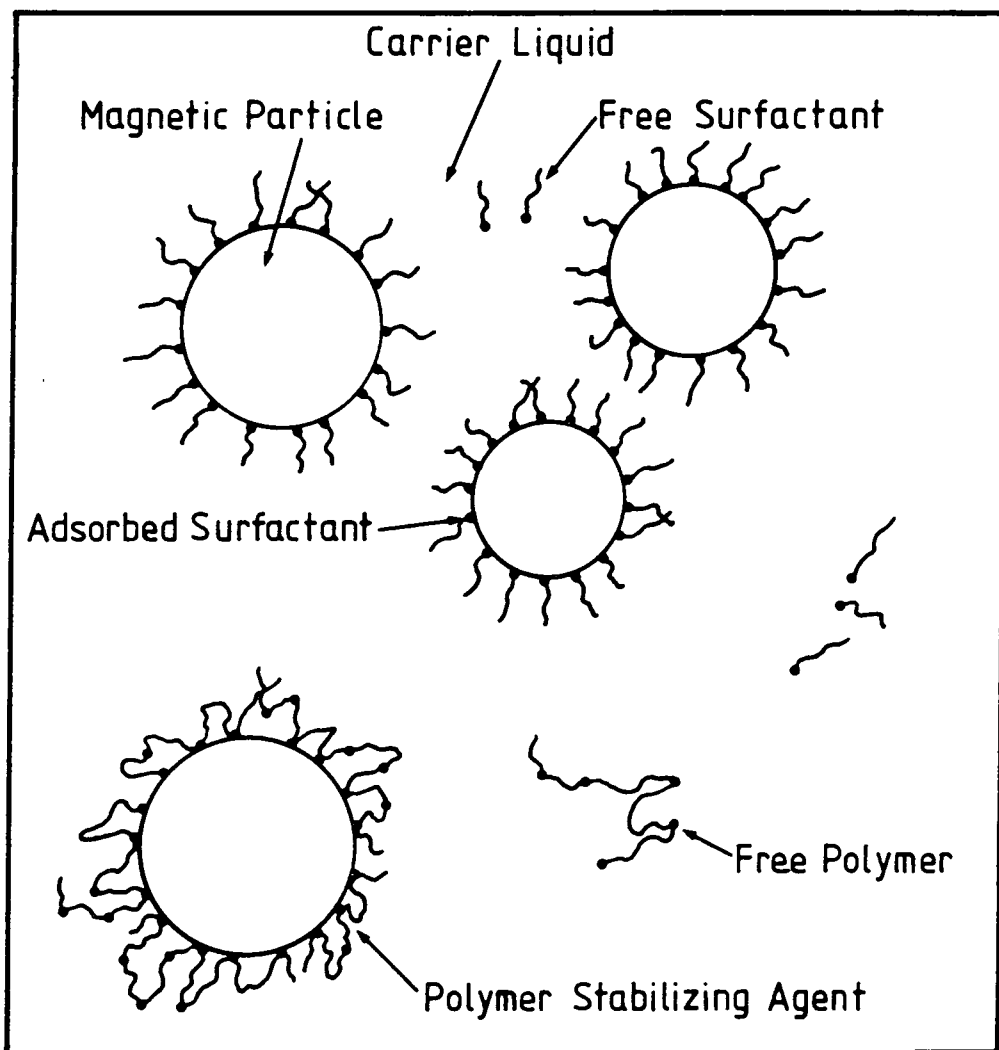


Fig. 1.1 The components of a magnetic fluid.

in more detail in section 1.4.

1.3 Historical Development

Gowan Knight's preparation of artificial lodestone reported in 1779 by Wilson³ involved the use of suspensions of iron filings in water. This is usually credited to be the earliest reported work on magnetic fluids, however Knight's suspensions were unstable and should not strictly be classed as magnetic fluids.

4,5

At the beginning of the 1930's Bitter used "temporary" suspensions of micron sized magnetic particles of $\gamma\text{-Fe}_2\text{O}_3$ in ethyl ethanoate to study domain structures on the surfaces of highly polished ferromagnetic materials, known as the Bitter pattern technique, which relies on the particles becoming concentrated in the regions of higher field gradient associated with the domain walls. McKeechan and Elmore⁶ (1934) used true sols of $\gamma\text{-Fe}_2\text{O}_3$ in water for the same purpose. In 1938 Elmore⁷ prepared 20nm particle sized Fe_3O_4 colloids for use in the Bitter pattern technique; this preparation bears a strong resemblance to some more recent preparative methods.⁸ These materials, as well as Rabinow's⁹ clutch fluids (1949) are not strictly magnetic fluids because they are made to solidify in a magnetic field, unlike true magnetic fluids which remain liquid. However, true magnetic fluids have been used more recently to detect magnetic domains in alloys and crystals.¹⁰

The history of modern day magnetic fluids began in the

mid 1960's when Papell¹¹ prepared magnetic fluids to control the flow of liquid rocket fuel propellant in zero-G conditions.

1.4 The Components of a Magnetic Fluid

Magnetic fluids are lyophobic colloids, i.e. colloidal dispersions of "insoluble" substances, a colloid being a suspension of finely divided particles in a continuous medium. In many respects magnetic fluids resemble a single phase ferromagnetic liquid, i.e. they respond to a magnetic field and have relatively large magnetizations. However, magnetic fluids are not homogenous, they are two phase systems.

Colloidal particles are usually sub-micron sized, but the ultrafine magnetic particles which form the solid phase of a magnetic fluid have a diameter typically less than 10nm in order that; (i) thermal effects (Brownian motion) maintain a stable dispersion and (ii) to ensure the particles are single domain. Although the six lanthanide elements Gd, Tb, Dy, Ho, Er and Tm can exhibit ferromagnetism, the magnetic particles in practice consist of one of the ferromagnetic transition metals iron, cobalt or nickel or a ferrimagnetic material, usually magnetite (Fe_3O_4) or another ferrite. Table 1.1 summarizes some properties of magnetic materials suitable for use in magnetic fluids.

The carrier liquid forms the liquid phase and in theory

TABLE 1.1

Some properties of magnetic materials which can be used for the particles in magnetic fluids.

Material	Crystalline Structure	T_c (K)	M_b^∞ at 290K ($\text{KJ}^{-1}\text{T}^{-1}\text{m}^{-3}$)
Iron (α)	bcc	1043	1707
Cobalt (α)	hcp	$\sim 1130^*$	1400
Cobalt (α)	fcc	1404	
Nickel (α)	fcc	631	485
Fe_3O_4	Inverse Spinel	858	484

* By Extrapolation

T_c Curie temperature

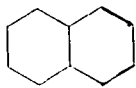
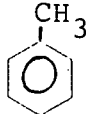
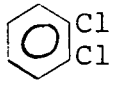
M_b^∞ Saturation Magnetization (per Unit Volume)

can be any material in the liquid phase (at ambient temperatures). Carrier liquids used include hydrocarbons, fluorocarbons, silicones, esters and water. Table 1.2 gives examples of some of the common types of carrier liquids. When a choice is allowed the carrier chosen may depend on the fluid application; for example, if the fluid is going to experience long term exposure to the atmosphere a high boiling oil with low volatility will be desirable. Dispersions of metal particles in which the carrier is a liquid metal, e.g. mercury, are usually classed as magnetic fluids, despite their stability problems.

The third component of a magnetic fluid is a surfactant or surface active agent. These are molecules able to alter the properties of an interface between two media. Most magnetic inorganic solids are insoluble in common liquids. Particles are made compatible with the carrier liquid by virtue of a surfactant molecule which has a lyophobic portion adsorbed onto the particle surface and a lyophilic portion which is compatible with the base fluid. Surfactant molecules form a surface coating on the particles which prevent particle aggregation due to the short range attractive interparticle forces present in all colloids. This aggregation can lead to sedimentation. Surface coatings in magnetic fluids consist of surfactant molecules with a polar "head" group and a "tail" compatible with the carrier liquid. Alternatively polymers with special polar groups spaced along the polymer backbone have been used. In

TABLE 1.2

Common classes of carrier liquids used in magnetic fluids

Type	Example	Formula/Structure
Aliphatic Hydrocarbon	Decalin	
Aromatic Hydrocarbon	Toluene	
Chlorinated Aromatic	o-dichlorobenzene	
Fluorocarbon	Freon-E3	$\text{F} \left[\begin{array}{c} \text{CF}_3 \\ \\ \text{---C---CF}_2\text{---O---} \\ \\ \text{F} \end{array} \right]_3 \text{CHFCF}_3$
Ester	Butyl ethanoate	$\text{CH}_3\text{COOC}_4\text{H}_9$
Silicone oil		$\text{R}_3\text{Si} \left[\begin{array}{c} \text{R} \\ \\ \text{---O---Si---} \\ \\ \text{R} \end{array} \right]_n \text{OSiR}_3$

this case the particle coating is made up of loops of polymer chain. Adsorption of the "active" group is preferably via chemical bonding to the particle surface. The tails or loops forming the coating are normally 1-2nm in length. Both these forms of coating are shown schematically in Figure 1.1. It is true that if the surfactant tail possesses a "kink" due to the presence of a double bond for example or "bulges" due to side chains, then this prevents crystallization of the surfactant chains with their own species which renders them useless as a surfactant.¹² This is illustrated by the comparison of oleic and stearic acids. Table 1.3 gives examples of the various types of surfactants used for the stabilization of magnetic fluids.

1.5 Magnetism

1.5.1 Electronic and Atomic Magnetic Moments

Magnetism can be considered to arise from the motion of electric charge, e.g. electrons. In the classical treatment, by considering the motion of an electron in a circular orbit it can be shown that the magnetic moment associated with this orbital motion is given by

$$\vec{\mu}_l = -(e/2m_0)\vec{p}_l \quad (1.1)$$

where $-e$ is the electronic charge, m_0 the electronic rest mass and p_l the orbital angular momentum. This classical treatment only considers simple orbital type motion.

Electrons however, have both orbital and spin motions, both

TABLE 1.3

Examples of the various classes of surfactant used for the stabilization of magnetic fluids

Type	Example
Anionic	$\text{CH}_3(\text{CH}_2)_{10}\text{COSO}_3^-\text{Na}^+$
Cationic	$\text{R-N}^+(\text{CH}_3)_3\text{Br}^-$
Non-ionic	$\text{CH}_3(\text{CH}_2)_{10}\text{CH}_2(\text{OCH}_2\text{CH}_2)_n\text{OH}$
Amphoteric	$\text{R} \text{---} \overset{+}{\text{N}} \begin{matrix} \text{---} \\ \text{CH}_3 \end{matrix} \begin{matrix} \text{---} \\ \text{CH}_3 \end{matrix} \text{---} \text{CH}_2\text{COO}^-$
Polymeric	4-vinylpyridine-styrene 0.1 : 1

motions giving rise to magnetic moments. Quantum mechanics shows the orbital angular momentum to be quantized in units of \hbar ($\hbar = h/2\pi$, where h is Planks constant), i.e.

$$p_l = [l(l+1)]^{1/2}\hbar \quad (1.2)$$

where l is the orbital angular momentum quantum number. It follows that the orbital magnetic moment has magnitude

$$\mu_l = [l(l+1)]^{1/2}(e\hbar/2m_e) \quad (1.3)$$

This introduces the Bohr magneton μ_B , an important unit of magnetic moment with value $\mu_B = e\hbar/2m_e$.

Electron spin motion is purely a quantum mechanical effect, the spin angular momentum is

$$p_s = [s(s+1)]^{1/2}\hbar \quad (1.4)$$

s being the spin quantum number. Experiment shows that the corresponding spin magnetic moment $\vec{\mu}_s$ for transition metals has a value given by

$$\mu_s = 2[s(s+1)]^{1/2}\mu_B \quad (1.5)$$

Since both types of electronic motion produce their own magnetic field, this effects the motion of the other, resulting in a spin-orbit interaction known as ls coupling.

This gives rise to a resultant angular momentum \vec{p}_j with magnitude

$$p_j = [j(j+1)]^{1/2}\hbar \quad (1.6)$$

and a total electronic magnetic moment $\vec{\mu}_j$ with magnitude

$$\mu_j = [j(j+1)]^{\frac{1}{2}} g \mu_B \quad (1.7)$$

j is the total angular momentum quantum number, g is known as the Landé factor with value

$$g = 1 + \frac{j(j+1) + s(s+1) - l(l+1)}{2j(j+1)} \quad (1.8)$$

In most cases except for the heaviest elements, spin-orbit interaction is weak compared to spin-spin and orbit-orbit interaction. For the whole atom spin motion gives rise to a resultant vector \vec{S} , and orbital motion, orbital momenta \vec{L} , with S and L being the respective total atomic quantum numbers. \vec{L} and \vec{S} combine to give the resultant vector \vec{J} with quantum number J . The corresponding atomic magnetic moments have magnitudes given by

$$\mu_L = [L(L+1)]^{\frac{1}{2}} \mu_B \quad (1.9)$$

$$\mu_S = 2[S(S+1)]^{\frac{1}{2}} \mu_B \quad (1.10)$$

and

$$\mu_J = g[J(J+1)]^{\frac{1}{2}} \mu_B \quad (1.11)$$

with g being the Landé factor given by

$$g = 1 + \frac{J(J+1) + S(S+1) - L(L+1)}{2J(J+1)} \quad (1.12)$$

The electrons of the atom interact to produce a number of states described in terms of L, S and J by the term state $2S+1L_J$, the state of lowest energy or ground state is determined by application of Hund's rules. It is these atomic magnetic moments which determine the magnetic properties of bulk materials.

1.5.2 Magnetism in Bulk Materials

Whatever their state or composition all substances exhibit some form of magnetic properties at all temperatures. Magnetism can be divided into five basic types: (i) Diamagnetism, (ii) Paramagnetism, (iii) Ferromagnetism, (iv) Ferrimagnetism and (v) Antiferromagnetism.

Atoms in diamagnetic materials have filled electronic subshells so that the summation of the individual electronic magnetic moments is such that the resultant atomic magnetic moment is zero. In the other four forms of magnetism the atoms have a resultant magnetic moment and in the latter three there is some form of ordering of these moments. The first four types of magnetism can be conveniently characterized by their susceptibility, χ . Volume susceptibility or simply susceptibility is defined by

$$\chi = M/H \quad (1.13)$$

where H is the applied magnetic field and M is the magnetization i.e. the total magnetic moment of dipoles per unit volume, both quantities have units of $JT^{-1}m^{-3}$.

A diamagnetic material has a small negative susceptibility which arises from the change induced in the orbital motion of the electrons by an applied magnetic field. Diamagnetism is often explained by an analogy with Lenz's law, i.e. the applied field induces a small moment which opposes the field causing the change. Examples of diamagnetic materials include the rare gases, the noble metals (Cu, Ag and Au) and most organic compounds. In materials which display other forms of magnetism a relatively small diamagnetic effect is always present due to the filled inner electron subshells.

The second type of magnetism is paramagnetism, of which there are three types. In classical Langevin paramagnetism each atom or molecule carries a magnetic moment. In the absence of an applied field these moments are aligned randomly because of thermal agitation and the lack of any magnetic interaction between neighbouring atoms or molecules, resulting in zero net magnetization. When a magnetic field is applied to a paramagnetic sample only partial alignment of magnetic moments is achieved since alignment is opposed by thermal effects resulting in a small positive susceptibility. The other two forms of paramagnetism, Pauli and Van Vleck paramagnetism are not discussed here. Examples of paramagnetic materials include liquid oxygen, most transition metal compounds and ferromagnetic materials above their Curie temperatures.

In ferromagnetic, ferrimagnetic and antiferromagnetic

materials there is spontaneous ordering of atomic magnetic moments, even in the absence of an applied field. The different types of ordering are shown schematically in Figure 1.2.

A ferromagnetic solid is a material which below a certain critical temperature (Curie temperature) is composed of regions called domains, in which there is parallel alignment of individual atomic magnetic moments. Ferromagnetic materials are broken up into domains in order to minimize the field energy. Although magnetic moment alignment within a domain is in one fixed direction even in the absence of an applied field, the orientation of domains is random resulting in zero magnetization in the absence of a field. Domains are separated by domain walls across which the direction of the atomic moment vector changes gradually over ~ 100 atoms. Each domain is said to be spontaneously magnetized to the saturation value of the material.

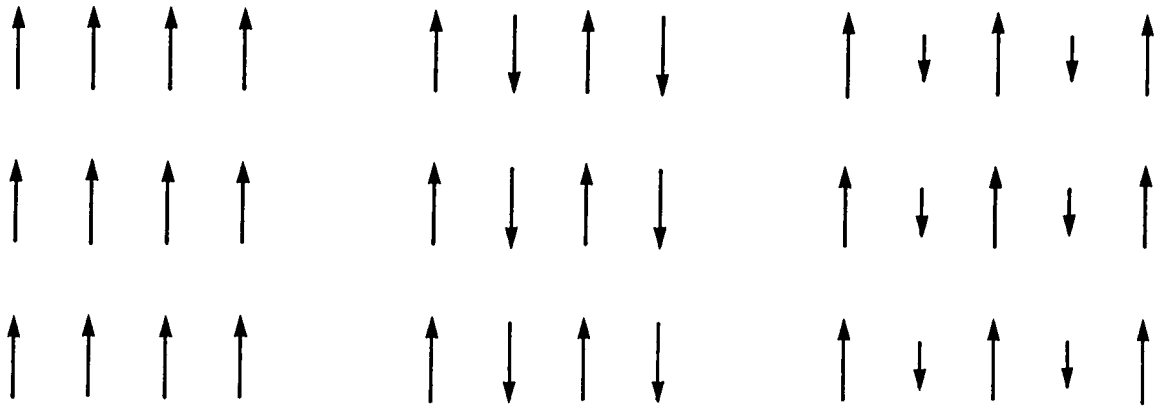
In order for the individual magnetic moments to spontaneously align there must be some form of interaction. Weiss in 1907 accounted for this spontaneous alignment by postulating the existence of an intense internal field known as the molecular field. For iron for example, this can be estimated at $\sim 1.7 \times 10^9 \text{ JT}^{-1} \text{ m}^{-3}$.

Spontaneous alignment is explained by the strong interatomic quantum mechanical exchange forces. In ferromagnetic materials the exchange integral is positive meaning parallel alignment of electron spin magnetic moments

is energetically favourable. Volume susceptibility is large and positive for ferromagnetic materials.

Magnetization of a bulk ferromagnetic solid occurs by the growth of domains aligned with the field at the expense of those which oppose it. Above the Curie temperature ferromagnetic materials exhibit paramagnetism. Examples of ferromagnetic materials are iron, nickel, cobalt and many of their alloys as well as the heavier Lanthanide elements.

Antiferromagnetic materials consist of domains in which the individual magnetic moments have antiparallel alignment (Figure 1.2(b)) below a certain critical temperature, the Néel temperature. This antiparallel alignment results in a net zero magnetization. Above the Néel temperature the antiferromagnetic alignment disappears. Examples of antiferromagnetic materials are MnO , FeCl_2 and MnSe . Ferrimagnetic materials are similar to ferromagnetic materials in that they consist of spontaneously magnetized domains below their Curie temperatures and have large positive susceptibilities. Ferrimagnetic materials must have two or more magnetic ions whose magnetic moment alignment is antiparallel as in antiferromagnetism. In ferrimagnetism however, one of the magnetic dipole moments is larger (Figure 1.2(c)) hence resulting in a net magnetization. Magnetite is an example of a ferrimagnetic material. In a unit cell of magnetite the atomic moments of the 8Fe^{3+} ions in the octahedral sites are aligned antiparallel with the 8Fe^{3+} ions in the tetrahedral sites



(a) Ferromagnetic (b) Antiferromagnetic (c) Ferrimagnetic

Fig. 1.2 Ordering of atomic magnetic moments.

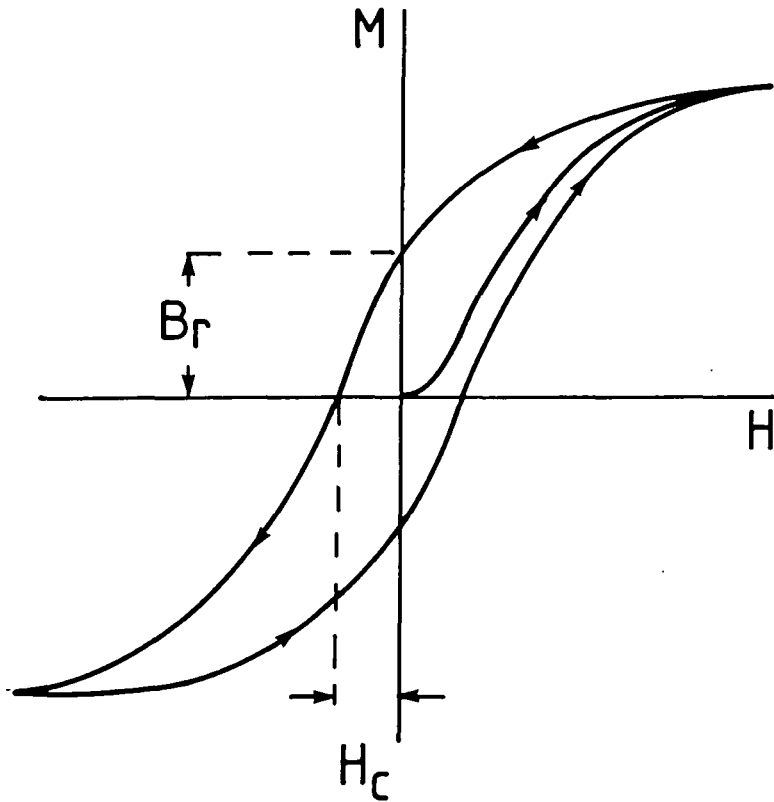


Fig. 1.3 A typical hysteresis loop for a bulk ferromagnetic material.

but parallel with those of the 8Fe^{2+} ions in the octahedral sites.

1.6 Magnetic Properties of Magnetic Fluids

1.6.1 Single Domain Particles

We must now consider what happens to the domain structure of a ferromagnetic material when the dimensions become comparable to those of a domain wall. Below a certain critical size it is energetically favourable for a sample of ferromagnetic material to become a single domain. Frenkel and Dorfman¹³ predicted from energy considerations that sufficiently small particles should consist of single domains. Kittel¹⁴ calculated the critical size to be $\sim 15\text{nm}$ for cubes or spheres of ferromagnetic material. Later Kittel et al.¹⁵ showed this value to be $\sim 60\text{nm}$ for nickel in an experiment giving evidence for the existence of single domain particles.

The particles of a magnetic fluid are typically less than 10nm in diameter, hence each particle is a single domain of ferro- or ferri- magnetic material. Like the individual domains in a bulk ferro- or ferri- magnetic material, each particle is spontaneously magnetized even in the absence of an applied magnetic field. The single domain particles in a magnetic fluid magnetize by a different mechanism to bulk ferromagnetic materials. In a bulk ferromagnetic material magnetization occurs by the growth of the domains which are aligned with the applied field at the

expense of those opposed to it. This process continues as the field increases until saturation of the material is achieved. A sample will never be converted to a single domain because of imperfections in the microstructure of the material which hinder domain wall motion. If the applied magnetic field (H) is reversed and reduced in magnitude, the magnetization (M) of the sample does not follow the same curve, instead a hysteresis loop is obtained. In Figure 1.3 H_C is known as the coercivity, this is the reverse field required to reduce the magnetization to zero after the sample has been magnetized in the forward direction. If saturation was achieved then H_C is the intrinsic coercivity, H_C is a measure of the resistance to demagnetization. The magnetization remaining when the applied field is reduced back to zero is called the Remanence (B_r), related to the amount of permanent magnetization induced in the material. In bulk ferromagnetic materials this hysteresis is due to domains not reverting to their original sizes on reduction/reversal of the applied field due to hindrance to domain wall motion.

In single domain materials there are no domain walls; magnetization occurs by a change in the orientation of the particle magnetic moment¹⁶ (the magnitude of the magnetic moment remains unaltered). Before we can understand the magnetization of single domain particles we must introduce the concept of magnetic anisotropy¹⁷ of single domain particles.

Magnetic anisotropy provides an energy barrier to particle magnetic moment rotation. There are several forms of magnetic anisotropy, the two most important being shape anisotropy and magnetocrystalline anisotropy. Shape anisotropy arises when particle shape deviates from being spherical; the magnetization vector will lie along the long axis of elongation. Magnetocrystalline anisotropy is an effect due to the lower energy associated with the magnetization vector lying along preferred crystallographic directions known as easy axes. The subject of particle anisotropy is complex and further in depth discussion is not necessary for this work. The important point to note is that particle anisotropy provides an energy barrier to changes in orientation of the particle magnetic moment within the particle as the applied field changes.

1.6.2 Variation of Coercivity with Particle Size

Single domain particles frozen in a solid matrix can have a coercivity (H_c) which arises because of the magnetic anisotropy.¹⁶ Coercivity arises because of the energetically difficult process of magnetic moment rotation, between crystallographic axes for example. When the applied field returns to zero some of the particles do not reorientate to the easy directions (cf. incomplete return to initial domain size in bulk magnetic materials).

Coercivity is a function of particle size. Figure 1.4 shows how coercivity varies with particle size.¹⁸ As the particle size decreases from the 10^4 \AA size range the

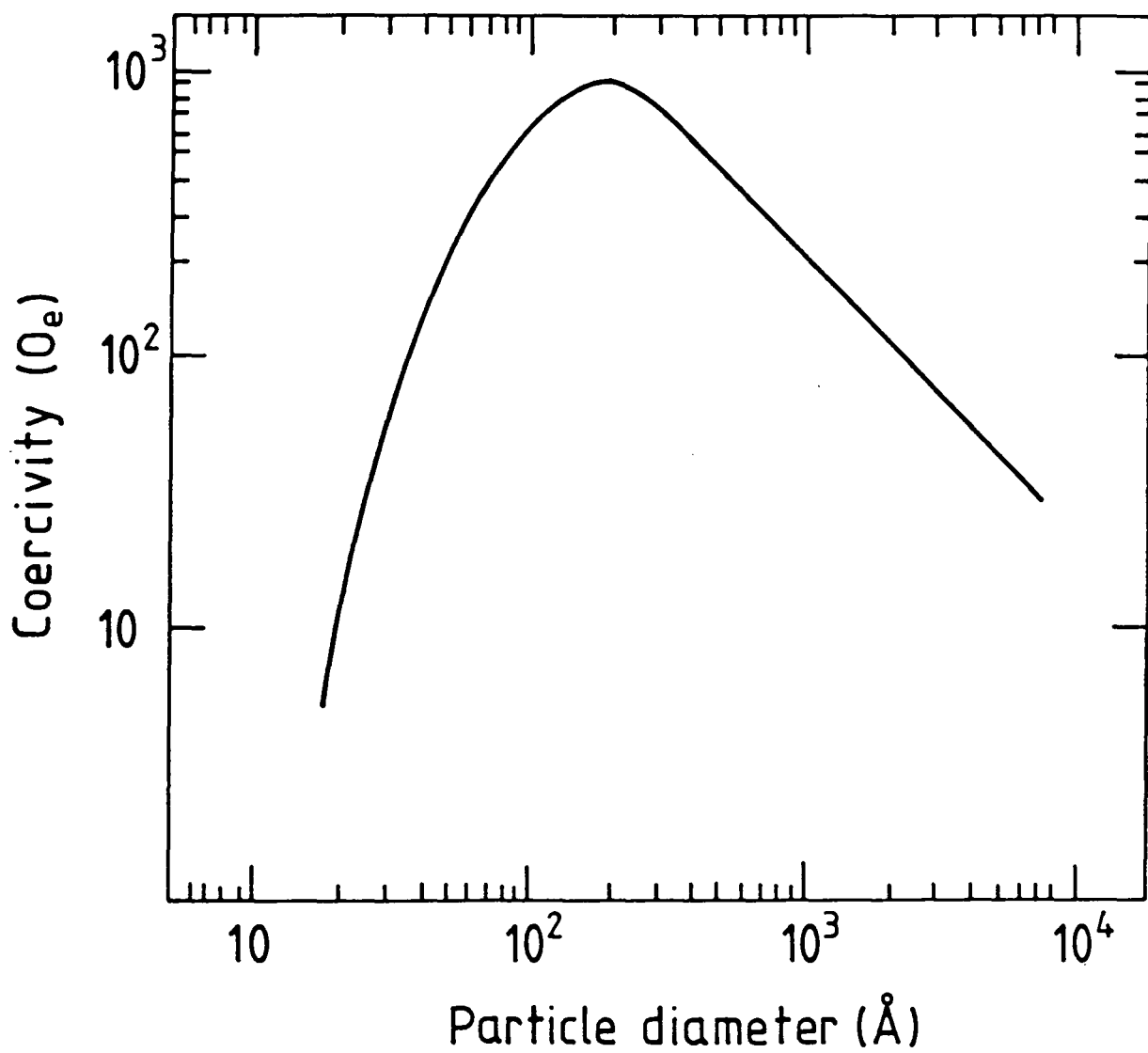


Fig. 1.4

Coercivity as a function of particle size for iron particles at 77K¹⁸.

coercivity increases as the particles make the transition from multi- to single domain, and the magnetization/demagnetization mechanism changes from domain wall movement to particle magnetic moment reorientation. The coercivity reaches a maximum in the 100-200Å range and then decreases and eventually reaches zero. This zero coercivity is explained by a phenomenon called superparamagnetism.

1.6.3 Superparamagnetism¹⁹

Let us consider the particles in a magnetic fluid. Each particle has a magnetic moment vector \vec{m} , with magnitude m . In the absence of an applied field the particles are randomly orientated and the magnetic fluid has no net magnetization (cf. a paramagnetic gas). When a magnetic field is applied to the sample the individual particle magnetic moments start to align with the field. However these alignments are partially overcome by thermal agitation. As the field increases in magnitude the alignment becomes more complete until saturation is achieved when all the particle magnetic moments are aligned with the applied field.

In simple paramagnetism the atomic or molecular moments are of the order of a few Bohr Magnetons. However, in ferrofluids the particles consist of several thousand atoms with their atomic magnetic moments spontaneously aligned (ferromagnetism). This produces a magnetic moment of the order of 10^5 Bohr Magnetons, hence the term superparamagnetism.

Langevins classical theory of paramagnetism can easily be adapted and applied to the single domain particles in ferrofluids.²⁰ This assumes there is negligible particle-particle interaction. By considering an assembly of independent identical particles each possessing a magnetic moment (m) which can fluctuate thermally at the temperature of the system T (degrees Kelvin), in an applied field (H), it can be shown²¹ that the average component of the magnetic moment along the field direction (\bar{m}) can be given by

$$\bar{m}/m = \coth(mH/kT) - kT/mH \quad (1.14)$$

where k is the Boltzmann constant. If $\alpha = mH/kT$ then

$$L(\alpha) = \coth(\alpha) - 1/\alpha \quad (1.15)$$

where $L(\alpha)$ denotes the Langevin function. The magnetization (per unit volume) of a ferrofluid M_{ff} at field H is in the direction of the applied field. Its magnitude is the total of the moments of the n magnetic particles in unit volume of the fluid, and is related to \bar{m} by

$$M_{ff} = n\bar{m} \quad (1.16)$$

Analogously the ferrofluid saturation magnetization per unit volume, M_{ff}^{∞} is given by

$$M_{ff}^{\infty} = nm \quad (1.17)$$

The saturation magnetization per unit volume can be related

to the saturation magnetization per unit volume (M_b^∞) of the bulk solid by

$$M_{ff}^\infty = \epsilon_v M_b^\infty \quad (1.18)$$

where ϵ_v is the volume packing fraction of solid in the ferrofluid. Combining equations 1.16, 1.17 and 1.18 gives

$$M_{ff}/\epsilon_v M_b^\infty = \bar{m}/m \quad (1.19)$$

Combining equations 1.15 and 1.19 gives the superparamagnetic magnetization law for a monodisperse colloidal ferrofluid.

$$M_{ff}/\epsilon_v M_b^\infty = \coth(\alpha) - 1/\alpha \equiv L(\alpha) \quad (1.20)$$

For a single domain particle the magnetic moment can be given in terms of the saturation magnetization of the bulk material and the particle volume, v

$$m = VM_b^\infty = \frac{\pi M_b^\infty d^3}{6} \quad (1.21)$$

It follows that we can write the magnetization per unit volume of the ferrofluid as

$$M_{ff} = \epsilon_v M_b^\infty \left[\coth\left(\frac{\pi M_b^\infty Hd^3}{6kT}\right) - \frac{6kT}{\pi M_b^\infty Hd^3} \right] \quad (1.22)$$

This is an important result and can be used to generate magnetization curves for ferrofluids. These curves have the

same shape as the magnetization curves for paramagnetic materials, in that they do not exhibit hysteresis, i.e. no coercivity or remanence. Figure 1.5 shows a series of curves computed for different particle diameters (for positive values of field only).

In this work the magnetization per unit mass (σ_{ff}) was measured rather than M_{ff} , the magnetization per unit volume. The applied magnetic field is actually B_0 , an induction field in Teslas. Despite the changes in symbols, the physical principles discussed above still apply.

The above derivation provides the basis of a method for deriving the particle sizes from experimentally measured magnetization curves, this will be discussed further in section 1.6.5. Before going on to this we need to distinguish between physical and magnetic particle size.

1.6.4 Physical and Magnetic Particle Diameters and the Nonmagnetic "Dead" layer

In the Langevin theory of superparamagnetism outlined in the previous sub-section it was assumed that the particles were uniform in size. In real magnetic fluids there is a distribution of particle sizes. Electron microscopy can be used to measure particle size distributions which are given in terms of the physical particle diameter (d_p). However, the so-called magnetic particle diameters derived from fluid magnetization curves are always found to be smaller than the corresponding

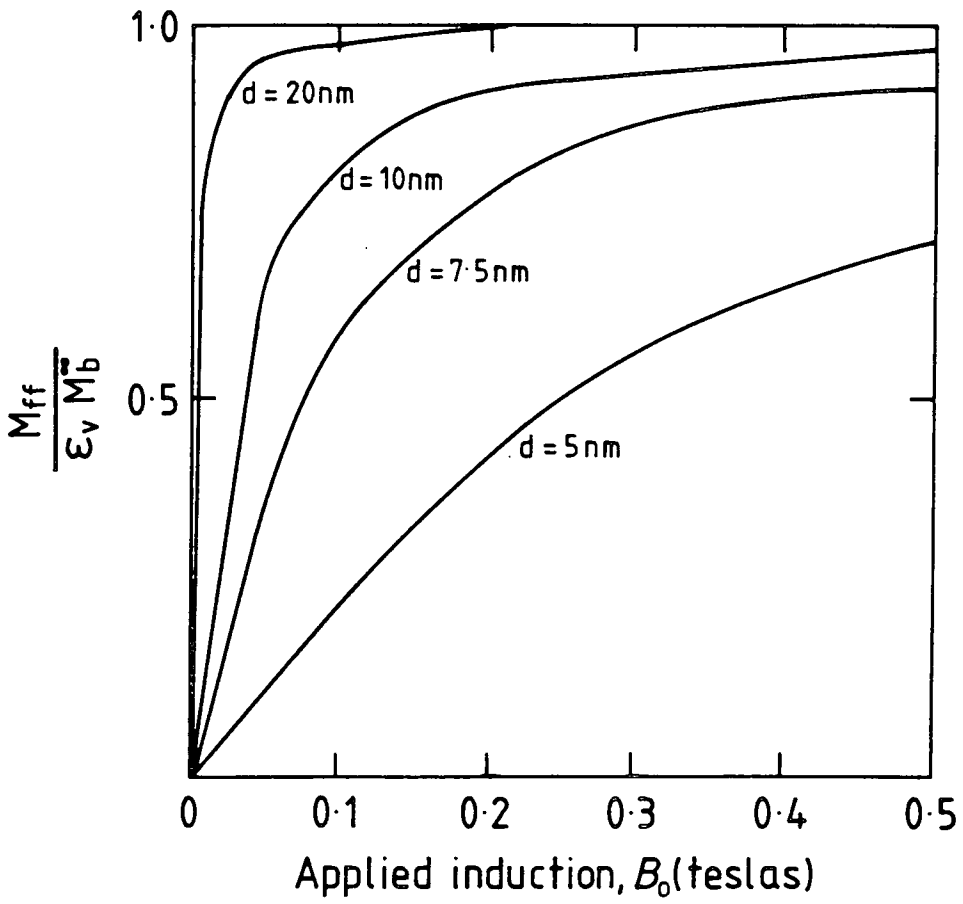


Fig. 1.5 Calculated magnetization curves for spherical particles of magnetite with various diameters.

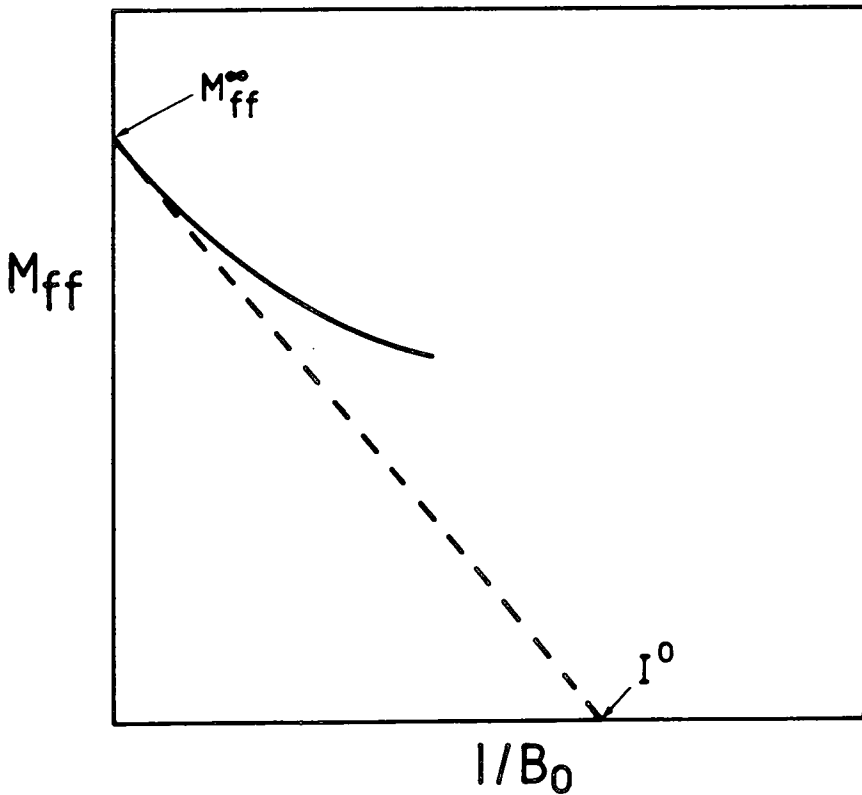


Fig. 1.6 A plot of M_{ff} against $1/B_0$ (solid line) and the limiting slope as $1/B_0 \rightarrow 0$ (dashed line) giving I^0 .

physical particle diameters. The difference arises due to a nonmagnetic layer on the surface of the particle, referred to as the nonmagnetic "dead" layer.¹⁹ This nonmagnetic surface of the particle is attributed to several reasons, which may well occur simultaneously (i) when a surfactant molecule adsorbs to the particle surface it is likely that adsorption occurs by a chemical reaction, producing some form of metal derivative of the surfactant. Such a derivative will possess negligible magnetic properties in comparison with the ferromagnetic material in the remainder of the particle. Hence adsorption of a surfactant onto the particle surface will produce an essentially nonmagnetic layer. (ii) Adsorption of surfactant on the particle surface is thought to cause a phenomenon called spin pinning. Essentially the magnetic moments of the surface metal atoms are "pinned" in an orientation such that their net magnetic moment vanishes.²² (iii) When the fluid particles consist of a metal, the particle surfaces will be highly susceptible to oxidation by an external source, producing a nonmagnetic or at least less magnetic oxide layer.

1.6.5 Determination of Particle Size Distributions from Magnetization Curves

In sub-section 1.6.3 the shape of the magnetization curve is essentially derived as a function of particle size.

In practice this is inverted and we deduce particle sizes from the shape of the experimentally determined

magnetization curve. This approach will be exploited extensively later in this work. Chantrell et al.²³ have developed a method from which details of the particle size distributions can be derived. The median particle diameter (\bar{d}_v) and the standard deviation (σ) can be calculated from equations derived assuming a lognormal particle size distribution. On transformation to quantities used throughout this text the equations become

$$\bar{d}_v = \left[18kT / \pi M_b^\infty \sqrt{\kappa I^0 / 3M_{ff}^\infty} \right]^3 \quad (1.23)$$

and

$$\sigma = 1/3 \sqrt{\ln(3K / M_b^\infty I^0)} \quad (1.24)$$

where κ is the initial susceptibility of the ferrofluid, I^0 is the intercept on the $1/B_0$ axis of the limiting slope of an M_{ff} vs $1/B_0$ plot as $B_0 \rightarrow \infty$. This is illustrated in Figure 1.6. Note M_{ff}^∞ is given by the same plot. These equations are used frequently in later chapters to calculate values of \bar{d}_v and σ .

The median diameter \bar{d}_v is derived from magnetic data. The shape of the magnetization curve is dependent on the distribution of particle magnetic moment magnitudes, which are dependent on the particle volume. Hence \bar{d}_v is referred to as a volume distribution median diameter. The physical size distribution mean diameter, \bar{d}_p , derived from electron microscopy is derived from a number distribution. In order to compare the two quantities directly it is necessary to

convert \bar{d}_v to a number fraction mean. This is done by application of the equation²⁴

$$\bar{d}_m = \bar{d}_v e^{-\frac{5}{2}\sigma^2} \quad (1.25)$$

\bar{d}_m is the mean magnetic particle diameter referred to frequently in this text. Comparison of \bar{d}_m and \bar{d}_p gives an estimate of the magnetic "dead" layer thickness.

1.6.6 Magnetic Relaxation

The magnetization of a magnetic fluid can relax following a change in applied field by either a Brownian or Néel mechanism.²¹ The Brownian rotational relaxation mechanism involves the physical rotation of the particle in the liquid medium, and is characterized by the relaxation time τ_B . Néel relaxation involves changes in the orientation of the particle magnetic moment between crystallographic axes, hence Néel rotation depends on particle anisotropy. Let us briefly consider the simplest example; in a single domain uniaxial particle the magnetic moment can have two possible orientations along the easy axis (i.e. in opposite directions). For the magnetic moment to change orientations an energy barrier (KV) must be overcome, where K is the anisotropy constant of the material and V is the particle volume. When the thermal energy kT is much greater than KV, then the magnetic moment will fluctuate thermally inside the particle with a characteristic relaxation time τ_N ²¹.

In magnetic fluids both Brownian and Néel relaxation

mechanisms both lead to apparent superparamagnetic behaviour. When $\tau_B \gg \tau_N$ the Néel mechanism dominates, and the material is said to be intrinsically superparamagnetic. Conversely when $\tau_N \gg \tau_B$ Brownian relaxation dominates, and the material exhibits extrinsic superparamagnetism. The values of τ_N and τ_B depend on particle size, for particles less than 10nm in diameter Néel rotation dominates. All but one of the systems described in this work fall into this category and are therefore, intrinsically superparamagnetic.

It follows that all of the room temperature magnetization curves obtained for samples described in this work will possess no coercivity or remanence at room temperature. The ferrofluids have to be frozen and cooled to very low temperatures ($\sim 4K$) before coercivity and remanence are observed. (Note Brownian relaxation cannot occur when a fluid sample is frozen).

1.7 Ferrofluid Stability

Magnetic fluids should be stable with respect to aggregation and sedimentation. Fluid stability generally relies on thermal agitation preventing aggregation. Each particle has thermal energy kT , and stability requires that kT is greater than any attraction energy, this restricts the maximum particle diameter. In this section internal stability with respect to particle aggregation is treated in terms of the simple physics of the interparticle forces present in magnetic fluids. Effects of gravitational and

applied magnetic fields on stability are then considered with particular emphasis on the limiting particle diameter.

1.7.1 Internal Stability - Interparticle Forces

Interparticle forces can be divided into destabilizing attractive forces and stabilizing repulsive forces. The attractive Van der Waals and magnetic dipole forces are considered first.

(i) London Type - Van der Waals forces

London or Dispersion type Van der Waals forces are present in all colloids. In neutral (non-polar) species the time averaged dipole moment is zero, however at any instant there exists an instantaneous dipole which induces a dipole in a neighbour. This dipole-induced dipole interaction gives rise to a time averaged finite force.²⁵ These forces are relatively short range with an r^{-6} dependence. Hamaker²⁶ derived an expression for the energy of interaction due to dispersion forces for two spherical particles. In the case when both particles have the same diameters Hamaker's original expression can be simplified to give the interaction energy due to Van der Waals dispersion forces as

$$E_w = -\frac{A}{6} \left[\frac{2}{s^2 - 4} + \frac{2}{s^2} + \ln \frac{s^2 - 4}{s^2} \right] \quad (1.26)$$

where $s = \frac{2x}{d} + 2$, x is the particle surface separation and d is the particle diameter. The constant $A \sim 10^{-19}$ J (within a factor of 3) depends on the nature of the particles and the medium and can be estimated from UV (or visible) dielectric

properties.²⁷ According to Hamaker,²⁶ for very small particle-particle distances, this expression reduces to

$$E_w = -\frac{Ad}{24x} \quad \text{for } d \gg x \quad (1.27)$$

This indicates that on particle contact the attraction energy tends to an infinite value. Obviously the prevention of contact is a necessity for a colloid to be stable. Figure 1.7 shows variation of Van der Waals attraction energy with particle surface separation for particles of various sizes. At room temperature for particle separations of approximately half that of the particle radius the attraction energy is much greater than the thermal energy (kT). It follows that thermal agitation as a mechanism for prevention of aggregation is not applicable in this case and we require the presence of the protective coating mentioned in section 1.4. This mechanism is discussed later in the section.

(ii) Magnetic Dipole-Dipole Attraction

The single domain particles in magnetic fluids have a magnetic dipole moment. It can be shown²⁸ that the interaction energy between two dipoles m_1 and m_2 separated by position vector \vec{r} is given by

$$E_m = \mu_0/4\pi \left[\vec{m}_1 \cdot \vec{m}_2 / r^3 - 3/r^5 (\vec{m}_1 \cdot \vec{r})(\vec{m}_2 \cdot \vec{r}) \right] \quad (1.28)$$

where μ_0 is the permeability of free space.

The interaction energy is a minimum (i.e. maximum attraction) when the dipoles are aligned, if $\vec{m}_1 = \vec{m}_2 = \vec{m}$,

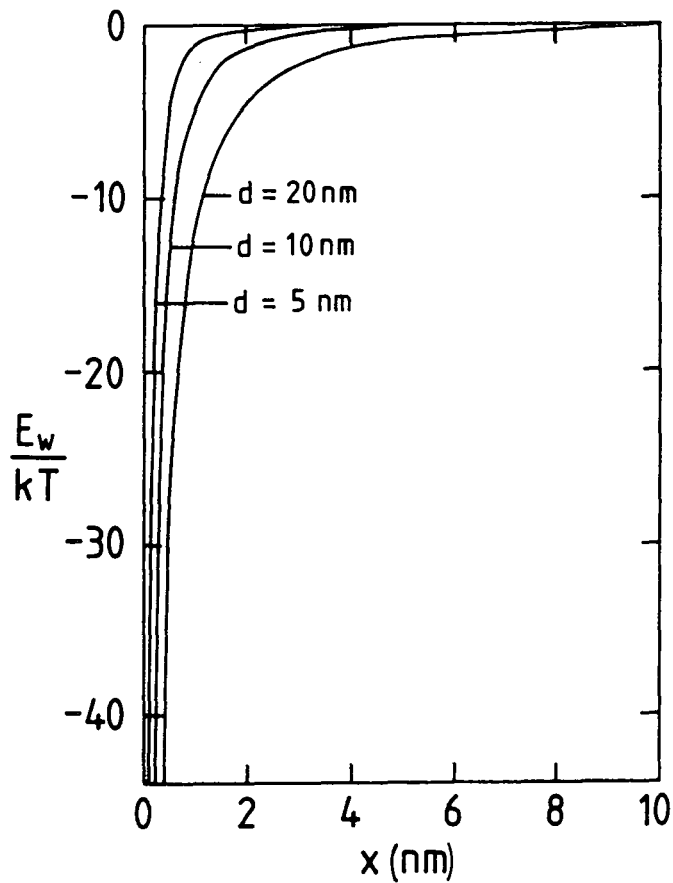


Fig. 1.7 Van der Waals attraction energy as a function of particle surface separation.

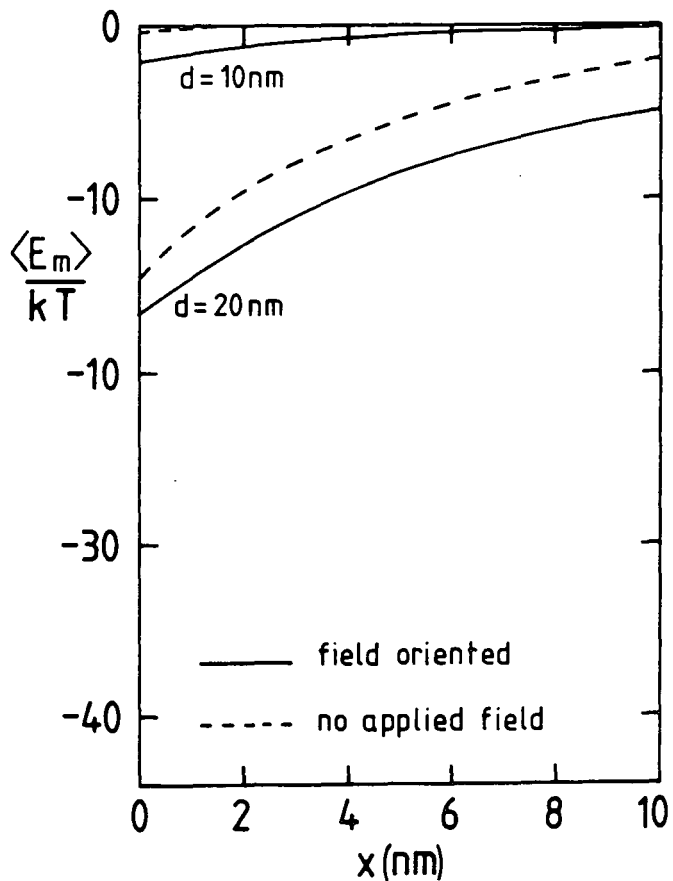


Fig. 1.8 Variation of magnetic attraction energy with particle surface separation for field orientated and non-orientated particles.

then for aligned dipoles $(\vec{m} \cdot \vec{r})(\vec{m} \cdot \vec{r}) = m^2 r^2$, the minimum attraction energy is given by

$$E_m(\text{min}) = -\frac{\mu_0 m^2}{2\pi r^3} \quad (1.29)$$

For two spherical particles with diameters d , the particle magnetic moment has a magnitude given by $m = M_b^\infty V = \pi M_b^\infty d^3/6$, (V is the particle volume) hence $E_m(\text{min})$ becomes

$$E_m(\text{min}) = -\pi\mu_0(M_b^\infty)^2 d^3/9s^3 \quad (1.30)$$

As defined before $s = \frac{2x}{d} + 2$ and M_b^∞ is the saturation magnetization of the bulk material. The particles are most difficult to separate when touching, i.e. when $x = 0$, hence the dipole-dipole contact energy is

$$E_m(\text{min})_{\text{contact}} = -\pi\mu_0(M_b^\infty)^2 d^3/72 \quad (1.31)$$

This shows the magnetic dipole-dipole attraction is very dependent on d . Monodispersity of orientated particles due to thermal agitation is only assured if

$$kT \geq \mu_0\pi(M_b^\infty)^2/72 \quad (1.32)$$

This restricts the particle size to

$$d \leq (72kT/\pi\mu_0(M_b^\infty)^2)^{1/3} \quad (1.33)$$

For Fe_3O_4 at 298K, $M_b^\infty = 4.84 \times 10^5 \text{ JT}^{-1}\text{m}^3$, giving $d < 6.8\text{nm}$.

Particles with diameters of 10nm or less are only likely to be orientated in the presence of an external magnetic field. This limiting diameter of $d < 6.8\text{nm}$ refers to the size of particles which would remain monodispersed even in the presence of an aligning external magnetic field. Even in the presence of a magnetic field this is an extreme estimate since particle contact is avoided by the presence of the surfactant coating.

Particle dipole moments fluctuate thermally and a more realistic value of the magnetic attraction energy due to the averaging of these fluctuating moments is given by¹²

$$\langle E_m \rangle = - E_m^2 / 12kT \quad (1.34)$$

Figure (1.8) shows how magnetic attraction energy varies for both orientated and non-orientated particles with particle surface separation.

Even for fully orientated particles the magnetic attraction is small compared to the Van der Waals attraction.

(iii) Steric Repulsion

Thermal effects alone are insufficient to prevent particle aggregation due to Van der Waals dispersion forces.

The surfactant or polymer coating on the particle surface provides a repulsion energy vital in preventing particle contact. It is the interaction of surfactant "tails" or polymer "loops", as described in Section 1.4, which gives rise to this repulsion. These non-adsorbed parts of the

molecule undergo thermal motions. As two particles approach these motions are restricted due to steric repulsion, and this loss of motion constitutes a loss of entropy. Hence this mechanism is known as either steric or entropic repulsion. Order of magnitude calculations give estimates of the repulsion energy. The mechanism can be considered in two ways.

In the first approach Mackor²⁹ gave the first quantitative explanation of this form of repulsion by considering the surfactant tail as a rigid rod attached to a flat surface via a ball joint. Mackor derived his expression by considering the loss of possible configurations of the hydrocarbon chains as the two surfaces came close enough for the chains to interact. This approach was modified by Rosensweig et al.³⁰ who obtained an expression for this steric repulsion between two spherical particles which can be written as

$$E_s = 2\pi kT \Gamma d^2 \left[2 - \frac{l+2}{t} \frac{(1+t)}{(1+t/2)} - \frac{l}{t} \right] \quad (1.35)$$

where $l = 2x/d$, $t = 2\delta/d$, δ is the thickness of the surfactant coating, and Γ is the number of surfactant molecules per unit area on the particle surface. These parameters are shown in Figure 1.9.

An alternative approach is given by Scholten¹² who considers repulsion between the surfactant chains as an osmotic effect. Surfactant tails are considered as free molecules and an expression is obtained by considering the

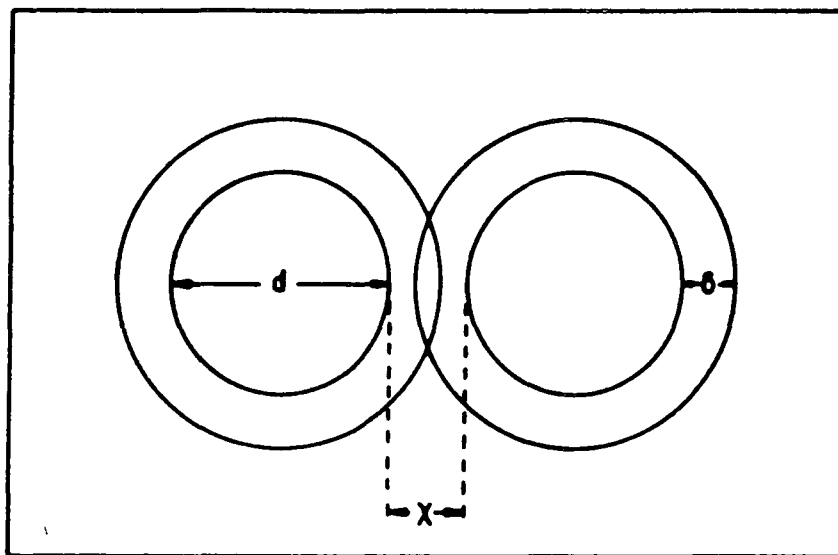


Fig. 1.9 An illustration of parameters d , x and δ .

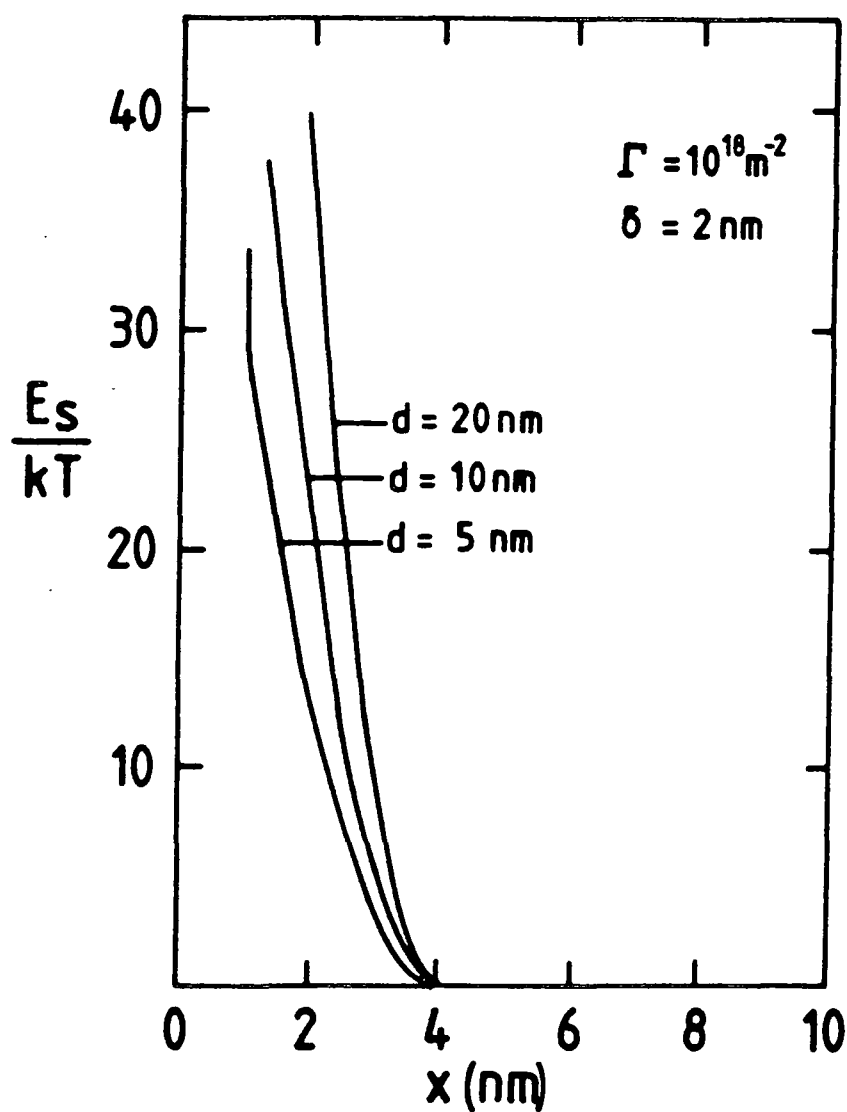


Fig. 1.10 Steric repulsion energy as a function of particle surface separation.

increase in osmotic pressure arising due to increased concentration of tails in the overlap volume. This approach produces an expression for the repulsion energy given by

$$E_s = \frac{2}{3} \pi kT \frac{\Gamma}{\delta} (\delta - x/2)^2 (1.5d + 2\delta + x/2) \quad (1.36)$$

The parameters are as before.

Graphical representations showing how these estimates vary with interparticle distance can be obtained by substituting in realistic values for the various parameters.

Figure 1.10 shows the curves obtained using equation 1.36 with $d = 2\text{nm}$ and $\Gamma = 10^{18} \text{m}^{-2}$.

(iv) Enthalpic Repulsion

This effect arises when the heat of solution of the surfactant is exothermic. If surfactant chain-solvent interactions are energetically more favourable than solvent-solvent and chain-chain interactions then a repulsive force will arise between two particles whose surfactant chains come into close contact. This effect is believed to be at least an order of magnitude less than the entropic effect.³¹

(v) Electrostatic Repulsion

In a polar medium colloidal particles can carry electric charge. This charge originates from either surface dissociation producing ions or preferential adsorption of ions from solution onto the particle surface. A repulsive force arises between the like charges on the particle surfaces. In aqueous solution the particle charge may be

effected by the pH of the solution. Variation of solution pH can lead to neutralization of the surface charge, known as the isoelectric point, and may cause flocculation of the colloid.²⁷

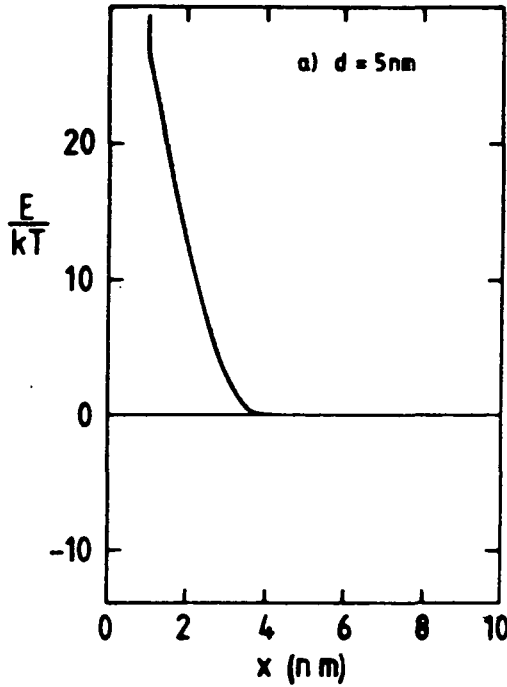
Electrostatic repulsion between charged particles is not simple Coulombic repulsion. In order to maintain electroneutrality an electric double layer is produced. The particle charge forms the first layer which is surrounded by a diffuse outer layer composed of oppositely charged ions to balance the charge of the inner layer. Electrostatic repulsion between particles is reduced by the screening effect of the surrounding ions. The corresponding repulsion energy depends on the particle size, surface potential and concentration of ions in the bulk solution.¹²

In general magnetic fluid stability relies on steric repulsion. There are exceptions; magnetic fluids have been prepared by Massart,³² in which stability depends on the presence of the electric double layer rather than surfactants. Although the electric double layer is not present in most magnetic fluids, it is important at an intermediate stage in some of the preparative methods discussed later.

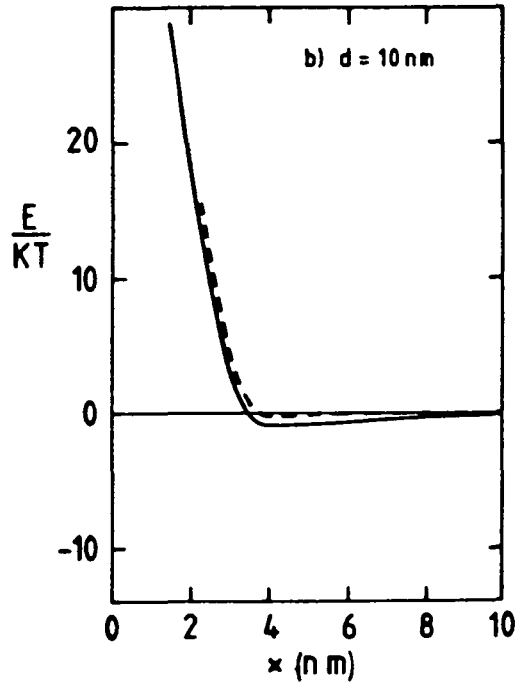
(vi) Net Potential Energy Curves

Fluid stability depends on a balance of the interparticle forces described. Net potential energy curves are obtained by summing the values for Van der Waals and magnetic attraction energy and steric repulsion energy.

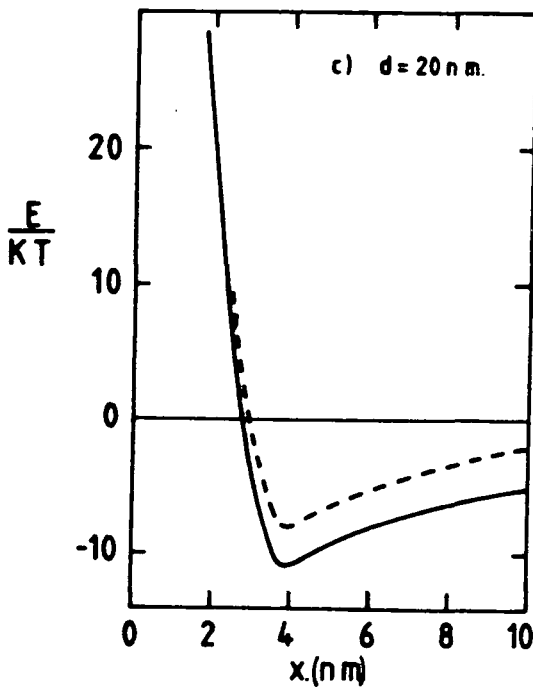
In Figure (1.11(a)) it can be seen that only repulsion at small interparticle distances remains for 5nm particles. For 10nm diameter non-orientated particles (Figure 1.11(b)) there is a potential energy minimum at $x \sim 4\text{nm}$, this minimum is shallow ($\sim 0.4\text{ kT}$) and thermal motions should keep the particles monodispersed. Again at very small separations repulsion dominates so closer approach is unlikely. For orientated particles the minimum is slightly deeper than kT . Hence in a strong field agglomeration for 10nm particles is to be expected, as predicted earlier. When the particle diameter is 20nm the potential energy minimum is now deep sided (Figure 1.11(c)). As particles approach they fall into this minimum and are unlikely to escape even in the absence of a magnetic field. It must be noted that these curves are from order of magnitude calculations. The overall potential energy curves in Figure 1.11 appear to tend to infinite repulsion as x tends to zero. If we continue to calculate the overall potential based on contributions from Van der Waals attraction, magnetic attraction and steric repulsion at very short distances ($x = 0.1\text{-}0.2\text{nm}$) the value becomes negative ie attraction dominates since the Van der Waals attraction energy tends to infinity as x tends to zero. In practice this would not happen because extremely short range Born repulsive forces would dominate for $x < 0.4\text{nm}$. These forces which arise due to overlap of atomic orbitals²⁵ are not taken into account when generating the energy curves.



(a) $d = 5 \text{ nm}$



(b) $d = 10 \text{ nm}$



(c) $d = 20 \text{ nm}$

Fig. 1.11 Net interparticle potential energy curves as a function of particle surface separation for (a) $d = 5 \text{ nm}$, (b) $d = 10 \text{ nm}$ and (c) $d = 20 \text{ nm}$.

1.7.2 Stability in External Fields

(i) Sedimentation in the Gravitational Field

The sedimentation caused by the gravitational field is opposed by thermal agitation which tends to keep particles evenly dispersed throughout the fluid. Gravitational settling is avoided if the thermal energy is greater than the gravitational energy i.e.

$$kT > V(\rho_s - \rho_L)gh \quad (1.37)$$

where V is the particle volume, ρ_s and ρ_L are the solid and liquid densities respectively, g is the acceleration due to gravity and h is the height of the particle in the liquid. For a spherical particle this gives the limiting diameter not to settle as

$$d = (6kT/\pi(\rho_s - \rho_L)gh)^{1/3} \quad (1.38)$$

For magnetite in water, setting $h = 0.05\text{m}$ and $g = 9.8\text{ms}^{-2}$, equation 1.38 gives $d = 16\text{nm}$. Hence only aggregates of particles will settle out in the gravitational field. Whatever the treatment gravitational settling is not a serious problem compared to the settling caused by a magnetic field gradient.

(ii) Stability in a Magnetic Field Gradient

When a magnetic fluid is placed in a magnetic field gradient (∇B) the particles are subjected to a magnetic force, F_m , given by³⁰

$$F_m = m\nabla B \quad (1.39)$$

where m is the particle magnetic moment. For spherical particles with volume $\pi d^3/6$ this becomes

$$F_m = \pi d^3 M_b^\infty \nabla B / 6 \quad (1.40)$$

where M_b^∞ is the saturation magnetization per unit volume of the bulk magnetic material. This force induces the particles to move at a steady terminal velocity v . Particle motion is opposed by the Stokes force given by³³

$$F_s = 3\pi d_h \eta_o v \quad (1.41)$$

where η_o is the viscosity of the carrier liquid and d_h is the particle hydrodynamic radius (i.e. including surfactant layers). At equilibrium these forces can be equated and by using the approximation $d = d_h$ and rearranging, the terminal velocity is given by

$$v = d^2 M_b^\infty \nabla B / 18 \eta_o \quad (1.42)$$

The net particle motion produces a particle flux which is opposed by a back diffusional flux.³⁴ If a 100% change in mean particle concentration per unit volume is taken as the criterion for magnetic separation, then it can be shown that the limiting diameter for stability is

$$d = [6kT / \pi M_b^\infty \nabla B]^{1/3} \quad (1.43)$$

It follows that the limiting size is dependent on the magnetic field gradient. For typical field gradients found in present day applications, the particle size is limited to the 2.5 - 10nm range.

1.8 The Properties of Magnetic Fluids

Magnetic fluids possess many interesting physical properties which have been studied specifically by a number of authors. These properties, however interesting, are not relevant to this text. This section gives a very brief review to make the reader aware of the range of properties which have been studied.

1.8.1 Mechanical Properties

When a magnetic field is applied to sample of a magnetic fluid some rather astonishing effects can be observed. The most spectacular phenomenon is known as surface instability. When a magnetic field is orientated perpendicular to the surface of a pool of ferrofluid, the flat surface can be observed to suddenly break up into a hexagonal pattern of spikes (Figure 1.12) as the field reaches some critical value. This surface instability is a critical phenomenon dependent on the fluid magnetization, surface tension and the applied field gradient.³⁵

A non-ferromagnetic body immersed in a ferrofluid which is subject to an applied field gradient experiences a magnetic pressure gradient.³⁶ By control of the field gradient non-ferromagnetic objects can be levitated or even

Fig. 1.12 Surface instability



expelled from the ferrofluid. This phenomenon has been applied to the design of a magnetic separator by Shimoizaka et al.³⁷ A ferromagnetic object such as a simple bar magnet can be self-levitated in a magnetic fluid.³⁶

1.8.2 Electrical Properties

In the hydrocarbon based magnetic fluids described in this text, electrical conductivity and electrophoresis will be negligible because of the insulating nature of the carrier liquid used. Electrophoresis would only be observed in fluids prepared in a polar medium, where an electric double layer (described in section 1.7.1(v)) gives the particles a net electric charge. The electrical conductivity of ferrofluids prepared in polar media is greater than that of the carrier liquid because of ions from the surfactant molecules or particle surfaces in solution.

1.8.3 Thermal Properties

The thermal conductivity of magnetic fluids has been studied by Popplewell et al.³⁸ These workers observed that a magnetic field had no effect on this property. The melting point of a magnetic fluid is less than that of the pure carrier liquid, because of the presence of surfactant molecules in solution.

1.8.4 Rheological Properties

The viscosity of a magnetic fluid is effected by the presence of a magnetic field, although fluid flowability is retained even when the fluid is magnetized to saturation.²¹ In the absence of a magnetic field, the rheological

behaviour is the same as for non-magnetic colloidal suspensions. Viscosity of a ferrofluid is related to hydrodynamic particle size, i.e. including the surfactant layer.³⁹

1.9 Applications of Magnetic Fluids

This section is not a comprehensive catalogue of the applications of magnetic fluids. It is simply an illustration of some of the uses magnetic fluids have been associated with in the relatively short time they have been available.

The most advanced application is that of dynamic sealing.⁴⁰ Figure 1.13 shows the essential components of a magnetic fluid seal. Fluid fills the gap between a rotating shaft and a stationary housing and acts as if it was a liquid O-ring. The fluid is maintained in position by an axially magnetized ring magnet focusing its field onto a small annular volume where the fluid is placed. These dynamic seals can be applied to both vacuum and high differential pressure systems. One seal can be used for both inclusion and exclusion purposes. For inclusion applications they are used not only for vacuum and gas pressure systems but can seal against immiscible liquids under pressure. Exclusion finds them protecting against harmful vapours or particles, for example preventing dust entering disc drives, in a static application. The performance of these seals compared to conventional seals is

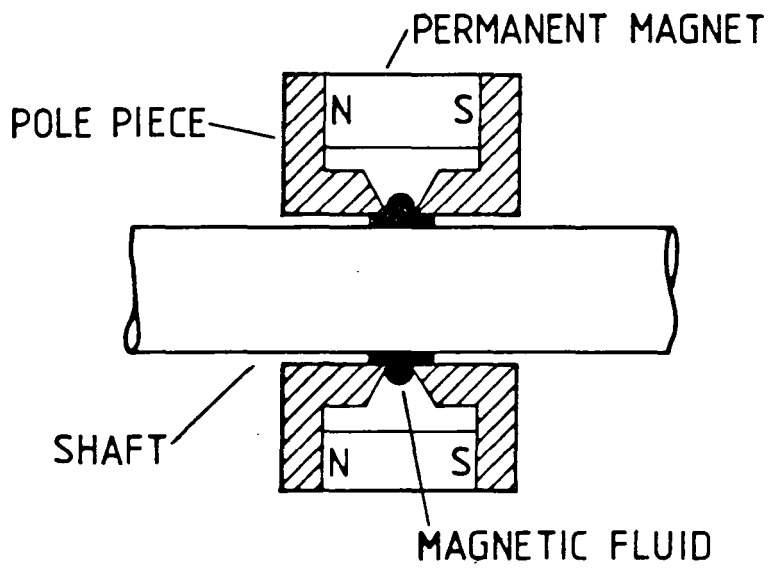


Fig. 1.13

The essential components of a magnetic fluid dynamic seal.

impressive. They have been known to withstand 10^{-9} atmospheres and if used in stages can hold 66 atmospheres. Rotation speeds of 10,000 r.p.m. are common and 120,000 r.p.m. has been achieved. Carrier liquid properties can be chosen to suit the specific requirements of the application. These seals exhibit no wear and do not require maintenance.

Lubrication is a bonus in the rotating seals described. However, magnetic fluids are used specifically as lubricants.⁴¹ The lubricating fluid is held in place by a magnetic field and the carrier liquid used is chosen for its lubricating properties.

Papell¹¹ first prepared magnetic fluids to allow pumping of rocket propellant in zero-gravity conditions. The carrier liquid is the fuel which is prevented from dispersing throughout the fuel tank by a magnet which essentially provides an artificial gravity.

Bailey⁴² describes some lesser known applications of magnetic fluids the most established of which is in loudspeakers. This application utilizes the thermal conductivity of the magnetic fluid. The fluid is held in position by the field gradients around the speaker voice coil and dissipates away generated heat. The fluid's presence allows the power output of the speaker to increase several fold.

The magnetic levitation phenomena observed when a magnetic fluid is subject to a magnetic field gradient can be applied to several separation processes for solid

non-magnetic materials which have different densities.^{36,37} This effect, which arises due to a balance of magnetic and pressure energies, results in non-magnetic objects which differ in density being levitated to different extents. An accurate densitometer relying on the fact that the apparent specific gravity of the fluid can be varied by variation of applied field gradient has been described by Kaiser and Miskolczy.⁴³

Magnetic fluids are used as magnetic inks. These inks are used in ink-jet printing⁴⁴ where a jet of fluid drops is directed by a magnetic field gradient. Magnetic inks containing coloured dyes are used in a plain paper recorded process described by Maruno et al.⁴⁵

Energy conversion was one of the original uses magnetic fluids were developed for.³⁰ This potential application is based on the fact that a ferromagnetic material suffers a reduction in magnetization when heated, especially as the Curie point is approached. In such a device magnetic fluid is contained in a tube and is drawn into a heat source by a magnetic field supplied by a solenoid. The fluid suffers a local decrease in magnetization in the region of the heat source. Ideally the Curie temperature of the particulate material is exceeded and the material becomes paramagnetic. The heated "demagnetized" fluid is moved out of the magnetic field and replaced by cool fluid. The hot fluid passes through a heat sink causing it to cool again and regain its original magnetization (in the ideal case when the Curie

temperature has been exceeded the particles become ferromagnetic again). These devices would convert heat energy to mechanical energy which would be subsequently converted to electrical energy. Such mechanisms would have no moving or mechanical parts and in theory have a very high efficiency.

Some of the proposed medical applications of magnetic fluids are rather ambitious. One of these involves the injection of fluid into various organs to use in radiodiagnosis as a contrast media.⁴⁶ Another proposal involves magnetic fluid emulsions for drug carrying applications.⁴⁷

1.10 Metal Particles in Other Areas of Chemistry

Fine metal particles have important uses in several areas of chemistry. Before going on to discuss the preparation of magnetic fluids in detail (chapter 2) it is relevant to consider the more common uses of fine metal particles in chemistry.

1.10.1 Heterogeneous Catalysis

Heterogeneous catalysis is a well established very broad area. Heterogeneous catalysts of relevance here are solids, consisting of a support, usually a silicate, aluminate or related material with a surface coating of the metal, which increase the rates of chemical reactions by virtue of their surface.⁴⁸ Large surface areas are desirable for efficient catalysts, hence the use of finely divided

metals. The metal particles in use can be divided into many categories. Reduction of metal salts at elevated temperatures using gaseous reducing agents, i.e. CO, H₂, usually forms the basis of particle preparation.⁴⁹

Unsupported single metal and alloy metal powders are prepared from hydroxides,⁵⁰ basic carbonates⁵¹ and metal salts in general, by decomposition to the oxide which is then hydrogen reduced.⁴⁹ Supported catalysts are prepared by soaking metal salt solutions into the carrier (support), drying them and then reducing the deposited salt with hydrogen at elevated temperatures. Alternatively the metal and carrier can be co-precipitated as a hydroxide, followed by drying and reduction.⁴⁸ Fine metal particles in colloidal suspension have even been prepared by depositing platinum onto alumina in suspension. Platinum particles as small as 1.5nm in diameter have been prepared in this manner.⁵²

Metal particles in heterogeneous catalysis are important because of their large surface area and associated properties, rather than magnetic properties (cf. magnetic fluids).

1.10.2 Metal Slurries

Rieke and co-workers have generated a series of reactive metal slurries in ethereal solvents and used them in organic synthesis. The work involves the alkali metal reduction of metal salts, almost exclusively halides in ethereal solution, to produce finely divided metal powders as slurries. The early work involved the preparation of

magnesium slurries in this manner and their use in preparing difficultly formed Grignard reagents.^{53,54} In an analogous way highly reactive zinc and first row transition metals cobalt, nickel and iron powders have been prepared.⁵⁶ Metal slurries have been applied to the synthesis of chromium hexacarbonyl and more recently dicobalt octacarbonyl.⁵⁸

1.10.3 Metal Atom Condensation

Small nickel particles have been produced by co-condensation of nickel atoms and alkanes at low temperatures (-196°C).⁵⁹ A Ni-solvent (alkane) complex is believed to form initially⁶⁰ which on melting and warming produces very small nickel particles/crystallites ($\sim 3\text{nm}$). At $\sim -130^{\circ}\text{C}$ the growing nickel particles are believed to react and cleave the alkane solvent.⁶¹ The alkane cleavage reaction competes with particle growth and produces a carbonaceous "layer".⁶¹ The ratio of Ni:organic material in the particles is dependent on the excess of alkane used in the co-condensation and the warm up conditions. The magnetic properties of the products were also dependent on the preparative conditions. Non-ferromagnetic powders were produced with very large excesses of alkane or when the mixture was held at -130°C during the warm up period. With smaller excesses of alkane and more rapid warm up, ferromagnetic powders were obtained. These magnetic properties were attributed to a higher carbonaceous content due to the nickel-alkane reaction at -130°C . ESCA showed the carbonaceous "layer" to consist of sp^2 or sp^3 carbon

bound species homogeneously dispersed throughout the nickel, rather than carbides.⁵⁹

These products are of interest because of the catalytic properties; indeed more recently Klabunde and Imizu⁶² have vaporized Mn and Co simultaneously to produce bimetallic particles which were deposited on powdered silica for catalytic purposes.

CHAPTER 2

A REVIEW OF MAGNETIC FLUID PREPARATIONS

Introduction

The work described in this thesis is largely concerned with the preparation of magnetic fluids. This chapter is a review of magnetic fluid preparations which are conveniently categorized by the preparative method employed. This however, simultaneously divides the fluids into particle composition types, i.e. non-metallic and metallic (with few exceptions).

2.1 Non-metallic Fluids

These fluids have magnetic particles which consist of either gamma ferric oxide ($\gamma\text{-Fe}_2\text{O}_3$), magnetite or other ferrites. Two general preparative methods are used, the first being by the physical process of size reduction where coarse material is literally ground down until it is the correct size. The second is a chemical method involving the precipitation of the relevant material from aqueous solution.

2.1.1. Size Reduction - Ball Milling

Commercially available magnetic fluids are prepared in this manner. In this procedure first used by Papell,¹¹ stainless steel mill jars of various capacities are loaded with small steel balls and a slurry consisting of a mixture of the relevant magnetic material, carrier liquid and

surfactant. Milling is achieved by rotating the mills for time scales of the order of weeks. During this process the powdered magnetic material with original particle size in the micron range is broken down until the particles are of colloidal size. The product is normally decanted off and subject to centrifugation to remove non-colloidal particles.

This simple physical process is highly versatile and can be subject to modifications. Papell¹¹ used magnetite with oleic acid as surfactant and a range of hydrocarbon carriers including rocket fuel.

Rosensweig and Kaiser⁶³ conducted a thorough study into the use of ball milling for the preparation of magnetic fluids. They used Fe_3O_4 , $\gamma\text{-Fe}_2\text{O}_3$ and MnZn ferrite as magnetic material with an extensive range of surfactants in a variety of carrier liquids. In the same report micron sized iron powder was ground in an attempt to produce a metallic iron fluid, the product was a slightly magnetic colloid which was rapidly oxidized to a non-magnetic state.

Manganese-Zinc ferrite ($\text{Mn}_{0.5} \text{Zn}_{0.5} 0.\text{Fe}_2\text{O}_3$) has a magnetization which varies considerably with temperature. Consequently $\text{Mn}_{0.5} \text{Zn}_{0.5} 0.\text{Fe}_2\text{O}_3$ has been successfully milled in the described manner³⁰ in studies directed toward producing a magnetic fluid for a heat exchange system.

This method is very time consuming and has the disadvantage that the particles produced tend to have a wide distribution of particle sizes, typically 2-50nm. However, by virtue of the following modifications this process is

capable of producing fluids with almost any carrier liquid and surfactant, i.e. this allows tailoring of fluid properties for specific applications.

(i) Substitution of Carrier Liquid

This modification of the milling process relies on the reversible flocculation of the particles.⁶⁴ A fluid is first prepared in the normal way. Flocculation is achieved by the addition of polar solvent such as acetone or ethanol. This works because surfactant tails are less compatible with the combined solvents causing the tails to fold hence reducing the thickness of the surfactant protective coat.

Subsequently the stabilizing steric repulsion mechanism fails and the particles flocculate and settle out. Figure 2.1 shows the reversibly flocculated particles, the surfactant still being attached to the particle surface. A new magnetic fluid is obtained by separating the particles and redispersing them in a new carrier liquid. This modification means that grinding can take place in a solvent with good grinding properties, i.e. low viscosity, but can be replaced with a carrier with a particular desired property, low volatility for example.

(ii) Substitution of Surfactant

Surfactant and carrier liquid can be exchanged via irreversibly flocculating the particles produced in the initial milling.⁶⁵ The procedure is summarized in a schematic chart form in Figure 2.2. The initial milling is carried out in water which is inexpensive, non-combustible and has a

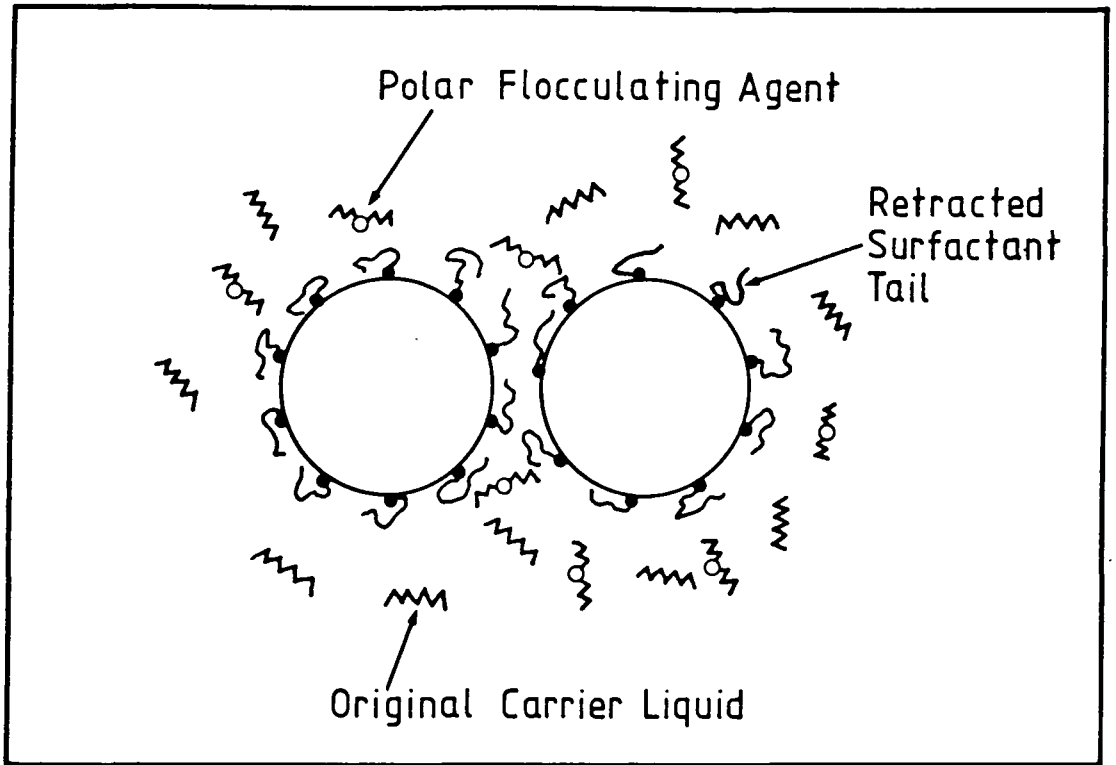


Fig. 2.1 Reversibly flocculated particles.

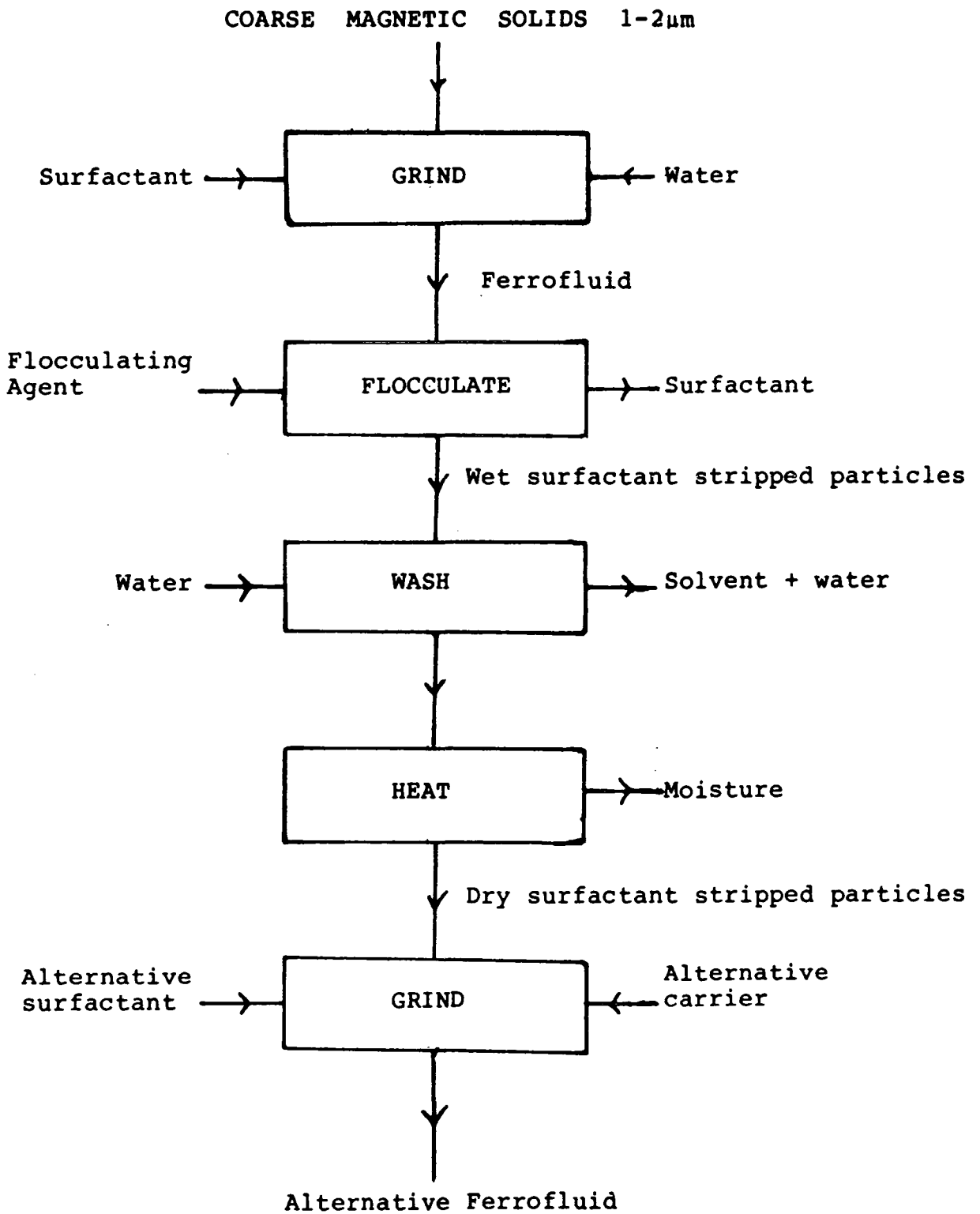


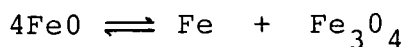
Fig. 2.2

Substitution of magnetic fluid carrier liquid and surfactant.

low viscosity. As before a second solvent such as acetone is added causing the particles to irreversibly flocculate as represented in Figure 2.3. During the irreversible flocculation the particles are stripped of surfactant. These particles are separated, washed and dried before they are redispersed by further milling with an alternative carrier in the presence of a new surfactant. This approach is very convenient since stocks of dry particles can be used to provide a magnetic fluid of predetermined concentration with a particular carrier/surfactant combination.

(iii) Magnetic Fluids via Milling of a Non-magnetic Precursor

A clever route to a magnetic fluid has been achieved by grinding a non-magnetic precursor to produce a stable colloid and then converting it to a magnetic colloid.⁶⁶ Micron sized ferric oxide powder is reduced to wustite using carbon monoxide at 650°C, this is then quenched producing wustite (Fe_{1-x}O , $x = 0.01$ to 0.2) in the metastable phase in the same micron size range. A stable non-magnetic suspension is then obtained by milling the wustite in kerosene/oleic acid. Subsequent refluxing of the colloid for 6 hours at 250°C causes the wustite to disproportionate according to



producing a stable magnetic suspension of magnetite (and iron).

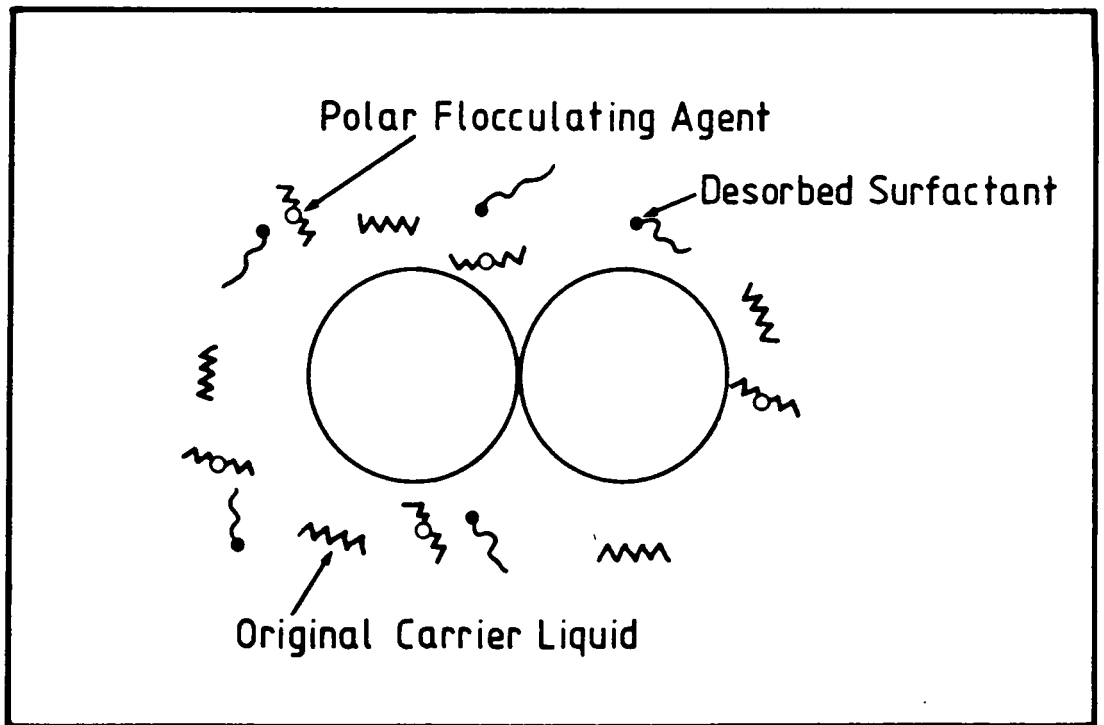


Fig. 2.3 Irreversibly flocculated particles.

2.1.2 Chemical Precipitation from Aqueous Solution

Many authors have applied this method (with surprisingly little variation) which is essentially based on the precipitation of magnetite from aqueous solutions of iron (II) and iron (III) salts with an excess of alkali.⁶⁷⁻⁸⁵ The precipitation of magnetite in this manner was used by Elmore⁷ to prepare his suspensions, the method however can be traced back to the nineteenth century.⁸⁶

True magnetic fluids were first prepared using this technique by Reimers and Khalafalla.⁶⁷ Their procedure is fairly typical; aqueous solutions of iron (II) chloride and iron (III) chloride are mixed so that the $\text{Fe}^{2+}:\text{Fe}^{3+}$ ratio is 1:2. An excess of aqueous ammonia solution is added rapidly to cause precipitation of colloidal sized iron oxide particles. A solution of oleic acid in the carrier liquid kerosene is then added with stirring, ammonium oleate being formed by reaction with the excess ammonia. The particles become coated with ammonium oleate in the aqueous phase. Heating to 80-90°C causes the ammonium oleate to decompose, giving off ammonia gas and leaving oleic acid on the surface of the particles. During this heating the co-precipitated hydrated iron (II) and iron (III) oxides are converted to magnetite. Transfer of the oleic acid coated particles to the organic phase is followed by phase separation. The aqueous phase is removed and the remaining organic phase heated to remove traces of water. In this particular variation of the general procedure if sodium hydroxide was

used as the precipitating agent the process would fail because sodium oleate does not thermally decompose in the same way as ammonium oleate.

In general both chloride and sulphates salts can provide the source of iron (II) and iron (III) ions. Likewise⁷⁶ sodium hydroxide has been employed to cause precipitation instead of aqueous ammonia. Normally the precipitated magnetite is separated prior to redispersion in an organic carrier. In the majority of cases the surfactant is added following the precipitation but before the separation of the particles. Hence when the particles are separated they are already coated with surfactant and easily dispersed in a carrier liquid. Particle separation is usually done magnetically. In some cases sedimentation of the precipitated magnetite can be achieved by neutralising the particle surface charge by control of the pH.⁷⁷ There are examples^{78,79} when the peptization occurs during the magnetite precipitation. One author claims adding the iron salt solution to the ammonia solution improves the quality of the product.⁸⁰ It is also possible to start with purely Fe(II) and oxidize the relevant amount to Fe(III).

This method has been successfully applied to the preparation of aqueous magnetic fluids.⁸¹⁻⁸⁵ After the coated particles are prepared and separated in the normal way they are redispersed in an aqueous solution of shorter tailed water-compatible-surfactants.^{84,85} Khalafalla and Reimers⁸⁷ studied the effects of dilution on aqueous magnetic fluids.

They showed that fluids stabilized with the cationic surfactant dodecylamine were unstable to dilution, whereas fluids stabilized with the anionic surfactant sodium dodecanoate were stable to considerable dilution.

Precipitation of the particles occurs in an aqueous alkaline medium. Hydroxide ions are adsorbed onto the particle surface forming the inner Helmholtz layer. Loosely bound cations form the outer Helmholtz layer. Dodecylamine is present as dodecylammonium chloride and is only loosely physisorbed to the outer Helmholtz layer. Dilution lowers the concentration of surfactant in the bulk solution and the loosely held cationic surfactant is desorbed to maintain the balance. In contrast the anionic surfactant sodium dodecanoate is chemisorbed to the inner Helmholtz layer and is not removed on dilution.

All the magnetic fluids discussed in this section have been sterically stabilized, although electrostatic repulsion has played a role in many of the preparations. Massart has prepared aqueous magnetic fluids stabilized in both alkaline and acidic media without the use of organic stabilizing agents. Magnetite is precipitated in one of the usual ways.

Precipitated magnetite is separated and peptized with aqueous tetraethylammonium hydroxide solution (1M) to give an alkaline magnetic fluid. To obtain an acidic sol the precipitate is treated with perchloric acid (2M), isolated by centrifugation and peptized into water. Stabilization of these fluids is electrostatic. If the pH of the solution is

altered to pH5 — pH9 then coagulation occurs due to neutralization of the surface charge responsible for stabilization.

As with the size reduction process described in the previous section some work deals with the production of specialized fluids for specific applications. Bottenberg and Chagnon⁸⁸ have developed low vapour pressure fluids for use in vacuum seals by using polyphenyl ethers as the carrier liquids. Phenoxy terminated aliphatic acids proved to be successful surfactants for use in this medium. Similarly silicone-oil based fluids with organosilicone surfactants have been prepared because their viscosity has a low temperature dependence.⁸⁹ Fluorocarbon based magnetic fluids have also been prepared using the precipitation technique.^{90,91}

The precipitation technique is less time consuming than grinding methods. It differs fundamentally from the size reduction route because it starts at the molecular level and grows particles to colloidal size. Milling begins essentially with the bulk material and reduces it to colloidal size. Particle size is in the 10 nm range and is dependent on the precipitation step. The number of particle nuclei produced increases as the excess in concentration of ions in solution above the equilibrium value at the time of precipitation increases. Particle size decreases as the number of nuclei increases. In accordance with this it has been observed that the larger the excess of hydroxide and

iron(III) ions the smaller the particles. A slower precipitation rate will produce less nucleation sites and hence larger particles. In the gravimetric determination of iron, precipitation is deliberately slow to avoid producing a colloid.

2.2 Metallic Magnetic Fluids

Some preparations of metallic ferrofluids are closely related to the preparation of fine metallic particles. Metals of interest are the ferromagnetic transition metals iron, cobalt and nickel, their alloys and the lanthanide element, Gadolinium. Liquid metal based systems are included in this section.

2.2.1 Evaporation Techniques

The preparation of fine metal particles by the evaporation of metals in inert gas atmospheres is a well established technique. Evaporation of a range of metals into argon gas at low pressures produced fine particles whose size was found to depend on the argon gas pressure.^{92,93} Analogous work involving evaporation of metals into helium⁹⁴ and xenon atmospheres has also been investigated. In these studies the particle size was observed to depend on the nature of the gas forming the inert atmosphere as well as its pressure. Operating at the same pressure particle size was found to increase in the order helium, argon, xenon.⁹⁵ Using this technique metal particles in the nanometre to micron size range can be prepared. Particle size is

independent of the metal. In argon 10nm sized particles could be obtained at an argon pressure of 1mm of mercury. Particles produced were usually single crystal and their structure and crystal habits were investigated. Structures were usually the same as the bulk with a few exceptions. Chaining of particles was always observed for the ferromagnetic elements.

Tasaki et al.⁹⁶ studied the magnetic properties of iron, cobalt and nickel particles produced by evaporation into argon. This is an extremely powerful technique for the preparation of fine particles since composition of the particles is easily predetermined. This is demonstrated by the preparation of alloy particles of the ferromagnetic transition elements. By evaporation of the desired bulk alloy into argon, this technique has been applied to study the magnetic properties of iron-cobalt,⁹⁷ iron-nickel⁹⁸ and even iron-cobalt-nickel⁹⁹ particles. Single domain particles are readily prepared in this manner whose compositions are very close to that of the bulk alloys. Considering the versatility of this technique it must be logical to adapt this method for the preparation of metallic and alloy magnetic fluids. Using this technique both the size and composition of particles can be controlled. In fact recently Japanese workers¹⁰⁰ have prepared magnetic fluids by evaporating ferromagnetic elements and alloys into an alkyl naphthalene carrier containing a surfactant.

In the following sub-section electrodeposition of

metals into liquid mercury is discussed. For gadolinium this proved difficult; however adaptation of the evaporation technique has allowed gadolinium to be evaporated into mercury in an argon atmosphere to produce gadolinium particles with 8-75nm diameters.¹⁰¹

Evaporation of metals into gases other than an inert gas can produce compound particles. For example iron being evaporated into ammonia has produced iron nitride particles.¹⁰²

Ultrafine iron particles in the 5-20nm size range have been prepared by decomposing iron pentacarbonyl in the vapour phase in a stream of heated helium.¹⁰³

2.2.2 Electrodeposition-Liquid Metal Based Systems

Systems with fine metal particles dispersed in liquid mercury are usually classified as magnetic fluids. Strictly this is untrue as these systems are not colloidally stable and have no means of protection against Van der Waals forces. However they are of great interest for energy conversion systems because of their superior thermal conductivity. This sub-section deals briefly with their preparation using an electrodeposition technique.

Basically this technique involves the electrodeposition of metals from aqueous or alcoholic solutions of salts of the ferromagnetic metals with the metallic liquid carrier (mercury) forming the cathode in the electrolytic cell.

Originally this type of work was aimed toward producing fine particle magnets rather than metal based "ferrofluids". Both elongated¹⁰⁴ and spherical¹⁰⁵ iron particles have been

prepared in this way. The authors being interested in magnetic properties rather than producing a stable suspension. In fact the systems were heat treated to deliberately cause particle growth to maximize coercivity. Similar work followed,¹⁶ producing cobalt and iron-cobalt particles and finally nickel-cobalt particles.¹⁰⁶

Iron-nickel alloy particle metallic based "ferrofluids" would be particularly useful for a potential heat exchange system. This is because their Curie temperature could be made to coincide with an operating temperature of 100-200°C by tailoring the alloy composition. A nickel content of ~ 25% would be required.¹⁰⁷

In work directed towards producing metal based "ferrofluids" preparation of small single domain particles is aided by agitation of the liquid mercury cathode during electrodeposition. This reduces dendritic growth of the particles. Agitation is achieved both mechanically and magnetically.

Nickel-iron particles have been prepared by simultaneous electrodeposition of ferrous and nickel ammonium sulphates.^{107,108} The alloy composition being determined by the $Fe^{2+}:Ni^{2+}$ ratio in the electrolyte. Electroprobe analysis of clusters implies true alloy formation. In these systems particle growth is an exceedingly restrictive problem. Coating the particles with tin was observed to reduce this growth.¹⁰⁸

In later studies¹⁰⁹ of this effect iron particles and

tin-coated iron particles were prepared by electrodeposition of ferrous ammonium citrate into mercury and tin-mercury amalgam cathodes respectively. Particle sizes of 2-4nm were obtained from the magnetization curves. The particles were "aged" by heating and the growth of the particles followed by the variation of coercivity with time. A tin coating did appear to reduce short term growth, possibly by reducing diffusion of atoms between particles. This tin coating although effective in slowing short term growth does not protect against clustering due to Van der Waals forces. Introduction of sodium into the freshly prepared system¹¹⁰ helps prevent longer term growth possibly due to some charge transfer mechanism on the particle/liquid surface.

2.2.3 Preparation of Fine Metal Particles by Chemical Reduction

Chemical reduction of ferromagnetic metal salts in aqueous solution has been used to prepare single domain metal and alloy particles. Oppegard et al.¹¹¹ prepared iron, iron-cobalt and nickel-iron particles by borohydride reduction. Recently small acicular particles of cobalt have been obtained by hypophosphite reduction of cobalt chloride between the poles of a magnet.¹¹² The method does not merit further discussion as the product can hardly be described as magnetic fluid.

2.2.4 The Organometallic Route

Preparation of truly colloidal suspensions of

ferromagnetic particles in non-metallic carrier liquids dates back to the mid-1960's. The method involves the decomposition of organometallic compounds of the ferromagnetic elements in the presence of surfactants or stabilizing polymers. Decomposition is usually thermal but UV radiation has also been used. Organometallic compounds employed are almost exclusively metal carbonyls of the ferromagnetic transition metals. Metal carbonyls are ideal as the carbon monoxide is displaced during thermolysis leaving metal in the inert medium. Electron microscopy shows that particles produced via this route usually have narrow size distributions. Work on cobalt has dominated this area with less reported on iron and nickel. As most of the original work in this thesis is concerned with the use and extension of this route, the next chapter is devoted to the chemistry of the type of organometallic compounds used and the mechanism of the decomposition process and particle formation. Hydrocarbon based metal particle fluid preparations are now discussed according to the metal used.

(i) Cobalt Magnetic Fluids

Cobalt magnetic fluids are easily prepared by decomposing dicobalt octacarbonyl. Polymer stabilized colloidal suspensions of cobalt metal are readily prepared.¹¹³⁻¹¹⁶ The experimental procedure is usually fairly simple and involves charging an appropriate vessel with the cobalt carbonyl and carrier liquid solution of polymer and bringing it to a rapid reflux with stirring. Heating is normally

continued until carbon monoxide evolution has ceased.

Variation of the polymer composition, average molecular weight and carrier liquid is observed to produce 1-100nm particles. Addition and condensation polymers with an average molecular weight of $\sim 100,000$ have proved most successful. Polymers with a non-polar backbone, non-reactive polar groups attached to alternate carbon atoms and very polar groups at wider intervals of about 200 backbone carbon atoms are especially useful. An increase in the concentration of polar groups is generally observed to produce smaller particles. Table 2.1 gives examples of polymers used.

Cobalt particles produced are observed to be largely in the high temperature fcc phase¹¹⁴ and not the usual bulk hcp phase. This is in agreement with results from the evaporation technique discussed earlier in this section.⁹⁵ When no polymer is used large (100nm) polydomain particles are obtained.

Carrier liquids used in conjunction with these polymers include aliphatic hydrocarbons, aromatic hydrocarbons such as toluene and xylene, halogenated aromatics such as chlorobenzene and p-dichlorobenzene and ethers. The carrier liquid acts as an inert medium for the thermolysis.

¹¹⁷ Smith demonstrated that hydroformylation reactions can be catalysed by colloidal cobalt dispersions prepared by the polymer catalysed thermal decomposition of dicobalt octacarbonyl. Using the same dispersions he also prepared

TABLE 2.1

Examples of polymeric surfactants used in ferrofluids

Metal	Polymer	Composition	Molecular Weight	Carrier Liquid	\bar{d}_p (nm)	Ref.
Co	Methyl methacrylate-ethyl acrylate-vinyl pyrrolidine	33:66:1	300,000	chloro-benzene	15-40	113
Co	Vinyl acetate-vinyl pyrrolidine	56:1	20,000	Toluene	2-15	116
Fe	Butadiene-styrene	5.8:1		Xylene	~6	122
Fe	4-vinylpyridine-styrene	0.10:1		o-dichloro-benzene	~16	122

\bar{d}_p = Physical Particle Diameter

bead supported cobalt catalysts in which polymer beads are formed which contain 2% of finely divided cobalt metal. Analogous work has been carried out by the same author on iron systems.¹¹⁸

More recently cobalt magnetic fluids have been prepared using surfactants rather than polymers. After their initial preparation¹¹⁸ the authors were largely concerned with investigating the effect of various experimental parameters¹²⁰ such as temperature, concentration and nature of surfactant and choice of carrier liquid. Finally they go on to discuss a possible mechanism for nucleation and growth of the cobalt particles.¹²¹ The surfactant di(ethyl-2-hexyl) sodium sulfosuccinate (Manoxol-OT) proved to be very successful and became standard in their work. Results of these experiments will be drawn upon in the next chapter.

(ii) Iron Magnetic Fluids

The polymer catalysed thermal decomposition of iron pentacarbonyl in a variety of solvents has been investigated.^{122,118} Work concerning the structure, magnetic properties and oxidation of the iron particles produced in this way has also been carried out.¹²³ Carrier liquids used were decalin, xylene, chloroform and o-dichlorobenzene. Examples of polymers are given in Table 2.1. Particle sizes of 1.5-20nm were recorded using electron microscopy. The structure of the particles is reported to depend on their size. Very small (< 6 nm) particles appeared to have a disordered structure initially and then "recrystallize" to

α -iron over a period of one year when stored under argon. Larger (16nm) particles appear to be α -iron with a disordered core. In dry air the particles suffer oxidation.

For the 16nm particles this reaches an equilibrium at which an oxide of Fe_3O_4 and $\gamma\text{-Fe}_2\text{O}_3$ of 2.8nm thickness is formed. In moist air the same result is observed for hydrocarbon solvents. However in the chlorocarbon solvents, chloride ion is formed which stabilizes the formation of $\beta\text{-FeOOH}$ which seems to break up many of the original particles leading to the formation of agglomerates.

Metallic iron magnetic fluids have been prepared by the thermal decomposition of the diiron nonacarbonyl and triiron dodecacarbonyl in toluene in the presence of non-polymeric surfactants.¹²⁴ In these studies particles in the 6-7 nm size range were obtained which had the bcc structure of bulk iron.

(iii) Nickel Magnetic Fluids

Thermal decomposition of nickel carbonyl has been used to prepare nickel magnetic fluids. Particles of $\sim 20\text{nm}$ diameter were produced using polymer solutions in benzene.¹¹⁶ Whereas Smith¹²⁵ used an autoclave to thermally decompose nickel tetracarbonyl under pressure in a xylene/polymer solution. More recently nickel ferrofluids have been obtained by decomposition of nickel tetracarbonyl using UV radiation¹²⁶ in toluene solution in the presence of non-polymeric surfactants. $\text{Di-}\eta^5\text{-cyclopentadienylnickel}$ has been reduced with hydrogen gas in refluxing toluene to

produce a nickel magnetic fluid.¹²⁶ Particles were observed to have a median diameter of 5nm and the bulk nickel fcc structure.

2.2.5 Spark Erosion

A rather novel method which in principle can be applied to preparing metal or alloy particle fluids is that of spark erosion.^{127,128} The process involves using a pair of electrodes of the desired material. These electrodes are immersed in a dielectric liquid such as an aliphatic hydrocarbon and adjusted until there is an electric discharge between the electrodes. This spark discharge produces highly localized superheated regions in the electrodes causing the ejection of both small molten droplets and vaporized material from at least one electrode. Particles are produced which become enmeshed in polymer produced from reaction of the dielectric on the hot particle surface or/and dielectric breakdown in the spark. The molten droplets produce a distribution of large particles in the 0.5 to 40 μ m range whereas colloidal sized particles in the 2.5-10nm range are produced from the vaporized material. Particles originating from electrodes of composition Fe₇₅Si₁₅B₁₀ have been produced. Magnetic recovery of the particles is followed by ultrasonic redispersion in a carrier such as kerosene. Although a promising method the fluids produced appear to lack colloidal stability.

CHAPTER 3

ORGANOMETALLIC STARTING MATERIALS AND THE DECOMPOSITION PROCESS

Introduction

The results reported in this work are concerned with the preparation and characterization of hydrocarbon-based metal particle magnetic fluids. The work to be described involved the use of selected organometallic compounds of the ferromagnetic transition elements cobalt, iron, nickel and some combinations thereof. More specifically ferrofluid preparation involved the controlled thermal decomposition of selected metal carbonyl compounds and related cyclopentadienyl derivatives. The preparations of complexes used are given in the relevant chapters. Although the simple carbonyl and cyclopentadienyl compounds are well known to the chemist, in this thesis on magnetic fluids a short section on these important compounds is included for completeness.

Details of the process by which metal particles are formed by the decomposition of metal carbonyls in hydrocarbon solutions of surfactants (including polymers) are not well documented in the literature. Most of the work on magnetic fluids to date has concentrated primarily on the physical properties and applications of magnetic fluids and

secondly on their preparation (as the work described herein). Despite this, there has been some excellent work carried out concerning the mechanism of the decomposition process; this is described in the second section of this chapter.

3.1 Transition Metal Complexes with Carbonyl and/or Cyclopentadienyl Ligands

3.1.1 Bonding and Structure

Carbon monoxide is an important π -acceptor ligand.¹²⁹ Bonding in metal carbonyl complexes is via (i) σ bonding arising from lone-pair donation from the carbon atom of the carbon monoxide ligand and (ii) through a type of π bonding associated with donation of electron density from full metal orbitals into vacant antibonding (π^*) orbitals of the carbon monoxide molecule.¹³⁰ In complexes between the d-group transition metals and neutral molecules such as carbon monoxide, the metals are in a low positive, zero or negative formal oxidation state. It is the ability of π -acceptor ligands (such as carbon monoxide) to delocalize the high electron density on the metal atom which stabilizes the low formal oxidation states associated with these complexes.

In the nickel and/or iron cyclopentadienyl containing complexes employed in this work, the cyclopentadienyl ligands are pentahapto ($\eta^5\text{-C}_5\text{H}_5$), ie. the ring is essentially covalently bonded to the metal through five carbon atoms, the metal being equidistant from the carbon

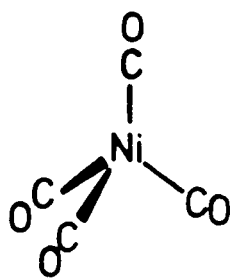
atoms (conveniently written as $\pi\text{-C}_5\text{H}_5$). In complexes containing both carbonyl and cyclopentadienyl groups the carbonyl and cyclopentadienyl groups are effectively trans to each other,¹³¹ resulting in a strengthening of the metal-CO bonding since $\pi\text{-C}_5\text{H}_5$ is a better donor and weaker acceptor of electron density than carbon monoxide.

The empirical 18-electron rule can be applied successfully to many (not all) of these types of complexes.¹²⁹ The rule is based on the tendency of the metal atom to use its valence orbitals as fully as possible in bonding to ligands.

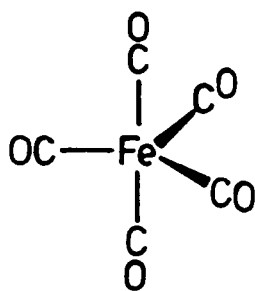
The simple mononuclear carbonyls $\text{Ni}(\text{CO})_4$ and $\text{Fe}(\text{CO})_5$ have tetrahedral and trigonal bipyramidal structures respectively¹³⁰ (Figure 3.1(a) and (b)), and contain only linear M-CO units. The polynuclear carbonyls e.g. $\text{Co}_2(\text{CO})_8$, $\text{Fe}_2(\text{CO})_9$ and $\text{Fe}_3(\text{CO})_{12}$ contain both carbon monoxide ligands which are bonded terminally and carbon monoxide ligands which bond to two (edge) or three (face) metal atoms.¹³² In solutions of dicobalt octacarbonyl an equilibrium is believed to exist between the solid state isomeric form containing bridging carbon monoxide ligands (Figure 3.1(c)) and at least two isomeric forms without bridging carbon monoxide groups¹³² (Figure 3.1(d)).

In $(\pi\text{-C}_5\text{H}_5)_2\text{Ni}$ the two rings are positioned above and below the metal atom, the rings are staggered (Figure 3.1(g)) in the solid state, but rotate freely in solution.¹³³

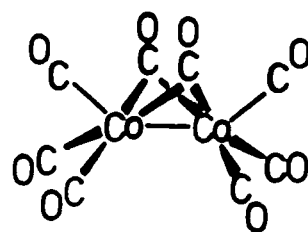
Figure 3.1 gives the structures of examples of mono-



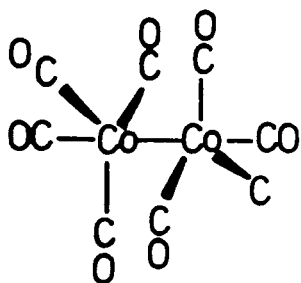
(a)



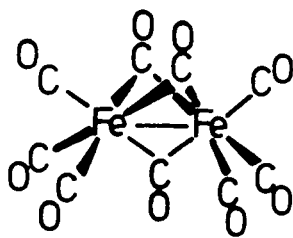
(b)



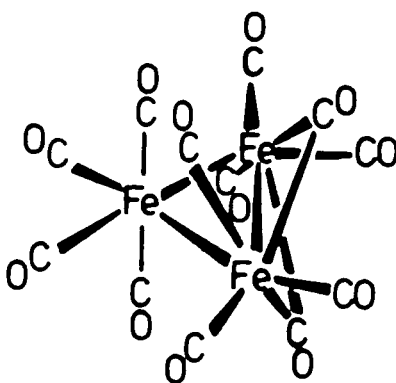
(c)



(d)



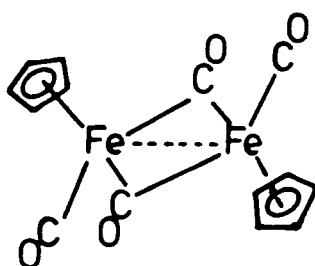
(e)



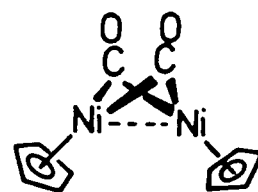
(f)



(g)



(h)



(i)

Fig. 3.1

Some structures of simple metal complexes with carbon monoxide and/or cyclopentadienyl ligands.

and polycarbonyls, cyclopentadienyl and cyclopentadienyl carbonyl containing complexes.

3.1.2 Preparation

Carbon monoxide reacts readily with nickel at room temperature and atmospheric pressure to form $\text{Ni}(\text{CO})_4$.¹³⁴ Although $\text{Fe}(\text{CO})_5$ can also be prepared by direct combination of finely divided iron and carbon monoxide, higher yields are obtained by using elevated temperatures and pressures.¹³⁴ In all other cases metal carbonyls must be prepared from metal compounds under reductive conditions (unless they are prepared from either $\text{Ni}(\text{CO})_4$ or $\text{Fe}(\text{CO})_5$). Carbon monoxide is often the reducing agent, sometimes used in conjunction with hydrogen; these reactions are called reductive carbonylations.¹³⁰ For example, dicobalt octacarbonyl is prepared by reducing cobalt (II) acetate with carbon monoxide (160 atmospheres) and hydrogen (40 atmospheres) at 160-180°C.¹³⁵

Compounds of the type $(\pi\text{-C}_5\text{H}_5)_2\text{M}$ are prepared by two general methods.¹³¹ The first is by reaction of an alkali metal cyclopentadienide with a metal halide, e.g. $\text{Na}^+\text{C}_5\text{H}_5^-$ and NiCl_2 in refluxing T.H.F. The second is by direct reaction of cyclopentadiene with a metal halide in the presence of a base to eliminate the methylene hydrogen from cyclopentadiene.

The simple cyclopentadienyl carbonyl compounds used in this work, i.e. $[\pi\text{-C}_5\text{H}_5\text{Fe}(\text{CO})_2]_2$ and $[\pi\text{-C}_5\text{H}_5\text{Ni}(\text{CO})]_2$, are prepared by direct reaction of $\text{Fe}(\text{CO})_5$ with

dicyclopentadiene $C_{10}H_{12}$, and combination of $Ni(CO)_4$ and $(\pi-C_5H_5)_2 Ni$ respectively.¹³⁵

3.2 Metal Particle Formation by the Thermal Decomposition of Metal Carbonyls in the Presence of Surfactants in Hydrocarbon Solution

Metal carbonyl complexes are ideal starting materials from which to produce metal by thermal decomposition. The metals are usually in a zero formal oxidation state, hence reduction/oxidation is not necessary in a decomposition to yield metal. Indeed, thermal decomposition of $Ni(CO)_4$ to produce highly pure nickel forms the basis of the Mond process.¹³⁴ Triiron dodecacarbonyl is thought to produce pyrophoric finely divided iron when allowed to decompose in the atmosphere at room temperature.¹³⁶

At the elevated temperatures used in the preparation of ferrofluids by the thermal decomposition of carbonyl complexes, the M-CO bonds are readily broken with the liberation of carbon monoxide. The liberated gaseous carbon monoxide is conveniently lost from the system and therefore cannot recombine with metal to produce carbonyl complexes.

The thermal decomposition of metal carbonyls in hydrocarbon solutions containing surfactant molecules (including polymers) is a rather complex process. In this section, work carried out to determine the mechanism by which discrete metal particles are formed in colloidal suspension is described.

3.2.1 Mechanism of Iron Pentacarbonyl Thermal Decomposition in the Presence of Polymeric Surfactants

The work reported in this sub-section is taken from a paper written by Smith and Wychick.¹²² The authors report the thermal decomposition of $\text{Fe}(\text{CO})_5$ in both dilute hydrocarbon solutions of functional polymers and "inert" solvent media, e.g. decalin. The polymers used were termed "active" or "passive". In the former case "active" polymers contained nucleophilic residues on the polymer backbone which can react directly with $\text{Fe}(\text{CO})_5$, for example pyridine groups in a copolymer formed from 4-vinylpyridine and styrene. In the latter case "passive" polymers containing alkene functionalities can only react with intermediates such as $[\text{Fe}(\text{CO})_4]$, for example copoly(butadiene-styrene). Decompositions were carried out at temperatures typically between 130 and 160°C. Decomposition was followed using Infra-red spectroscopy, transmission electron microscopy and kinetic studies which involved monitoring the rate of carbon monoxide evolution.

When an "active" polymer is used the nucleophilic groups on the polymer backbone react directly with $\text{Fe}(\text{CO})_5$ causing disproportionation and the formation of ligand substituted metal cluster complexes, which are attached to the polymer, this attachment is referred to as being "in the polymeric domain". These clusters are postulated to be more thermally labile than $\text{Fe}(\text{CO})_5$ and decompose to polynuclear

intermediate metal clusters (still in the polymeric domain).

When sufficient metal is present in the polymer domain, particle nucleation occurs. Once nucleation has occurred, the reaction is believed to continue by the decomposition of iron carbonyl species on the growing particle surfaces. This growth phase coincides with the appearance of particles (electron microscopy) and zero order carbon monoxide evolution. The zero order evolution of carbon monoxide is explained by the heterogeneous decomposition of iron carbonyl species on the particle surfaces. The reaction rate is limited by carbon monoxide adsorbed onto the particle surface which must desorb before more iron carbonyl species can adsorb and react at the site.

The "passive" polymers used cannot react directly with $\text{Fe}(\text{CO})_5$. Instead decomposition occurs by an uncatalysed loss of carbon monoxide to produce reactive intermediates such as $[\text{Fe}(\text{CO})_4]$ (in the formation of these intermediates the decomposition is analogous to the decomposition of $\text{Fe}(\text{CO})_5$ in an inert solvent). These reactive intermediates can then react with alkenyl groups in the polymer backbone and form complexes, these complexes isomerize to produce butadienyl-iron tricarbonyl residues in the polymer (detected by IR spectroscopy). Particles are then believed to nucleate from these residues and zero order evolution of carbon monoxide follows, as with the "active" polymers, which is thought to correspond to the decomposition of $\text{Fe}(\text{CO})_5$ on the particle surfaces.

In the absence of polymer, the thermal decomposition of $\text{Fe}(\text{CO})_5$ in an inert hydrocarbon medium proceeds slowly, an equilibrium between $\text{Fe}(\text{CO})_5$ and $\text{Fe}_2(\text{CO})_9$ is attained with further decomposition occurring very slowly.

The process by which metal particles are formed by the "catalytic" decomposition of $\text{Fe}(\text{CO})_5$ by functional polymers is referred to as a "locus control mechanism".

3.2.2 Mechanism of Dicobalt Octacarbonyl Thermal

Decomposition in a Toluene Solution of Surfactant

The work described in this sub-section concerning the thermal decomposition of dicobalt octacarbonyl in toluene solutions of the surfactant Manoxol-OT was carried out by French research workers.^{120,121} In the first of these papers Papirer et al.¹²⁰ studied in detail the experimental conditions necessary to produce stable cobalt ferrofluids. One of their observations was that the percentage of carbon monoxide (% CO) evolved plotted as a function of time always produced the same general shape of "decomposition curve". Figure 3.2 shows a typical decomposition curve taken from this first paper. In all cases ~ 25% of total CO evolution occurred rapidly during the first few minutes of decomposition (A), this corresponds to the formation of $\text{Co}_4(\text{CO})_{12}$ (detected by IR spectroscopy). This initial rapid evolution is observed to slow down and CO evolution becomes linear with respect to time (B). This is followed by an acceleration of CO evolution to a different linear dependence on time (C). Finally the rate decreases as the

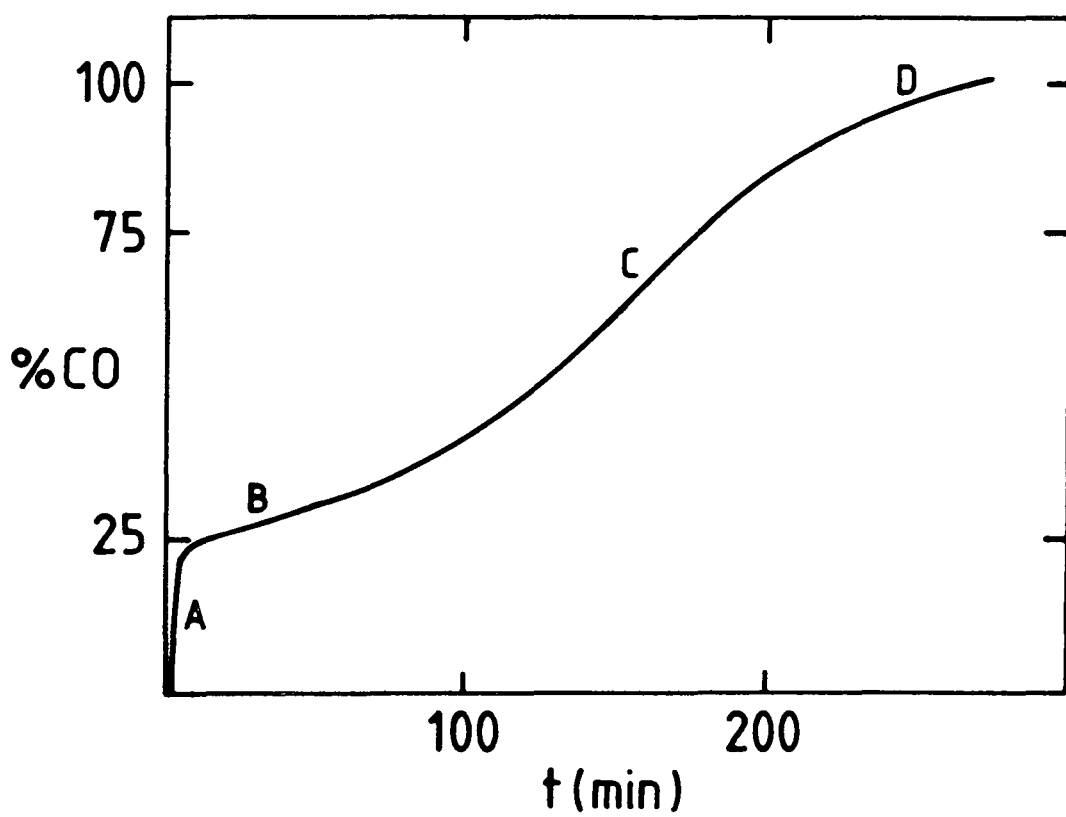


Fig. 3.2

Carbon monoxide evolution as a function of time for the decomposition of $\text{Co}_2(\text{CO})_8$ in a toluene solution of the surfactant Manoxol-OT¹²⁰.

reagents became exhausted (D). In the same investigation the authors also noted that the particles produced had very narrow size distributions.

In the second paper, Papirer et al.¹²¹ attempt to explain these observations. In the study described, the decomposition reactions were quenched at known times corresponding to known extents of decomposition. Samples of the quenched reaction mixtures were analysed by small angle X-ray scattering (SAXS), transmission electron microscopy, IR spectroscopy and vibrating sample magnetometry (magnetic measurements).

By using SAXS the authors deduced that $\text{Co}_2(\text{CO})_8$ (before heating) and $\text{Co}_4(\text{CO})_{12}$ (after heating) are concentrated into large cluster/aggregates (5nm radii of gyration) which were termed "microreactors". This phenomenon was not observed for $\text{Co}_2(\text{CO})_8$ and $\text{Co}_4(\text{CO})_{12}$ in toluene in the absence of surfactant under the same conditions. Papirer et al. explained the observed enhancement of the decomposition rate in the presence of the surfactant to be a consequence of the increased concentration of $\text{Co}_2(\text{CO})_8$ in these "microreactors".

The decomposition process was first studied at 130°C (oil bath temperature). At this temperature they observed (i) particle growth to be most important during the 40-80% CO evolution stage, (ii) that the concentration of particles remained approximately constant throughout the decomposition and (iii) that the microreactors disappear during the 40-80%

decomposition period.

A second study was carried out at 120°C in order to observe the changes occurring more distinctly. During the first linear section of the decomposition curve (~ 31% decomposition) they observed that the large "microreactors" were still present but that no isolated particles had formed. At about 40% decomposition the large aggregates start disappearing and very small particles were observed for the first time.

Using IR spectroscopy the authors detected the presence of the complex $\text{Co}_4(\text{CO})_9\text{C}_6\text{H}_5\text{CH}_3$ after 25% decomposition (as well as $\text{Co}_4(\text{CO})_{12}$). The concentration of this complex relative to $\text{Co}_4(\text{CO})_{12}$ increases to a maximum at about 40% decomposition. The authors postulate that by ~ 40% decomposition particle nucleation has occurred in the microreactors via a series of complex and unobserved intermediates. Once nucleation has occurred the particles grow on these nucleation sites only (i.e. a constant concentration of growing particles). During the 40-50% decomposition stage, the microreactors are observed to begin disappearing, this being explained by the dissolution of $\text{Co}_4(\text{CO})_{12}$ to form $\text{Co}_4(\text{CO})_9\text{C}_6\text{H}_5\text{CH}_3$, which accumulates in solution. Simultaneously, it is thought that there is only a small degree of decomposition in the microreactors as the particle size does not increase significantly over this crucial stage.

After the 40-50% period the particles suddenly and

inexplicably begin to grow rapidly with the simultaneous disappearance of the microreactors. This coincides with the second linear portion of the decomposition curve (C) which is explained by the decomposition of cobalt carbonyl species on the surfaces of the growing particles (cf growth of iron particles in section 3.2.1). The rate of this heterogeneous stage is limited by the desorption of carbon monoxide from the particle surface which is a zero order process and consequently CO evolution is linear with respect to time. The final "tailing off" of the decomposition curve (D) is simply due to the depletion of carbonyl species from solution and the loss of CO remaining on the particle surfaces.

The narrow size distributions observed were attributed to the constant number of growing particles in the decomposition medium. This growth is thought to be further regulated by a diffusion process which causes a narrowing of any size distribution produced.

From the work described in this section it is obvious that the thermal decomposition processes occurring during the preparation of ferrofluids from simple metal carbonyls are extremely complex, and are not fully understood. The work described in this thesis involves the decomposition of more complicated molecules, with possibly even more complicated decomposition pathways, which can only be speculated upon.

CHAPTER 4

GENERAL EXPERIMENTAL TECHNIQUES AND INSTRUMENTATION

4.1 General Experimental Techniques

4.1.1 General Handling Techniques

The organometallic compounds employed in this study were assumed to be air and moisture sensitive. All manipulations were consequently performed under an atmosphere of dry nitrogen in 2-necked flasks and Schlenk tubes. Dry degassed solvents and solutions were transferred by syringe against a counter current of dry nitrogen, septum caps being used when appropriate. Air sensitive solids were handled in a glove box.

Positive pressure breathing apparatus were worn when handling materials of extreme toxicity such as nickel tetracarbonyl.

4.1.2 Nitrogen Supply

Nitrogen was supplied to the laboratory as the boil off from a tank containing liquid nitrogen. The gas was passed through a de-oxygenating plant and dried at the bench by passage through columns packed with phosphorus pentoxide and molecular sieve. Nitrogen flow was regulated by use of an oil bubbler.

4.1.3 Glove Box

Solid compounds were handled in a glove box. A dry

nitrogen atmosphere was maintained by continuous recycling through columns packed with phosphorus pentoxide and molecular sieve. A dish of exposed phosphorus pentoxide was kept in the box to further minimize the moisture content of the box atmosphere.

4.1.4 Solvents

Hydrocarbon solvents were normally dried and stored over freshly extruded sodium wire. Toluene in particular was dried by refluxing with sodium metal in the presence of benzophenone. Ethanol was dried by refluxing with magnesium and distilling onto molecular sieve for storage.

Solvents were de-oxygenated prior to use by repeated freezing and thawing under vacuum.

4.1.5 Starting Materials

(i) Organometallics

All organometallic materials synthesized and employed in this work were prepared from the simple metal carbonyls (and di- η^5 -cyclopentadienylnickel(II)) which were used as supplied by the manufacturer.

(ii) Surfactants

The surfactants used in this work were commercial products and are referred to by their trade-names for convenience. Table 4.1 gives the chemical formulae and suppliers of surfactants used throughout this work. The formulae of I.C.I. Solsperse reagents used in this work have been withheld.

TABLE 4.1

Surfactants used in this work

Trade-name	Supplier	Formula
Sarkosyl-O	Ciba-Geigy	$R_1 \overset{\overset{O}{\parallel}}{C}N(CH_3)CH_2COOH$
Manoxol-OT	B.D.H.	$Na^+ SO_3^- \overset{\overset{CH_2COOR_2}{ }}{C}HCOOR_2$
Duomeen-TDO	Akzo Chemie	$(R_3NH_2^+ (CH_2)_3NH_3^+) (C_{17}H_{33}COO^-)_2$
Duomeen-T	Akzo Chemie	$R_3NH(CH_2)_3NH_2$

R_1 is $CH_3(CH_2)_7CH = CH(CH_2)_7$

R_2 is $CH_2-\overset{\overset{C_2H_5}{|}}{C}H-C_4H_9$

R_3 is a mixture of saturated and unsaturated alkyl chains with average chain distribution: $C_{12}, 1$; $C_{14}, 3$; $C_{16}, 27$; $C_{18}, 24$;

$C_{14}^=, 1$; $C_{16}^=, 4$; $C_{18}^=, 39$; $C_{18}^{\prime=}, 1\%$.

Where = represents one degree of unsaturation.

4.1.6 Infra-red Spectroscopy

Infra-red spectra in the range 4000 cm^{-1} to 250 cm^{-1} were recorded on Perkin-Elmer 457, 577 and 580 grating spectrometers. Spectra recorded on the PE 580 could be stored on disc and manipulated using a data station. Samples were mounted as nujol mulls between KBr plates. Liquid samples (generally solutions) were syringed into a solution cell with KBr windows and employing spacers of 0.05mm or 0.1mm thickness.

4.1.7. Analytical Methods

Carbon, hydrogen and nitrogen were determined using a Perkin-Elmer 240 elemental analyser. Metals were determined using a Perkin-Elmer 403 atomic absorption spectrometer.

4.2 Instrumentation

This section outlines the use and purpose of the "specialist" techniques employed in this project.

4.2.1 Electron Microscopy

Transmission electron microscopy was used routinely to examine products and determine the physical particle size distribution. Shadow electron micrographs were taken using a Philips EM400T electron microscope. Magnifications of 100,000 and 220,000 and a column voltage of 80 or 100kV proved by experience to be normally most successful in yielding prints suitable for analysis.

Samples were prepared by diluting the normally black product with a solution of surfactant in the carrier liquid.

A drop of the diluted product is then placed on a 3.05 mm copper grid coated with either a carbon or carbon/formvar film.

Calibration at these magnifications was achieved using catalase crystals mounted on a 3.05 mm copper grid (supplied by Agar Aids). These crystals have lattice spacings of 8.75 nm and 6.85 nm which appear as a series of parallel lines. Since these lines are of known spacings they can be used to calibrate the microscope. Taking into account the results obtained from this type of calibration and the fact that particle images are not always sharp, the precision of the measurements is taken to be of the order of $\pm 10\%$.

4.2.2 Electron Diffraction

X-ray powder diffraction was found to be an unsuitable method to determine the structure of the ultrafine particles produced in this study. The particles produced are in the 5-10nm range and are small enough to cause severe line broadening in the diffraction pattern. Further problems arise due to the low concentration of the samples.

The wavelength of electrons commonly used in electron diffraction is one to two orders of magnitude smaller than the X-ray wavelengths used in X-ray diffraction. Although difficult, electron diffraction patterns can be obtained for fluid samples. Analysis of these patterns gives important information concerning particle structures.

Transmission electron diffraction was performed using a Philips EM400T and a JOEL JEM 120 electron microscope. Samples were mounted on grids as for shadow electron microscopy. An aluminium grid (supplied by Agar Aids) was used to calibrate the microscope each time. This grid gives a well defined face centred cubic diffraction pattern. About 6 rings corresponding to known d-spacings are used to calibrate the microscope for a particular camera length and accelerating voltage.

Electron diffraction patterns for the iron-cobalt and nickel-iron systems discussed in chapters 6 and 7 respectively were obtained by Dr. G.J. Russell of the Department of Applied Physics using the JOEL JEM 120 instrument. These results are also reported by Lambrick who indexed the patterns.

4.2.3 EDX

Energy dispersive analysis of X-rays is performed using the electron microscope. Samples are mounted on grids as usual. X-rays are emitted from the sample (particles) as atoms excited by the microscope beam return to lower energy levels. A detector close to the sample receives the whole spectrum of X-ray energy. The energy of X-rays emitted by a sample are characteristic of the element concerned. Analysis of these X-ray energies gives the elemental composition of the sample. On a high resolution microscope small groups of particles (local area) or even individual particles can be examined to determine their atomic

composition. Unfortunately use of this powerful technique was very restricted.

4.2.4 The Automated Electro-optic Image Size Analyser (Particle Size Analysis)

An automated electro-optic image size analyser is used to obtain particle size distributions from electron micrographs. Electron micrograph negatives are enlarged ($\sim 3 \times$) and printed onto Kodak (P.84) lightweight projection paper. Prints are positioned on a working surface over a light spot projected from below whose diameter is adjusted via an iris to coincide with the particles image. Once the image is matched a foot pedal is depressed causing the spot area to be automatically recorded onto a disc. To avoid multiple image counting a pen automatically marks each particle image as it is counted. A more detailed description of this instrument is given by Hoon et al.¹³⁷

This instrument is interfaced with a BBC microcomputer which has programmes which (i) correct the raw data to particle diameters, (ii) bin the data, (iii) statistically analyse the data giving the mean diameter and standard deviation of the distribution, and (iv) produce a histogram which can be printed out. Normally at least 500 particle images are counted to ensure good statistics. These histograms give the physical particle size distribution of the magnetic fluids. The distribution standard deviation is an indication of the range of particle sizes.

4.2.5 The Vibrating Sample Magnetometer

A vibrating sample magnetometer (VSM) is used to obtain the magnetization curve of a magnetic fluid. A schematic diagram of the VSM is given in Figure 4.1. Magnetic fluid is weighed into a small glass bulb and is positioned between the poles of a variable electromagnet. The sample is vibrated in a direction perpendicular to the applied field thus inducing an e.m.f. in the detection coils on the magnetic pole pieces. As the sample vibrates the applied magnetic field is varied from zero to a maximum value of 1.2 Tesla in discrete stages of ~ 0.01 Tesla. The field is then reduced in discrete stages back through zero to a negative field of magnitude 1.2 Tesla. Vibration of the sample in the magnetic field induces an A.C. voltage in the detection coils, simultaneously a cobalt permanent magnet used as a reference sample is positioned so it vibrates between a pair of reference coils inducing a voltage (A.C.). Both coil outputs are fed into a phase sensitive detector, which essentially improves the signal to noise ratio of the sample voltage. The output is a D.C. voltage, proportional to the magnetic moment of the sample. Calibration of the VSM with a nickel standard gives the magnetic moment of the sample.

The magnetization curves obtained consist of a plot of σ_{ff} (the magnetization per unit mass of sample) in $\text{JT}^{-1}\text{Kg}^{-1}$ against B_0 (the inductance field) in Teslas.

As a fluid sample approaches saturation the

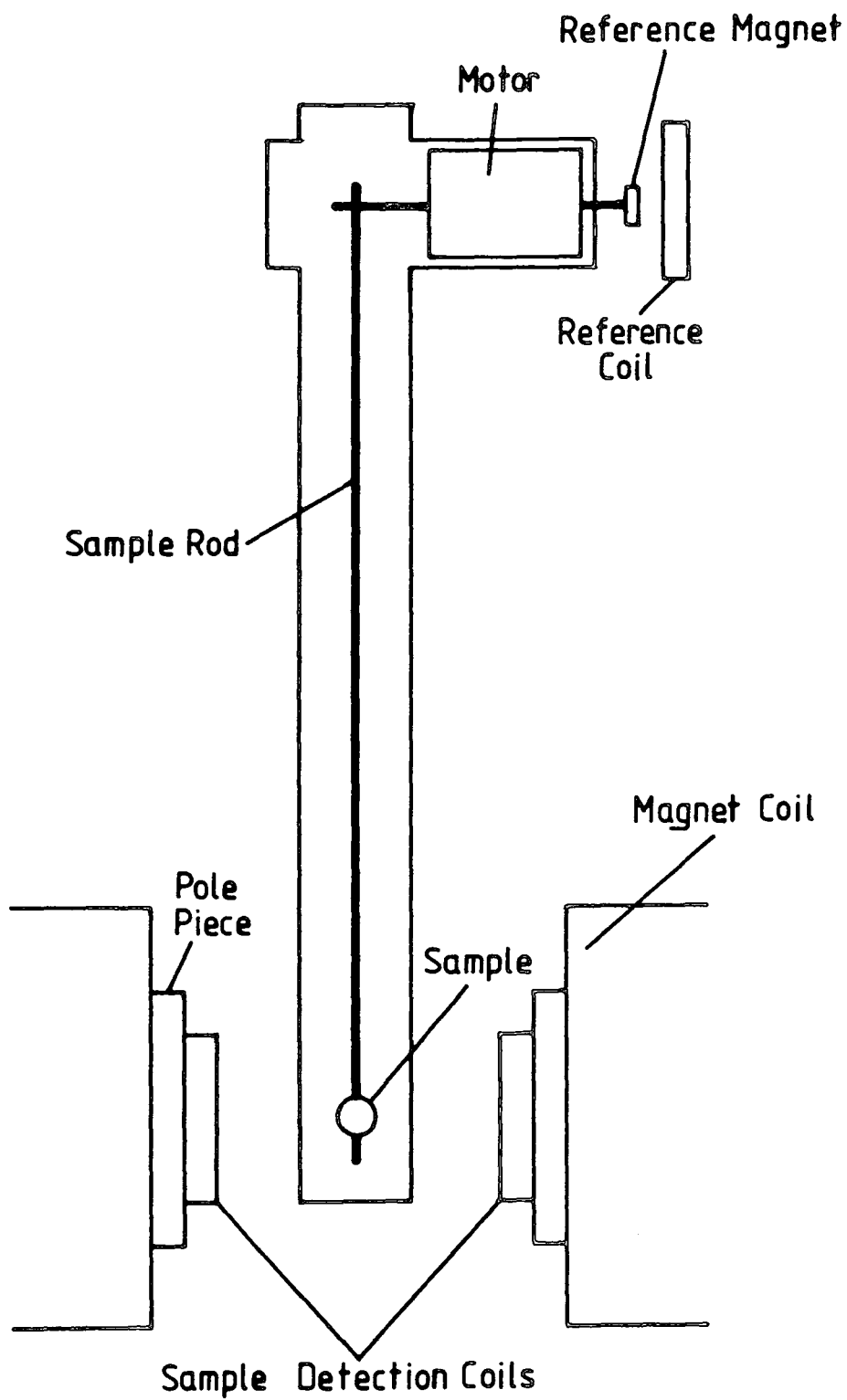


Fig. 4.1 The essential components of the vibrating sample magnetometer.

magnetization is observed to asymptotically approach the saturation magnetization. This indicates the quantity of magnetic material in the sample. Magnetic particle size distributions can be derived from these curves as illustrated in section 1.6.5. The room temperature magnetization curves described in this work were kindly recorded by D.B. Lambrick of the Physics Department. Lambrick reports the full magnetic analysis of the iron-cobalt (chapter 6) and nickel-iron (chapter 7) systems prepared by the author in his thesis.

4.2.6. EXAFS Spectroscopy

Extended X-ray Absorption Fine Structure spectroscopy is based on X-ray absorption spectroscopy. As X-rays impinge on the sample photoionization results. Back scattering of the ejected photoelectron results in a modification of the photoionization cross section. EXAFS are the oscillations superimposed on the absorption coefficient as a result of these back scatterings. The EXAFS effect is dependent on (i) the number of coordinating atoms, (ii) their elemental identity, and (iii) their distances from the central atom. In principle, information on these properties can be extracted from EXAFS spectra.

The laboratory scale EXAFS spectrometer consists of a continuous X-ray source, a monochromater and detectors to measure the incident and transmitted X-ray intensities. A computer system controls the movement of the various spectrometer components as well as storing and manipulating

data.

To record spectra neat fluid is syringed into a small brass cell with mylar windows. The cell is positioned between the monochromater and detector. Scanning in X-ray energy (wavelength) through the absorption edge of the relevant element produces the EXAFS spectra.

EXAFS spectra recorded show the spectrum of X-rays incident on the sample $N_0(E)$ and the spectrum of X-rays transmitted through the sample $N(E)$. $N_0(E)$ and $N(E)$ are ratioid to give the total X-ray absorption coefficient $\mu(E)$ as a function of the X-ray energy.

$$\mu(E).t = \ln\left(\frac{N_0(E)}{N(E)}\right) \quad (4.1)$$

At the time of these studies the relevant computer programmes necessary to fully analyse this data to obtain information on atomic spacings and the number of coordinating atoms were not available. Hence spectra obtained can only be treated qualitatively.

CHAPTER 5

SOME STUDIES OF COBALT MAGNETIC FLUIDS

Introduction

Hydrocarbon based cobalt magnetic fluids are readily prepared by the thermal decomposition of dicobalt octacarbonyl (the carbonyl route).^{113-117,119-121} Details of particle size, particle structure and magnetic properties have been reported in the literature. In this chapter cobalt magnetic fluids prepared by the conventional "carbonyl" method are compared with a fluid prepared by the novel method of cobalt metal evaporation. There is also a brief section concerned with the first study of magnetic fluids with EXAFS spectroscopy. The final section deals with an infra-red spectroscopic study of the cobalt ferrofluids prepared.

5.1 Comparison of Cobalt Magnetic Fluids Prepared by the Carbonyl Route and the Metal Atom Technique

5.1.1. Fluid Preparation

(i) Via Thermal Decomposition of Dicobalt Octacarbonyl

Cobalt magnetic fluids were prepared by thermally decomposing dicobalt octacarbonyl dissolved in a toluene solution of a surfactant. Decomposition was carried out in a 3-necked 100cm³ round bottomed flask fitted with a teflon paddle stirrer, reflux condenser and a tap. The reflux

condenser was connected to an oil bubbler to allow monitoring of carbon monoxide evolution. A typical preparation was as follows:

Dicobalt octacarbonyl (2.066g, 6.04mmol), weighed out in a glove box was transferred to the nitrogen purged flask against a nitrogen flow. A solution of the surfactant Sarkosyl-0 (0.7222g) in toluene (20.0cm³) was then syringed into the flask against a nitrogen flow to give a brown solution. The system was purged briefly with nitrogen and stirred at room temperature. Purging was ceased and a pre-heated oil bath at 145-150°C was used to heat the system. Heating caused rapid reflux with carbon monoxide evolution and darkening of the brown solution to black. Heating was continued until the evolution of carbon monoxide had ceased. The system was then allowed to cool to room temperature under a nitrogen atmosphere and the black liquid product was removed and stored under nitrogen. Table 5.1 summarizes the preparative details for cobalt fluids produced in this manner.

(ii) Using Metal Atom Techniques

A cobalt magnetic fluid was prepared by P.D. Hooker of Bristol University using a metal atom technique. A more detailed description of the preparation is given in his report.¹³⁸ The preparation involved the use of apparatus normally employed for the study of metal atom chemistry. Essentially the preparation involved the evaporation of cobalt metal (16.837g, 285.71mmol) into a toluene solution

TABLE 5.1

Preparation of cobalt fluids from $\text{Co}_2(\text{CO})_8$

Fluid	Mass of $\text{Co}_2(\text{CO})_8$ (g)	Surfactant	Mass of surfactant (g)	Vol. of Toluene (cm^3)	R = Mass $\text{Co}_2(\text{CO})_8$: surfactant	Oil Bath Temp. ($^\circ\text{C}$)
5.1	2.066	Sarkosyl-0	0.722	20.0	2.86	145-150
5.2	1.111	Manoxol-OT	0.533	13.0	2.08	145-150
5.3	0.999	Duomeen-TDO	0.464	12.0	2.15	145-150

(150cm³) of Manoxol-OT (6.782g, 15.27mmol). Evaporation of the cobalt metal was from an alumina crucible resistively heated to ~1600°C using 1.5mm Mo wire. The reaction vessel was a 10 litre flask rotated at 60 r.p.m. to maintain a thin film of the surfactant solution on the inside of the flask. A pressure of 10⁻³ - 10⁻⁴ Torr was maintained inside the flask during evaporation. To prevent the loss of excessive amounts of solvent the flask was cooled with a slush bath at - 115°C. Evaporation lasted for 80 minutes. The black magnetic product was filtered through powdered quartz under nitrogen to remove excess cobalt in the form of sedimented residue. Finally the product was stored under nitrogen.

5.1.2 Particle Size Analysis

The ferrofluids were examined using transmission electron microscopy and shadow electron micrographs were taken. Analysis of the printed micrographs gave the corresponding physical particle size distributions. A summary of this TEM data is given in Table 5.2. Figure 5.1 shows the individual distributions in histogram form, each distribution being derived from 500 particle images.

For both preparative methods electron microscopy revealed well dispersed roughly spherical particles. In all cases the distributions appeared approximately Gaussian in shape with a fairly narrow range of sizes. These features are normal in ferrofluids prepared via the carbonyl route.

All fluids examined had mean particle diameters within the single domain size limit for cobalt, ie 14nm.¹⁴ Although

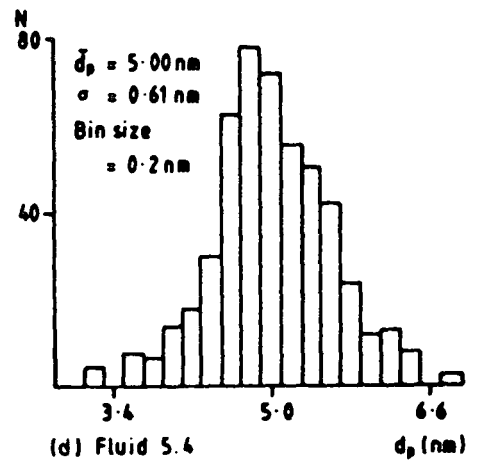
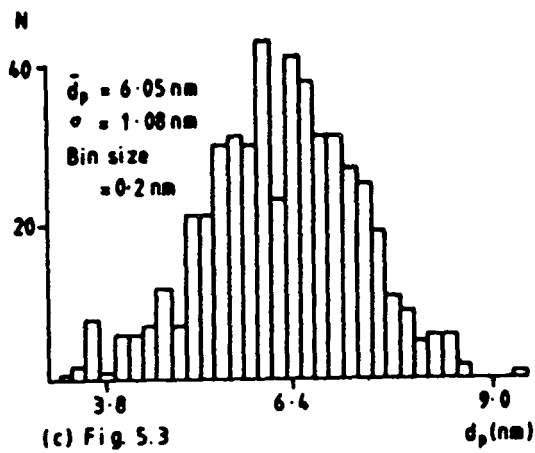
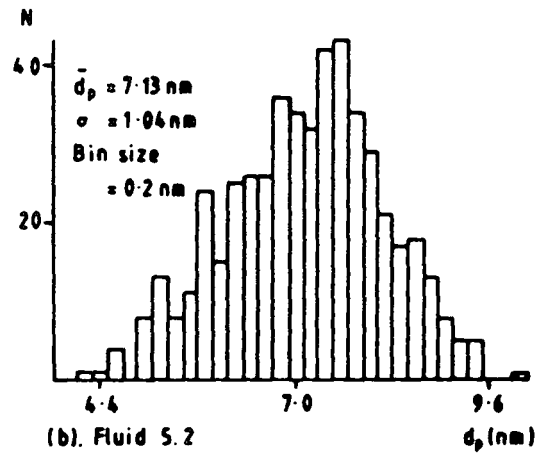
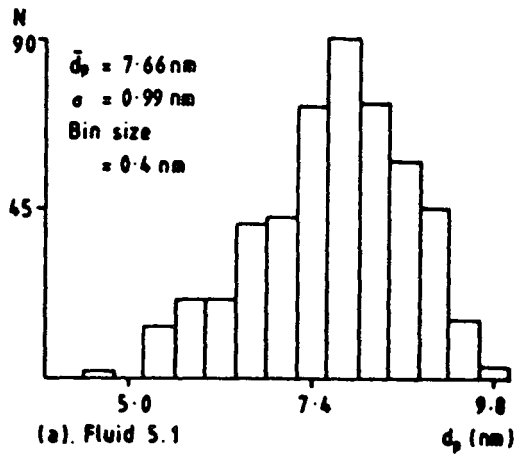


Fig. 5.1

Physical particle size distributions for cobalt magnetic fluids (a) Fluid 5.1, (b) Fluid 5.2, (c) Fluid 5.3 and (d) Fluid 5.4.

TABLE 5.2

Physical data for cobalt fluids

Fluid	TEM \bar{d}_p (nm)	data S.Dev(nm)	σ_{ff}^{∞} (JT ⁻¹ Kg ⁻¹)	Density (Kgm ⁻³)	ϵ_v	\bar{d}_v (nm)	\bar{d}_m (nm)	σ (nm)
5.1	7.66	0.99	4.08	900	0.0025	5.16	4.24	0.28
5.2	7.13	1.04	2.01	867	0.0012	2.76	2.52	0.19
5.3	6.05	1.08	2.58	867	0.0015	4.10	3.37	0.28
5.4	5.00	0.61	10.4	-	-	3.06	2.98	0.10

particles prepared by both techniques were similar in size, those prepared by the decomposition method were consistently larger. Fluid 5.4 had a notably smaller standard deviation which is desirable for good magnetic properties.

5.1.3 Magnetization Curves

Figure 5.2 shows the room temperature magnetization curves for the cobalt fluids obtained using a vibrating sample magnetometer. These curves are needed to determine the ferrofluids saturation magnetizations (σ_{ff}^{∞}) by inverse field extrapolations. This is demonstrated for fluid 5.3 in Figure 5.3, in which the magnetization per unit mass of the ferrofluid (σ_{ff}) is plotted against $1/B_0$, extrapolating to $1/B_0 = 0$ gives σ_{ff}^{∞} . Volume packing fractions (ϵ_v), which are a measure of the concentration of ferromagnetic cobalt in the ferrofluid, are calculated from the saturation magnetization (σ_{ff}^{∞}) using

$$\epsilon_v = \frac{\sigma_{ff}^{\infty} \rho_{ff}}{M_b^{\infty}} \quad (5.1)$$

where ρ_{ff} is the ferrofluid density and M_b^{∞} is the saturation magnetization per unit volume of the bulk metal. Values of σ_{ff}^{∞} and ϵ_v for the cobalt fluids are given in Table 5.2. The different shapes of the magnetization curves reflect the differences in particle sizes. Application of Chantrell's method allows the calculation of the mean magnetic particle diameter. (This is described in more detail in Section 1.6). The value calculated straight from the magnetic data is \bar{d}_v , this is the median magnetic

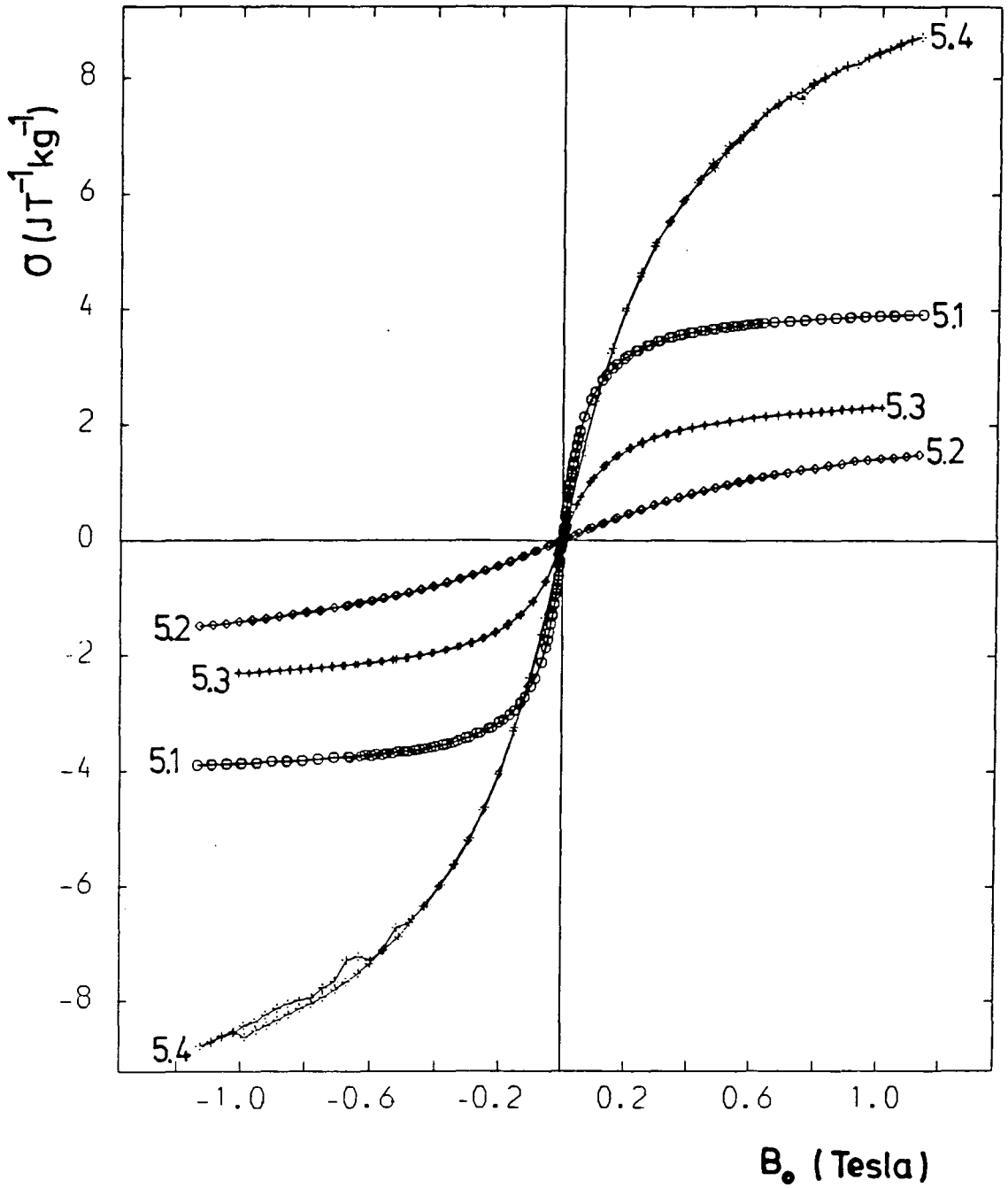


Fig. 5.2 Room temperature magnetization curves for cobalt magnetic fluids 5.1, 5.2, 5.3 and 5.4.

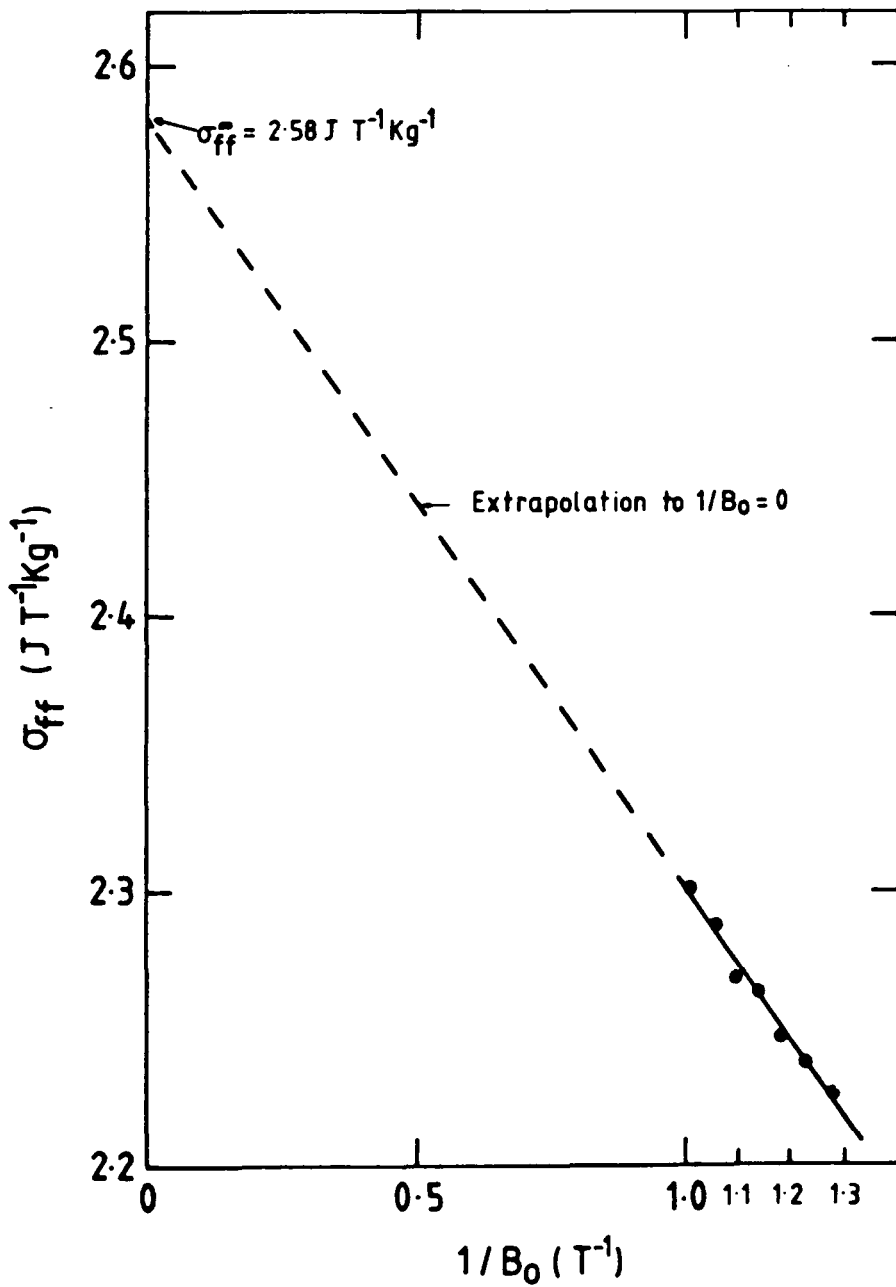


Fig. 5.3 Inverse field plot for fluid 5.3 to obtain σ_{ff}^{∞} .

particle diameter based on the particle volume distribution. However, this must be converted to the mean magnetic particle diameter, \bar{d}_m , (based on the particle number distribution) before it can be directly compared to the mean physical particle diameter (\bar{d}_p). A comparison of the mean physical diameter (\bar{d}_p) with the mean magnetic diameter (\bar{d}_m) indicates the relative amounts of the particle in a ferromagnetic and non-ferromagnetic state.

5.1.4 Electron Diffraction

Structural analysis of the particles in this series of magnetic fluids using electron diffraction proved to be very difficult because of the very small particle sizes. A diffraction pattern consisting of four lines was eventually obtained for fluid 5.3 using an electron accelerating voltage of 120kV. Indexing of the pattern ring diameters confirmed that the particles consisted of cobalt in the high temperature face centred cubic phase. A lattice parameter of $a_0 = 3.53\text{\AA}$ was derived from this diffraction data, this compares reasonably well with the literature value of 3.548\AA .¹³⁹ Table 5.3 compares the observed d-spacings with the literature values. From the table it is obvious there are several d-spacing values missing; considering the weakness and diffuse nature of the pattern this is not surprising.

5.1.5 A Qualitative Kinetic Study of the Decomposition Process

For the ferrofluids 5.1, 5.2 and 5.3, prepared by the thermal decomposition of dicobalt octacarbonyl, the

TABLE 5.3

Cobalt fluid electron diffraction data

d-observed Å	hkl assignment	d-lit. (fcc). Å
2.11	111	2.048
-	200	1.774
1.23	220	1.254
1.06	311	1.070
-	222	1.024
-	400	0.887
-	331	0.814
0.78	420	0.793

evolution of carbon monoxide was monitored. The purpose of this study was, (i) to discover the extent of the $\text{Co}_2(\text{CO})_8$ decomposition and (ii) to determine whether the mechanism of decomposition was consistent with that reported in the literature.

The procedure consisted of following the rate of carbon monoxide evolution by collecting the gas over water. In these experiments the volume of carbon monoxide evolved was not corrected for barometric pressure or temperature and the solubility of carbon monoxide in water was ignored ($2.3\text{cm}^3/100\text{cm}^3$ of water at 20°C)¹⁴⁰. The results, presented in graphical form, are being used only for comparative purposes and are considered sufficiently accurate. Figures 5.4(a), (b) and (c) show the results for this sub-section, each figure consists of plots of the percentages of the total carbon monoxide content evolved against time. The curves resemble those obtained by Papirer et al.¹²⁰ in similar work. Figure 5.4(d) taken from Papirer's work, shows how the shape of the decomposition curves change with temperature for a $\text{Co}_2(\text{CO})_8$:surfactant ratio of $R = 10$. Figure 5.4(d) shows Papirer's result using $R = 2$ at 130°C , these conditions are similar to those used in our experiments. It is reasonable¹²⁰ therefore, to assume that if Papirer et al. had used a temperature of $145\text{--}150^\circ\text{C}$ they would have observed more rapid evolution of carbon monoxide and therefore steeper decomposition curves. We can conclude that a decomposition¹²¹ mechanism of the form proposed by Papirer et al. was

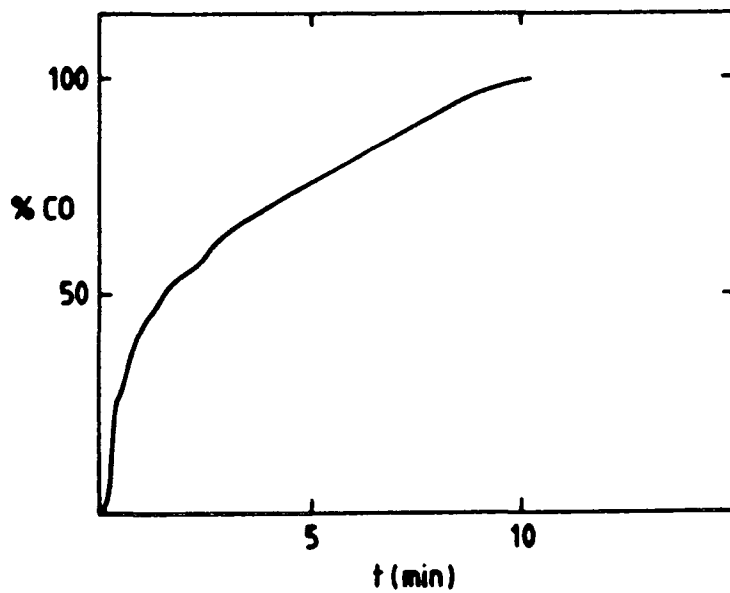
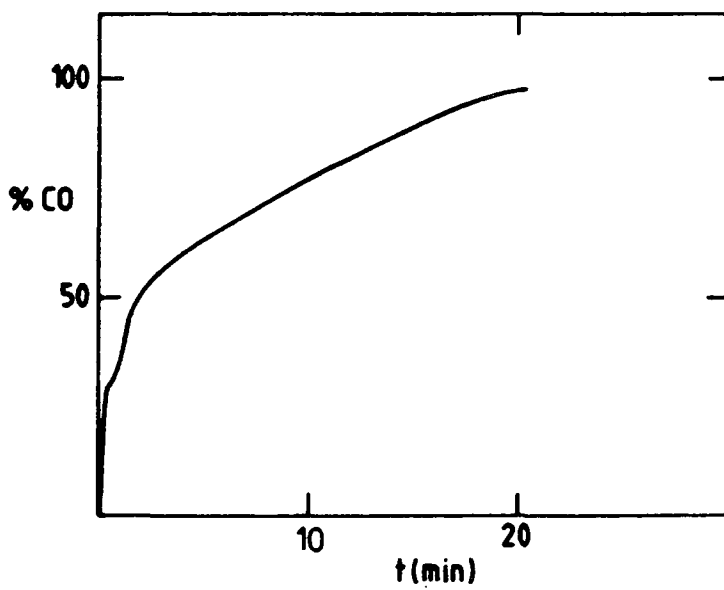
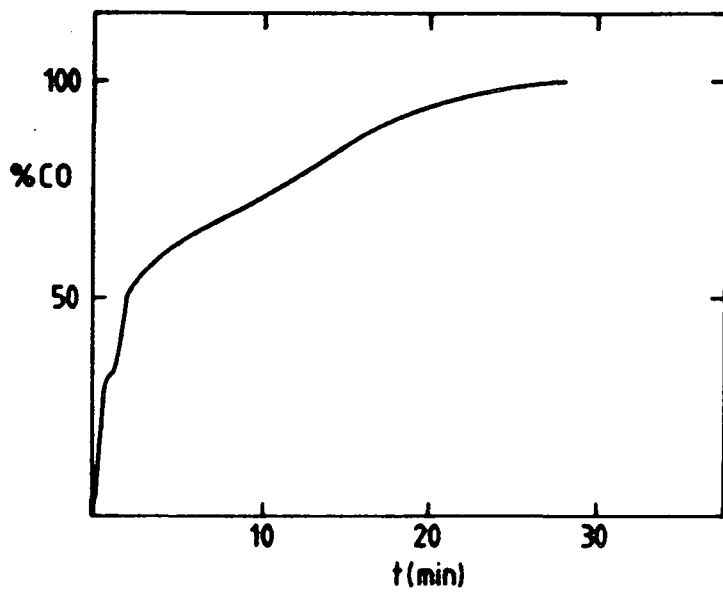
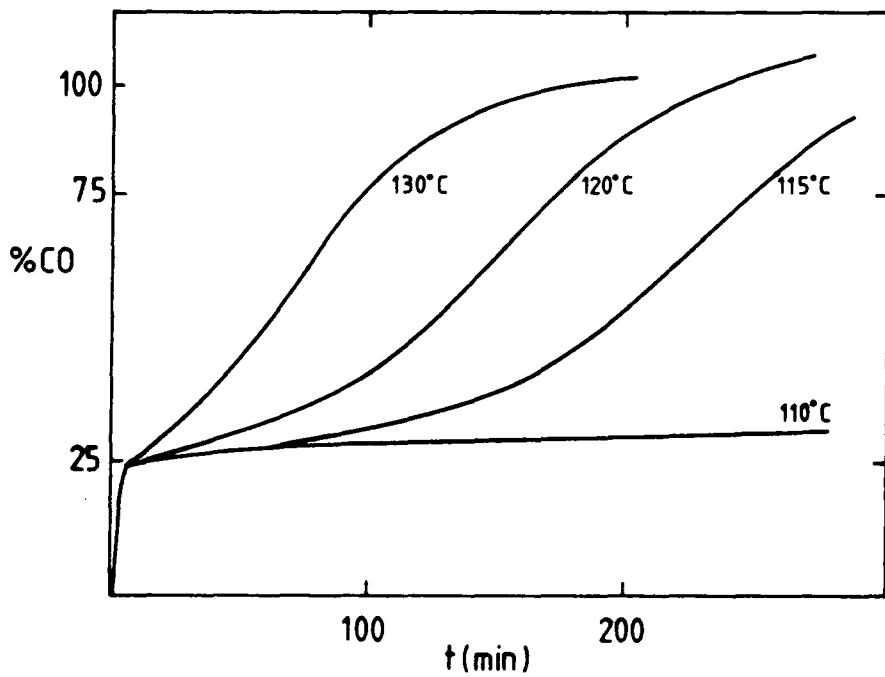


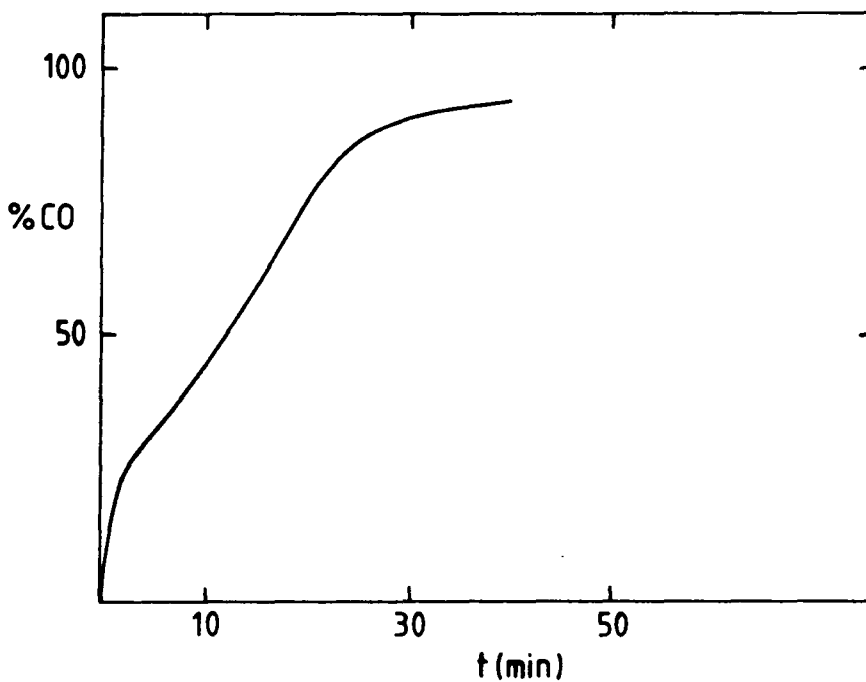
Fig. 5.4

Plots of percentage CO evolved against time for (a) Fluid 5.1, (b) Fluid 5.2 and (c) Fluid 5.3

continued overleaf



(d)



(e)

Fig. 5.4 continued

(d) $\text{Co}_2(\text{CO})_8/\text{Manoxol-OT}/\text{toluene}$ at various temperatures for $R = 10$ (Papirer et al.120).

(e) $\text{Co}_2(\text{CO})_8/\text{Manoxol-OT}/\text{toluene}$ at 130°C with a $\text{Co}_2(\text{CO})_8:\text{Manoxol-OT}$ ratio of 2 (Papirer et al.120).

operating (i.e. formation of $\text{Co}_4(\text{CO})_{12}$ which decomposes via a complex mechanism to produce cobalt particles of uniform size, this mechanism is described in more detail in section 3.2.2.

The solution infra-red spectra of fluids 5.1 to 5.4 in the $2200\text{-}1700\text{cm}^{-1}$ region were recorded. Only the carbonyl stretching frequency region was studied because of strong solvent absorptions in other regions of the spectra. For ferrofluids 5.1, 5.3 and 5.4 the $2200\text{-}1700\text{cm}^{-1}$ regions were virtually identical to that of toluene. However, for fluid 5.2 metal carbonyl bands at 2071 , 2026 , 2008 and 1992 cm^{-1} were observed. It appears that a thermally stable metal carbonyl was formed in the magnetic fluid prepared from dicobalt octacarbonyl with Manoxol-OT as the surfactant. The same complex was not present in fluid 5.4, prepared using the same surfactant but by another method.

5.1.6 Discussion and Conclusions

The decomposition and evaporation methods appear to produce equivalent magnetic fluids. The differences in σ_{ff}^{∞} the ferrofluid saturation magnetization, are thought not to be significant because higher values of σ_{ff}^{∞} could easily be attained simply by increasing the concentration of dicobalt octacarbonyl in the decomposition route. In all other respects the fluids appeared identical, with only minor differences in mean particle sizes.

Papirer et al.¹²¹ have proposed a mechanism for cobalt particle formation from the thermal decomposition of $\text{Co}_2(\text{CO})_8$

in toluene solution in the presence of a surfactant. The results in sub-section 5.1.5 of this chapter are comparable to Papirer's and indicate that the same type of mechanism is occurring, namely the formation of $\text{Co}_4(\text{CO})_{12}$ which decomposes via a complex mechanism to produce cobalt particles (described in detail in Chapter 3). However, there must be another process responsible for the formation of virtually identical particles from the completely different procedure of metal evaporation.

As the cobalt atoms enter the toluene solution it is believed that they initially react with the toluene to produce an unstable toluene-cobalt complex.⁶⁰ The complexes then decompose to form cobalt particles. This occurs slowly at -95°C but more rapidly on warming to room temperature. A remarkably uniform particle size was observed for the fluid prepared by this route. It is possible that as the particles form and grow at the lower temperature of -95°C , the surfactant becomes adsorbed restricting particle growth.

This is only a possibility as the particle formation mechanism was not studied specifically. During the cobalt condensation the solution was observed to become yellow, then green and finally black. The initial colour changes indicate some reaction of the metal atoms with either the surfactant or the toluene solvent..

The use of a metal atom technique is a logical method of preparing ferrofluids. In fact very recently Nakatami et al.¹⁴¹ have reported a similar procedure for preparing cobalt,

iron and nickel magnetic fluids. In the work described the particles were initially formed at room temperature and then flocculated by annealing at 270°C under argon, before redispersing. In the future this method is likely to be extended to include alloy materials provided the constituent metals have similar evaporation rates. It is even feasible that more exotic materials such as the lanthanide metals may be used.

The principle intention of this section was to compare the novel metal evaporation method with the conventional metal complex decomposition method. However, some additional points of interest arose from examining the ferrofluids prepared using the carbonyl route i.e. fluids 5.1, 5.2 and 5.3. Table 5.4 essentially compares the efficiency of the surfactants employed in the decomposition process. $(\bar{d}_p - \bar{d}_m / 2)$ is a measure of the thickness of the magnetic dead layer, i.e. the non-ferromagnetic layer on the particle surface. The three surfactants used did vary in the thickness of dead layer produced, as well as in the fraction of cobalt being converted to the ferromagnetic state.

Without further data it is impossible to explain the differences in the dead layer thicknesses and the percentage conversions. All previous work appears to neglect the latter area in particular. I believe it is likely that there are a number of reactions between surfactant and $\text{Co}_2(\text{CO})_8$ competing with the decomposition process. These

TABLE 5.4

A comparison of mass packing fractions and "Dead"
layer thickness for cobalt magnetic fluids discussed
in the text

Fluid	ϵ_m (100%)	ϵ_m	% Conversion	$\frac{\bar{d}_p - \bar{d}_m}{2}$ (nm)
5.1	0.0396	0.0247	62	1.71
5.2	0.0340	0.012	35	2.30
5.3	0.033	0.015	45	1.34
5.4	-	-	-	1.01

ϵ_m (100%) is calculated assuming 100% decomposition of $\text{Co}_2(\text{CO})_8$ to ferromagnetic cobalt.

reactions produce cobalt containing species which are stable or unstable, and which may react further. The exceptionally large dead layer observed for Manoxol-OT may be due to water, an impurity difficult to remove from this surfactant.

The dead layer thickness of fluid 5.4, the fluid prepared by metal evaporation was thinner than for ferrofluid 5.2, though both are Manoxol-OT stabilized fluids.

5.2 An EXAFS Spectroscopic Study of Cobalt Magnetic Fluids

5.2.1 Introduction

The laboratory scale EXAFS spectrometer described in section 4.2.6 was used to obtain EXAFS spectra of cobalt magnetic fluids and related samples. EXAFS spectroscopy can be used to study samples in any state and therefore samples of neat magnetic fluid could be examined directly. In this particular study only qualitative analysis of the EXAFS spectra was possible. Analysis consisted of a visual comparison of the spectra of interest with spectra of known materials.

An EXAFS spectrum of a magnetic fluid will be derived from all forms of cobalt present. Cobalt in the metallic state will form the major component; however, contributions to the overall spectra will arise from non-metallic cobalt on the particle surface i.e. oxides, cobalt surfactant derivatives and any cobalt in solution.

5.2.2 Spectra

Figure 5.5 shows the EXAFS absorption spectra for

freshly prepared magnetic fluid 5.1. Figure 5.5 also shows the EXAFS spectrum of a sample of (solid) cobalt metal. The cobalt absorption edge will always occur at the same X-ray energy. It is the oscillations superimposed on the general decrease in absorption coefficient (as X-ray energy increases beyond the absorption edge) which are of interest.

Although there are some slight differences in the two spectra in Figure 5.5, the positions of the EXAFS oscillations are in the same positions. In comparing the two spectra it is important to remember that only 62% of the cobalt in the fluid is in the ferromagnetic state (see Section 5.2.4); this accounts for the slight deviations between the spectra.

Figure 5.6 shows the EXAFS spectrum of fluid 5.1 partially oxidized after 2 months exposure to the atmosphere in comparison with the EXAFS spectrum of the freshly prepared fluid. The general appearances of the spectra are different, with the first absorption peak becoming more prominent. Figure 5.7 illustrates the EXAFS spectrum of $\text{Co}(\text{Sarkosyl-0})_2$. This sample was prepared using a metal atom technique at Bristol University. The spectrum of the partially oxidized fluid shows a strong resemblance to that of the surfactant derivative. From this we must not necessarily conclude that the metallic content of the fluid has been partially converted to a surfactant derivative, although it remains a possibility. In Figure 5.8 the spectrum of the partially oxidized fluid is plotted

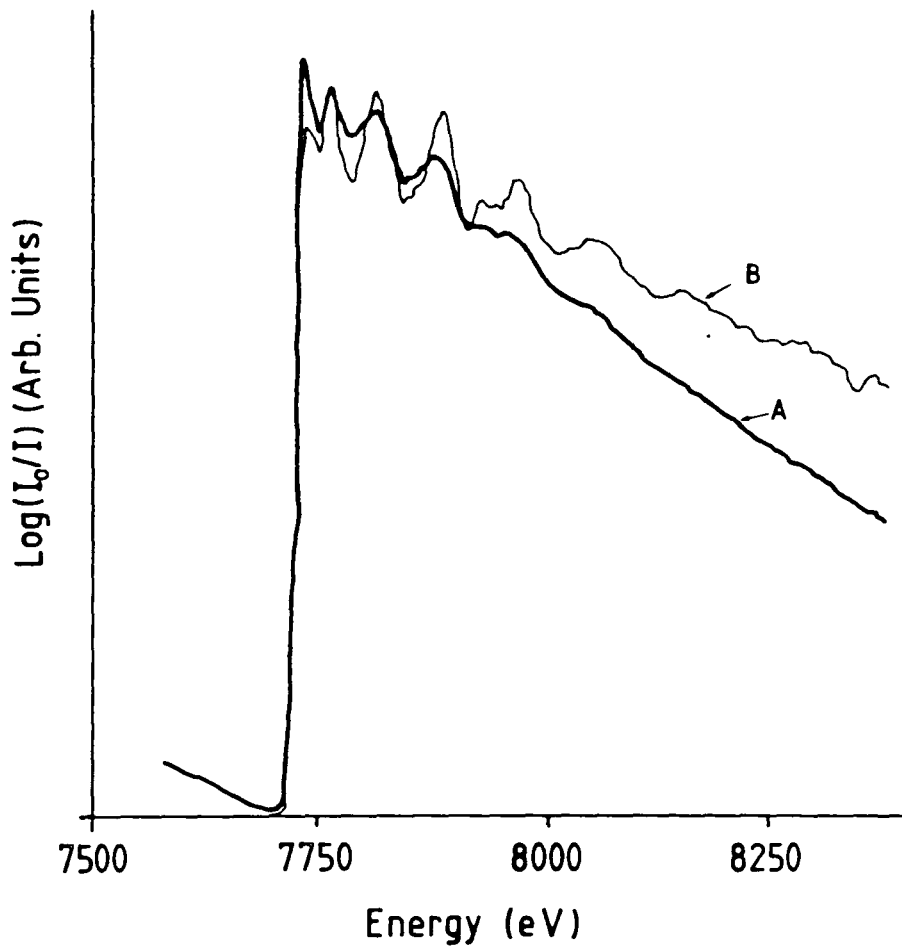


Fig. 5.5 EXAFS spectra for a freshly prepared cobalt magnetic fluid (A) and cobalt metal (B).

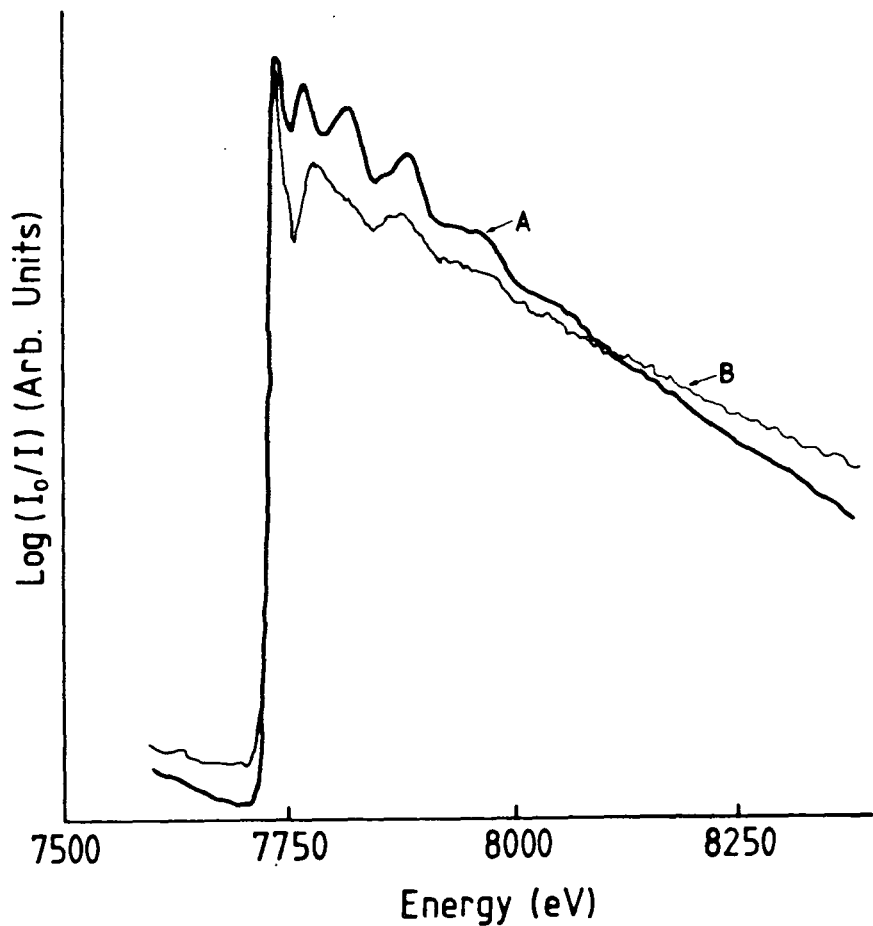


Fig. 5.6 EXAFS spectra for a freshly prepared cobalt magnetic fluid (A) and the same fluid partially oxidized (B).

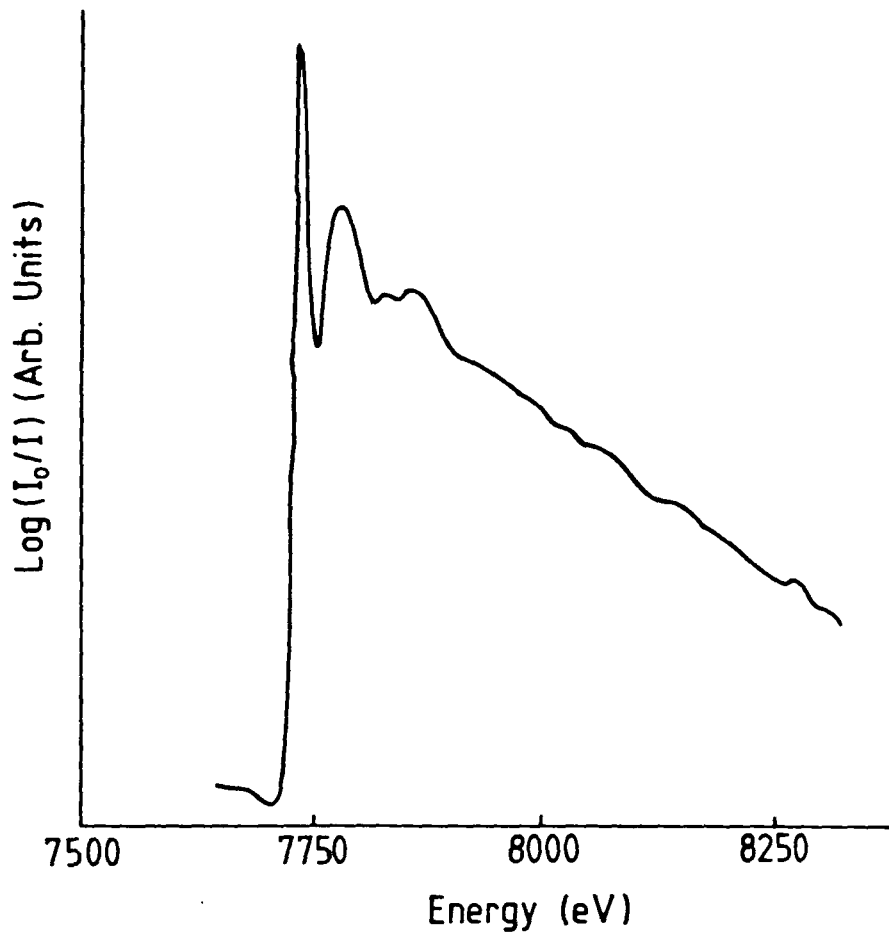


Fig. 5.7 EXAFS spectrum of $\text{Co}(\text{Sarkosyl-O})_2$.

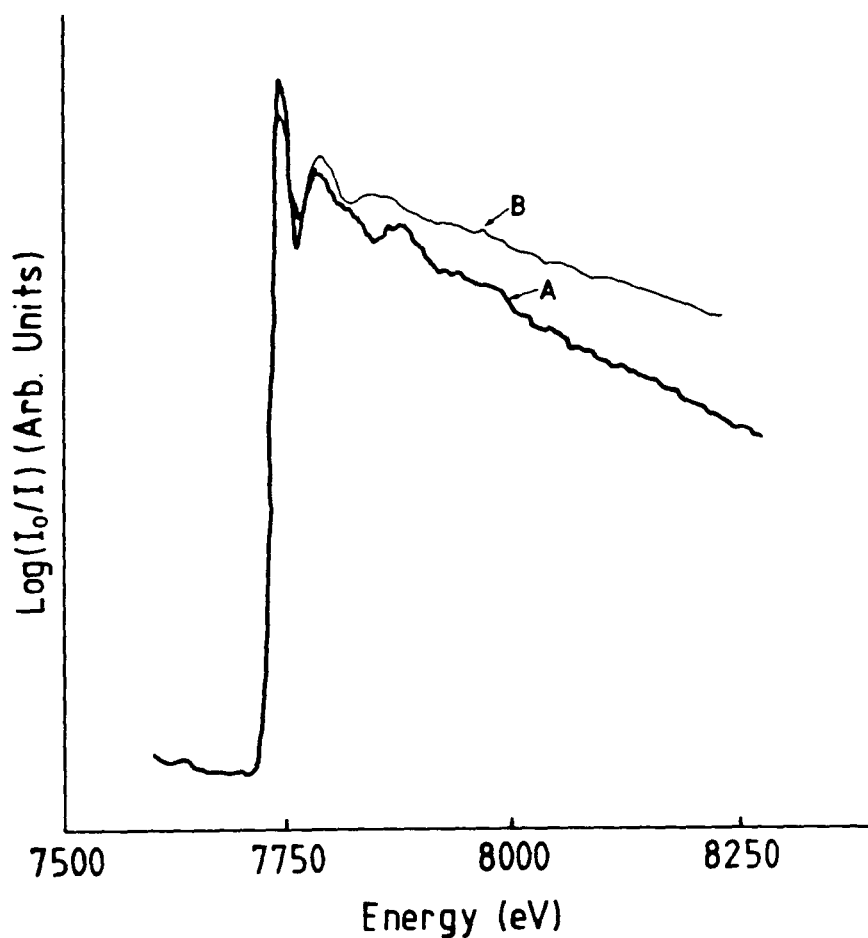


Fig. 5.8 EXAFS spectra of a partially oxidized cobalt fluid (A) and an aqueous solution of cobalt nitrate (B).

alongside that of an aqueous solution of cobalt nitrate. Again there are strong similarities between the two spectra, as might be expected if cobalt is coordinated to six oxygen atoms in both cases. From these spectra it is safe to conclude that cobalt in the freshly formed fluid was largely in the metallic state. The other spectra imply that the aged fluid consisted of a much higher proportion of cobalt coordinated by oxygen, i.e. an oxide or surfactant derivative layer. The EXAFS spectrum of dicobalt octacarbonyl in toluene solution did not resemble the spectrum of the freshly prepared ferrofluid.

5.2.3 Supporting Magnetic Data

A vibrating sample magnetometer was used to obtain a magnetization curve for the aged fluid. This curve is given in Figure 5.9 together with the corresponding curve for the freshly prepared fluid. An inverse field plot gave the saturation magnetization, $\sigma_{ff}^{\infty} = 2.49\text{JT}^{-1}\text{kg}^{-1}$ for the aged fluid (cf. $4.08\text{JT}^{-1}\text{kg}^{-1}$ for the freshly prepared fluid). This magnetic data indicated there was $\sim 61\%$ of the initial ferromagnetic cobalt content remaining. The mean magnetic particle diameter (\bar{d}_m) for the aged fluid, derived from the magnetization curve was 3.64nm (cf. 4.24nm for the freshly prepared fluid). Therefore approximately 63% of the original volume of ferromagnetic cobalt had survived oxidation. These percentages are in good agreement, and indicate that oxidation essentially "eats" away the particle magnetic core.

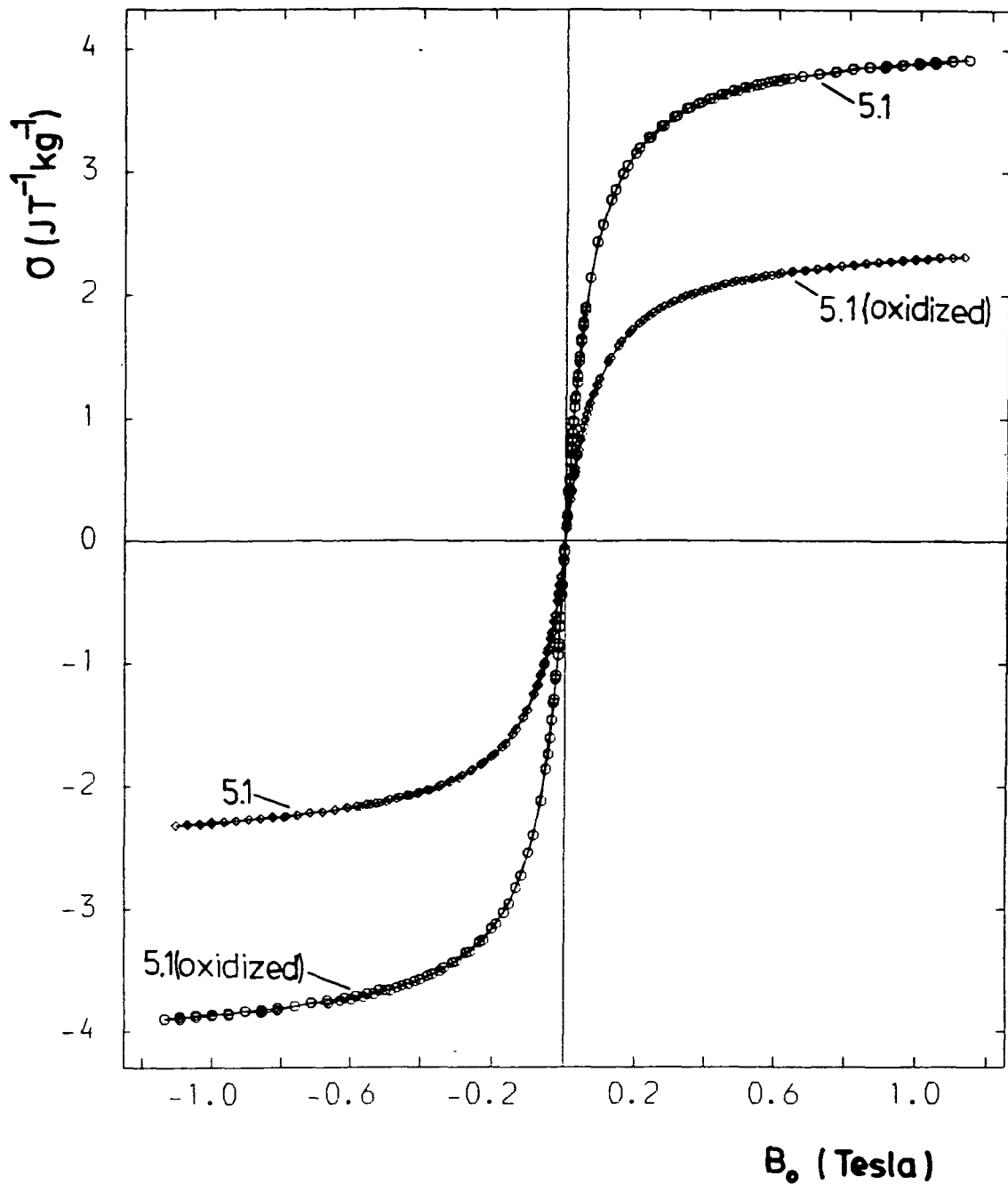


Fig. 5.9 Room temperature magnetization curves for freshly prepared cobalt fluid 5.1 (curve A) and the same fluid partially oxidized (curve B).

5.2.4 Discussion

If there was 100% decomposition of $\text{Co}_2(\text{CO})_8$ to ferromagnetic cobalt metal then we calculate that fluid 5.1 would be 3.96% by mass of ferromagnetic cobalt. The magnetic data indicates that only 2.47% by mass of the ferrofluid was ferromagnetic cobalt (this assumes that the particles have the same saturation magnetization per unit volume as bulk cobalt). Hence $\sim 62\%$ of the cobalt in the dicobalt octacarbonyl was converted to cobalt in the ferromagnetic form, and $\sim 38\%$ of the cobalt was in a non-ferromagnetic state. The EXAFS spectrum of the freshly prepared ferrofluid will be a combination of this cobalt metal and cobalt in other forms. The other forms will be non-metallic cobalt in solution and in the particles. In the partially oxidized fluid there was only $\sim 38\%$ (61% of 62%) of the total possible ferromagnetic cobalt remaining, hence the majority of the cobalt in the fluid was in a non-ferromagnetic form.

The recorded EXAFS spectra are consistent with the above observations. Firstly, the EXAFS spectrum of the freshly prepared sample of fluid 5.1 consisted largely of metallic cobalt absorptions with relatively minor contributions from other cobalt containing materials. The aged sample contained a much larger proportion of non-metallic cobalt. The spectra are consistent with the cobalt content being reduced by atmospheric oxidation and/or reaction with the surfactant to produce some oxygen

co-ordinated species. Unfortunately this study did not enable us to determine the exact nature of the non-ferromagnetic products. As far as it is known this was the first study of magnetic fluids using EXAFS spectroscopy.

I believe that this technique could be used in the future to solve some of the structural problems occurring in magnetic fluid study. Future studies would require data computation to obtain structural parameters, and would consist of combining spectra of possible components in various proportions to model the observed spectra.

5.3 Infra-red Spectroscopic Study of Cobalt Magnetic Fluids

5.3.1 Introduction

Despite ferrofluids being in existence for about 20 years, there has been no infra-red study reported in the literature. In this work the objectives were limited to trying to discover the nature of the particle-surfactant bonding and the nature of the "solution" cobalt. The strategy adopted was to examine changes in surfactant "head" group infra-red absorption frequencies. The study was restricted to cobalt ferrofluids because of all the metallic fluid systems they are the most well defined and easiest to prepare. There are several practical problems connected with this type of study: (i) The ferrofluids are produced in a hydrocarbon medium (normally toluene). In such a fluid the bulk of the organic fraction is solvent, which dominates the infra-red spectrum, overlapping regions of interest in

the spectrum of the surfactant. For this reason only strongly absorbing groups can be studied. (ii) Ferrofluids are intensely black and only a low path length of sample can be used; dilution of the ferrofluid exaggerates problem (i).

(iii) The study of "real" surfactants means investigating complex molecules with little or no reported work for comparative purposes. Simpler surfactants such as oleic acid (9-octadecenoic acid) would be far more convenient for study but do not stabilize cobalt ferrofluids effectively.

5.3.2 Experimental

(i) Systems Examined

The surfactants chosen initially for study were Sarkosyl-0 and Manoxol-OT because these molecules have polar head groups whose infra-red absorption frequencies would be expected to change on coordination/interaction with a metal.

(ii) Technique

A solution cell with KBr windows with either a 0.05mm or 0.025mm spacer was employed throughout the study. A PE580 grating spectrometer connected to a data station was used to record and manipulate spectra. This equipment allowed subtraction of the solvent spectra from those of the ferrofluid or surfactant solution.

5.3.3 Results and Discussion

(i) Sarkosyl-0

Toluene would be the ideal choice of solvent (carrier liquid) for this study from preparative considerations, as cobalt magnetic fluids are easily prepared in this medium.

Unfortunately toluene absorbs strongly in part of the infra-red region of interest. To partially overcome this problem petroleum ether (b.p. 100-120°C) and decalin (decahydronaphthalene) were used in addition to toluene as solvents. Surfactant concentrations were also varied in order to help distinguish genuine surfactant infra-red absorption bands. Infra-red spectra in the 1850-1550 cm^{-1} region were recorded for Sarkosyl-0 in solutions of the hydrocarbon solvents toluene, petroleum ether (b.p. 100-120°C) and decalin. Subtraction of the pure solvent spectra from the respective solution spectra (over the 1850-1550 cm^{-1} region) consistently produced what appeared to be three absorption bands in the 1850-1550 cm^{-1} region suitable for analysis. The observed absorption band frequencies are summarized as follows:

Carrier Liquid	Absorption band frequencies(cm^{-1})
Toluene	1721.9, 1667.4*, 1624.0*
Pet. Ether (b.p. 100-120°C)	1734.8, 1661.4*, 1618.8*
Decalin	1731.6, 1658.6*, 1621.5*

The absorption bands marked by * were observed to be poorly resolved. In all three solvents the band in the 1720-1735 cm^{-1} region was clearly resolved. However, the other "two" absorptions appeared as two peaks of roughly equal intensity on a single broad absorption band. To distinguish if two absorption bands really exist in the 1620-1670 cm^{-1} range or whether there was only one absorption and the appearance of two "peaks" was connected with the subtraction of the

solvent spectra, the infra-red spectrum of a concentrated nujol solution of Sarkosyl-0 was recorded. Nujol does not absorb in the $1850-1550\text{cm}^{-1}$ region. In nujol solution two absorption bands at frequencies 1729 and 1625cm^{-1} were observed. The bands were both broad, especially the band with maximum intensity at frequency 1625cm^{-1} . It would appear that Sarkosyl-0 gives only two absorption bands in the $1850-1550\text{cm}^{-1}$ frequency range. The apparent appearance on inspection of three absorption bands illustrates a problem with this type of study, i.e. subtraction of solvent absorption bands giving rise to the appearance of "extra" bands in the spectrum of the surfactant.

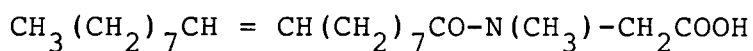
Ferrofluids were prepared for this study by the thermal decomposition of dicobalt octacarbonyl as outlined in section 5.1.1(i). With petroleum ether (b.p. $100-120^\circ\text{C}$) as the carrier liquid a stable ferrofluid could not be produced, hence the study was restricted to the cobalt/Sarkosyl-0/toluene and the cobalt/Sarkosyl-0/decalin systems. In these systems two absorption bands were observed in the $1850-1550\text{cm}^{-1}$ region. The band frequencies are summarized as follows:

Carrier Liquid	Absorption band frequencies (cm^{-1})
Toluene	$1647.4, 1615.1^*, 1594.5^*$
Decalin	$1651.8, 1604.4$

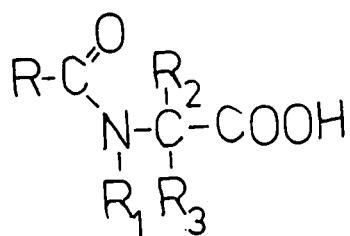
As before * denotes what appeared to be a single broad absorption band with two poorly resolved "peaks" in

intensity. Toluene has a very strong absorption band in the 1600 cm^{-1} frequency region. Subtraction of this band from the ferrofluid spectrum produces what appears to be two absorption bands. Fortunately in decalin there is no equivalent absorption band and only a single absorption band was clearly observed in the infra-red spectrum of the ferrofluid.

The first step in interpreting these spectra is the assignment of the absorption bands in the Sarkosyl-0 in hydrocarbon solution spectra. Sarkosyl-0 has the systematic name N-methyl-N-(1-oxo)-9-octadecenylglycine, with structure:



In hydrocarbon solution the carboxylic acid group will be in the undissociated form. By inspection we would expect the molecule to give rise to two strong absorption bands due to C=O stretching vibrations, i.e. the carboxylic acid C=O and an Amide I band. An Amide II band is not expected as a N-H bond would be necessary. A literature search did not produce any suitable reference concerning the infra-red spectra of Sarkosyl-0. To assign the observed absorption bands we must rely on a comparison of the observed band frequencies with those of similar molecules reported in the literature. The surfactant molecule Sarkosyl-0 has a "head" group of the general form:



i.e. an α -amido-acid. Randall et al.¹⁴² have recorded the infra-red spectra of a series of α -amido-acids and suggest that the carboxyl group absorption occurs at frequencies above 1695cm^{-1} (see Table 5.5).¹⁴² In all the examples given only two absorption bands are associated with this type of functionality, in the region of interest (excluding Amide II bands).

By comparing the observed absorption frequencies with those recorded by Randall et al.¹⁴² we can assign the absorption band in the $1720\text{-}1730\text{cm}^{-1}$ region as the acid C=O stretching absorption. The other absorption in the $1620\text{-}1760\text{cm}^{-1}$ region must be the Amide I band.

On conversion to the ferrofluid the two absorption bands due to C=O stretching in the Sarkosyl-O molecule had shifted in frequency. In the ferrofluid the carboxylic acid C=O stretching frequency band had completely disappeared, which indicates that all the surfactant had reacted to produce some form of cobalt derivative. According to Bellamy,¹⁴³ when α -amido-acids form "salts" the Amide I absorption band shifts to higher frequencies. Salt/complex formation results in conversion of the carboxylic acid group to a carboxylate functionality and the occurrence of a band

TABLE 5.5

Infra-red absorption frequencies for some α -amido acids
in the 1850-1550 cm^{-1} region.¹⁴²

Molecular Structure	$\bar{\nu}(\text{cm}^{-1})$	Assignment
$\begin{array}{c} \text{O} \\ \parallel \\ \text{C}_6\text{H}_5\text{CH}_2\text{C} \\ \diagdown \quad \diagup \\ \text{N} \quad \text{CH}_2\text{---COOH} \\ \\ \text{CH}_3 \end{array}$	1709.4 1602.6	Acid C=O Amide I
$\begin{array}{c} \text{O} \\ \parallel \\ \text{C}_6\text{H}_5\text{CH}_2\text{C} \\ \diagdown \quad \diagup \\ \text{N} \quad \text{CH}_2\text{---COOH} \\ \\ \text{H} \end{array}$	1724.1 1607.7 1529.1	Acid C=O Amide I Amide II
$\begin{array}{c} \text{O} \\ \parallel \\ \text{C}_6\text{H}_5\text{CH}_2\text{C} \\ \diagdown \quad \diagup \\ \text{N} \quad \text{CH}_2\text{---COOH} \\ \\ \text{C}_6\text{H}_5 \end{array}$	1751.3 1636.7	Acid C=O Amide I
$\begin{array}{c} \text{O} \\ \parallel \\ \text{C}_6\text{H}_5\text{CH}_2\text{C} \\ \diagdown \quad \diagup \\ \text{N} \quad \text{---CH---COOH} \\ \diagup \quad \diagdown \\ \text{CH}_2 \quad \text{CH}_2 \\ \diagdown \quad \diagup \\ \text{CH}_2 \end{array}$	1715.3 1589.7	Acid C=O Amide I
$\begin{array}{c} \text{O} \\ \parallel \\ \text{C}_6\text{H}_5\text{CH}_2\text{C} \\ \diagdown \quad \diagup \\ \text{N} \quad \text{---CH(CH}_3\text{)---COOH} \\ \\ \text{H} \end{array}$	1715.3 1644.7 1545.6	Acid C=O Amide I Amide II

at a lower frequency.¹⁴³ It follows that the band at $\sim 1650\text{cm}^{-1}$ in the ferrofluid will be the Amide I band shifted from 1625cm^{-1} in Sarkosyl-0. The band at $\sim 1604\text{cm}^{-1}$ will be due to the carboxylate group.

(ii) Manoxol-OT

The head group in Manoxol-OT is a sulphonic acid salt, i.e. $\text{R-SO}_3^-\text{Na}^+$. The characteristic infra-red absorptions are in the 1175 and 1055cm^{-1} frequency regions for this functional group.¹⁴⁴ However these bands could not be resolved with sufficient clarity from the solvent infra-red spectra to monitor any frequency shifts.

5.3.4 Conclusion

From the results obtained in the study of the cobalt/Sarkosyl-0 systems, we can conclude that in the preparation of the ferrofluid all of the surfactant had reacted to give the anion of Sarkosyl-0 present possibly as some form of cobalt derivative. This means that the "free" surfactant present in solution in the ferrofluid is actually a cobalt derivative and not in the original form (a previously unreported result). This is interesting and explains the fate of some of the cobalt which is not converted to a ferromagnetic state.

The results obtained are insufficiently sensitive to differentiate between surfactant on the particle surface and in solution. Hence we cannot make any deductions concerning the nature of the particle-surfactant bonding.

IRON-COBALT ALLOY MAGNETIC FLUIDS

Introduction

The preparation of hydrocarbon-based metal particle magnetic fluids was discussed in Chapter 2. Simple cobalt fluids were discussed more specifically in the previous chapter. This chapter and the one which follows are devoted to the preparation and characterization of the first colloidal alloy magnetic fluids. Alloy systems are of interest because magnetic properties such as Curie temperature and saturation magnetization depend on the alloy composition.¹⁴⁵

Metallic systems in general are of interest because they offer higher saturation magnetizations than ferrite systems. In this respect the iron-cobalt alloy is important because those alloys whose compositions lie in the range of 0 to 75% cobalt have a saturation magnetization higher than that of iron,¹⁴⁵ which possesses the highest saturation magnetization of the ferromagnetic elements. In fact iron-cobalt alloys with 35% cobalt content have the highest saturation magnetization value of any magnetic material.¹⁴⁶

The strategy used for alloy fluid preparation was to decompose specially synthesized heteronuclear organometallic compounds of the ferromagnetic elements. The idea was based

on the carbonyl route, the difference being that suitable mixed-metal compounds needed to be synthesized specifically.

Since this was the first time such a study had been attempted there were no guidelines to follow with respect to which compounds were likely to be successful. This chapter reports the preparation and characterization of two series of iron-cobalt magnetic fluids from different iron-cobalt organometallic precursors.

6.1 Iron-Cobalt Magnetic Fluids from $[(\pi\text{-C}_5\text{H}_5)\text{Fe}(\text{CO})_2\text{Co}(\text{CO})_4]$

6.1.1 Fluid Preparation

The series of ferrofluids described in this section were prepared from $[(\pi\text{-C}_5\text{H}_5)\text{Fe}(\text{CO})_2\text{Co}(\text{CO})_4]$.

(i) Preparation of $[(\pi\text{-C}_5\text{H}_5)\text{Fe}(\text{CO})_2\text{Co}(\text{CO})_4]$

Hexacarbonylcyclopentadienylcobaltiron was prepared via a method adapted from that of Manning.¹⁴⁷ In the original preparation $(\pi\text{-C}_5\text{H}_5)\text{Fe}(\text{CO})_2\text{Cl}$ was reacted with $\text{Na}^+\text{Co}(\text{CO})_4^-$ in T.H.F. solution, the $\text{Na}^+\text{Co}(\text{CO})_4^-$ being prepared from reaction of $\text{Co}_2(\text{CO})_8$ with sodium amalgam in T.H.F. Our preparation differed slightly from this in that the source of $\text{Co}(\text{CO})_4^-$ was from $[(\text{Co}(\text{CH}_3\text{OH})_n)^{2+}][\text{Co}(\text{CO})_4^-]_2$. This method was used repeatedly to prepare 3-4g batches of $[(\pi\text{-C}_5\text{H}_5)\text{Fe}(\text{CO})_2\text{Co}(\text{CO})_4]$ for fluid preparation. A typical preparation was as follows:

Dicobalt octacarbonyl (5.18g, 15.15mmol) was stirred in methanol (60cm³) under nitrogen at $\sim 30^\circ\text{C}$ until infra-red spectroscopy indicated the absence of $\text{Co}_2(\text{CO})_8$. A rose



coloured solution containing $[\text{Co}(\text{CH}_3\text{OH})_n^{2+}][\text{Co}(\text{CO})_4^-]_2$ (10.10mmol) was obtained (the source of $\text{Co}(\text{CO})_4^-$ (20.20mmol)),¹⁴⁸ this was filtered under nitrogen through a sinter into a solution of $(\pi\text{-C}_5\text{H}_5)\text{Fe}(\text{CO})_2\text{Cl}$ (4.29g, 20.20mmol) in methanol (40cm³) at room temperature. $(\pi\text{-C}_5\text{H}_5)\text{Fe}(\text{CO})_2\text{Cl}$ was prepared from $[(\pi\text{-C}_5\text{H}_5)\text{Fe}(\text{CO})_2]_2$ as described by Piper et al.¹⁴⁹ The methanol solution was stirred at room temperature under nitrogen for ~ 16 hours, after which a brown coloured solution was obtained. A brown solid product was isolated by removal of the solvent under reduced pressure. It was purified by column chromatography (alumina, toluene solvent) and finally recrystallized from pentane. Yields were of the order of ~ 15% (pure product), 50% crude product. Confirmation that $[(\pi\text{-C}_5\text{H}_5)\text{Fe}(\text{CO})_2\text{Co}(\text{CO})_4]$ had been prepared was by elemental analysis and comparison of the observed carbonyl stretching frequencies with those in the literature. Found: C, 38.32; H, 1.14; Fe, 15.81; Co 17.04. $[(\pi\text{-C}_5\text{H}_5)\text{Fe}(\text{CO})_2\text{Co}(\text{CO})_4]$ requires: C, 37.90; H, 1.30; Fe, 16.05; Co, 16.94%. Infra-red spectrum (cyclohexane): (obs): 2070s, 2015vs, 2000m, 1980vs, 1960w and 1831lw. (lit) 2071s, 2017vs, 2015, 2000m, 1982vs, 1958w, 1857, 1851, 1836 and 1831 w cm⁻¹.

(ii) Magnetic Fluid Preparation

Fluid preparation consisted of thermally decomposing $[(\pi\text{-C}_5\text{H}_5)\text{Fe}(\text{CO})_2\text{Co}(\text{CO})_4]$ in a toluene solution containing a surfactant. Fluids were prepared in one of two sets of apparatus, either a 3-necked round bottomed flask system

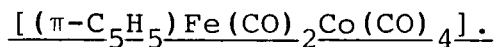
(described in 5.1.1.(i)) or alternatively, a glass tube fitted with a reflux condenser and gas inlet tube allowing nitrogen to be bubbled through the solution to cause agitation. In both sets of apparatus the reflux condenser was connected to an oil bubbler. A pre-heated oil bath was used as the heat source, typically at 130°C. Table 6.1.1 summarizes the preparative details for fluids prepared from $[(\pi\text{-C}_5\text{H}_5)\text{Fe}(\text{CO})_2 \text{Co}(\text{CO})_4]$. Attempts to prepare fluids using the surfactants Solsperse-17000 and Sarkosyl-0 were unsuccessful. Fluid 6.1.6 was centrifuged at 2000 r.p.m. for 90 minutes in order to remove non-colloidal material produced in this preparation. The remaining fluid was magnetically weak and not fully analysed.

6.1.2 Transmission Electron Microscopy

Figure 6.1.1 shows a typical shadow electron micrograph (fluid 6.4) taken at a magnification of 220,000 and enlarged approximately a further 3 fold. As with other ferrofluids the particles do not appear to have a particular shape, but are roughly spherical. Figure 6.1.2 gives the particle size distributions for fluids analysed. The corresponding mean physical size data is given in Table 6.1.2. These distributions are all typical for ferrofluids prepared by the "carbonyl" route. All sizes are in the 5-8nm range with fairly narrow distributions. The fact that there is nothing unusual about the micrographs and particle size distributions is encouraging. From this we can conclude the preparation is analogous to the preparation of simple cobalt

TABLE 6.1.1

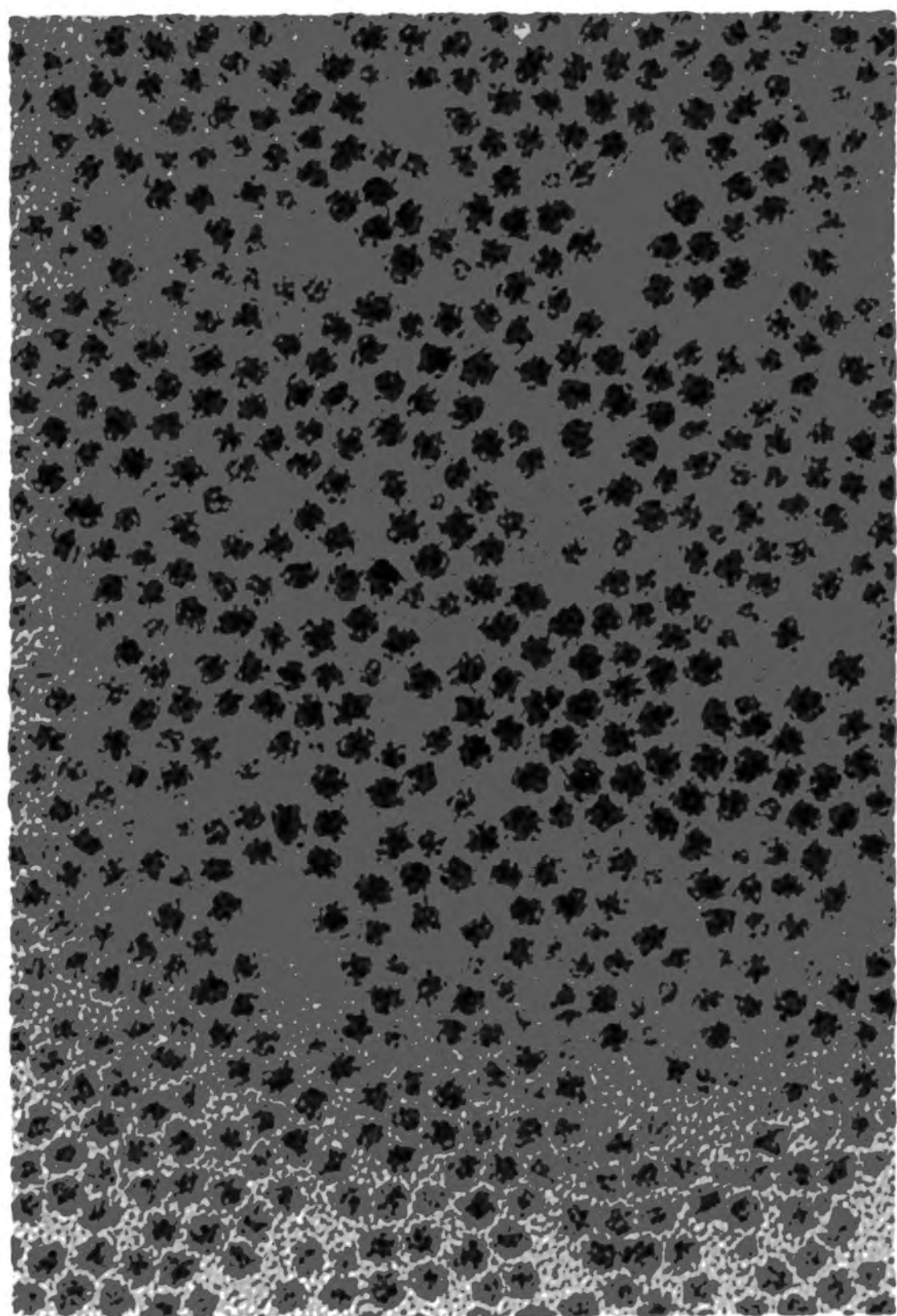
Preparative details for magnetic fluids prepared from



Fluid	Mass of * (g)	Surfactant	Mass of Surfactant (g)	Vol. of Toluene (cm ³)	R = Mass * : Mass surf.	Oil Bath Temp. (°C)	Heating Time (hrs)
6.1.1	3.10	Solsperse -3000	3.00	20.0	1.03	130	3
6.1.2	1.4973	Solsperse -3000	1.4962	10.0	1.00	130	2
6.1.3	1.4067	Duomeen -TDO	0.6984	10.0	2.01	130	2
6.1.4	1.0012	Duomeen -TDO	1.0427	10.0	0.96	140	2
6.1.5	0.8299	Duomeen -TDO	0.5881	10.0	1.411	155-160	2
6.1.6	0.9654	Duomeen-T	0.9962	10.0	0.97	130	2

* is $[(\pi\text{-C}_5\text{H}_5)\text{Fe}(\text{CO})_2\text{Co}(\text{CO})_4]$

Fig.6.11 Typical shadow electron micrograph of an iron-cobalt fluid (X 600 000)



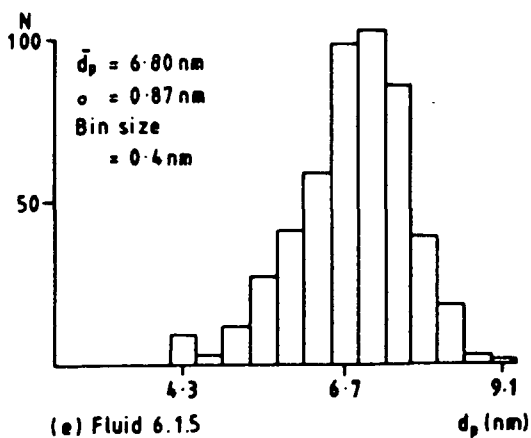
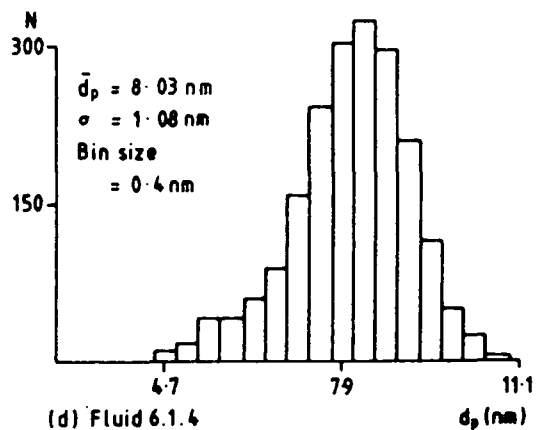
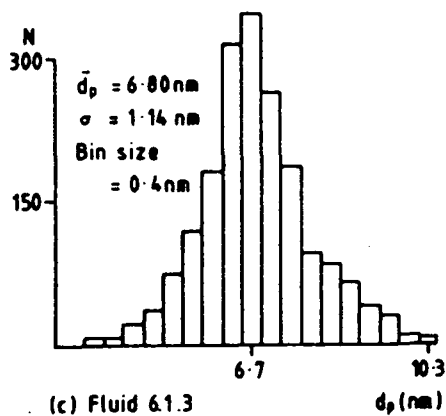
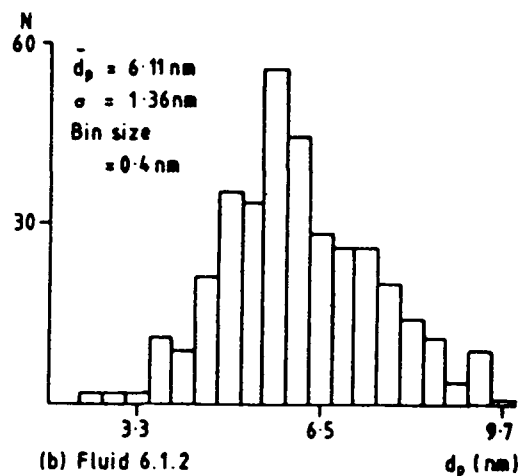
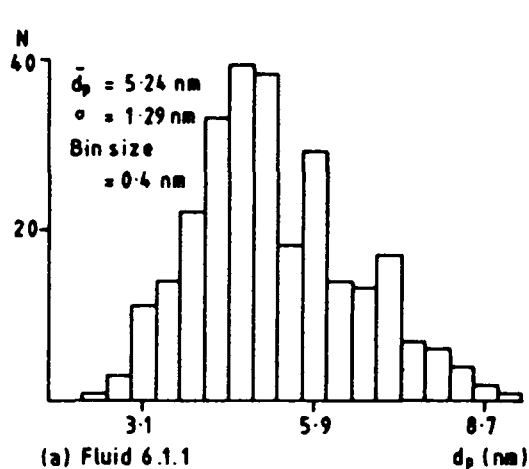


Fig. 6.1.2 Physical particle size distributions for iron-cobalt fluids 6.1.1., 6.1.2, 6.1.3, 6.1.4 and 6.1.5.

TABLE 6.1.2

Magnetic and Particle Size data for magnetic fluids prepared

from $[(\pi\text{-C}_5\text{H}_5)\text{Fe}(\text{CO})_2\text{Co}(\text{CO})_4]$

Fluid	TEM Data		σ_{ff}^{∞} ($\text{JT}^{-1}\text{Kg}^{-1}$)	Density (Kgm^{-3})	ϵ_v	\bar{d} (nm)	\bar{d}_m (nm)	σ (nm)
	\bar{d}_p (nm)	S.Dev (nm)						
6.1.1	5.24	1.66	2.80	965	0.14	4.3	3.3	0.32
6.1.2	6.11	1.85	0.98	909	0.05	4.2	3.4	0.29
6.1.3	6.80	1.14	2.52	913	0.12	4.9	3.9	0.30
6.1.4	8.03	1.08	1.25	906	0.06	5.39	-	-
6.1.5	6.80	0.87	1.82	910	0.09	4.62	3.90	0.26

fluids from dicobalt octacarbonyl.

The mean particle size for fluids 6.1.3 and 6.1.4 differ by 1.2nm. 2000 particle images were counted in both cases, giving good statistics and therefore reliable data. This is interesting as the only significant difference in their preparation was the value of R, i.e. relative amount of surfactant (see Table 6.1.1). This result implies that particle size is dependent on surfactant concentrations, smaller size particles being obtained when the surfactant concentration is relatively high compared with the amount of organometallic starting material.

6.1.3 Particle Structure and Composition

(i) Electron Diffraction

The elucidation of the particle structure is crucial in verifying that the particles are genuinely alloy particles. Shadow electron micrographs and magnetization curves would be indistinguishable if the particles were composed of a single (ferromagnetic) metal. Transmission electron diffraction was used to obtain the diffraction pattern shown in figure 6.1.3. The lines ratio unambiguously as a body centred cubic structure. Indexing as such produced a lattice parameter of $\sim 3.8\text{\AA}$, which is not compatible with any iron, cobalt or iron-cobalt system.¹³⁹ However, bulk iron-cobalt alloys with compositions in the range 40-60% cobalt in iron are known to exist in one of two forms. The atoms are arranged either in an ordered or disordered structure,¹⁴⁶ Lambrick (priv. comm.) proposed the occurrence of

Fig. 6.1.3 Electron diffraction pattern for the
iron-cobalt system

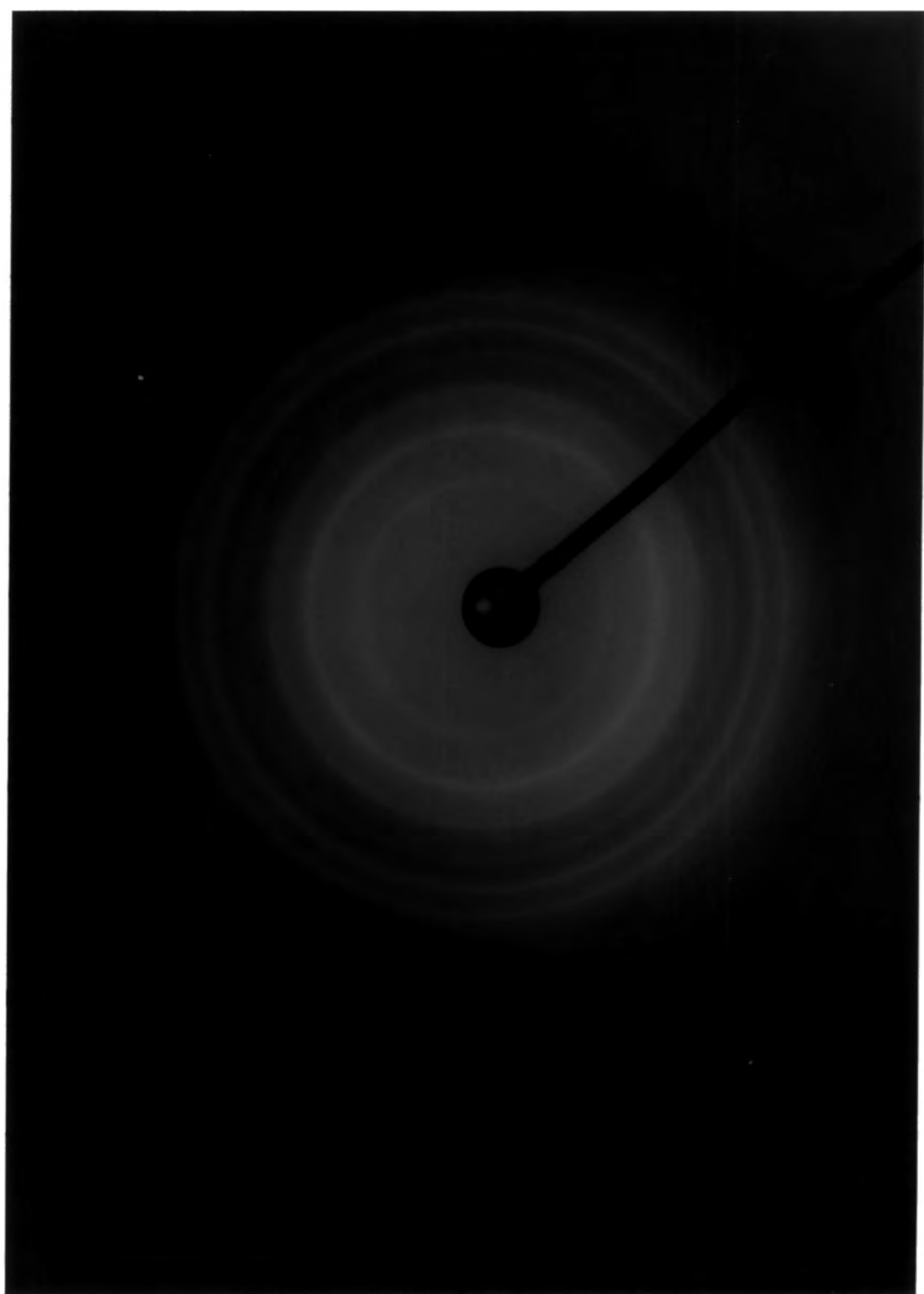


TABLE 6.1.3

Observed d-spacings and hkl assignments
for the Fe-Co system

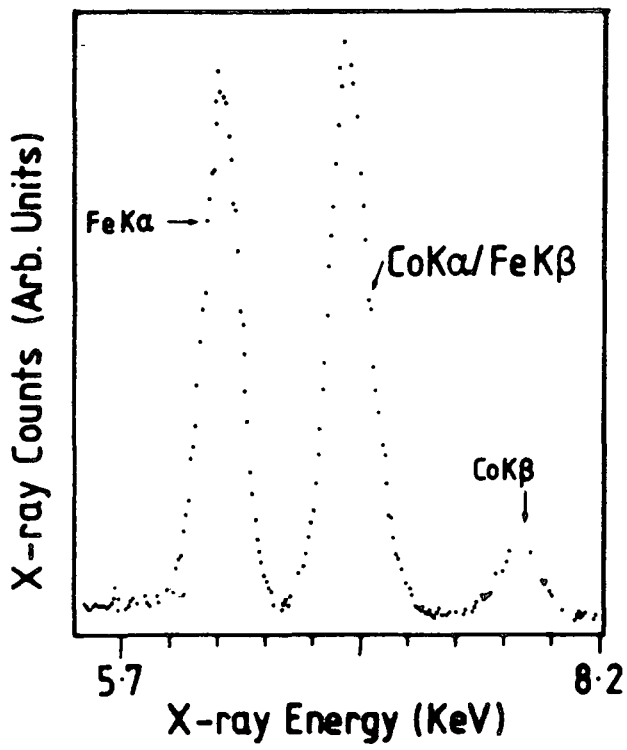
$d(\text{\AA})$	hkl
2.61	100*
1.91	110
1.55	111*
1.34	200
1.20	210*
1.10	2.11

* Denotes superlattice reflections

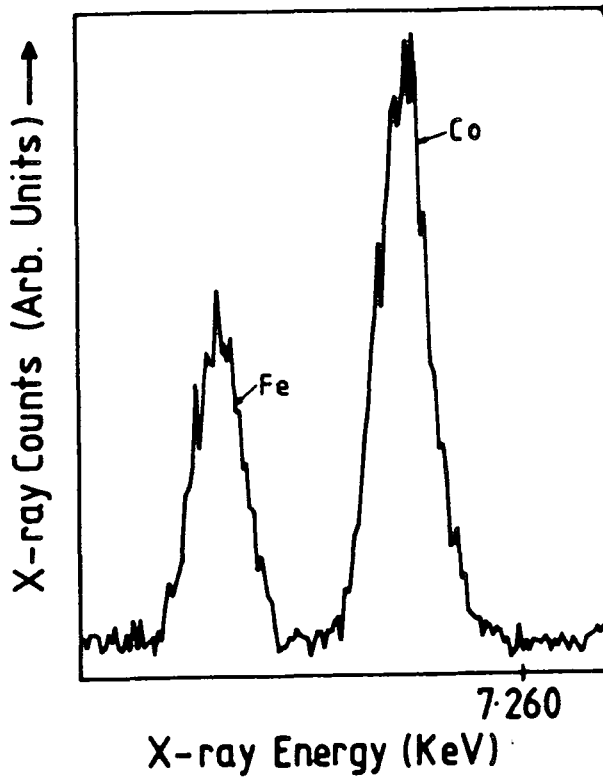
the ordered iron-cobalt phase in the fluid particles. Indeed, if we assume (i) a composition in the 40-60% cobalt in iron range, and (ii) an iron-cobalt ordered structure, then we must allow for the extra reflections due to the iron and cobalt primitive cubic systems, i.e. (100), (111), (210) etc. Ratioing of the diffraction pattern ring diameters is consistent with the superlattice structure. If the observed d-spacings are indexed with the "superlattice" reflections then a lattice parameter of $\sim 2.7\text{\AA}$ is obtained. This is within a 5% error of the bulk iron-cobalt value. From this important result we conclude the particles produced have the ordered iron-cobalt structure with a composition of 40-60% cobalt in iron. The structure overall is bcc, derived from two interpenetrating simple cubic lattices of iron and cobalt. It appears that the 1:1 iron to cobalt ratio in the organometallic precursor is at least approximately reproduced in the metallic particles. Table 6.1.3 summarizes these findings, giving the observed d-spacings and hkl assignments.

(ii) EDX Spectroscopy

SEM EDX spectroscopic analysis of a sample of fluid was not very revealing. The results shown in Figure 6.1.4(a) merely show that the iron-cobalt ratio in the bulk fluid was approximately 1:1 which was to be expected as the iron:cobalt ratio in the precursor molecule was 1:1. However, local area EDX spectroscopy revealed variations in particle composition. In an aged sample of fluid, small



(a) SEM large area



(b) TEM local area.

Fig. 6.1.4 EDX spectra for magnetic fluids prepared from $[(\pi\text{-C}_5\text{H}_5)\text{Fe}(\text{CO})_2\text{Co}(\text{CO})_4]$

groups and chains of particles were examined. The technique which essentially gives a local area elemental analysis indicated iron:cobalt ratios of up to 3 and 4 to 1. This means a substantial proportion of particle iron content had been lost. It must be emphasized that the sample examined was several months old at the time of analysis and had been exposed to the atmosphere. Figure 6.1.4(b) shows a typical result for the examination of an area of well dispersed particles. It is the peak area which is of importance, this example has an elemental composition of Co (65.2%) and Fe (34.8%) i.e. the cobalt:iron ratio is 1.88:1. Throughout this work metallic ferrofluids have been found to be air/moisture sensitive, particularly iron containing particles. These results therefore follow the general trend of loss of iron from the particles with ageing, presumably into solution as a surfactant derivative.

6.1.4 Magnetic Data

Figure 6.1.5 shows the room temperature magnetization curves for the "iron-cobalt" fluids. All the curves are of a classical Langevin form, showing no hysteresis or coercivity. This is a characteristic of a superparamagnetic material. The saturation magnetizations (σ_{ff}^{∞}) derived from inverse field plots are presented in Table 6.1.2. The strongest of the fluids had a saturation magnetization about 30% of that of a commercial ferrite ferrofluid. In order to calculate values for the volume packing fraction, ϵ_v , and the magnetic particle size we must know M_b^{∞} , i.e. the

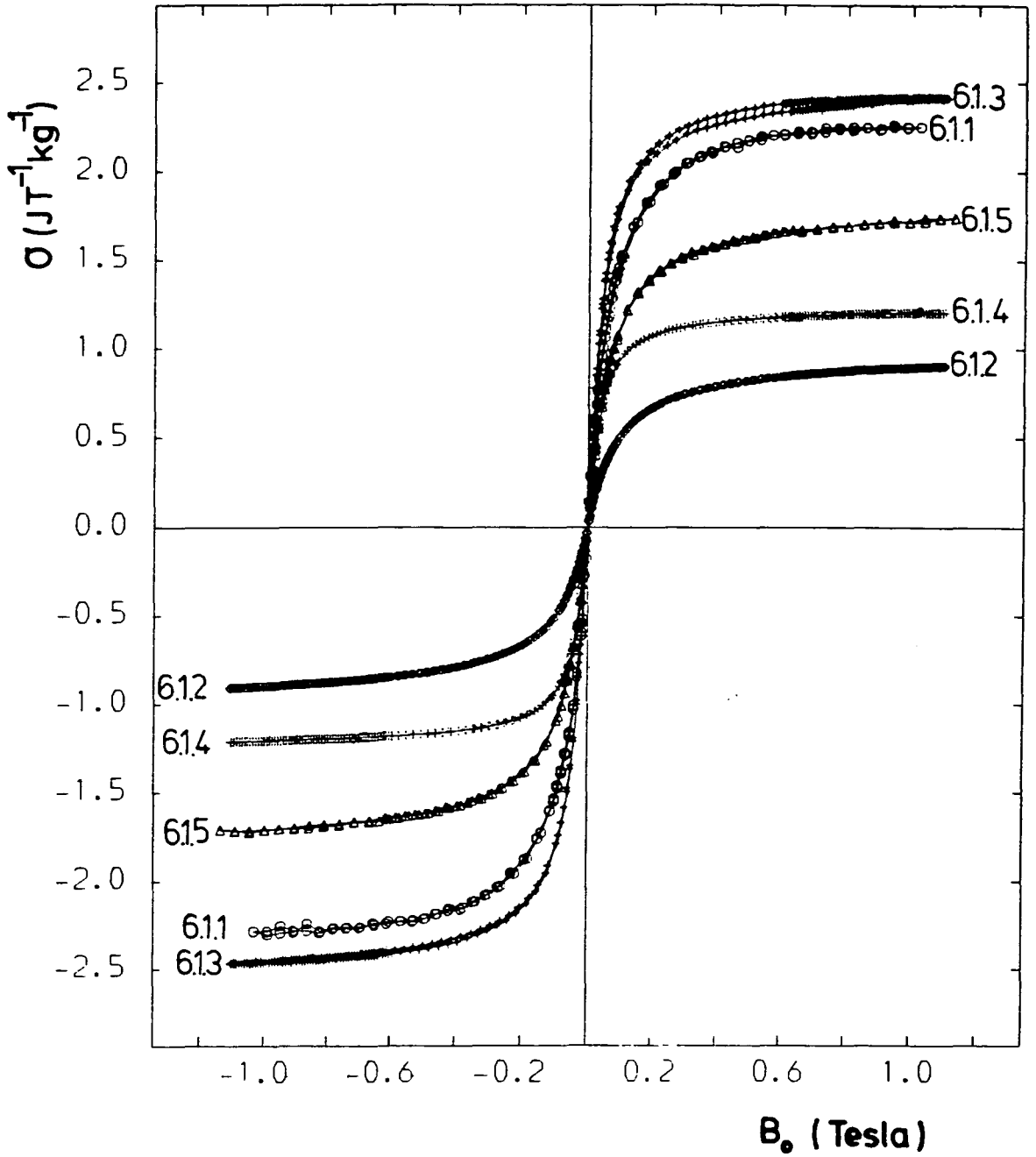


Fig. 6.1.5 Room temperature magnetization curves for iron-cobalt magnetic fluids 6.1.1, 6.1.2, 6.1.3, 6.1.4 and 6.1.5.

saturation magnetization of the bulk material per unit volume. For this a 1:1 iron-cobalt alloy was assumed for the freshly prepared material with the corresponding value of M_b^∞ of $1.899 \times 10^6 \text{ JT}^{-1} \text{ m}^{-3}$. The calculated values of ϵ_v , \bar{d}_v , \bar{d}_m and σ are given in Table 6.1.2. As with the single metal fluids there were considerable differences between \bar{d}_p and \bar{d}_m , the thickness of the dead layer, which for these fluids was of the order of 1.4nm.

A mass fraction for the fluids can be calculated easily from the magnetic data. Comparing this to the total mass of "FeCo" metal in the starting material gives the fraction of metal converted to the ferromagnetic state. For this series of preparations the degree of conversion was in the 10-25% range (cf. 35-62% for cobalt). It is feasible that whatever process was responsible for this low conversion to metal is also responsible for the loss of an even larger proportion of iron. Iron is more reactive than cobalt and will be more susceptible to both oxidation and reaction with surfactant.

6.2 Magnetic Fluids from $\text{HFeCo}_3(\text{CO})_{12}$

To extend the study of iron-cobalt magnetic fluids a second iron-cobalt containing organometallic carbonyl was utilized. $\text{HFeCo}_3(\text{CO})_{12}$ was chosen because of its similarity to $\text{Co}_4(\text{CO})_{12}$. In the preparation of cobalt ferrofluids from dicobalt octacarbonyl, tetracobalt dodecacarbonyl is an intermediate in the decomposition process.¹²⁰ Hence $\text{HFeCo}_3(\text{CO})_{12}$ ¹²⁰ would seem to be a logical choice of starting material, as it has a very similar structure to $\text{Co}_4(\text{CO})_{12}$.¹⁵⁰

6.2.1 Preparations

(i) Preparation of $\text{HFeCo}_3(\text{CO})_{12}$

$\text{HFeCo}_3(\text{CO})_{12}$ was first prepared by Italian workers.¹⁵¹

$\text{HFeCo}_3(\text{CO})_{12}$ was prepared by the reaction of iron pentacarbonyl with dicobalt octacarbonyl in propanone to produce $[\text{Co}(\text{CH}_3\text{CO}\cdot\text{CH}_3)_6]^{2+} [\text{FeCo}_3(\text{CO})_{12}]^{-}$, which was converted to $\text{HFeCo}_3(\text{CO})_{12}$. The resulting purple solid was confirmed as $\text{HFeCo}_3(\text{CO})_{12}$ by infra-red spectroscopy and by iron and cobalt content. Found: Fe, 9.19; Co, 29.21; $\text{HFeCo}_3(\text{CO})_{12}$ requires: Fe, 9.80; Co, 29.21%. Infra-red spectrum (hexane) $\bar{\nu}_{\text{CO}}$ (obs): 2061s, 2056s, 2030m, 1985m and 1880m. (lit)¹⁵²: 2059s, 2050m, 2026m, 1986m and 1885 cm^{-1} .

(ii) Ferrofluid Preparation

Ferrofluids were prepared readily from $\text{HFeCo}_3(\text{CO})_{12}$ by decomposing it in toluene solution containing a surfactant. The apparatus and technique used for the reaction were the same as used for producing cobalt fluids (see 5.1.1(i)). A pre-heated oil bath was used to bring the mixture to a rapid reflux. Heating produced an extremely rapid evolution of carbon monoxide, the decomposition being normally complete within 10 minutes, although heating was continued for one hour to ensure complete destruction of the carbonyl. After the reaction was complete the flask was allowed to cool to room temperature under nitrogen. The black magnetically responsive liquid products were transferred by syringe through a serum cap to a storage vessel and kept under

TABLE 6.2.1

Preparative details for magnetic fluids prepared

from $\text{HFeCo}_3(\text{CO})_{12}$ and $[\text{Co}(\text{CH}_3\text{COCH}_3)_6]^{2+}[\text{Co}_3\text{Fe}(\text{CO})_{12}]_2^-$

Fluid	Mass of $\text{HFeCo}_3(\text{CO})_{12}$	Surfactant	Mass of Surfactant (g)	Vol. of Toluene (cm^3)
6.2.1	0.8169	Duomeen-TDO	0.5856	10.0
6.2.2	0.8139	Solsperse-3000	0.6957	10.0
6.2.3	0.8578	Sarkosyl-O	0.5060	10.0
6.2.4	0.9431*	Sarkosyl-O	0.5007	10.0

*Denotes use of $[\text{Co}(\text{CH}_3\text{COCH}_3)_6]^{2+}[\text{Co}_3\text{Fe}(\text{CO})_{12}]_2^-$

nitrogen while awaiting further analysis. Table 6.2.1 summarizes the successful ferrofluid preparations. Use of surfactants Manoxol-OT and oleic acid in toluene as carrier liquid was found to be unsuccessful in producing a magnetic colloid. Preparations in which petroleum ether (b.p. 100-120°C) replaced toluene as the decomposition medium were all unsuccessful. The table includes the preparation of fluid 6.2.4 which was prepared from $[\text{Co}(\text{CH}_3\text{CO}\cdot\text{CH}_3)_6^{2+}][\text{FeCo}_3(\text{CO})_{12}^-]_2$ rather than $\text{HFeCo}_3(\text{CO})_{12}$. This preparation was attempted to determine if the presence of the cation $[\text{Co}(\text{CH}_3\text{CO}\cdot\text{CH}_3)_6^{2+}]$ interfered with the decomposition process.

6.2.2 TEM Analysis

Samples of the four ferrofluids in Table 6.2.1 were diluted in toluene and examined on carbon coated copper grids using transmission electron microscopy. In all cases except fluid 6.2.2 electron microscopy revealed well dispersed discrete particles. Shadow electron micrographs were taken at a magnification of 220,000. These were enlarged and analysed using the electro-optic image size analyser described in section 4.2.4. The physical particle size distributions are shown in Figure 6.2.1. The particles are in the 6-8nm size range, with characteristically small standard deviations (uniform size) produced by the organometallic decomposition route.

In fluid 6.2.2. electron microscopy revealed massive aggregates consisting of several thousands of particles.

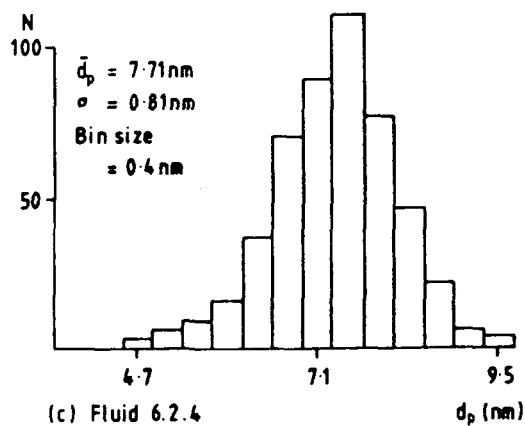
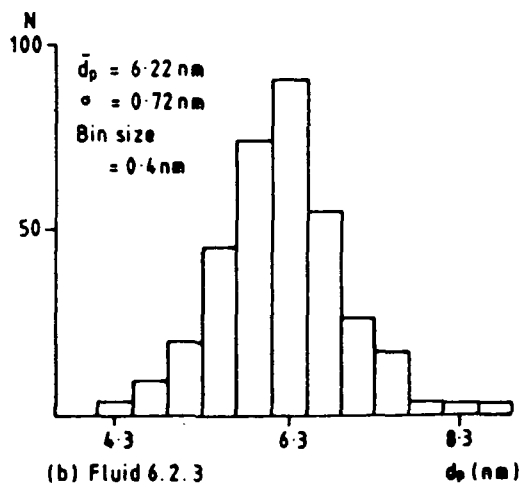
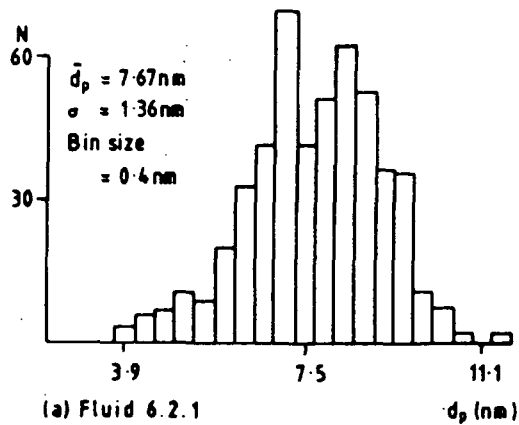


Fig. 6.2.1 Physical particle size distributions for iron-cobalt fluids 6.2.1, 6.2.3 and 6.2.4.

TABLE 6.2.2

Magnetic and Particle Size data for
Fluid 6.2.1, 6.2.2, 6.2.3 and 6.2.4

Fluid	TEM Data		σ_{ff}^{∞} ($\text{JT}^{-1}\text{Kg}^{-1}$)	$\bar{d}_{1/2}$ (nm)	\bar{d}_m (nm)	σ (nm)
	d_p (nm)	S.Dev (nm)				
6.2.1	7.67	1.36	5.91	5.80	4.77	0.28
6.2.2	Aggregates Observed		1.96	4.62	3.90	0.26
6.2.3	6.22	0.72	-	-	-	-
6.2.4	7.31	0.81	-	-	-	-

The particles appeared to be enmeshed together in a "gel" like medium. This observation was consistent with the general appearance of this fluid which contained black sediment within hours of preparation. Both sediment and liquid fractions were visibly magnetic. It seems as if metal particles were being produced initially but the surfactant Solsperse-3000 does not stabilize the majority of the particles in suspension. The particles then become enmeshed in the unused surfactant producing aggregates too large to remain in suspension which sediment out of suspension.

Note that there is little difference in mean diameter of particles for fluids 6.2.3 and 6.2.4 prepared from different starting materials, indicating that the use of $[\text{Co}(\text{CH}_3\text{CO}\cdot\text{CH}_3)_6]^{2+}[\text{FeCo}_3(\text{CO})_{12}]_2^-$ makes little difference to the preparation.

6.2.3 Composition and Structure

(i) Electron Diffraction

Four individual unsuccessful attempts were made to obtain an electron diffraction pattern for this series of fluids. On every occasion faint and diffuse diffraction lines were observed using the electron microscope. Unfortunately these patterns could not be photographically recorded with sufficient clarity to determine the particle structure.

(ii) Local Area EDX Spectroscopy

The vital evidence that alloy particles were produced

from $\text{HFeCo}_3(\text{CO})_{12}$ comes from local area EDX spectroscopy. A fresh sample of ferrofluid was prepared as described in 6.2.1(ii) specifically for this study. The work was carried out in conjunction with J. Chapman of Glasgow University. A HP4 high resolution electron microscope was employed for the analysis.

Each "spectrum" collected consisted of number of counts of X-rays characteristic (by energy) of the elements cobalt and iron. In all cases the counts were accumulated over a 60 second sampling time. Using this procedure, regions of isolated particles, particles in and near aggregates and even single particles could be analysed. The data collected is corrected for background.

Figure 6.2.2 presents the data collected in a graphical form. The results of each EDX spectrum obtained are represented by a point. The position of each point depends on the number of counts for iron (ordinate) and cobalt (abscissa). The points are numbered and the corresponding cobalt:iron ratio for this "spectrum" is given in Table 6.2.3.

From these observations we can conclude that the particles have a mixed metal composition. The spectra of both single particles and regions of well dispersed discrete particles show a cobalt:iron ratio of almost 3:1. Hence reproducing the starting material cobalt:iron ratio. It is interesting that analysis of particles in the aggregates consistently show a cobalt content in excess of the expected

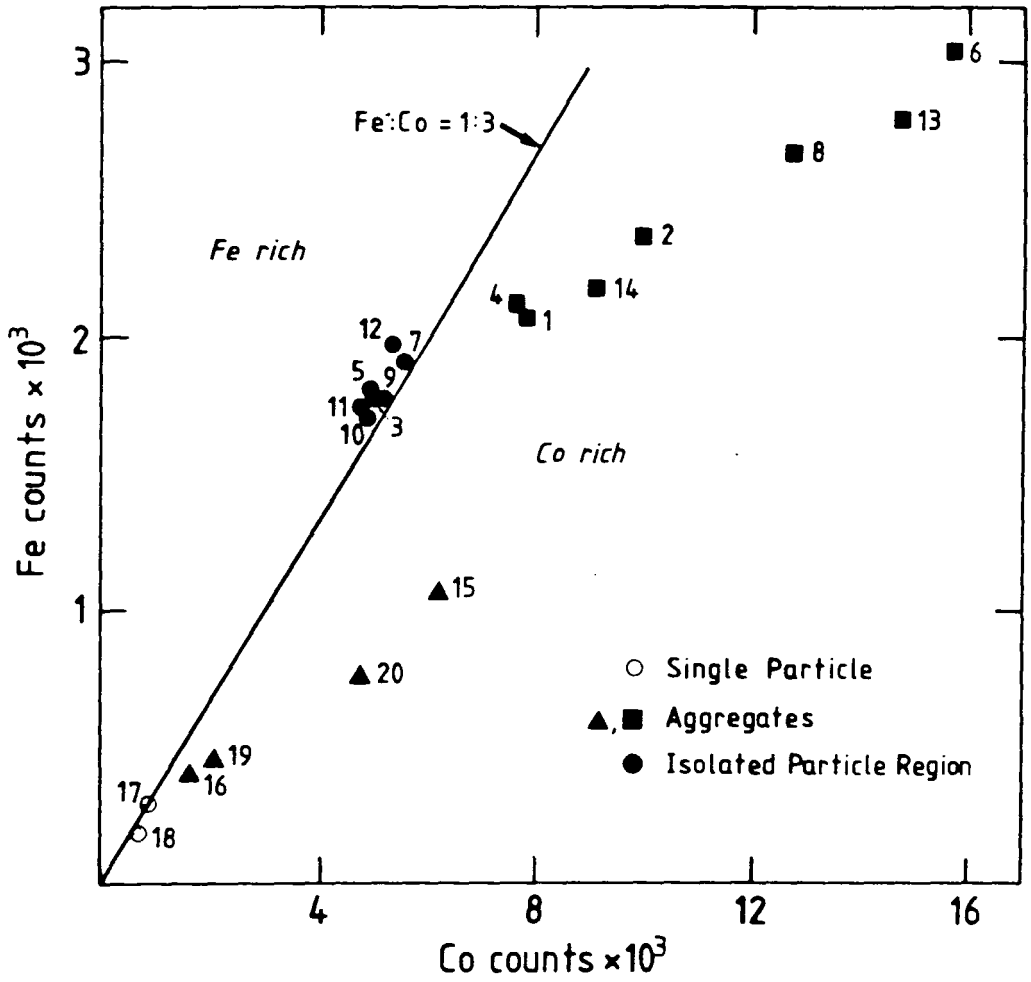


Fig. 6.2.2 Local area EDX data for a magnetic fluid prepared from $\text{HFeCo}_3(\text{CO})_{12}$, each point represents a separate EDX spectrum.

TABLE 6.2.3

Local Area EDX data for a magnetic fluid

prepared from $\text{HFeCo}_3(\text{CO})_{12}$

Spectrum No.	Co:Fe	Type of Region
1	3.85	A
2	4.30	A
3	2.88	IP
4	3.66	A
5	2.79	IP
6	5.26	A
7	2.93	IP
8	4.85	A
9	3.01	IP
10	2.89	IP
11	2.81	IP
12	2.80	IP
13	5.37	A
14	4.28	A
15	5.83	A
16	4.08	A
17	2.73	SP
18	3.58	SP
19	4.75	A
20	6.34	A

A : Aggregate Region

IP : Region of Isolated Particles

SP : Single Particle analysed

cobalt:iron ratio of 3:1. Loading samples into the electron microscope involves unavoidable exposure to air. Some oxidation of the sample is expected, but this does not explain the high cobalt content of the particles in or near aggregates. An excess of cobalt or deficit of iron was also observed in the iron-cobalt particles discussed in the previous section. In general iron loss during decomposition might be explained by (i) preferential oxidation of iron, (ii) a higher reactivity towards surfactant or (iii) formation and loss of a volatile or thermally stable iron species. However, why this loss of iron appears to occur predominantly in particles in aggregates for ferrofluids prepared from $\text{HFeCo}_3(\text{CO})_{12}$ is not immediately apparent.

One possible explanation may be connected with the dilution of the ferrofluid. It is necessary to dilute the sample of ferrofluid (with carrier liquid) prior to electron microscopic (and EDX) examination. Chantrell et al.¹⁵³ have studied the dilution induced instability of ferrofluids. Dilution of the ferrofluid disturbs the equilibrium between the surfactant adsorbed onto the particle surface and "free" surfactant in the bulk solution. On dilution the concentration of surfactant in solution is lowered, this causes surfactant adsorbed on the particle surface to desorb and restore equilibrium between "free" and adsorbed surfactant.

From the results of the infra-red spectroscopic study of cobalt ferrofluids described earlier in this work

(section 5.3), we believe that all of the surfactant molecules are converted to some form of cobalt derivative during the decomposition process. It is reasonable to assume that this will also occur for the ferrofluids prepared from $\text{HFeCo}_3(\text{CO})_{12}$, i.e. all the surfactant is converted to cobalt and iron surfactant "derivatives" (we are not specifying the form of these derivatives). In the starting material $\text{HFeCo}_3(\text{CO})_{12}$ there is a cobalt:iron ratio of 3:1. If this ratio is reproduced in the particles formed initially, as is implied by the EDX spectra of the dispersed particles, then the metal-surfactant species in solution will also be produced in a cobalt:iron ratio of 3:1. Dilution will cause surfactant adsorbed on the particle surface to be desorbed. If surfactant molecules desorb associated with a metal atom (as we would expect in a non-polar medium), then we can explain loss of metal atoms from the particle surface. If the iron-surfactant species desorb preferentially then this will increase the proportion of cobalt in the particles, and increase the proportion of iron-surfactant species in solution. If particle aggregation occurs before this desorption mechanism has reached equilibrium, then the aggregates would consist of particles richer in cobalt content. The experimental observation that particles in the aggregates are richer in cobalt than in the dispersed (isolated) particles is difficult to explain, hence this explanation or any alternative can only be speculative.

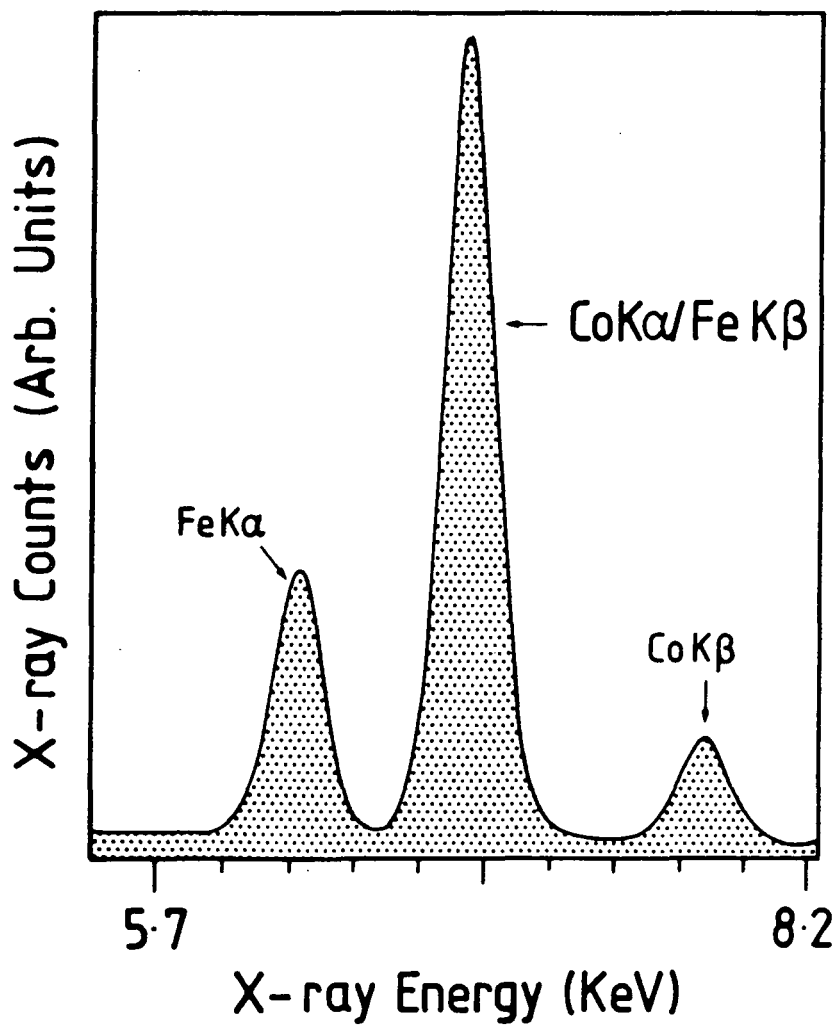


Fig. 6.2.3 SEM EDX (large area) spectrum for a magnetic fluid prepared from $\text{HFeCo}_3(\text{CO})_{12}$

Large area ($\sim 5\text{mm}^2$) SEM EDX analysis (Figure 6.2.3) indicated that the overall cobalt:iron ratio for a sample of fluid was 3:1 as expected. Iron and cobalt widely dispersed in soluble form in the carrier liquid would also be detected by this technique.

6.2.4 Magnetic Measurements

The room temperature magnetization curves for fluids 6.2.1 and 6.2.2 are shown in Figure 6.2.4. The data extracted from these curves i.e. σ_{ff}^∞ , \bar{d}_p , \bar{d}_m and σ are given in Table 6.2.2. For these calculations a value of $M_b^\infty = 1.6 \times 10^6 \text{JT}^{-1} \text{m}^{-3}$ is assumed which is the value for the Co_3Fe alloy. It is found that fluid 6.2.1 is a magnetically "strong" fluid. It is interesting to compare the relative values of σ_{ff}^∞ for fluids 6.2.1 and 6.2.2 since both fluids are prepared from virtually the same concentration of $\text{HFeCo}_3(\text{CO})_{12}$, and for which similar values of σ_{ff}^∞ would be expected. The factor of 3 difference is almost definitely connected with the sedimentation of fluid 6.2.2., which leaves a colloid more dilute in metal content with a corresponding lower saturation magnetization.

The proportion of metal atoms in the carbonyl compound converted to metal in the ferromagnetic state is very favourable for fluid 6.2.1. By calculating the initial mass of " Co_3Fe " which could be converted to the ferromagnetic state and comparing this to the mass of " Co_3Fe " in the fluid, calculated from σ_{ff}^∞ we find that $\sim 84\%$ conversion has taken place. This compares very favourably with the cobalt

C03FE

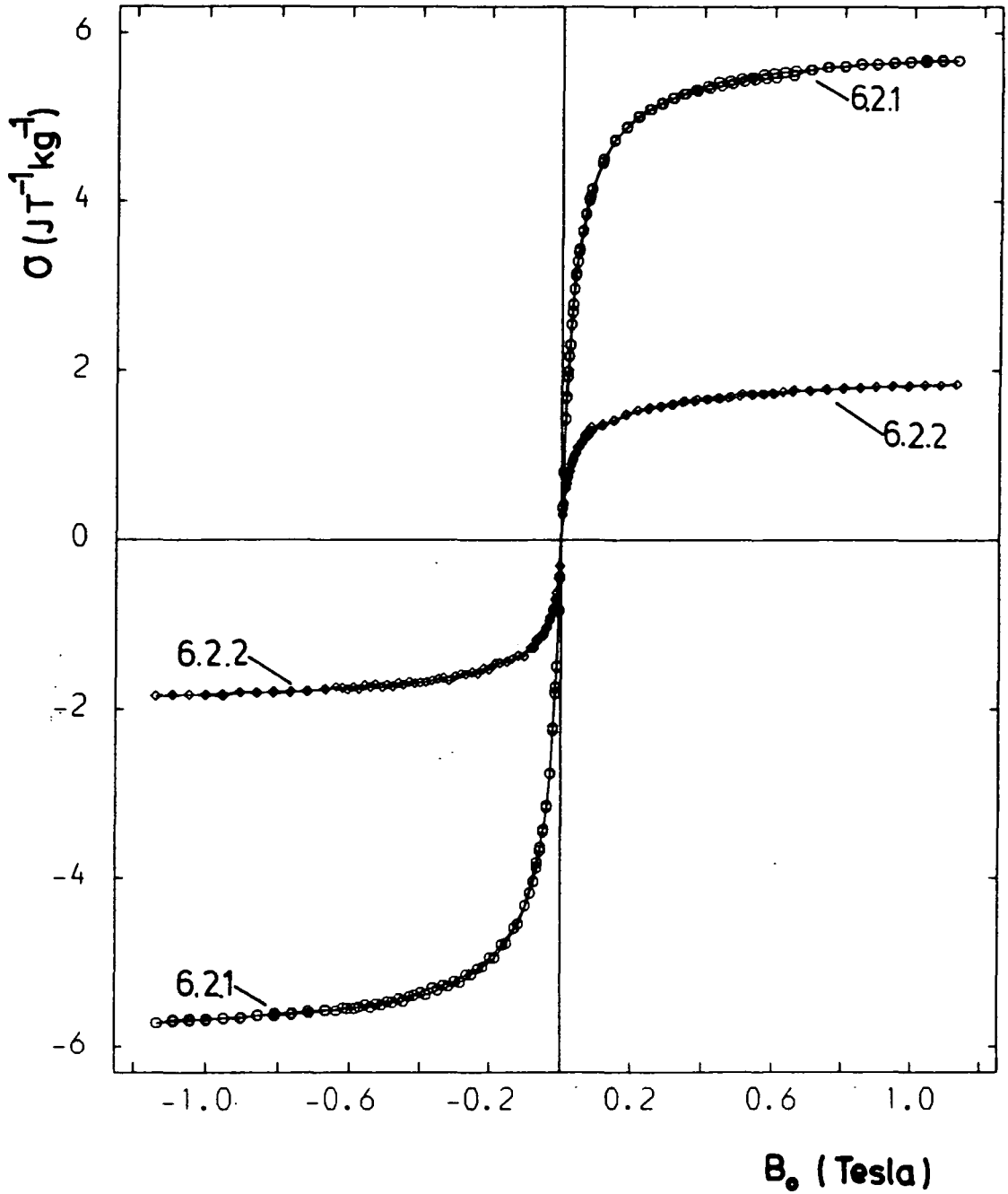


Fig. 6.2.4 Room temperature magnetization curves for iron-cobalt fluids 6.2.1 and 6.2.2.

fluids reported in the previous chapter.

6.2.5 Kinetics of $\text{HFeCo}_3(\text{CO})_{12}$ Decomposition

Tetracobalt dodecacarbonyl ($\text{Co}_4(\text{CO})_{12}$) is produced during the thermal decomposition of $\text{Co}_2(\text{CO})_8$ in the preparation of cobalt magnetic fluids. This explains the rapid evolution of the first 25% of the total carbon monoxide content during decomposition (see Chapter 3). Tetracobalt dodecacarbonyl then decomposes more slowly to cobalt metal.

Since $\text{HFeCo}_3(\text{CO})_{12}$ is very similar to $\text{Co}_4(\text{CO})_{12}$ it will be of interest to compare the evolution of carbon monoxide from $\text{HFeCo}_3(\text{CO})_{12}$ with evolution from $\text{Co}_4(\text{CO})_{12}$, or rather from $\text{Co}_2(\text{CO})_8$ after the first 25% of carbon monoxide has been evolved. For this purpose a magnetic fluid was prepared from $\text{HFeCo}_3(\text{CO})_{12}$ with Sarkosyl-0 as the surfactant in the normal way. The evolved carbon monoxide was collected over water, and as in section 5.1.5 the solubility of carbon monoxide in water was ignored. In the preparation of fluids from $\text{HFeCo}_3(\text{CO})_{12}$ described in sub-section 6.2.1(ii), very rapid carbon monoxide evolution was observed. Indeed, this study recorded that carbon monoxide evolution was complete after ~ 7 minutes with approximately 95% of the total possible carbon monoxide being evolved. Figure 6.2.5(a) shows % carbon monoxide evolved plotted against time. Plotted in Figure 6.2.5(b) is the equivalent curve for the cobalt fluid 5.1. This curve is for comparative purposes and shows the 25-100% carbon monoxide

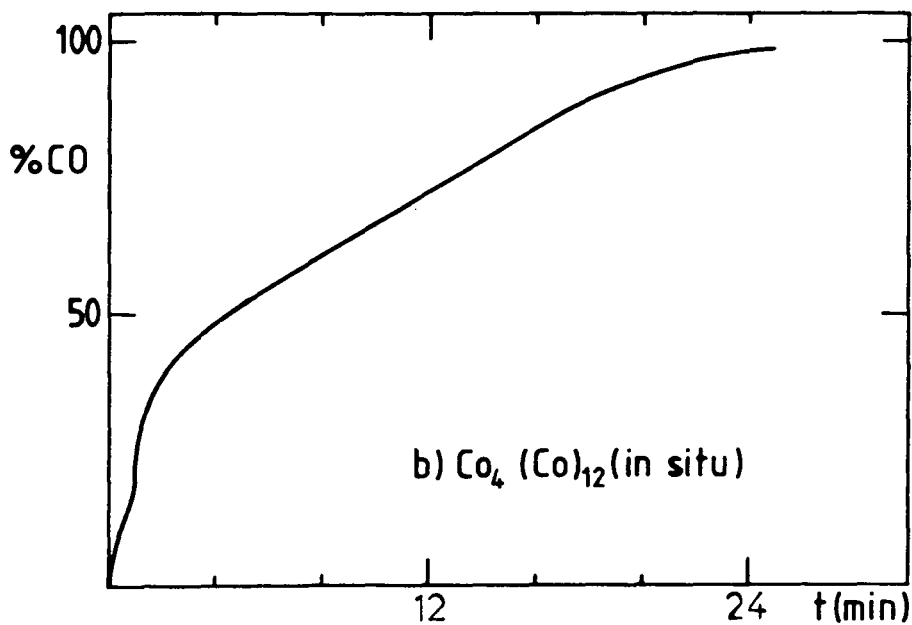
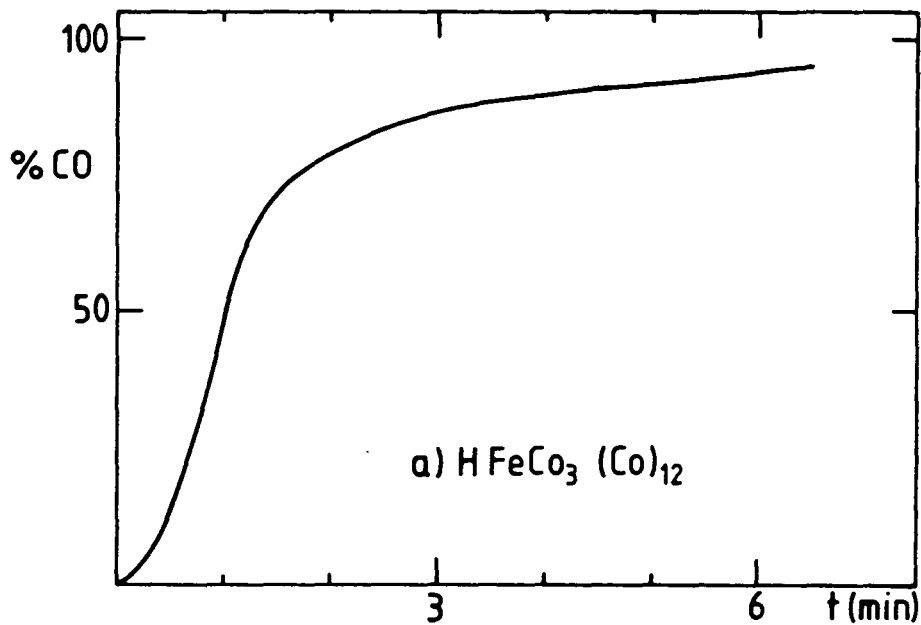


Fig. 6.2.5 %CO evolved plotted against time for
 (a) $\text{HFeCo}_3(\text{CO})_{12}$ /Sarkosyl-O/toluene.
 (b) " $\text{Co}_4(\text{CO})_{12}$ "/Sarkosyl-O/toluene
 (i.e. $\text{Co}_2(\text{CO})_8$ after 25% decomposition).

evolution portion of the curve, i.e. the portion associated with the decomposition of $\text{Co}_4(\text{CO})_{12}$. The curves do differ in appearance even with different scales on the abscissa which accommodate the differing lengths of time taken to reach complete decomposition. However, the decomposition of $\text{HFeCo}_3(\text{CO})_{12}$ is so rapid that any minor details in appearance of the curve shape may be "smoothed" out. It is distinctly possible that a complex decomposition process is in operation as with $\text{Co}_2(\text{CO})_8/\text{Co}_4(\text{CO})_{12}$ systems.¹²¹ Analogously, $\text{HFeCo}_3(\text{CO})_{12}$ could be concentrated into "microreactors" by the surfactant. In these microreactors a series of complex intermediates such as a toluene- $\text{Fe}_n\text{Co}_m(\text{CO})_x$ complex can form. Once a particle nucleation site has been formed both $\text{HFeCo}_3(\text{CO})_{12}$ and "complex" species can decompose on these sites, leading to particle growth. The particle growth period would explain the almost linear section of the curve between ~15 and 65% carbon monoxide evolution, the rate of this process being limited by the rate of desorption of carbon monoxide from the particle surface (a zero order process). After ~70% carbon monoxide evolution the curve indicates a slowing down of the process, consistent with a drop in "carbonyl" species concentration.

Alternatively the process occurs so rapidly that a completely different mechanism is operating. Possibly there are no aggregates/microreactors of $\text{HFeCo}_3(\text{CO})_{12}$ to limit the rate of decomposition; rather many nucleation sites are simultaneously formed by rapid destruction of solution

molecular $\text{HFeCo}_3(\text{CO})_{12}$ to form small metal clusters. These clusters can then act as sites to which other molecules diffuse and decompose. This process would also give a rapid and constant rate of carbon monoxide evolution which would tail off as the reagent became depleted. Without further information it is not immediately obvious which process is in operation.

6.3 Other Work

6.3.1 Attempted Thermal Decomposition of $\text{PNP}^+\text{FeCo}(\text{CO})_8^-$

Dicobalt octacarbonyl is the most established organometallic compound in use for preparing magnetic fluids by thermal decomposition. The anion $\text{FeCo}(\text{CO})_8^-$ ¹⁵⁴ is isoelectronic and is believed to have a similar structure to $\text{Co}_2(\text{CO})_8$ and would therefore be an ideal choice of organometallic compound from which to prepare iron-cobalt magnetic fluids.

The PNP^+ derivative was prepared from $\text{PNP}^+\text{Co}(\text{CO})_4^-$ ¹⁵⁵ and $\text{Fe}(\text{CO})_5$, a UV reaction in T.H.F. solution. The solid red compound $\text{PNP}^+\text{FeCo}(\text{CO})_8^-$ was virtually insoluble in a range of hydrocarbon solvents. Consequently several attempts to thermally decompose the ionic compound to metal proved unsuccessful. Presumably the presence of the bulky cation along with the insolubility explain the lack of success with this particular reagent.

To overcome the problem it may be possible to replace the cation in order to increase the solubility in organic

solvents. Attempts to prepare a surfactant derivative of $\text{FeCo}(\text{CO})_8$ proved unsuccessful.

6.3.2 Simultaneous Thermal Decomposition of Single Metal Carbonyls

Several attempts to thermally decompose dicobalt octacarbonyl and triiron dodecacarbonyl simultaneously proved unsuccessful in producing a mixed-metal iron-cobalt magnetic fluid. In each experiment a magnetic fluid was produced but electron diffraction analysis showed that the particles obtained were only cobalt.

The different thermal stabilities of the two compounds would explain the lack of iron, i.e. dicobalt octacarbonyl decomposes preferentially. These experiments emphasize the need to use specially prepared organometallic compounds to prepare alloy particle magnetic fluids.

6.4 Discussion and Conclusion

The results reported in this chapter are very significant in the field of magnetic fluids. It is the first time truly colloidal hydrocarbon based magnetic fluids containing alloy particles have been produced. The results show that the "carbonyl" or now more strictly "organometallic" route can be extended to include heteronuclear organometallics. In the next chapter this strategy will be applied to the preparation of the first nickel-iron magnetic fluids.

There are several additional points of interest which are demonstrated by these studies. The role of the surfactant is obviously more than the colloidal stabilization of the ferrofluids. The surfactant is observed to influence the effectiveness of the conversion of "molecular" metal atoms to particulate metal. Also the role of the surfactant in having some control over particle size is demonstrated (cf. fluids 6.1.3 and 6.1.4).

The difference between the amount of ferromagnetic metal present in the fluids (calculated from σ_{ff}^{∞}) and the theoretical amount calculated from the mass of organometallic is a challenging problem. The loss of iron content is likewise difficult to explain. To rationalize these observations the decomposition process would have to be followed. This would be difficult as decomposition occurs very quickly and we would predict complex mixtures of unknown species (and fragments) in low concentrations. The most plausible way to follow such a process would be via solution infra-red spectroscopy. Even here there would be severe difficulties as only species with very strong absorption bands would be likely to show up against the hydrocarbon solvent background. For example species such as ferrocene which may be produced in the decomposition of $[(\pi-C_5H_5)Fe(CO)_2Co(CO)_4]$ would be unlikely to be observed in low concentrations against a toluene background. In addition only species which survive the decomposition process (i.e. 1-3 hours at 110.6°C) would be present. Although the

aim of the study was to prepare and characterize the first iron-cobalt magnetic fluids, it would be interesting to understand what is happening during the decomposition process.

A result relevant to this question came from vacuum transfer of the volatile material from a sample of ferrofluid prepared from $[(\pi\text{-C}_5\text{H}_5)\text{Fe}(\text{CO})_2\text{Co}(\text{CO})_4]$. This sample was faintly orange in colour. GLC analysis indicated that the sample was almost pure toluene with a trace of "impurity". Infra-red spectroscopy and further GLC work showed this orange species to be iron pentacarbonyl which could arise from the initial decomposition process or from reaction of particulate iron with carbon monoxide.

In the future it would be interesting to evaporate iron-cobalt alloys into hydrocarbon surfactant solutions, primarily to discover if alloy particle magnetic fluids can be prepared in this way. Secondly, further investigations to determine whether alloy composition can be varied and controlled are of importance. Finally, a comparison of the particle structures with those of the particles in this chapter is of interest.

CHAPTER 7

NICKEL-IRON MAGNETIC FLUIDS

Introduction

In this chapter the application of heteronuclear organometallic compounds to alloy particle magnetic fluid synthesis is extended to the nickel-iron system. A nickel-iron particle fluid is of interest because the nickel-iron alloy has magnetic properties dependent on alloy composition, in particular Curie temperature¹⁵⁷ and magnetocrystalline anisotropy.¹⁵⁷ Nickel-iron particles have been electrodeposited into mercury for this very purpose.^{107,108} This short yet compact chapter reports a study of the first hydrocarbon based nickel-iron ferrofluids, which were prepared from a cyclopentadienyl nickel-iron carbonyl compound.

7.1 Fluid Preparation

The ferrofluids to be discussed in this chapter were all prepared from the trinuclear cluster $[(\pi-C_5H_5)_2Ni_2Fe(CO)_5]$. This dark green solid compound was prepared by the reaction of $[\pi-C_5H_5Ni(CO)]_2$ with $Fe_2(CO)_9$ in light petroleum (b.p. 60-80°C) as described by Hsieh and Knight.¹⁵⁸ Due to the nature of the preparative method only

small ($\sim 0.5\text{g}$) quantities of the trinuclear species could be synthesized at a time. Hence repeated preparations were required to build up a sufficient supply of starting material for fluid preparations. The compound is reported to be reasonably air-stable in the solid state while solutions deteriorate in air. On handling the material, air sensitivity and high toxicity were assumed.

Figure 7.1 shows the probable structure proposed by Hsieh and Knight¹⁵⁸ as deduced from infra-red spectroscopy.

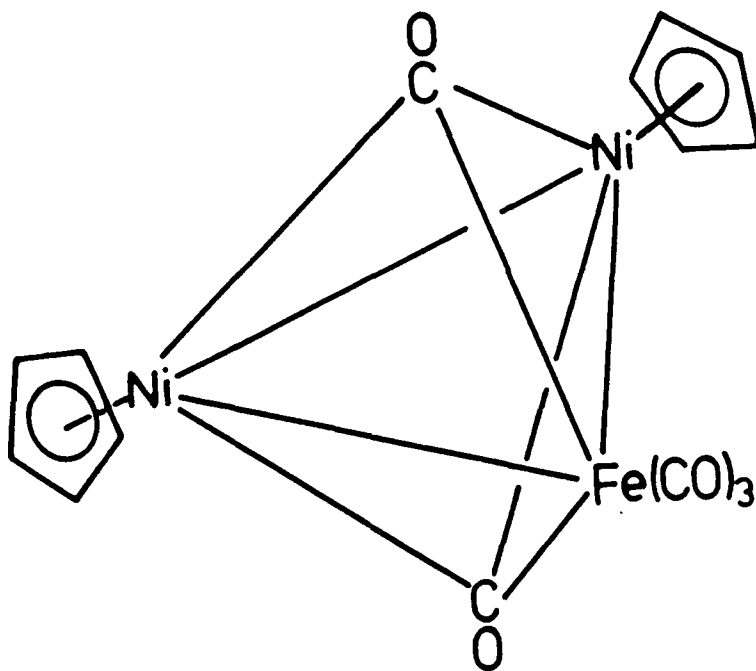


Fig. 7.1 Proposed structure of $[(\pi\text{-C}_5\text{H}_5)_2\text{Ni}_2\text{Fe}(\text{CO})_5]^{158}$

Magnetic fluids were prepared by the thermal decomposition of $[(\pi\text{-C}_5\text{H}_5)_2\text{Ni}_2\text{Fe}(\text{CO})_5]$ in hydrocarbon carrier liquid/surfactant solutions. A 3-necked round bottomed 100cm^3 flask was used as the reaction vessel,

fitted with teflon paddle stirrer, reflux condenser and a gas inlet. Air sensitivity of the complex was assumed throughout.

The first attempts to prepare nickel-iron fluids employed the use of toluene as carrier liquid because of the success with this solvent in preparing cobalt and iron-cobalt ferrofluids. However, after several hours of refluxing, the solutions remained green with no evidence that a successful decomposition had occurred. The organometallic compound is presumably stable at 110.6°C. Subsequent attempts involved the use of hydrocarbon solvents with higher boiling points. Both petroleum ether (b.p. 200-260°C) and 1-methyl-naphthalene (b.p. 242.6°C) were found to be satisfactory carrier liquids.

To achieve decomposition, higher temperatures were required and a molten metal bath was employed as the heat source. At metal bath temperatures in the 170-210°C range the green solution turned black and gas evolution took place. The gas evolution was slower than for the cobalt and iron-cobalt systems discussed in the previous two chapters. Gas evolution is not assisted by the refluxing of the solvent since the reaction temperature is below the solvent boiling point.

Details of carrier liquid, surfactant and reaction conditions are gathered in Table 7.1. In each case a black liquid was the product which was weakly magnetically responsive.

TABLE 7.1

Preparative details for magnetic fluids prepared from $[(\pi\text{-C}_5\text{H}_5)_2\text{Ni}_2\text{Fe}(\text{CO})_5]$

Fluid	Mass of Complex (g)	Surfactant	Mass of Surfactant (g)	Carrier Liquid	Vol. of Carrier Liquid (cm ³)	Metal Bath Temp. (°C)	Reaction Time (hrs)
7.1	0.7018	Manoxol-OT	0.4542	1-m-N	10.0	170	3
7.2	0.6027	Sarkosyl-O	0.3654	1-m-N	10.0	170-180	3.5
7.3	0.4482	Sarkosyl-O	0.4152	1-m-N	15.0	200-205	5.5
7.4	0.5683	Sarkosyl-O	0.4212	Pet.Eth.	10.0	200-210	3
7.5	0.4550	Duomeen-TDO	0.4544	1-m-N	10.0	170-180	3

1-m-N = 1-methyl naphthalene

Pet.Eth = Petroleum Ether (200-260°C)

7.2 Particle Size Analysis

Samples of each ferrofluid were diluted in their relevant carrier liquid and examined using electron microscopy in the usual way. For fluids 7.1-7.4 roughly spherical particles were observed which were clearly well dispersed. In fluid 7.5 large aggregates were observed at a magnification of 28,000. Electron micrographs were taken of fluids 7.2-7.4 at a magnification of 220,000 and examined to give particle size distributions. Figure 7.2 shows the physical size distributions for the ferrofluids 7.2 to 7.4. All the distributions appear to be Gaussian, with narrow size ranges. The mean physical particle sizes and standard deviations are given in Table 7.2. The reaction conditions, i.e. the choice of solvent, temperature, and duration of heating, do not appear to significantly effect the particle size in the fluids examined, all the diameters being in the 7-8nm range.

7.3 Particle Structure and Composition

7.3.1 Electron Diffraction

As with the iron-cobalt alloy particles discussed in the previous chapter it is essential to prove that the particles formed in the fluids prepared in section 7.1 have an alloy composition. Figure 7.3 is a print of a diffraction pattern obtained from transmission electron diffraction analysis of one of the ferrofluids (fluid 7.2).

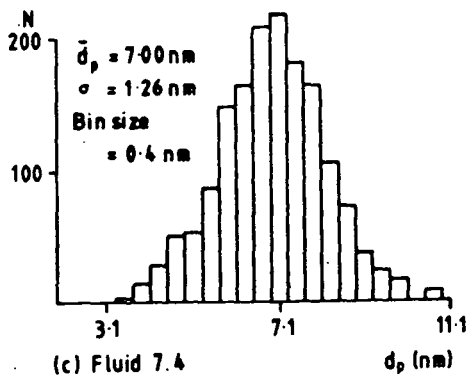
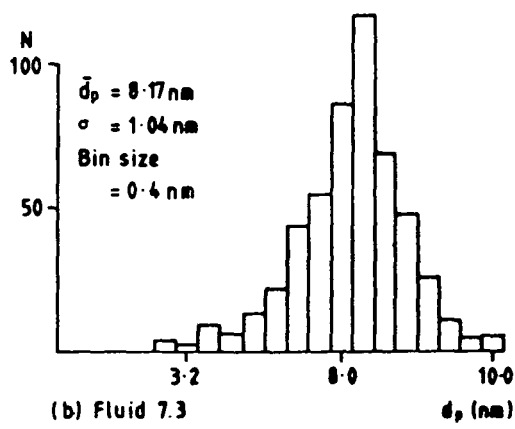
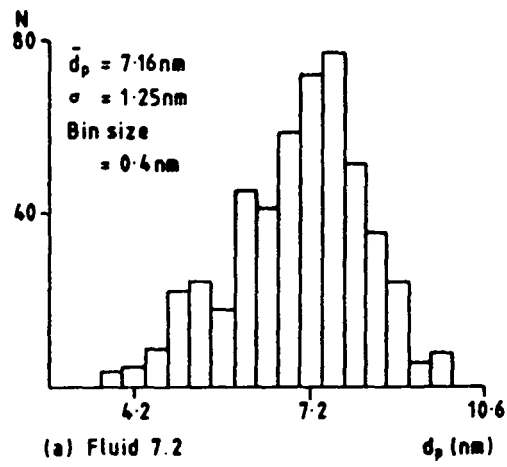


Fig. 7.2

Physical particle size distributions for nickel-iron fluids 7.2, 7.3 and 7.4.

TABLE 7.2

Magnetic and Particle Size data for Ni-Fe

Magnetic Fluids

Fluid	\bar{d}_p (nm)	S.Dev (nm)	σ_{ff}^{∞} (JT ⁻¹ Kg ⁻¹)	\bar{d}_m (nm)	σ (nm)
7.1	-	-	0.572	4.8	1.79
7.2	7.16	1.25	0.386	3.2	0.74
7.3	8.17	1.04	0.224	2.8	1.03
7.4	7.00	1.26	0.287	3.7	0.98

Fig. 7.3 Electron diffraction pattern for the nickel-iron system



Seven lines can be analysed but do not ratio clearly as fcc or bcc structures. An fcc or bcc structure would be expected, as nickel and nickel-iron alloys have fcc structures while iron has a bcc structure. If the calculated d-spacings are fitted to a fcc structure, then the values of the lattice parameter are distributed about an average of $\sim 4.8\overset{\circ}{\text{Å}}$. This value is incompatible with any nickel, iron or nickel-iron lattices.

However, in bulk nickel-iron alloys with approximately 75% nickel content an ordered superlattice has been detected by X-ray diffraction.^{159,160} If we allow for the extra reflections due to the superlattice (cf. section 6.1.3) and include the reflections (110), (210) and (211) into the indexing scheme then a lattice parameter of $\sim 3.56\overset{\circ}{\text{Å}}$ is obtained. This is in excellent agreement with the value obtained by Leech and Sykes¹⁵⁹ ($a_0 = 3.544\overset{\circ}{\text{Å}}$) using X-ray diffraction on bulk alloys. Table 7.3 gives the calculated d-spacings, their hkl assignments and denotes which lines are due to the superlattice. The superlattice reflection (100) is likely to be present but unresolved in the bright centre of the diffraction pattern.

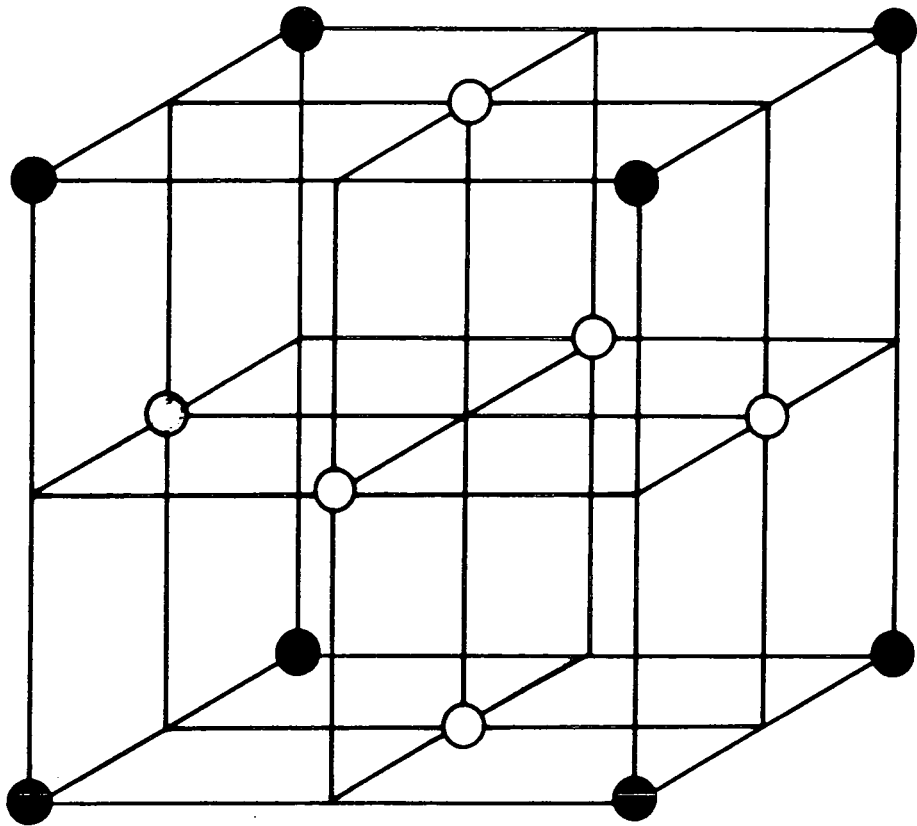
In nickel-iron bulk alloys the ordered phase occurs in the region at 75% nickel content, i.e. a superlattice structure exists for compositions around a nickel:iron ratio of 3:1. Therefore there will almost certainly be some slight variations in particle compositions even though the superlattice structure is maintained. In short, the

TABLE 7.3

Electron Diffraction data for the Ni-Fe system

$d(\text{\AA})$	hkl
2.49	110*
2.06	111
1.76	200
1.60	210*
1.48	211*
1.26	220
1.07	311

* Denotes superlattice reflection



● = Fe

○ = Ni

Fig. 7.4 Ni_3Fe superlattice unit cell.

particles have an ordered "superlattice" structure of composition Ni_xFe , where $x \approx 3$.

The Ni_3Fe lattice is an overall fcc structure, but consists of four interpenetrating simple cubic systems. Figure 7.4 shows the lattice unit cell which consists of four atoms. Iron atoms are positioned at the corners in the perfectly ordered structure, while nickel atoms occupy the faces.

One disturbing consequence of this result is the difference in the nickel:iron ratio in the starting material and in the final alloy particles, namely a change from 2:1 to 3:1. Again a loss of iron content on decomposition is evident. There are some similarities with the iron-cobalt work but the iron discrepancy here is more extreme.

7.3.2 EDX Spectroscopy

Large area SEM EDX spectroscopy showed the fluids to have an overall Ni:Fe composition of approximately 2:1 (Figure 7.5). Hence the "missing" iron appears to have remained in the fluid (as opposed to having been lost as a volatile iron species, e.g. $\text{Fe}(\text{CO})_5$).

A sample of a "nickel-iron" ferrofluid was examined by Dr. N. McCormack using a Philips 400T electron microscope with a LINK Si(Li) detector at Surrey University. Using this instrument three individual particles were analysed. Figure 7.6 shows one of the spectra recorded. The three spectra give nickel:iron atomic percent ratios as 3.63, 3.25 and 2.57 respectively. This data is in good agreement with

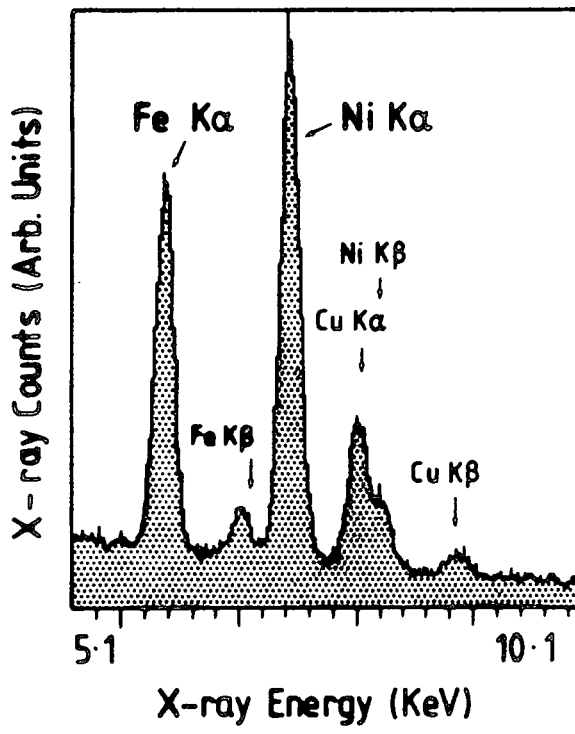


Fig. 7.5 Large area EDX spectrum for nickel-iron magnetic fluid.

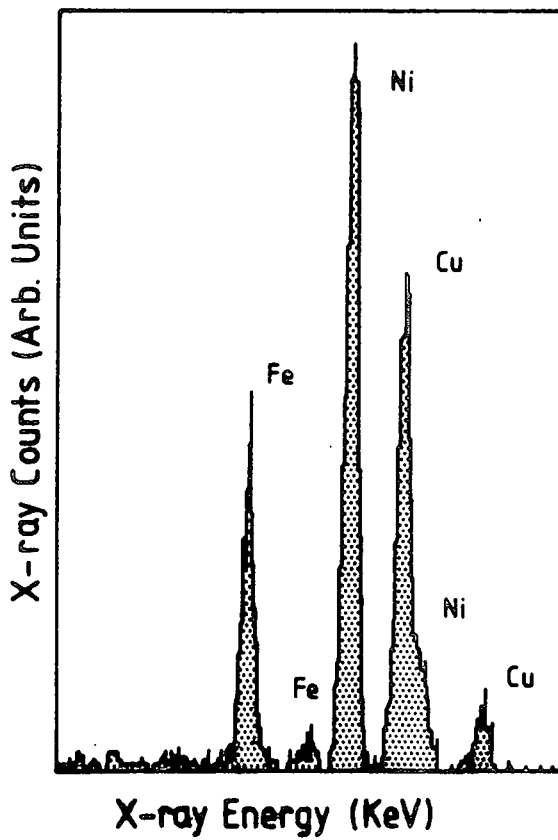


Fig. 7.6 Local area EDX spectrum for a nickel-iron magnetic fluid.

the electron diffraction analysis which indicated a nickel:iron ratio of three.

7.4 Magnetic Data

Room temperature magnetization curves were obtained using a vibrating sample magnetometer. The curves obtained immediately following fluid preparation are shown in figure 7.7. Saturation magnetizations (Table 7.2) as extracted from inverse field plots are low, with corresponding low volume packing fractions in the 0.02 to 0.06% range (assuming $M_b^\infty = 983100 \text{JT}^{-1} \text{m}^{-3}$). The conversion of "molecular" metal to particulate metal is in the 7-22% range. The shape of the curves are interesting. They all pass through the origin as is expected for single domain magnetic particles in suspension. At a field of 1.0 Tesla the fluids do not appear to have reached magnetic saturation, indicating a very small magnetic particle size. Indeed the mean magnetic particle diameters (\bar{d}_m) derived from these curves (given in Table 7.2) are 2.8 to 4.8nm. In all magnetic fluids \bar{d}_p is always larger than \bar{d}_m , the common explanations being surface oxidation, reaction with surfactant and/or spin pinning,²² the combined effect of which is referred to as the magnetic dead layer. In these nickel-iron systems this dead layer is exceptionally large, in the order of 2nm, i.e. twice the normal value. In calculating the mean magnetic particle diameter (\bar{d}_m), we assume that the particles have the same saturation

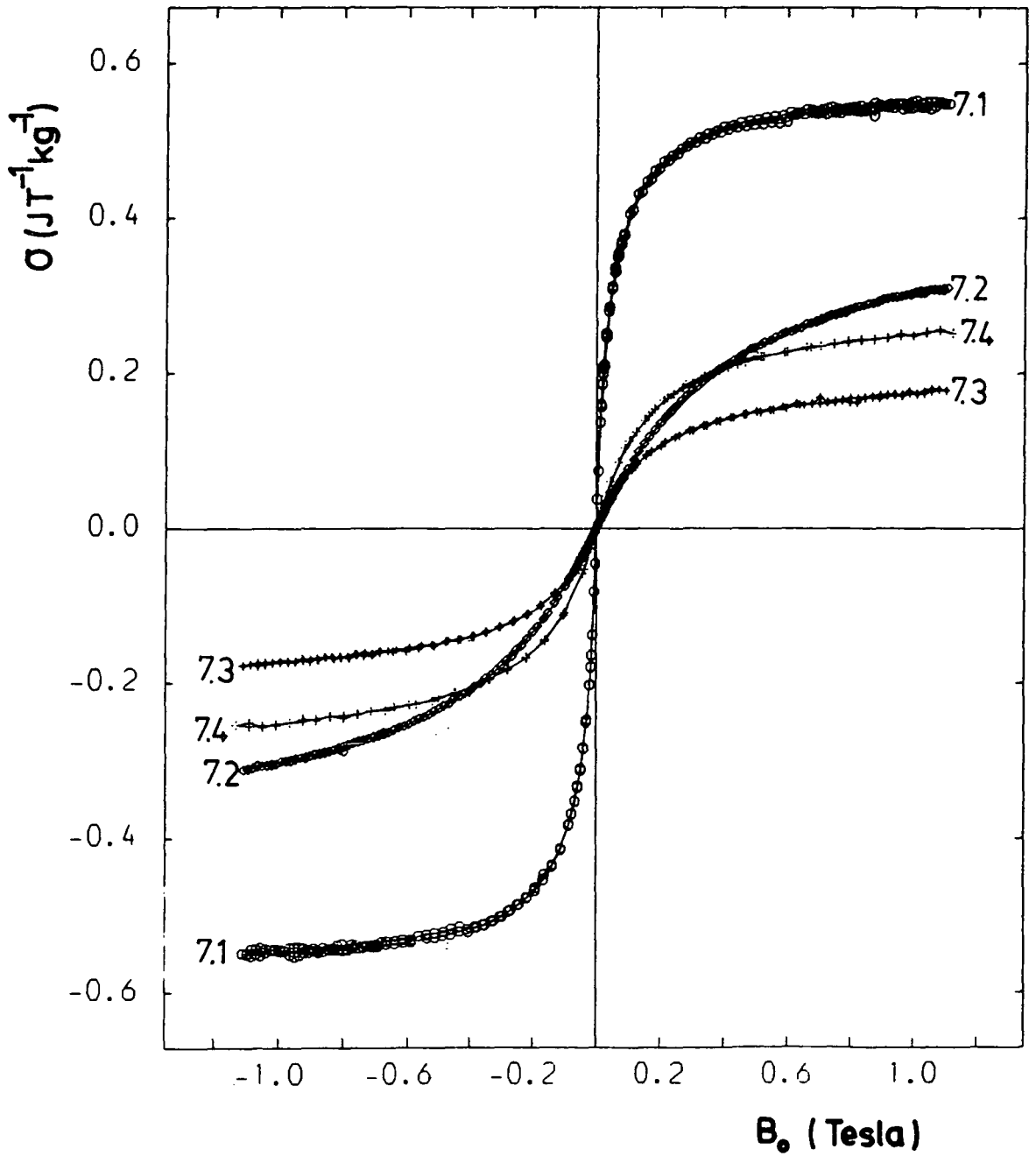


Fig. 7.7 Room temperature magnetization curves for nickel-iron fluids 7.1, 7.2, 7.3 and 7.4.

magnetization per unit volume as the bulk alloy Ni_3Fe . An allowance for a small increase in nickel content in the alloy in the calculation increases the value of \bar{d}_m calculated, consequently reducing the calculated value of the dead layer thickness slightly.

The nickel-iron particles in these magnetic fluids are very susceptible to oxidation. Magnetization measurements showed a 39% reduction in magnetic saturation in 8 days.

Comparison of the relative amounts of organometallic starting material and the relative saturation magnetizations of fluids 7.2 and 7.4, indicates that 1-methyl-naphthalene is a superior decomposition medium in comparison with petroleum ether (b.p. 200-260°C). Perhaps the aromatic hydrocarbon participates in the decomposition mechanism whereas the aliphatic hydrocarbon does not.

7.5 Attempted Infra-red Spectroscopic Study of the Decomposition Process

In an attempt to explain the difference in nickel-iron content in the starting material and alloy particles, and to understand the decomposition pathway in general, a typical preparation was followed by Infra-red spectroscopy. As the decomposition proceeded samples were removed by syringe at known times over a 4 hour period. It was hoped to be able to identify the nature of some intermediate species by recording their carbonyl stretching frequencies. Although this idea is simple in principle, it is rather optimistic as

the trinuclear cluster is believed to exist in isomeric forms in hydrocarbon solution. Any one of the two (or more) isomers has a maximum of five carbonyl absorptions, and in solution at least six absorptions are observed. These can be divided into three terminal CO stretching frequencies and three bridging $\bar{\nu}(\text{CO})$. The disappearance of the original carbonyl stretching absorptions was clearly observed.

Unfortunately no bands due to recognizable intermediates were recorded. Some absorption bands in both terminal and bridging regions were observed to disappear more rapidly than others. This could be due to one isomer decomposing more readily than the other(s) or possibly one form being converted to the other in the high temperatures of the decomposition medium. Eventually the surviving bands disappear to leave the carbonyl region virtually absorption free. At approximately 1880cm^{-1} a broad and very weak band appears as the other bands become weak, this increases slightly in intensity and then disappears. This band is not due to any of the likely carbonyl containing intermediates or side products such as $[\text{C}_5\text{H}_5\text{Ni}(\text{CO})]_2$ or $[(\text{C}_5\text{H}_5)_3\text{Ni}_3(\text{CO})_2]$.

The band is not due to carbon monoxide adsorbed on to a metal (particle) surface, these bands occur at frequencies higher than 2000cm^{-1} .

7.6 Conclusion

In this chapter we have reported the first successful preparations of hydrocarbon based nickel-iron magnetic

fluids. The particles were found to have physical diameters in the 7-8nm range. Analysis of the particles using EDX spectroscopy and electron diffraction proved the particles had a genuine alloy composition. From the electron diffraction data we can deduce that the particles possess an ordered "superlattice" structure, with a composition of Ni_xFe , where x has values near 3.

There are several similarities between these results and the results reported in the previous chapter concerning iron-cobalt alloy systems. Both nickel-iron and iron-cobalt systems have particles with diameters in the 5-8nm range. Further, in both we have observed a tendency for superlattice formation. Taken together, the data contained within these chapters prove that heteronuclear organometallic compounds can be used for the preparation of alloy particle magnetic fluids.

Future work of interest and importance will surely involve the evaporation of nickel-iron alloys to prepare nickel-iron particle magnetic fluids. If nickel-iron fluids can be prepared with control of alloy composition, it would be interesting to determine whether or not a superlattice is obtained for a Ni_3Fe particle composition using this alternative method. Indeed work in this area is already under way in collaboration with Dr. P.L. Timms of Bristol University.

NICKEL AND IRON MAGNETIC FLUIDS

Introduction

Following the success in preparing mixed-metal systems, we now focus on the remaining single metal systems i.e. nickel and iron. Neither metal has been as extensively investigated as that of cobalt.

Very little work has been reported on the preparation of nickel magnetic fluids (see chapter 2). This is probably because of the three ferromagnetic transition metals, it has the lowest saturation magnetization. In addition, the most obvious starting material, nickel tetracarbonyl, is extremely toxic and deters non-specialized researchers. Nickel does have the advantage that it is less susceptible to oxidation. In the two previous chapters on mixed-metal systems we have shown that starting materials for the preparation of metal particles need not be limited to compounds with carbon monoxide as the only ligand. The use of cyclopentadienyl containing compounds widens the range of possibilities. In the first section of the chapter some new routes to nickel ferrofluids are explored. This involves the use of starting materials previously unused. Success in preparing nickel ferrofluids has been limited but some of the results are interesting.

Iron fluids are of interest because pure iron has the highest magnetization of all elements. We have observed loss of iron from our mixed metal systems and consequently the properties of iron fluids are of particular relevance. The simple iron carbonyls, i.e. $\text{Fe}(\text{CO})_5$, $\text{Fe}_2(\text{CO})_9$, and $\text{Fe}_3(\text{CO})_{12}$ are readily available or easily prepared. Hence the preparation and study of iron ferrofluids would seem a straight forward matter. However, after a lengthy investigation, several inconsistencies were uncovered. The experimental results are discussed in the second section of this chapter.

8.1 Nickel Fine Particle Systems

8.1.1. Preparative Studies

The compounds investigated for the preparation of nickel ferrofluids were: η^5 -dicyclopentadienylnickel(II), $(\text{C}_5\text{H}_5)_2\text{Ni}$; cyclopentadienylnickelcarbonyl dimer, $([\text{C}_5\text{H}_5\text{Ni}(\text{CO})]_2)$; and the cluster $[\text{Me}_4\text{N}^+]_2[\text{Ni}_5(\text{CO})_{12}^{2-}]$. Only $(\text{C}_5\text{H}_5)_2\text{Ni}$ gave any success. This subsection takes the compounds in turn and summarizes both the unproductive and successful work.

(i) Studies of η^5 -dicyclopentadienylnickel(II)

This dark green solid is fairly air stable ¹³⁵ and has nickel formally in a plus two oxidation state. To produce nickel particles the compound will have to be simultaneously thermally decomposed and reduced. To achieve this high temperature and a reducing agent of molecular hydrogen were

used.

Reactions 1,2,3 and 4 (Table 8.1.1) were undertaken in a glass tube, which allowed hydrogen to be bubbled through the reaction mixture, simultaneously causing agitation. The tube was fitted with a reflux condenser and connected to a bubbler system. Prior to the reaction the system was purged with nitrogen. In each case, a pre-heated oil bath at a pre-set temperature was used to cause rapid heating.

In reactions 5 and 6 a high pressure autoclave was used as the reaction vessel, with hydrogen as the reducing agent under high pressures.

Although nickel metal was produced in several reactions, a stable magnetic colloid was not formed from η^5 -dicyclopentadienylnickel(II).

(ii) Studies of $[\text{Me}_4\text{N}^+]_2[\text{Ni}_5(\text{CO})_{12}]^{2-}$

The above cluster was prepared from nickel tetracarbonyl by the method described by Longoni et al.¹⁶¹ The sodium salt is first prepared by the reduction of nickel tetracarbonyl with sodium metal in T.H.F. The product is precipitated by the addition of tetramethyl ammonium chloride.

The rationale for using this cluster was that a degree of nickel-nickel association exists in the starting material and the cluster begins to decompose at 75°C.¹⁶¹ Unfortunately decompositions of the cluster in toluene solutions of Duomeen-TDO, Manoxol-OT, Sarkosyl-0, Solsperse-3000 and Solsperse-20000 to form a colloidal metal suspension were

TABLE 8.1.1

Reductive decompositions of $(\pi\text{-C}_5\text{H}_5)_2\text{Ni}$ using H_2

Reaction	Mass of $(\text{C}_5\text{H}_5)_2\text{Ni}$ (g)	Carrier Liquid	Mass of Carrier (cm^3)	Surfactant	Mass of surf. (g)	H_2	Temp. ($^\circ\text{C}$)	Duration of Reaction
1	4.10	Kerosene	60	Manoxol-OT	0.4513	Bubbled	160	2 hrs
2	5.00	Kerosene	60	Oleic acid	0.80	Bubbled	160	3 hrs
3	1.5528	Toluene	18	Solsperse 3000	0.4995	Bubbled	Reflux	6 hrs
4	1.8789	1-m-N	15	Manoxol-OT	0.7002	Bubbled	160	7.5 hrs
5	1.0423	Kerosene	12	Solsperse-3000	0.3286	75 Atm	100	1 hr
6	1.0253	Kerosene	12	solsperse-20000	0.4278	75-80 Atm. 70 Atm.	130 150	1 hr 5 mins

1-m-N = 1-methyl-naphthalene

Notes

- Reaction 1 : Nickel mirror formed, magnetic sediment.
 Reaction 2 : Nickel mirror formed.
 Reaction 3 : No observable change
 Reaction 4 : Grey Magnetic Sediment.
 Reaction 5 : Black solution and sediment (non-magnetic)
 Reaction 6 : 'Flakes' of metal.

completely unsuccessful, though metal formation did appear to have been achieved.

(iii) Studies of Cyclopentadienylnickelcarbonyl dimer

In chapters 6 and 7 we used cyclopentadienyl carbonyl compounds to prepare metal particles.

Cyclopentadienylnickelcarbonyl dimer is therefore a logical choice of starting material from which to prepare nickel particles. On heating, the complex decomposes on melting at 146-147°C.¹³¹ However, in organic solvents, heating produces the trinuclear cluster $[(\pi-C_5H_5)_3Ni_3(CO)_2]$. The trinuclear species is stable up to 200°C.¹³¹ In order to avoid mere conversion to the trinuclear, high decomposition temperatures were used to achieve rapid decomposition to metal.

Cyclopentadienylnickelcarbonyl dimer is prepared by the reaction of nickel tetracarbonyl and η^5 -dicyclopentadienylnickel(II) in benzene, the preparation being described by King.¹³⁵

$[C_5H_5Ni(CO)]_2$ is very dark green in the solid state (reflected light) but produces deep red solutions in organic solvents (transmitted light), whilst $[(C_5H_5)_3Ni_3(CO)_2]$ is green in both the solid state and in solution. All the reactions with cyclopentadienylnickelcarbonyl dimer were carried out in a 3-necked 100 cm³ round bottomed flask, fitted with teflon paddle stirrer, reflux condenser and nitrogen inlet. A molten metal bath was used for the heat source. Table 8.1.2 gives the essential details of the

TABLE 8.1.2

Thermal decompositions of $[\pi\text{-C}_5\text{H}_5\text{Ni(CO)}]_2$

Conc. of $[\text{C}_5\text{H}_5\text{Ni(CO)}]_2$ (g cm ⁻³)	Surfactant	Conc. of Surfactant (g cm ⁻³)	Metal Bath Temp. (°C)	Reaction Time (hrs)	Remarks
0.0419	Manoxol-OT	0.0323	160	3	Green solution produced
0.0509	Manoxol-OT	0.0448	200-210	3	Weakly magnetic product, sedimentation within 24 hrs.
0.0320	Sarkosyl-O	0.0345	200-210	3	Black liquid product
0.101	Duomeen-TDO	0.0820	205-210	2	Black product-weakly magnetic:Fluid 8.4.

attempted preparations. In all cases the carrier liquid was 1-methyl-naphthalene.

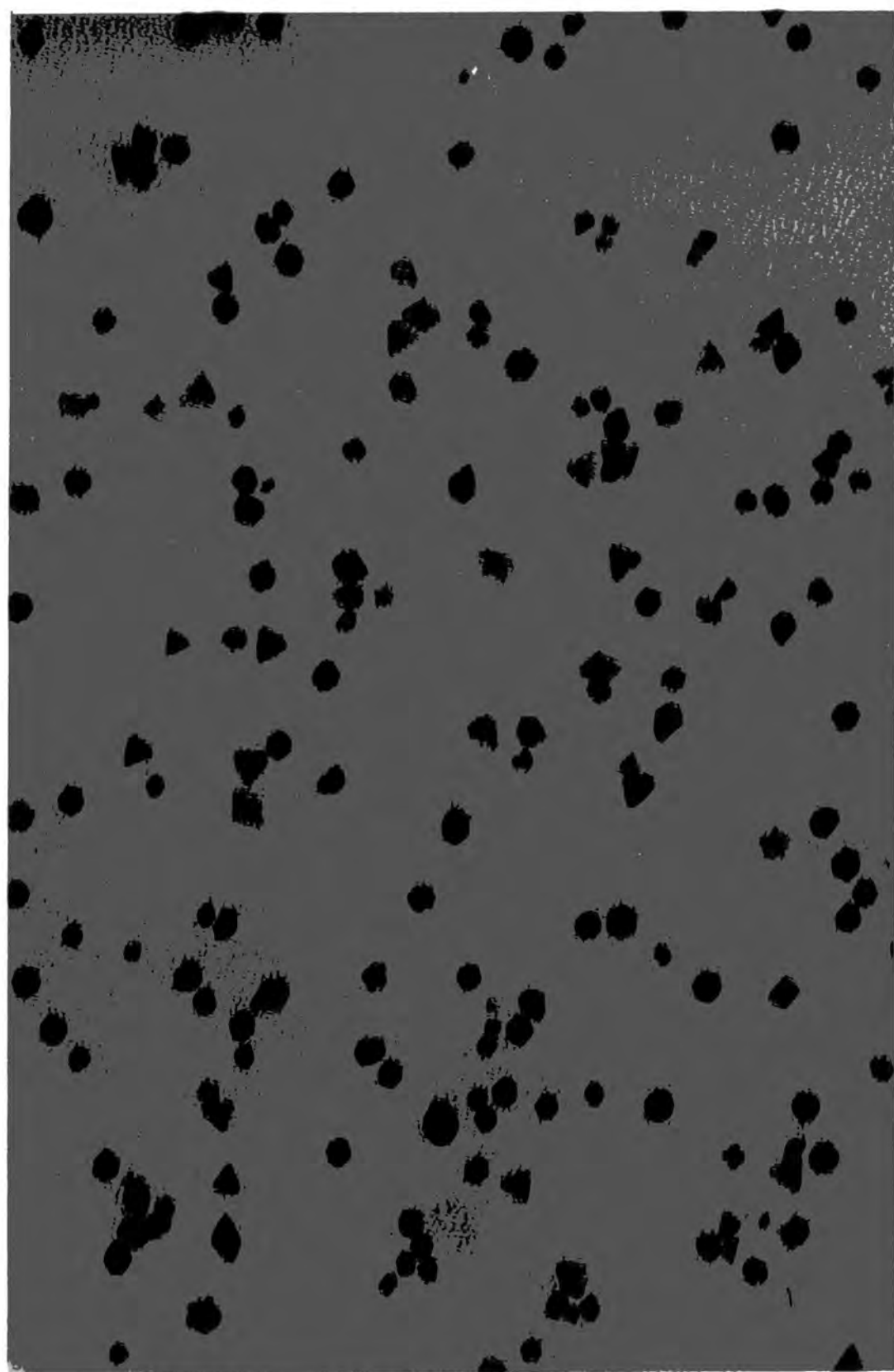
After many experiments only one weakly magnetically responsive fluid was produced and results discussed in the remainder of the section refer to this "fluid" (8.4).

8.1.2 Electron Microscopy

All of the ferrofluids containing cobalt, iron-cobalt and nickel-iron particles reported in the previous three chapters had particles in the 5-8nm diameter range. This is irrespective of starting material and preparation conditions. In addition all of the physical particle size distributions have been approximately Gaussian in shape with small standard deviations about the mean (i.e. narrow particle size range). Particles which are roughly spherical with no definite shape is another common feature observed.

The nickel "ferrofluid" 8.4 was examined using transmission electron microscopy. The sample after dilution in 1-methyl-naphthalene was placed on a carbon-formvar coated copper grid. Electron microscopy revealed large particles in the 13-27nm size range. Many of the particles had regular crystal habits. The main recognizable image shapes being triangles and hexagons. Figure 8.1.1. shows a shadow micrograph (total magnification 270,000). The triangular images are likely to be projections of tetrahedrally or octahedrally shaped particles, while the hexagons will be projections of polyhedral shaped particles. The diamond shaped images could be twinned particles.

Fig.8.11 Shadow electron micrograph of fluid 8.4 (X 270 000)



Prints from these micrographs were analysed in the usual way to give a physical size distribution (e.g. Figure 8.1.2). The mean diameter is 18.9nm with a standard deviation of 2.44nm. The accuracy of this particular distribution is not expected to be as good as for the other types of ferrofluid, because the light beam in the image size analyser is roughly circular in cross-section and therefore cannot be exactly matched to a triangular image. The distribution is uncharacteristic of fluids produced by the organometallic route in that the particle sizes and their range are large.

In nickel suspensions prepared from nickel tetracarbonyl by thermal decomposition in hydrocarbon polymer solutions, particles with diameters in the 8-15nm and 20nm size range were reported by Thomas¹¹⁶ and Smith¹²⁵ respectively. These authors reported no distinct particle shapes. In a nickel ferrofluid prepared by Hoon et al.¹²⁶ by the UV decomposition of nickel tetracarbonyl the small regular shaped particles (mainly triangles) obtained were found to be in the 6nm range. These particles were prepared in the aromatic hydrocarbons xylene,¹¹⁶ benzene¹²⁵ and toluene¹²⁶ respectively. Particles prepared by Hoon et al. from dicyclopentadienylnickel(II) were also in the 6nm range but possessed no regular shape.

In work involving the preparation of fine metal particles by evaporation of metals in inert atmospheres, Japanese workers observed crystal habits. When nickel was

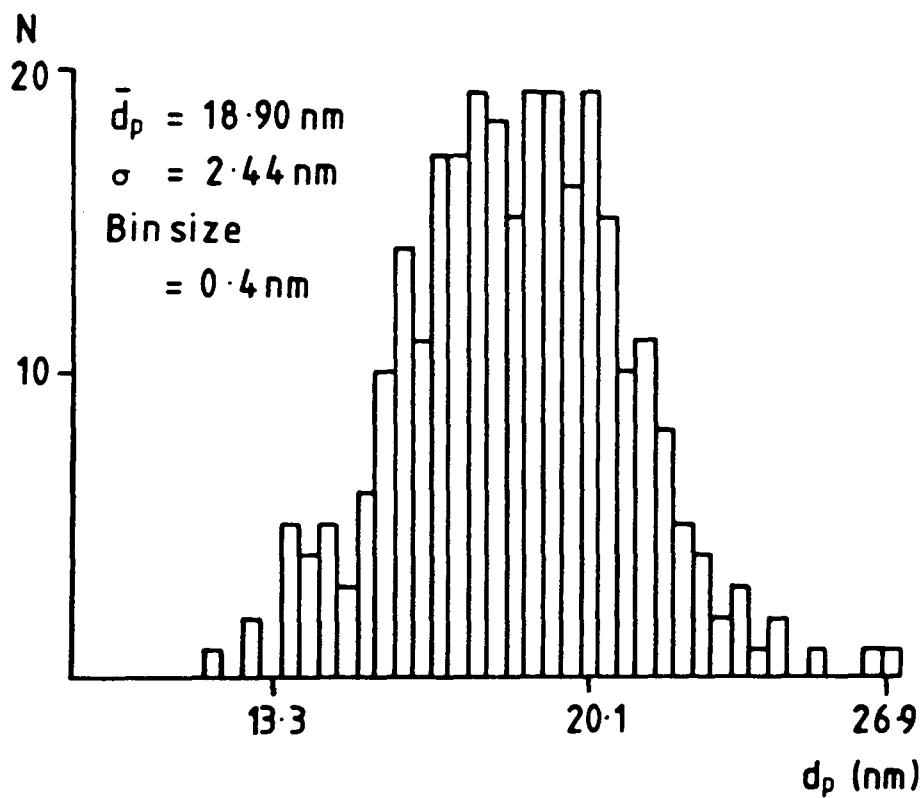


Fig. 8.1.2 Physical particle size distribution for the nickel particle system 8.4.

evaporated in argon many of the particles produced had polyhedral shapes with hexagonal profiles, provided the crystals were not smaller than 20-30nm. When the atmosphere was xenon, particles in the 30-100nm size range gave octahedron and hexagonal images, when the particles were 20nm or smaller the images were hexagonal, triangular and even pentagonal in shape.⁹⁵ These observations will be discussed further in the conclusion to this section.

8.1.3 Magnetization Curve

A room temperature magnetization curve was measured using the vibrating sample magnetometer (Figure 8.1.3). The saturation magnetization was extremely low ($\sigma_{ff}^{\infty} \approx 0.19 \text{ JT}^{-1} \text{ Kg}^{-1}$) giving a very small volume packing fraction of 0.04% i.e. approximately 0.4% by mass of the ferrofluid was ferromagnetic nickel, (this assumes the magnetic particle core is metallic nickel, with $M_b^{\infty} = 491,280 \text{ JT}^{-1} \text{ m}^{-3}$). This represents around 10% conversion of the organometallic compound to ferromagnetic nickel.

The shape of the curve indicates the particles become magnetized in a low magnetic field (~ 0.2 Tesla), which is compatible with the large particle size measured using electron microscopy.

8.1.4 Particle Composition and Structure

It would be very easy to assume the particles in "fluid" 8.4 were composed of elemental nickel. This would be a reasonable assumption as metallic nickel is the obvious ferromagnetic nickel material which could have been produced

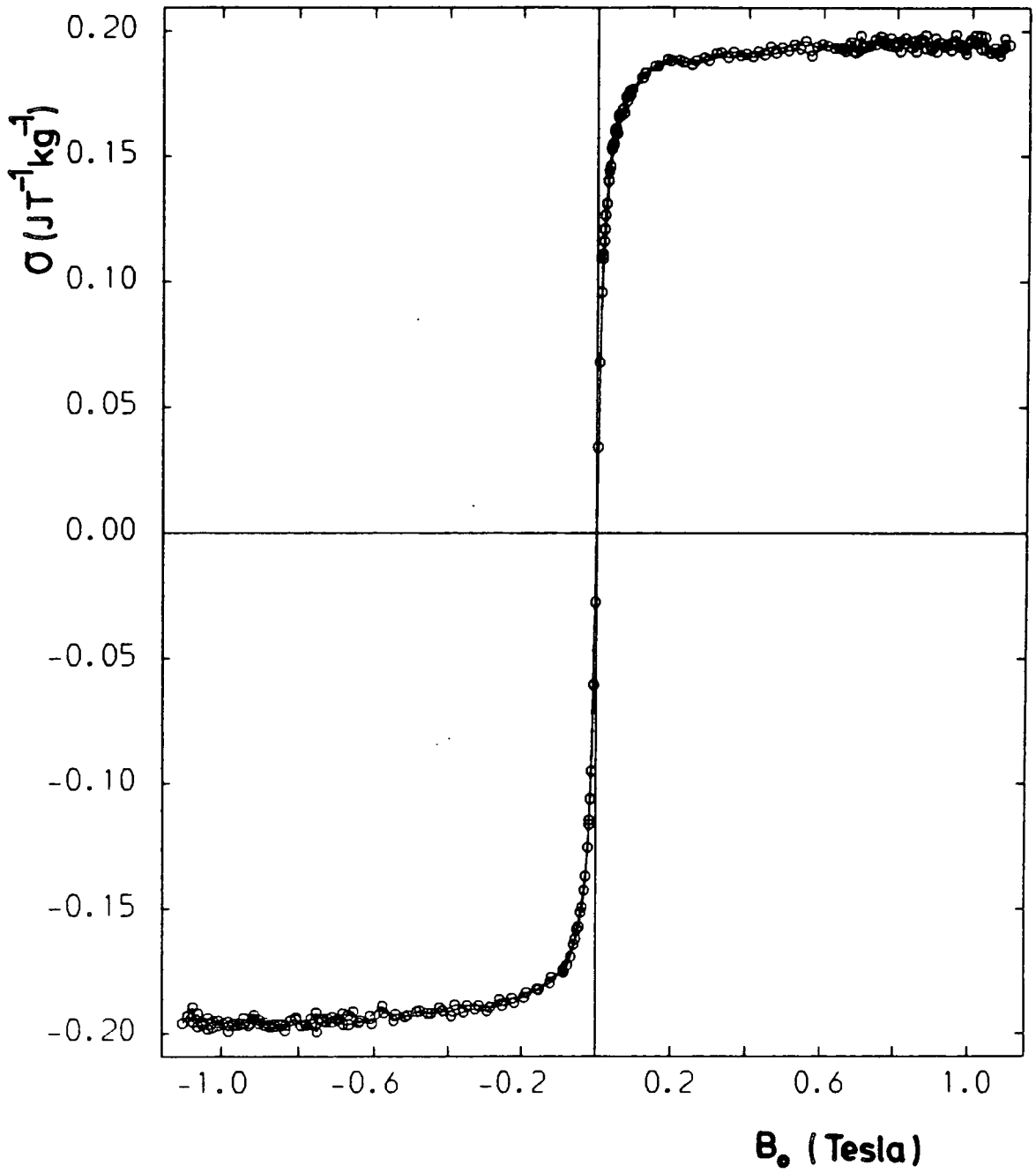


Fig. 8.1.3 Room temperature magnetization curve for "fluid" 8.4.

in this preparation. In order to confirm this, transmission electron diffraction was used to obtain a diffraction pattern

The pattern consisted of a number of intense broad continuous rings, the diameters of which ratioed as a face centred cubic structure. Indexing of the d-spacings calculated from these rings as fcc gave a lattice parameter of $a_0 = 3.64\text{\AA}$ which is rather large when compared to the value for bulk nickel, $a_0 = 3.516\text{\AA}$,¹⁶² i.e. a discrepancy of approximately 3.5%.

A closer examination of the diffraction pattern revealed a number of additional very weak lines. The most obvious explanation for these extra rings is the presence of a small amount of NiO in the sample. This is a conceivable explanation as NiO was observed in the electron diffraction patterns of the fine nickel particles produced by evaporation in inert atmospheres.^{92,93} NiO like nickel has a fcc structure with a larger lattice parameter and therefore larger d-spacings than nickel.¹⁶² However, by assuming NiO is responsible for the very weak lines and using the ASTM¹⁶² d-spacing values for NiO, we can calculate the corresponding ring diameters we would expect to observe in the pattern. Table 8.1.3 compiles the observed data and the various calculated values of relevance to this subsection.

It could be possible that the NiO (200) line and the nickel (111) line would be superimposed, explaining the broadness of the Ni (111) line. Likewise the NiO (331) line and the nickel Ni (220) line could be superimposed; again

TABLE 8.1.3

Electron diffraction for nickel particle system and related data

Measured ring dia. (nm)	Estimated Intensity	Calculated d-spacing (Å)	hkl assignment	ASTM values for d(Å) and (hkl)		Estimated ring dias. for NiO lines (mm).
				nickel	NiO	
93.5*	vs	2.07	111	2.03(111)	2.410(111)	80.2
106.5*	vs	1.81	200	1.76(200)	2.088(200)	92.6
119	w	1.62				
142	vw	1.36				
148.75*	s	1.30	220	1.24(220)	1.476(220)	131.0
154	vw	1.26				
173.75*	s	1.11	311	1.06(311) 1.015(222)	1.259(311) 1.206(222)	153.5 160.3

* Taken to be fcc nickel

this line is observed to be very broad in the diffraction pattern. However, from the predicted position of the NiO (111) line, i.e. 80.21 mm one would expect this line to be clearly visible in the pattern, as it would be fairly intense. This line is definitely absent from the observed pattern. In addition the other observed weak lines give d-spacing values which do not correspond well with those of NiO. These results certainly do not support the presence of NiO in the material.

Another possible explanation is the presence of a small proportion of nickel in the hexagonal phase. Le Clerc and Michel¹⁶³ prepared hexagonal nickel by the reduction of NiO. From their work we can calculate the d-spacings for the hexagonal close packed nickel system to be: 2.29, 2.16, 2.02, 1.57, 1.32Å etc. These values do not explain the presence of the "extra" lines and we conclude hexagonal close packed nickel is not present. These results are discussed further in the conclusion of this section.

Conclusion

The results in this section on nickel "ferrofluids" have shown some interesting irregularities. We have to explain the formation of distinctly polyhedral shaped particles which are considerably larger than all other particles produced in this work. In addition some unexpected lines in the electron diffraction pattern have been observed. These lines have extremely low intensities

and do not correspond to NiO or nickel in the hexagonal phase. The d-spacings calculated from the pattern are consistently slightly larger than the bulk nickel values.

There seems to be no obvious single explanation for all of these experimental observations. In attempting to provide an explanation let us first consider the starting material cyclopentadienylnickelcarbonyl dimer. The cyclopentadienyl group stabilizes the Ni-CO bonding. This will make the removal of carbon monoxide more difficult than for dicobalt octacarbonyl for example. In addition heating is almost certain to at least partially convert $[\text{C}_5\text{H}_5\text{Ni}(\text{CO})]_2$ to the trinuclear $[(\text{C}_5\text{H}_5)_3\text{Ni}_3(\text{CO})_2]$, which is even more thermally stable than the original complex.

At the temperatures of the decomposition medium ($\sim 200^\circ\text{C}$) let us suppose a small proportion of the organometallic material does thermally decompose to very small nickel clusters. (Note that Davis and Klabunde report Ni_3 clusters deposited on silica gel from the decomposition of $[(\text{C}_5\text{H}_5)_3\text{Ni}_3(\text{CO})_2]$). These very small nickel clusters may act as nucleation sites for particle growth. In colloid chemistry the formation of a new phase during precipitation involves two stages; firstly nucleation i.e. the formation of centres of crystallization, and secondly crystal growth. It is the relative rates of these two processes which determine particle size. (In the decompositions described in the previous chapters, the small particle sizes (5-8nm) may be explained by a high rate of nucleation). The final

crystal/particle size therefore depends on the initial number of nucleation sites formed. If few nickel nucleation sites are formed then the formation of larger particles in a controlled decomposition process follows automatically, the particles being produced by the decomposition of organometallic material on the nucleation sites. We would expect particle growth to cease when the material from which the particles are produced i.e. $[\text{C}_5\text{H}_5\text{Ni}(\text{CO})]_2$ and/or $[(\text{C}_5\text{H}_5)_3\text{Ni}_3(\text{CO})_2]$ is exhausted. In addition surfactants are believed to play a role in controlling particle size, giving rise to the characteristic narrow size distributions for the organometallic route. If in the case of nickel the surfactants used did not interact with the growing particles, then particle growth would not be controlled, explaining the formation of large particles.

For very small particles (5-8m), spheroids would be expected as the number of atoms in the surface layers is a minimum for spheres, hence minimizing the surface energy of the particles. As the particles become larger these surface considerations become less important and polyhedral shaped particles can be formed. Kimoto et al. observed the formation of polyhedral particles when the crystals were not smaller than 20-30nm. So far the formation of large particles with distinct crystal habits has been explained. The irregularities in the diffraction pattern still require rationalization.

Small nickel particles prepared for catalytic studies

may be covered in a layer of organic fragments from the solvent.⁶¹ In another similar example⁵⁹ nickel particles/clusters were found to contain CH units inside the nickel structure (some of the powders produced exhibited ferromagnetic properties). These species are not carbides. Ni_3C ¹⁶² does exist, but the d-spacings do not fit those of the "weak" lines observed in our diffraction work. This carbonaceous content is believed to arise from fragmentation of both aliphatic and aromatic hydrocarbons by reaction with the highly reactive nickel clusters. If a similar process is occurring during our decompositions a small proportion of "interstitial" carbon may be present in the nickel structure. If the proportion of carbon was low, then the fcc structure may not be significantly effected. This may even account for the large d-spacings observed (cf. bulk nickel) as well as the extra lines. An organic layer on the particle surface may even aid colloidal stability. Indeed¹⁶⁶ Wada and Ichikawa managed to temporarily redisperse fine metal particles produced by evaporating the metal into frozen diethylether. The authors believed the particles were coated in fragmented solvent molecules which prevented immediate aggregation.

Alternative and simpler explanations must not be overlooked. For example, the crystal habit of the larger particles may only be observed because the microscope resolution is not good enough to observe the crystal habit of 5-8nm particles. The weak lines in the electron

diffraction pattern could be simply due to an impurity in the bulk sample.

A general observation in this work has been the production of nickel metal from the decomposition (reductive and/or thermal) of the nickel organometallic compounds; $(C_5H_5)_2Ni$, $[Me_4Ni^+]_2[Ni_5(CO)_{12}^{2-}]$ and $[C_5H_5Ni(CO)]_2$. Although nickel metal was produced in each case it was only produced in colloidal suspension for $[C_5H_5Ni(CO)]_2$, and this was only in one of several preparations. Compared to iron and cobalt, nickel is relatively inert. It may be the lack of sufficient coordination of surfactant which prevents colloid formation in general, i.e. the surfactant does not control the growth of the nickel particles which prefer to bond to each other rather than other atoms, i.e. oxygen and nitrogen.

8.2 Preparative Studies of Iron Ferrofluids

Investigations into the preparation of iron particle magnetic fluids reported in this section have involved the use of the iron containing organometallic compounds; $Fe(CO)_5$, $Fe_2(CO)_9$, $Fe_3(CO)_{12}$, $[C_5H_5Fe(CO)_2]_2$ and $Fe(CO)_2(NO)_2$. Iron pentacarbonyl was readily available from Fluka. Diiron nonacarbonyl was obtained from Strem or prepared by the UV photolysis of iron pentacarbonyl as described by King.¹³⁵ The other compounds were all prepared by the standard literature method as given by King.¹³⁵

In this section the compounds will be discussed

individually for convenience and to avoid confusion.

However, this is not necessarily the chronological order in which the research progressed.

The simple iron carbonyls $\text{Fe}(\text{CO})_5$, $\text{Fe}_2(\text{CO})_9$ and $\text{Fe}_3(\text{CO})_{12}$ have been investigated previously for the preparation of iron magnetic fluids (see Chapter 2).

8.2.1 Studies of Cyclopentadienylirondicarbonyl Dimer

In the previous section the preparation of "nickel" particles from cyclopentadienylnickelcarbonyl dimer was reported. $[\text{C}_5\text{H}_5\text{Fe}(\text{CO})_2]_2$ was investigated to determine whether analogous results were obtained for the equivalent iron containing compound. Due to the high stability of $[\text{C}_5\text{H}_5\text{Fe}(\text{CO})]_2$ (decomposes on melting at 194°C)¹³⁵ extremely high decomposition temperatures were used ($> 200^\circ\text{C}$). 1-methylnaphthalene was used as the carrier liquid/decomposition medium.

The use of $[\text{C}_5\text{H}_5\text{Fe}(\text{CO})_2]_2$ as a starting material for iron ferrofluids was not particularly successful. Table 8.2.1 summarizes details of the two most successful preparations. In both cases extremely weakly magnetically responsive, black liquids were obtained as products. Both products exhibited a high degree of sedimentation within hours of preparation. A magnetization curve was measured for ferrofluid 8.2.1, giving a saturation magnetization of $0.25 \text{ JT}^{-1} \text{ kg}^{-1}$ (a low value). No further investigation was made into the use of $[\text{C}_5\text{H}_5\text{Fe}(\text{CO})_2]_2$.

FLUID 8. 2.1

Details of attempted ferrofluid preparation

from $[\pi\text{-C}_5\text{H}_5\text{Fe}(\text{CO})_2]_2$

Fluid	Conc. of $[\pi\text{-C}_5\text{H}_5\text{Fe}(\text{CO})_2]_2$ (g cm ⁻³)	Surfactant	Conc. of Surfactant (g cm ⁻³)	Reaction time (hrs)	Metal Bath temp. (°C)
8.2.1	0.0995	Duomeen-TDO	0.0412	2	220-240
8.2.2	0.103	Sarkosyl-O	0.0414	5	220

8.2.2 The Simple Carbonyls

Preparations involving the use of the three iron carbonyls $\text{Fe}(\text{CO})_5$, $\text{Fe}_2(\text{CO})_9$ and $\text{Fe}_3(\text{CO})_{12}$ are too numerous to include, even when tabulated. The most interesting results were observed for $\text{Fe}(\text{CO})_5$ and $\text{Fe}_3(\text{CO})_{12}$. Use of $\text{Fe}_2(\text{CO})_9$ proved to be completely unsuccessful.

(i) Diiron Nonacarbonyl ($\text{Fe}_2(\text{CO})_9$)

Although there is a report of the successful use of diiron nonacarbonyl in the literature,¹²⁴ all attempts to expand and even repeat this route were unsuccessful. The hydrocarbons kerosene, toluene and 1-methyl-naphthalene were used in conjunction with many of the surfactants used earlier in this work. No combination was successful in producing a colloiddally stable magnetic suspension. The very low solubility of diiron nonacarbonyl in organic solvents is probably responsible for the lack of success.

(ii) Studies of Triiron Dodecacarbonyl

(a) Preparations

There is a report in the literature of triiron¹²⁴ dodecacarbonyl being used to prepare iron ferrofluids. In this subsection the preparation of ferrofluids involving triiron dodecacarbonyl is discussed, the intention being to use this route as a convenient method of preparing iron ferrofluids for an EXAFS spectroscopic study.

Table 8.2.2 summarizes the experimental details of three typical preparations. Mean physical particle sizes (\bar{d}_p)

TABLE 8.2.2.

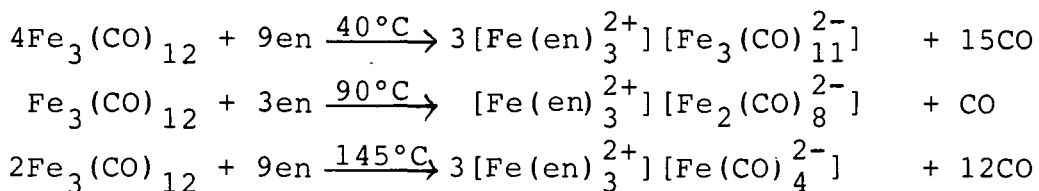
Preparative details and TEM data for magnetic fluids prepared from $\text{Fe}_3(\text{CO})_{12}$

Fluid	Mass of $\text{Fe}_3(\text{CO})_{12}$ (g)	Surfactant	Mass of surfactant (g)	Carrier Liquid	Volume of carrier (cm^3)	Bath Temp ($^{\circ}\text{C}$)	Reaction Duration (hrs)	TEM data	
								\bar{d}_p (nm)	S.Dev
8.2.3	1.5069	Sarkosyl-O	0.7288	1-m-N	15.0	195	3	7.98	1.92
8.2.4	1.6155	Duomeen-TDO	0.5722	Toluene	10.0	130	1.5	10.60	0.92
8.2.5	0.5908	Duomeen-TDO	0.5591	1-m-N	10.0	200	2.5	10.85	1.46

1-m-N = 1-methyl naphthalene

and standard deviations (σ) derived from transmission electron microscopic analysis are included in the table. On inspection the "fluids" were all black and weakly magnetically responsive. Electron microscopy showed the particles to have diameters in the 8-11nm range. This was slightly larger than for the cobalt and alloy particles discussed in previous chapters.

In the organic solvents used in the preparations, triiron dodecacarbonyl dissolved to give intense green solutions. On heating these green solutions were observed to rapidly turn an intense red-purple colour. This was followed by the evolution of a gas and a gradual darkening of the solution to black. Heating was continued until gas evolution had ceased. The surfactants present during decomposition were essentially nitrogen or oxygen bases; these types of compound are known to cause the disproportionation of triiron dodecacarbonyl to produce anions of the type $[\text{Fe}_x(\text{CO})_y]^{2-}$ where $x = 3, 2$ or 1 and $y = 11, 8$ or 4 respectively. The presence of such a series of anions would explain the intense purple colour of the reaction medium during decomposition. It is likely that the whole series of anions would be present in equilibrium, as the exact nature of the species present is dependent on temperature. Zeiss has compiled a series of reactions of triiron dodecacarbonyl with ethane-1, 2-diamine (en) at different temperatures which illustrate the type of reaction occurring:



a similar series of reactions is likely to have occurred as the temperature of the decomposition median increased. Petroleum ether (b.p. 200-260°C) was found to be a completely unsuitable decomposition medium.

Fluids 8.2.3 and 8.2.4 were prepared in apparatus consisting of the normal 3-necked 100cm³ round bottomed flask arrangement described in Chapter 5. This equipment was replaced by apparatus designed to further reduce the risk of oxidation of freshly prepared "iron" ferrofluids. Essentially it consisted of a glass tube which could be fitted with a specially shaped teflon paddle stirrer. The tube had two short side arms fitted with Youngs taps. One of these side arms could be connected to a reflux condenser which exhausted to a bubbler/nitrogen system. The other arm provided a tap which allowed the system to be purged with nitrogen. This system was designed to be small enough to be transferred to a nitrogen glove box for loading with the relevant reagents. When heating ceased, the system was purged with nitrogen, isolated by closing the Youngs taps and then returned to the glove box. Fluid 8.2.5 was the product of one of the many decompositions carried out using this apparatus.

(b) EXAFS Spectra and Discussion

EXAFS spectroscopy has been used for a qualitative study of the ferrofluids prepared from $\text{Fe}_3(\text{CO})_{12}$. As in section 5.3 analysis is only by comparison of spectra. Figure 8.2.1 compares the EXAFS spectra of freshly prepared ferrofluids 8.2.4 and 8.2.5 with the EXAFS spectra of iron foil (assumed to be α -iron). There are two disturbing observations on inspection of the spectra. Firstly neither of the "iron" ferrofluids appear to contain metallic α -Fe, and secondly the ferrofluid spectra are both slightly different.

One possibility is that only a small proportion of the triiron dodecacarbonyl had actually been decomposed. This would explain the poor magnetic properties observed. Figure 8.2.2 compares the EXAFS spectra of fluid 8.2.4 and a disc of $\text{Fe}_3(\text{CO})_{12}$. There are very strong similarities between the spectra. This implies that in refluxing toluene triiron dodecacarbonyl has largely remained in a carbonyl form, i.e. in the form of one or more $[\text{Fe}_x(\text{CO})_y]^{2-}$ anions. Some of the carbonyl must have decomposed to "metal", as ferrofluid 8.2.4 was black and it had a weak magnetic response.

The EXAFS spectrum of α -FeOOH was recorded. Figure 8.2.3 shows this spectrum in comparison to that of fluid 8.2.5. Again there are distinct similarities. From these results it is possible to cautiously conclude that the "iron" fluids had oxidized to one or a combination of iron oxides and/or iron (II) or an iron (III) surfactant complex

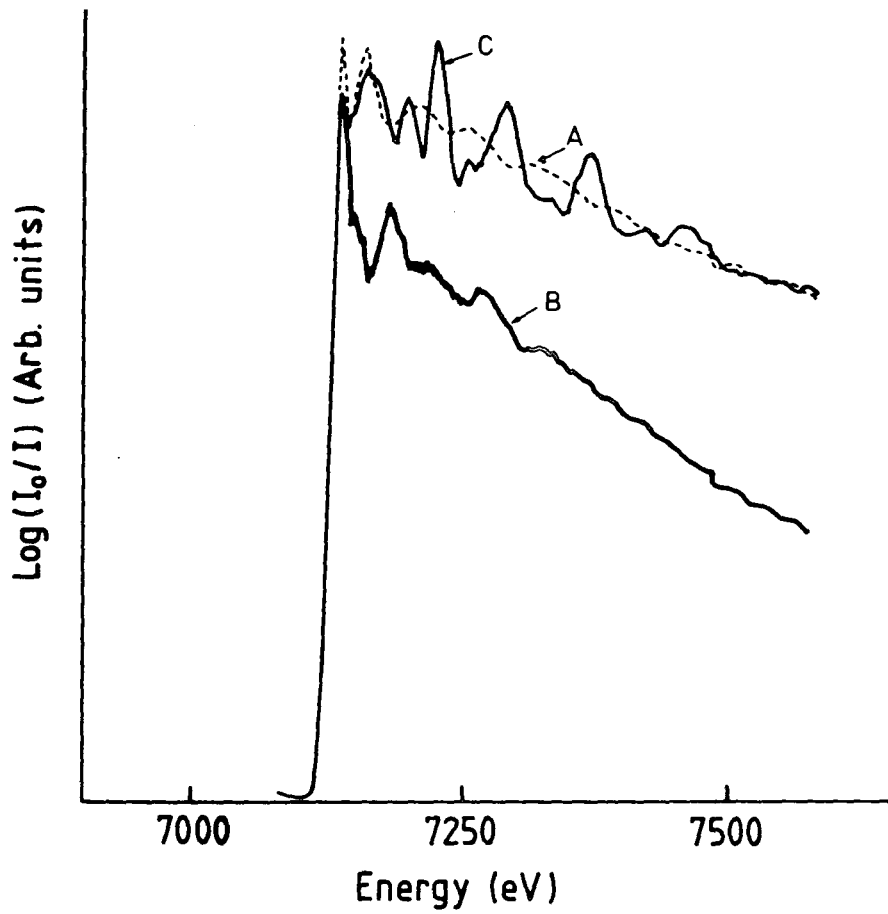


Fig. 8.2.1 EXAFS spectra of fluids 8.2.4(A) and 8.2.5(B) in comparison with the EXAFS spectrum of iron metal (C).

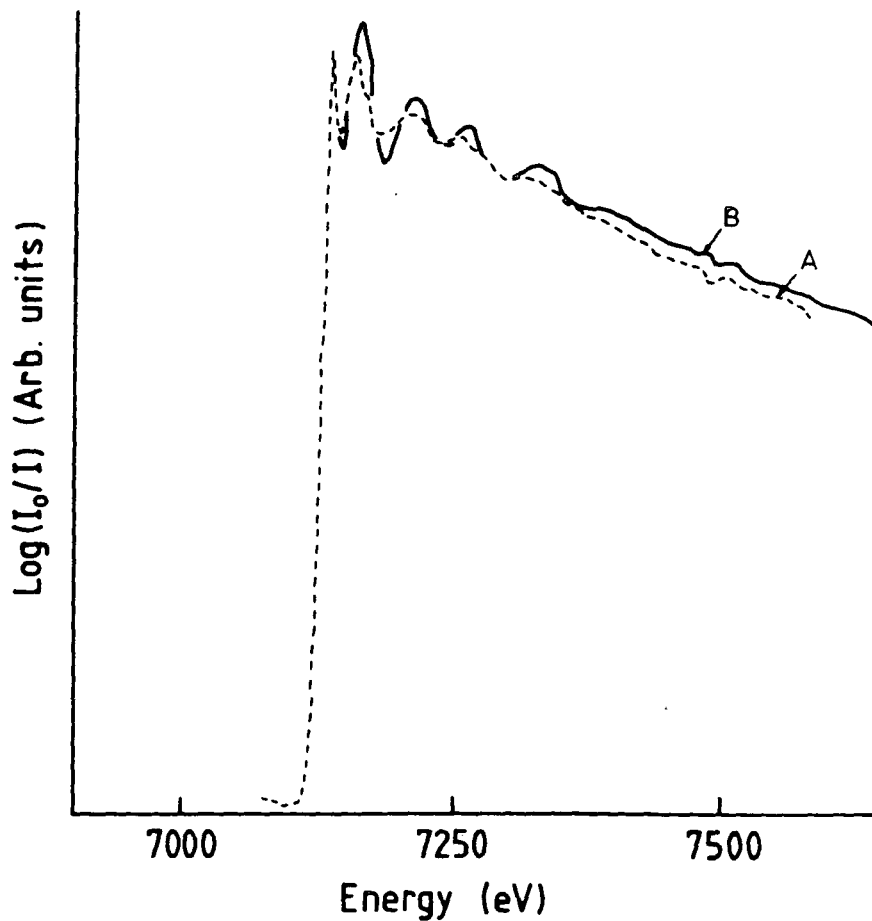


Fig. 8.2.2 EXAFS spectra of fluid 8.2.4(A) and $\text{Fe}_3(\text{CO})_{12}$ (B).

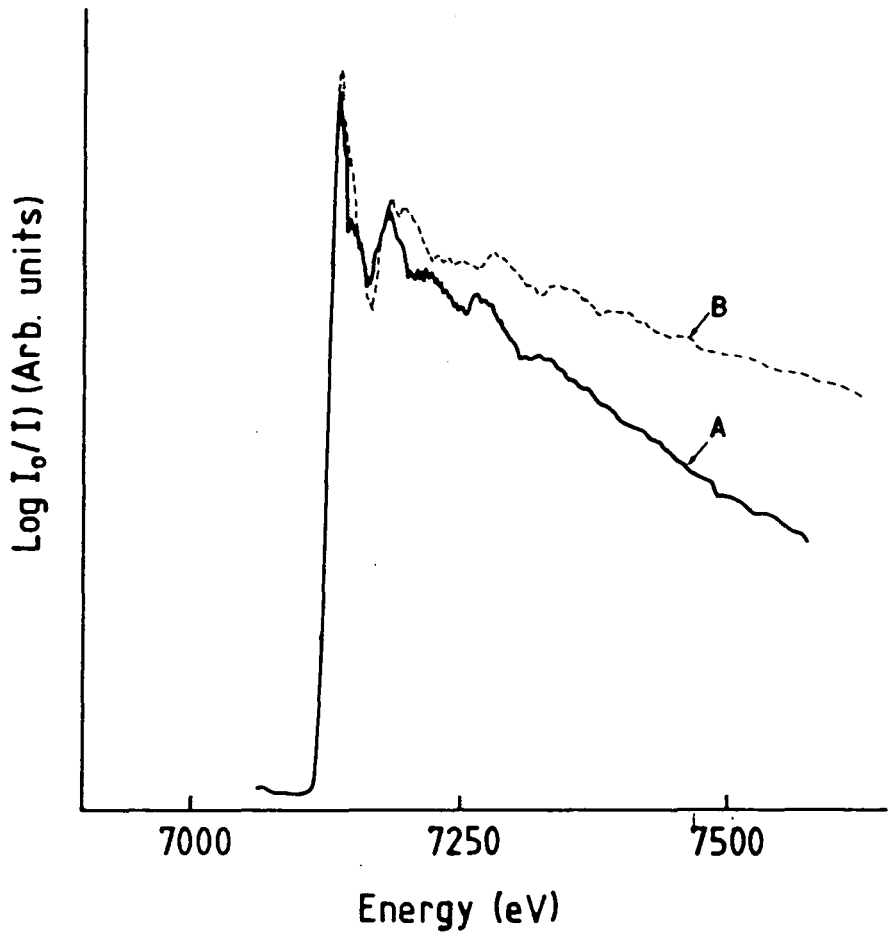


Fig. 8.2.3 EXAFS spectra of fluid 8.2.5(A) and α -FeOOH(B).

(more generally, an oxygen coordinated species). These preparations were repeated several times, taking every precaution possible to avoid oxidation of the ferrofluids. Spectra were recorded immediately following fluid preparation. Although there were slight variations in the EXAFS spectra recorded, they all indicated a lack of α -iron in the "ferrofluids" produced.

All attempts to obtain an electron diffraction pattern from these fluids failed to produce any diffraction lines. This is a feature of amorphous materials.

The EXAFS data recorded does not give sufficient detail to identify the species present in the fluid medium. One conclusion we can make from the combination of EXAFS spectra, lack of electron diffraction pattern and lack of good magnetic properties is that a magnetic fluid with α -iron as the magnetic particle has not been produced. Also we can conclude that triiron dodecacarbonyl despite initially encouraging results is not a suitable starting material for iron magnetic fluids.

One point which must not be overlooked is that whatever iron containing species was obtained, it was ferro- or ferrimagnetic. If the initial product of the decompositions is α -iron, which then undergoes oxidation, then the magnetic product is likely to be γ -Fe₂O₃ or Fe₃O₄ with one or more hydrated oxides present (α -FeOOH for example).

(iii) Studies of Iron Pentacarbonyl

¹²²
Smith and Wychick reported the preparation of colloidal

iron dispersions by the polymer catalysed thermal decomposition of iron pentacarbonyl in hydrocarbon solution. In the reactions the polymer is believed to catalyse the decomposition allowing the use of a lower temperature. Particle structures were reported to depend on particle size. Small (< 6nm) particles being initially amorphous, whereas larger (16nm) particles were largely α -iron. The aim of the present work was to prepare iron fluids from iron pentacarbonyl using the surfactants discussed previously rather than polymeric type surfactants.

(a) Preparations

A 5-necked round bottomed 500cm³ flask was used as the reaction vessel for this series of preparations. The flask was fitted with a teflon paddle stirrer, reflux condenser, thermometer, septum and gas inlet tap. The tap and condenser outlet were connected to an arrangement of taps/plastic tubing/T-pieces and bubblers which allowed either purging of the system or a stream of nitrogen to be blown over the top of the reflux condenser to encourage the removal of any evolved gas (carbon monoxide). In a typical preparation the flask was charged with a decalin solution (50cm³) of the surfactant (\sim 2.6g) following several hours of purging with dry nitrogen.

An isomantle was used to heat the system to a steady temperature in the 160-180°C range. Iron pentacarbonyl was then syringed into the flask via the septum in 1cm³ (1.46g) portions. Each addition would be followed by a rapid

evolution of gas. When gas evolution had ended, the system was briefly purged before a further addition. Normally six additions were made. The initial colour of the solutions was yellow, after two to three additions this darkened to brown, then black after four to six additions. When the decomposition was judged to be complete the flask was cooled to room temperature and thoroughly purged with nitrogen. The black liquid products were syringed into another flask, then the flask evacuated to remove any excess iron pentacarbonyl. Fluids 8.2.6 and 8.2.7 were prepared in this way using the surfactants Solsperse-3000 (2.6887g) and Duomeen-TDO (2.5616g) respectively.

(b) Analysis of Fluids 8.2.6 and 8.2.7 and Discussion

Transmission electron microscopy of diluted samples of these fluids on carbon coated copper grids showed the particles to be virtually spherical and well dispersed.

After much persistence electron diffraction patterns were obtained from both fluids. Each pattern consisted of four lines. The patterns were very similar in appearance. Most of the lines in both patterns were rather diffuse, hence the d-spacings calculated are not likely to be highly accurate. Table 8.2.3 gives the calculated d-spacings for a selection of possible iron containing decomposition products along with the values obtained by Griffiths et al.¹²³ for 16nm and 6nm particles.

The EXAFS spectrum of fluid 8.2.7 was very similar to that of fluid 8.2.5, prepared from $\text{Fe}_3(\text{CO})_{12}$ in

TABLE 8.2.3

"Iron" ferrofluid electron diffraction data (d-spacings) for
fluids 8.2.6 and 8.2.7 compared with literature data

Fluid 8.2.6	Fluid 8.2.7	Griffiths 16nm*	6nm	α -Fe	α -Fe ₂ O ₃	γ -Fe ₂ O ₃	Fe ₃ O ₄	α -FeOOH
3.68s	4.3vs					2.95	2.97	4.21
2.61m	2.58w				2.69	2.52	2.53	2.69 2.44
2.15m	2.08s	2.03	2.12	2.03	2.19			
1.52*	1.48s	1.44		1.43	1.61	1.48	1.48	
			1.2	1.17				

* very diffuse

** 16nm particles also exhibited an unidentified second phase

1-methyl-naphthalene with the same surfactant (i.e. Duomeen-TDO). Both spectra resemble the EXAFS spectra of α -FeOOH, implying the presence of some oxygen or nitrogen coordinated iron species i.e. an oxide, hydrated oxide or surfactant coordinated species (nitrogen coordination would give a very similar effect as oxygen coordination in the EXAFS spectra).

By taking into account both the EXAFS spectra and electron diffraction data we can start making some tentative conclusions. The decomposition of iron pentacarbonyl in hydrocarbon media initially produces particles which contain metallic iron. Electron diffraction suggests that some of this iron may be crystalline α -iron, because in both observed diffraction patterns there were lines which gave d-spacing values close to the 2.03\AA or 1.47\AA d-spacings for α -iron. The EXAFS data suggests the presence of an oxygen (or nitrogen) coordinated iron species. This could be due to oxidation by reaction with the surfactant, rather than oxidation by an external source. This is a likely possibility as the EXAFS spectra were recorded without exposure to the atmosphere. However, the electron diffraction data suggests the presence of an iron oxide species. The diffraction line due to a d-spacing of $\sim 2.6\text{\AA}$ could arise from any combination of the species α -Fe₂O₃, γ -Fe₂O₃, Fe₃O₄ or α -FeOOH. These species may arise through unavoidable contact with moist air in loading the sample for electron diffraction analysis. These observations do not

satisfactorily explain the possible presence of iron oxides in samples of ferrofluids which have not been exposed to air. EXAFS implies it is not α -iron, but from the data available a ferrimagnetic iron oxide cannot be eliminated entirely (whatever the identity of the material(s) it was ferro- or ferrimagnetic). Interestingly Mössbauer spectroscopy has recently revealed the presence of a magnetic material not previously considered.

Recently a sample of fluid 8.2.7 was studied using Mössbauer spectroscopy by Dr. J. Williams of Sheffield University. His initial studies indicate the absence of both α -iron and iron oxides (private communication). Instead the spectra resembled an iron-carbide type species; unfortunately his present analysis is not more specific about the identity of the species. Danish workers have also reported virtually identical results.¹⁶⁸ In their work, iron pentacarbonyl was thermally decomposed in decalin containing the surfactant Sarkosyl-0 under very similar conditions to those described in this work. From the Mössbauer spectra the Danes were able to conclude that a metallic glass had been produced from the thermal decomposition of iron pentacarbonyl. More specifically an amorphous iron-carbon alloy with 5-10 atomic % carbon had been formed. This metallic glass was crystallized into α -iron and an iron-carbide on heating.

These conclusions about the identity of the material¹⁶⁹ are reasonable as Niemantsverdriet et al. found that α -iron

catalysts used for Fischer-Tropsch synthesis were converted to a range of iron-carbides by passing carbon monoxide (along with hydrogen and helium) at elevated temperatures (160-450°C) over the catalysts. The nature and composition of the carbides present were dependent on the reaction temperature and synthesis time.

The formation of an iron-carbon alloy with hindsight is a logical explanation. We can easily envisage the decomposition of carbon monoxide on the growing surfaces of the iron particles. This would explain the incorporation of carbon into the particle structure. Secondly such a reaction would produce oxygen in the immediate vicinity of the iron particles. This would also explain why oxidation was always observed even after extreme precautions had been taken to exclude air. Further, if under the conditions of a typical decomposition carbon monoxide decomposed to carbon and oxygen preferentially on iron surfaces as compared to nickel and cobalt, we may have found some form of explanation for the "loss" of iron from our alloy systems. Iron-carbon alloys are ferromagnetic. The saturation magnetization decreases as the proportion of carbon increases (approximately 25% loss of saturation magnetization for 2% carbon). Hence we would still expect to observe typical magnetic properties for these systems.

8.2.3 Study of Iron Dicarbonyl Dinitrosyl

Iron dicarbonyl dinitrosyl was investigated as a potential new starting material for iron ferrofluids because

it is thermally unstable relative to the simple carbonyls
(dec. 50°C)¹⁷⁰. The aim of the study was to thermally decompose
the species at a relatively low temperature and avoid the
forcing conditions required by the binary carbonyls and thus
excessive oxidation or side reactions. (At the time of this
study simple oxidation was believed to be the principle
problem with the preparation of iron fluids).

Iron dicarbonyl dinitrosyl melts at 18°C.¹³⁵ At room
temperature it is a dark red volatile liquid. In these
studies the material was transferred using a vacuum system
into a Schlenk tube. A hydrocarbon surfactant solution would
then be syringed via a septum into the schlenk tube to
produce a blood red solution. These solutions were then
heated at various temperatures to cause decomposition to
metallic iron. Toluene was used initially as the carrier
liquid. Decomposition was attempted in the presence of a
range of surfactants. In each case a temperature of $\sim 70^\circ\text{C}$
was used initially; this produced no observable change.
Increasing the temperature to cause refluxing of the toluene
(110.6°C) only caused a slight darkening of the red solution
to brown. Further experiments using higher temperatures
available in decalin solution gave similar results. In all
cases there was no evidence of extensive gas evolution and
formation of metal. Consequently the carbonyl-nitrosyl
compound is not a suitable replacement for $\text{Fe}(\text{CO})_5$.

Conclusion

Although the results presented in this section concerning the preparation of "iron" fluids are interesting, the preparation of stable iron particle ferrofluids was not achieved. It was concluded that any α -iron particles produced are susceptible under the conditions used to reaction with carbon monoxide and other sources of oxygen leading to "carbide" and oxide formation.

From the results presented in this chapter we conclude that "metallic" particles produced by the thermal decomposition of organometallic carbonyl or carbonyl cyclopentadienyl derivatives incorporate a carbon based "impurity". In the interpretation of data collected on cobalt, iron-cobalt and nickel-iron systems reported in the previous three chapters, evidence of this particular phenomena was not observed. However we cannot neglect that this may have occurred also in the other systems. It may simply not cause any noticeable effect in the recorded data.

Incorporation of a carbon (or other) impurity would have a detrimental effect on the magnetic properties of the ferrofluids by reducing the particle magnetic moment. In turn this would lower the saturation magnetization of the ferrofluid. In the calculation of the dead layer thickness and %conversion of "molecular" metal to particulate metal in the ferromagnetic state it is assumed that the magnetic particle core has the same saturation magnetization per unit volume as the bulk metal (or alloy). Using this

assumption , the size of the dead layer may have been over estimated and the degree of conversion of the carbonyl to metal may have been under estimated.

CHAPTER 9

CONCLUSIONS AND FUTURE WORK

9.1 Conclusions

To date, the majority of research on magnetic fluids has been carried out by physicists; after all it has been traditionally a "physics" subject. The work described in this thesis gives a chemical bias to the subject, although inevitably there has been considerable overlap with other fields. In the future, development of magnetic fluid science will almost certainly lie with the physicists and engineers as more applications are developed. However, I believe solutions to many of the more fundamental problems of magnetic fluid research will lie with the chemist.

The aims of this particular study were (i) the preparation and characterization of new magnetic fluids, and (ii) investigation into alternative routes to existing magnetic fluids. Substantial progress has been made with respect to the first of these goals. A number of interesting and thought provoking discoveries have been made with respect to the second.

In Chapters 6 and 7 herein, the preparation of the first hydrocarbon based alloy particle magnetic fluids has been reported. This has been achieved by the controlled

thermal decomposition of specifically prepared heteronuclear organometallic carbonyl compounds of the ferromagnetic transition metals in hydrocarbon solution in the presence of a surfactant. Using this strategy iron-cobalt and nickel-iron particle magnetic fluids were prepared. Two series of iron-cobalt particles were produced with initial particle compositions of CoFe and Co_3Fe from different organometallic starting materials with cobalt:iron atomic ratios of 1:1 and 3:1 respectively. A series of nickel-iron particle fluids were prepared by the decomposition of a nickel-iron cluster with a nickel:iron ratio of 2:1; however the particle composition was observed to be Ni_xFe where $x \sim 3$. From electron microscopic examination and magnetic analysis we concluded that all of these fluids contained well dispersed, roughly spherical particles with physical diameters in the 5-8nm size range which were superparamagnetic. In these respects the fluids were virtually identical to simple cobalt particle magnetic fluids prepared by the thermal decomposition of dicobalt octacarbonyl in this and in previous work. Evidence that the particles were of a genuine alloy composition came from local area EDX spectroscopy. In two of the three alloy particle systems (FeCo and Ni_3Fe), electron diffraction revealed the presence of ordered "superlattice" structures. In the third system (Co_3Fe) a diffraction pattern was not obtained. This is an interesting result. The fact that the same tendency was observed in two different systems gives

credence to the result. Further support for superlattice formation comes from completely independent work by Marignier et al.¹⁷¹ who prepared CuPd and Cu₃Pd particles by the radiation-induced reduction of solutions of metal ions. Electron diffraction indicated these particles had superlattice structures.

An interesting trend was observed in all three series of alloy fluids; in all cases, and to varying extents, iron appeared to be "lost" either during the decomposition process (nickel-iron system) or possibly after particle formation (iron-cobalt systems). These observations were discussed in the relevant sections.

In a collaborative venture, a cobalt particle magnetic fluid has been prepared by the condensation of cobalt atoms into a toluene solution of surfactant. Fluid preparation was carried out at Bristol University under the supervision of Dr. P.L. Timms. Characterization of the fluid at Durham revealed that the fluid was virtually identical to cobalt ferrofluids prepared by the conventional method of thermal decomposition of dicobalt octacarbonyl, with respect to particle size and magnetic properties. This is an important result, and may well represent the beginning of a new general route to metallic particle magnetic fluids. It must be noted however, that recently Japanese workers have reached the same conclusions.¹⁷²

An infra-red spectroscopic study of cobalt magnetic fluids prepared by the thermal decomposition of Co₂(CO)₈ and

stabilized with the surfactant Sarkosyl-0 revealed that all of the surfactant present during decomposition reacts to produce a cobalt derivative, probably a form of carboxylate-type complex. This result means that the "free" surfactant present in magnetic fluids is in fact likely to be a metal derivative, when the fluids are prepared by the thermal decomposition of a carbonyl complex. This result, not being previously reported, at least partially explains why only a fraction of the metal in the organometallic starting material is converted to ferromagnetic metal.

An EXAFS spectroscopic study of magnetic fluids prepared by the thermal decomposition of $\text{Co}_2(\text{CO})_8$ indicated that the particles did consist of metallic cobalt as expected. Using the same technique the oxidation of this fluid to give an oxygen coordinated species was observed.

A similar study of "iron" particle magnetic fluids prepared by the thermal decomposition of iron carbonyls indicated a lack of α -iron in the particles. The spectra recorded were more consistent with an oxygen coordinated species, possibly a surfactant derivative or an oxide. It is now believed however, that these so called "iron" fluids consist of iron-carbon alloy particles. This represents an important result. If carbon is incorporated into the "iron" particles, as Mössbauer work seems to imply, then we must be aware of the possibility that this may occur in the other metallic systems. If the extent of carbon incorporation is very small, this may not be detectable from the observable

properties of magnetic fluids. Carbon incorporation into particles would almost certainly reduce the particle magnetic moment. Indeed, this effect may contribute to the observation that ferrofluid saturation magnetization is always lower than predicted assuming 100% decomposition of the organometallic to ferromagnetic metal.

In the work described, it has been demonstrated that the decomposition of organometallic carbonyl complexes to produce magnetic fluids can be extended to include bimetallic alloy systems. Considering the fluids discussed so far collectively, the systems containing cobalt, iron-cobalt and nickel-iron particles appear to be very similar with respect to particle size, shape, magnetic properties and structure (in as much as the particles consist of a crystalline form of the metallic material(s) present in the organometallic starting material). This implies the same type of decomposition process is occurring in these systems. Previous to this work it seemed logical to include nickel and iron single metal systems into this general conclusion. In the case of nickel the "organometallic" route was not observed to be particularly fruitful, with the preparation of large regularly shaped particles being the nearest to a successful preparation. A combination of the work described in section 8.2 and in work reported in the literature indicate that the thermal decomposition of iron carbonyl species is not a suitable method to prepare iron particle magnetic fluids.

9.2 Future work

This section is divided into (i) work concerning existing problems, and (ii) extension of the work described in the text.

9.2.1 Existing Problems

The most serious problem concerning metallic particle magnetic fluids is their susceptibility to atmospheric oxidation which has prevented their commercial application to date. Solution of the oxidation problem is of extreme importance. At this stage we can only speculate on possible methods of reducing oxidation. For example, a surface coating of inert material, preferably with one which is itself ferro- or ferrimagnetic (e.g. magnetite). Alternatively, it may be possible to incorporate a second element into the particle which inhibits oxidation. Chromium, for example, is known to inhibit the oxidation of iron at high temperatures.¹⁷³ By thermolysis of iron-chromium organometallic starting materials or simultaneous evaporation of the two metals, it may be possible to produce iron-chromium particles with a higher resistance to oxidation than pure iron. Unfortunately, incorporation of a nonferromagnetic element into the metallic particle or introduction of a surface coating would have a detrimental effect on the magnetic properties.

In the preparation of nickel-iron particle magnetic fluids from $[(\pi-C_5H_5)_2Ni_2Fe(CO)_5]$ (Ni:Fe = 2.1), the

particle composition was shown to be Ni_xFe , where $x \sim 3$. As a chemist, it would be of interest to understand what is happening during the thermal decomposition of these mixed metal complexes. From section 3.2.2. we know that the thermal decomposition of $\text{Co}_2(\text{CO})_8$ in toluene solution in the presence of a surfactant is a complex process. It is likely that the decomposition of mixed metal carbonyl species is even more complex. Full elucidation of the decomposition process would be a highly involved project. When iron is "lost" during the actual decomposition (nickel-iron systems) it may be possible to determine the fate of the "missing" iron by separating the components of the reaction mixture using chromatography for example (after removing the particles) and identify any residual metal containing components using techniques such as mass spectroscopy and infra-red spectroscopy.

9.2.2 Extension of Present Work

In the future there is a great deal of scope for the extension of the work described in this thesis. Iron-cobalt particles with composition Fe_2Co would probably be prepared by the thermal decomposition of $[(\pi\text{-C}_5\text{H}_5)\text{Fe}_2\text{Co}(\text{CO})_9]$. This particular alloy has the highest saturation magnetic moment of all known magnetic materials. The extension of the route to the preparation of nickel-cobalt particles is also a possibility by utilizing compounds such as $[(\pi\text{-C}_5\text{H}_5)\text{NiCo}_3(\text{CO})_9]$.

Preparation of an iron-rhodium particle system is also potentially very interesting. The iron-rhodium alloy undergoes an antiferromagnetic to ferromagnetic transition on heating through $\sim 77^{\circ}\text{C}$.¹⁷⁵ If we could prepare iron-rhodium particles from organometallics such as $[(\pi\text{-C}_5\text{H}_5)_2\text{Fe}_2\text{Rh}(\text{CO})_9]$,¹⁷⁴ then we could produce in theory a magnetic fluid whose magnetic properties could be "switched" on and off by a temperature change.

Finally, we must consider the use of metal evaporation to prepare metal and alloy particle magnetic fluids. This is a very logical method by which to prepare magnetic fluids containing alloy particles because this approach offers the possibility of controlling the final alloy composition. Indeed in collaborative work with Dr. P.L. Timms of Bristol University, initial investigations are now being made into the preparation of alloy particle fluids using this technique. However, very recently a very similar technique¹⁷² has been patented by Nakatami and Masumoto.

APPENDIX

RESEARCH COLLOQUIA, SEMINARS, LECTURES, MEETINGS AND
CONFERENCES

The Board of Studies in Chemistry requires that each postgraduate research thesis contains an appendix, listing:

- (a) all research colloquia, research seminars and lectures arranged by the Department of Chemistry during the period of the author's residence as a postgraduate student;
- (b) lectures organised by Durham University Chemical Society;
- (c) all research conferences and meetings attended and papers presented by the author during the period when research for the thesis was carried out;
- (d) details of the postgraduate induction course.

(a) LECTURES ORGANISED BY DURHAM UNIVERSITY 1983 - 1986

- 5.10.83 Prof. J.P. Maier (Basel, Switzerland)
"Recent approaches to spectroscopic characterization of cations".
- 12.10.83 Dr. C.W. McLeland (Port Elizabeth, Australia),
"Cyclization of aryl alcohols through the intermediacy of alkoxy radicals and aryl radical cations".
- 19.10.83 Dr. N.W. Alcock (Warwick),
"Aryl tellurium (IV) compounds, patterns of primary and secondary bonding".

- 26.10.83 Dr. R.H. Friend (Cavendish, Cambridge).
"Electronic properties of conjugated polymers".
- 30.11.83 Prof. I.M.G. Cowie (Stirling),
"Molecular interpretation of non-relaxation
processes in polymer glasses".
- 2.12.83 Dr. G.M. Brooke (Durham),
"The fate of the ortho-fluorine in 3,3-sigmatropic
reactions involving polyfluoro-aryl and
-hetero-aryl systems".
- 14.12.83 Prof. R.J. Donovan (Edinburgh),
"Chemical and physical processes involving the
ion-pair states of the halogen molecules".
10. 1.84 Prof. R. Hester (York)
"Nanosecond Laser Spectroscopy of Reaction
Intermediates".
18. 1.84 Prof. R.K. Harris (UEA)
"Multi-nuclear solid state magnetic resonance".
8. 2.84 Dr. B.T. Heaton (Kent),
"Multi-nuclear NMR studies".
15. 2.84 Dr. R.M. Paton (Edinburgh)
"Heterocyclic Syntheses using Nitrile Sulphides".
7. 3.84 Dr. R.T. Walker (Birmingham),
"Synthesis and Biological Properties of some
5-substituted Uracil Derivatives; yet another
example of serendipity in Anti-viral
Chemotherapy".
21. 3.84 Dr. P. Sherwood (Newcastle)
"X-ray photoelectron spectroscopic studies of
electrode and other surfaces".
21. 3.84 Dr. G. Beamson (Durham/Kratos)
"EXAFS: General Principles and Applications.
23. 3.84 Dr. A. Ceulemans (Leuven)
"The Development of Field-Type models of the
Bonding in Molecular Clusters".
2. 4.84 Prof. K. O'Driscoll (Waterloo)
"Chain Ending reactions in Free Radical
Polymerisation".
3. 4.84 Prof. C.H. Rochester (Dundee).
"Infrared Studies of adsorption at the
Solid-Liquid Interface".

25. 4.84 Dr. R.M. Acheson (Biochemistry, Oxford)
"Some Heterocyclic Detective Stories".
27. 4.84 Dr. T. Albright (Houston, U.S.A.)
"Sigmatropic Rearrangements in Organometallic
Chemistry".
14. 5.84 Prof. W.R. Dolbier (Florida, U.S.A.).
"Cycloaddition Reactions of Fluorinated Allenes".
16. 5.84 Dr. P.J. Garratt (UCL)
"Synthesis with Dilithiated Vicinal Diesters and
Carboximides".
22. 5.84 Prof. F.C. de Schryver (Leuven)
"The use of Luminescence in the study of micellar
aggregates" and
"Configurational and Conformational control in
excited state complex formation".
23. 5.84 Prof. M. Tada (Waseda, Japan)
"Photochemistry of Dicyanopyrazine Derivatives".
31. 5.84 Dr. A. Haaland (Oslo)
"Electron Diffraction Studies of some
organometallic compounds.
11. 6.84 Dr. J.B. Street (IBM, California)
"Conducting Polymers derived from Pyrroles".
19. 9.84 Dr. C. Brown (IBM, California)
"New Superbase reactions with organic compounds".
21. 9.84 Dr. H.W. Gibson (Signal UOP, Illinois)
"Isomerization of Polyacetylene".
- 19.10.84 Dr. A. Germain (Languedoc, Montpellier)
"Anodic Oxidation of Perfluoro Organic Compounds
in Perfluoroalkane Sulphonic Acids".
- 24.10.84 Prof. R.K. Harris (Durham)
"N.M.R. of Solid Polymers".
- 28.10.84 Dr. R. Snaith (Strathclyde)
"Exploring Lithium Chemistry: Novel Structures,
Bonding and Reagents".
- 7.11.84 Prof. W.W. Porterfield (Hampden-Sydney College,
USA)
"There is no Borane Chemistry (only Geometry)".
- 7.11.84 Dr. H.S. Munro (Durham)
"New Information from ESCA Data".

- 21.11.84 Mr. N. Everall (Durham)
"Picosecond Pulsed Laser Raman Spectroscopy".
- 27.11.84 Dr. W.J. Feast (Durham)
"A Plain Man's Guide to Polymeric Organic Metals".
- 28.11.84 Dr. T.A. Stephenson (Edinburgh)
"Some recent studies in Platinum Metal Chemistry".
- 12.12.84 Dr. K.B. Dillon (Durham)
"³¹P N.M.R. Studies of some Anionic Phosphorus Complexes".
11. 1.85 Emeritus Prof. H. Suschitzky (Salford)
"Fruitful Fissions of Benzofuroxanes and Isobenzimidic azoles (umpolung of o-phenylenediamine)".
13. 2.85 Dr. G.W.J. Fleet (Oxford)
"Synthesis of some Alkaloids from Carbohydrates".
19. 2.85 Dr. D.J. Mincher (Durham)
"Stereoselective Synthesis of some novel Anthracyclines related to the anti-cancer drug Adriamycin and to the Steffimycin Antibiotics".
27. 2.85 Dr. r. Mulvey (Durham)
"Some unusual Lithium Complexes".
6. 3.85 Dr. P.J. Kocienski (Leeds)
"Some Synthetic Applications of Silicon-Mediated Annulation Reactions".
7. 3.85 Dr. P.J. Rodgers (I.C.I. plc. Agricultural Division, Billingham)
"Industrial Polymers from Bacteria".
12. 3.85 Prof. K.J. Packer (B.P. Ltd./East Anglia)
"N.M.R. Investigations of the Structure of Solid Polymers".
14. 3.85 Prof. A.R. Katritzky F.R.S. (Florida)
"Some Adventures in Heterocyclic Chemistry".
20. 3.85 Dr. M. Poliakoff (Nottingham)
"New Methods for detecting Organometallic Intermediates in Solution".
28. 3.85 Prof. H. Ringsdorf (Mainz)
"Polymeric Liposomes as Models for Biomembranes and Cells?".

24. 4.85 Dr. M.C. Grossel (Bedford College, London)
"Hydroxypyridone dyes - Bleachable one-dimensional metals?".
25. 4.85 Major S.A. Shackelford (U.S. Air Force)
"In Situ Mechanistic Studies on Condensed Phase Thermochemical Reaction Processes: Deuterium Isotope Effects in HMX Decomposition, Explosives and Combustion".
1. 5.85 Dr. D. Parker (I.C.I. plc. Petrochemical and Plastics Division, Wilton)
"Applications of Radioisotopes in Industrial Research".
7. 5.85 Prof. G.E. Coates (formerly of University of Wyoming, USA)
"Chemical Education in England and America: Successes and Deficiencies".
8. 5.85 Prof. D. Tuck (Windsor, Ontario)
"Lower Oxidation State Chemistry of Indium".
8. 5.85 Prof. G. Williams (U.C.W. Aberystwyth)
"Liquid Crystalline Polymers".
9. 5.85 Prof. R.K. Harris (Durham)
"Chemistry in a Spin: Nuclear Magnetic Resonance".
14. 5.85 Prof. J. Passmore (New Brunswick, U.S.A.)
"The Synthesis and Characterisation of some Novel Selenium-Iodine Cations, aided by Se N.M.R. Spectroscopy".
15. 5.85 Dr. J.E. Packer (Auckland, New Zealand)
"Studies of Free Radical Reactions in aqueous solution using Ionising Radiation".
17. 5.85 Prof. I.D. Brown (McMaster University, Canada)
"Bond Valence as a Model for Inorganic Chemistry".
21. 5.85 Dr. D.L.H. Williams (Durham)
"Chemistry in colour".
22. 5.85 Dr. M. Hudlicky (Blacksburg, USA)
"Preferential Elimination of Hydrogen Fluoride from Vicinal Bromofluorocompounds".
22. 5.85 Dr. S. Grimmett (Otago, New Zealand)
"Some Aspects of Nucleophilic Substitution in Imidazoles".

4. 6.85 Dr. P.S. Belton (Food Research Institute, Norwich)
"Analytical Photoacoustic Spectroscopy".
13. 6.85 Dr. D. Woolins (Imperial College, London)
"Metal -Sulphur - Nitrogen Complexes".
14. 6.85 Prof. Z. Rappoport (Hebrew University, Jerusalem)
"The Rich Mechanistic World of Nucleophilic
Cinylic Substitution".
19. 6.85 Dr. R.N. Mitchell (Dortmund)
"Some Synthetic and NMR - Spectroscopic Studies of
Organotin Compounds".
26. 6.85 Prof. G. Shaw (Bradford)
"Synthetic Studies on Imidazole Nucleosides and
the Antibiotic Coformycin".
12. 7.85 Dr. K. Laali (Hydrocarbon Research Institute,
University of Southern California)
"Recent Developments in Superacid Chemistry and
Mechanistic Considerations in Electrophilic
Aromatic Substitutions: A Progress Report".
13. 9.95 Dr. V.S. Parmar (University of Delhi),
"Enzyme Assisted ERC Synthesis".
- 30.10.85 Dr. S.N. Whittleton (University of Durham),
"An Investigation of a Reaction Window".
- 5.11.85 Prof. M.J. O'Donnell (Indiana-Purdue University),
"New Methodology for the Synthesis of Amino
acids".
- 20.11.85 Dr. J.A.H. MacBride (Sunderland Polytechnic).
"A Heterocyclic Tour on a Distorted
Tricycle-Biphenylene".
- 28.11.85 Prof. D.J. Waddington (University of York),
"Resources for the Chemistry Teacher".
15. 1.86 Prof. N. Sheppard (University of East Anglia),
"Vibrational and Spectroscopic Determinations of
the Structures of Molecules Chemisorbed on Metal
Surfaces".
29. 1.86 Dr. J.H. Clark (University of York),
"Novel Fluoride Ion Reagents".
12. 2.86 Prof. O.S. Tee (Concordia University, Montreal),
"Bromination of Phenols".

12. 2.86 Dr. J. Yarwood (University of Durham),
"The Structure of Water in Liquid Crystals".
19. 2.86 Prof. G. Procter (University of Salford),
"Approaches to the Synthesis of some Natural
Products".
26. 2.86 Miss C. Till (University of Durham),
"ESCA and Optical Emission Studies of the Plasma
Polymerisation of Perfluoroaromatics".
5. 3.86 Dr. D. Hathway (University of Durham),
"Herbicide Selectivity".
5. 3.86 Dr. M. Schroder (University of Edinburgh),
"Studies on Macrocyclic Complexes".
12. 3.86 Dr. J.M. Brown (University of Oxford),
"Chelate Control in Homogeneous Catalysis".
14. 5.86 Dr. P.R.R. Langridge-Smith (University of
Edinburgh),
"Naked Metal Clusters - Synthesis,
Characterisation and Chemistry".
9. 6.86 Prof. R. Schmutzler (University of Braunschweig),
"Mixed Valence Diphosphorous Compounds".
23. 6.86 Prof. R.E. Wilde (Texas Technical University),
"Molecular Dynamic Processes from Vibrational
Bandshapes".

(b) LECTURES ORGANISED BY DURHAM UNIVERSITY CHEMICAL
SOCIETY DURING THE PERIOD 1983 - 1986

- 20.10.83 Prof. R.B. Cundall (Salford)
"Explosives".
- 3.11.83 Dr. G. Richards (Oxford)
"Quantum Pharmacology".
- 10.11.83 Prof. J.H. Ridd (U.C.L.)
"Ipso-Attack in Electrophilic Aromatic
Substitution".
- 17.11.83 Dr. J. Harrison (Sterling Organic),
"Applied Chemistry and the Pharmaceutical
Industry"
(Joint Lecture with the Society of Chemical
Industry).

- 24.11.83 Prof. D.A. King (Liverpool)
"Chemistry in 2-Dimensions".
- 1.12.83 Dr. J.D. Coyle (The Open University),
"The Problem with Sunshine".
26. 1.84 Prof. T.L. Blundell (Birkbeck College, London).
"Biological Recognition: Interactions of
Macromolecular Surfaces".
2. 2.84 Prof. N.B.H. Jonathan (Southampton),
"Photoelectron Spectroscopy - A Radical Approach".
16. 2.84 Prof. D. Phillips (The Royal Institution),
"Luminescence and Photochemistry - a Light
Entertainment".
23. 2.84 Prof. F.G.A. Stone F.R.S. (Bristol),
"The Use of Carbene and Carbyne Groups to
Synthesise Metal Clusters"
(The Waddington Memorial Lecture).
1. 3.84 Prof. A.J. Leadbetter (Rutherford Appleton Labs.),
"Liquid Crystals".
8. 3.84 Prof. D. Chapman (Royal Free Hospital School of
Medicine, London)
"Phospholipids and Biomembranes: Basic Science and
Future Techniques".
28. 3.84 Prof. H. Schmidbaur (Munich, F.R.G.),
"Ylides in Coordination Sphere of Metal:
Synthetic, Structural and Theoretical Aspects"
(R.S.C. Centenary lecture).
- 18.10.84 Dr. N. Logan (Nottingham),
" N_2O_4 and Rocket Fuels".
- 23.10.84 Dr. W.J. Feast (Durham),
"Syntheses of Conjugated Polymers. How and Why?".
- 8.11.84 Prof. B.J. Aylett (Queen Mary College, London),
"Silicon - Dead Common or Refined?".
- 15.11.84 Prof. B.T. Golding (Newcastle-upon-Tyne),
"The Vitamin B_{12} Mystery".
- 22.11.84 Prof. D.T. Clark (I.C.I. New Science Group),
"Structure, Bonding, Reactivity and Synthesis as
revealed by ESCA".
(R.S.C. Tilden lecture).
- 29.11.84 Prof. C.J.M. Stirling (University College of North
Wales)

- 6.12.84 Prof. R.D. Chambers (Durham),
"The Unusual World of Fluorine".
24. 1.85 Dr. A.K. Covington (Newcastle-upon-Tyne),
"Chemistry with Chips".
31. 1.85 Dr. M.L.H. Green (Oxford),
"Naked Atoms and Negligee Ligands".
7. 2.85 Prof. A. Ledwith (Pilkington Bros.),
"Glass as a High Technology Material"
(Joint Lecture with the Society of Chemical
Industry).
14. 2.85 Dr. J.A. Salthouse (Manchester),
"Son et Lumiere".
21. 2.85 Prof. P.M. Maitlis, F.R.S. (Sheffield)
"What Use is Rhodium?".
7. 3.85 Dr. P.W. Atkins (Oxford),
"Magnetic Reactions".
- 17.10.85 Dr. C.J. Ludman (University of Durham)
"Some Thermochemical aspects of Explosions".
(A Demonstration Lecture).
- 24.10.85 Dr. J. Dewing (U.M.I.S.T.),
"Zeolites - Small Holes, Big Opportunities".
- 31.10.85 Dr. P. L. Timms, (University of Bristol),
"Some Chemistry of Fireworks"
(A Demonstration Lecture).
- 7.11.85 Prof. G. Ertl, (University of Munich),
"Heterogeneous Catalysis",
(R.S.C. Centenary lecture).
- 14.11.85 Dr. S.G. Davies (University of Oxford),
"Chirality Control and Molecular Recognition".
- 21.11.85 Prof. K.H. Jack, F.R.S. (University of
Newcastle-upon-Tyne),
"Chemistry of Si-Al-O-N Engineering Ceramics"
(Joint Lecture with the Society of Chemical
Industry).
- 28.11.85 Dr. B.A.J. Clark (Research Division, Kodak ltd.)
"Chemistry and Principles of Colour Photography".

23. 1.85 Prof. Sir Jack Lewis, F.R.S. (University of Cambridge),
"Some More Recent Aspects in the Cluster Chemistry of Ruthenium and Osmium Carbonyls"
(The Waddington Memorial Lecture).
30. 1.86 Dr. N.J. Phillips (University of Technology, Loughborough)
"Laser Holography".
13. 2.86 Prof. R. Grigg (Queen's University, Belfast),
"Thermal Generation of 1,3-Dipoles".
(R.S.C. Tilden lecture).
20. 2.86 Dr. C.J.F. Barnard, (Johnson Matthey Group Research),
"Platinum Anti-Cancer Drug Development - From Serendipity to Science".
27. 2.86 Prof. R.K. Harris, (University of Durham),
"The Magic of Solid State NMR".
6. 3.86 Dr. B. Iddon (University of Salford),
"The Magic of Chemistry"
(A Demonstration lecture).

(c) RESEARCH CONFERENCES AND MEETINGS ATTENDED

February 1984, Scottish Dalton meeting, Glasgow University.

April 1984, Graduate Symposium, Durham University.

April 1985, Graduate Symposium, Durham University.

*December 1986, Royal Society of Chemistry, Poster Meeting, Newcastle University.

**April 1986, Graduate Symposium, Durham University.

**July 28-August 1, 1986, Fourth International Conference on Magnetic Fluids, Tokyo and Sendai, Japan.

* indicates poster presentation.

** indicates oral presentation.

(d) FIRST YEAR INDUCTION COURSE, OCTOBER 1983

This course consists of a series of one hour lectures on the services available in the Department.

1. Departmental organisation.
2. Safety matters.
3. Electrical appliances and infrared spectroscopy.
4. Chromatography and Microanalysis.
5. Atomic absorptiometry and inorganic analysis.
6. Library facilities.
7. Mass spectroscopy.
8. Nuclear magnetic resonance spectroscopy.
9. Glassblowing technique.

REFERENCES

1. S.W. Charles and R.E. Rosensweig, *J. Magn. Mag. Mat.*, 1983, 39, 190.
2. S.W. Charles and J. Popplewell, In *Ferromagnetic Materials*, Vol. 2, Ed., E.P. Wohlfarth, North-Holland, Amsterdam, 1980, 509.
3. E.G. Wilson, *Phil. Trans.*, 1779, 480.
4. F. Bitter, *Phys. Rev.*, 1931, 38, 1903.
5. F. Bitter, *Phys. Rev.*, 1932, 41, 507.
6. L.W. McKeehan and W.C. Elmore, *Phys. Rev.*, 1934, 46, 226.
7. W.C. Elmore, *Phys. Rev.*, 1938, 54, 309.
- 8.* N.M. Griбанov, I.S. Lavrov and I. Yu. Mishuris, *Dispersnye Sist. Ikh. Povedenie Elektr. Magn. Polyakh.*, 1976, 1, 27. *Chem. Abs.*, 90, 33104y.
9. J. Rabinow, *Franklin Inst.*, 1949, 248, 155.
10. R.W. Wolfe and J. North, *Appl. Phys. Lett.*, 1974, 25, 122.
11. S.S. Papell, U.S. Patent 3,215,572, 1965.
12. P.C. Scholten, In *Thermomechanics of Magnetic Fluids*, Ed., B. Berkovsky, Hemisphere, Washington D.C., 1978, 1.
13. J. Frenkel and J. Dorfman, *Nature*, 1930, 126, 274.
14. C. Kittel, *Phys. Rev.*, 1946, 70, 965.
15. C. Kittel, J.K. Gault and W.E. Campell, *Phys. Rev.*, 1950, 77, 735.
16. F.E. Luborsky and T.O. Paine, *J. Appl. Phys.* 1960, 31, 68S.
17. R.W. Tebble, *Magnetic Domains*, Butler and Tanner, London, 1960.
18. F.E. Luborsky, *J. Appl. Phys.*, 1961, 32, 171S.
19. C.P. Bean and J.D. Livingston, *J. Appl. Phys.*, 1959, 30, 120S.

20. R. Kaiser and G. Miskolczy, *J. Appl. Phys.*, 1970, 41, 1064.
21. R.E. Rosensweig, *Ferrohydrodynamics*, Cambridge University Press, Cambridge, 1985.
22. A.E. Berkowitz, J.A. Lahut, I.S. Jacobs, L.M. Levison and D.W. Forester, *Phys. Rev. Lett.*, 1975, 34, 594.
23. R.W. Chantrell, J. Popplewell and S.W. Charles, *IEEE Trans. Magn.*, 1978, 14, 975.
24. D.B. Lambrick, Ph.D. Thesis, 1986.
25. J.N. Israelachvilli and D. Tabor, *Progr. in Surface and Membrane Sci.*, 1973, 17, 1.
26. H.C. Hamaker, *Physica*, 1937, 4, 1058.
27. J. Th. G. Overbeek, In *Colloidal Dispersions*, Ed., J.W. Goodwin, Royal Society of Chemistry, London, 1982.
28. M.I. Shiomis, *Sov. Phys. USP.*, 1974, 17, 153.
29. E.L. Mackor, *J. Colloid Sci.*, 1951, 6, 492.
30. R.E. Rosensweig, J.W. Nestor and R.S. Timmins, *Mater. Assoc. Direct Energy Convers. Proc. Sym. AICHE. I Chem. Eng. Ser. 5*, 1965, 5, 104.
31. K.D. O'Grady, Ph.D. Thesis, 1982.
32. R. Massart, *IEEE Trans. Magn.*, 1981, 17, 1247.
33. H. Lamb, *Hydrodynamics*, Sixth Edition, Cambridge Univ. Press, London, 1932.
34. S.W. Charles and J. Popplewell, In *Thermomechanics of Magnetic Fluids*, Ed., B. Berkovsky, Hemisphere, Washington D.C., 1978, 27.
35. J. Popplewell and S.W. Charles, *Physics Bull.*, 1979, 30, 474.
36. R.E. Rosensweig, *Sci. Am.*, 1982, 247, 124.
37. J. Shimoizaka, K. Nakatsuka, T. Fujita and A. Kounosu, *IEEE Trans. Magn.*, 1980, 16, 368.
38. J. Popplewell, A. Al-Qenaie, S.W. Charles, R. Moskowitz and K. Raj, *Coll. and Polym. Sci.*, 1982, 260, 333.

39. R.E. Rosensweig, R. Kaiser and G. Miskolczy, *J. Colloid and Interface Sci.*, 1969, 29, 680.
40. R. Moskowitz, *ASLE Trans.*, 1975, 18, 135.
41. M.P. Perry, In *Thermomechanics of Magnetic Fluids*, Ed., B. Berkovsky, Hemisphere, Washington D.C., 1978, 219.
42. R.L. Bailey, *J. Magn. Mag. Mat.*, 1983, 39, 178.
43. R. Kaiser and G. Miskolczy, *IEEE Trans. Mag.*, 1970, 6, 694.
44. L. Kuhn and R.A. Myers, *Sci. Am.*, 1979, 240, 120.
45. S. Maruno , K. Yubakami and M. Soga, *J. Magn. Mag. Mat.*, 1983, 39, 187.
46. A.F. Tsyb, I.S. Amosov, B.M. Berkovsky, V.I. Sharley, R.G. Nikitina, M.M. Rozhinsky, L.V. Suloyova and G.M. Shakhlevich, *J. Magn. Mag. Mat.*, 1983, 39, 183.
47. Y. Morimoto, M. Akimoto and Y. Yotsumoto, *Chem. Pharm. Bull.*, 1982, 30, 3024.
48. R.P.H. Gasser, *An Introduction to Chemisorption and Catalysis by Metals*, Clarendon Press, Oxford, 1985.
49. G.C. Bond, *Catalysis by Metals*, Academic Press, London, 1962.
50. P.H. Emmett and N. Skau, *J. Am. Chem. Soc.*, 1943, 65, 1029.
51. G.C. Bond and R.S. Mann, *J. Chem. Soc.*, 1959, 3566.
52. G.C. Bond, *Trans. Faraday Soc.*, 1956, 52, 1235.
53. R.D. Rieke and P.M. Hudnall, *J. Am. Chem. Soc.*, 1972, 94, 7178.
54. R.D. Rieke and S.E. Bates, *J. Am. Chem. Soc.*, 1974, 96, 1775.
55. R.D. Rieke, S.J. Uhm and P.M. Hundall, *J. Chem. Soc. Chem. Comm.*, 1973, 269.
56. A.V. Kavaliunas and R.D. Ricke, *J. Am. Chem. Soc.*, 1980, 102, 5944.
57. R.D. Rieke, W.F. Wolf, N. Kuzundzic and A.V. Kavaliunas, *J. Am. Chem. Soc.*, 1977, 99, 4159.

58. R.D. Rieke, K. Öfele and E.O. Fischer, *J. Organomet. Chem.*, 1974, 76, C19.,
59. S.C. Davis and K.J. Klabunde, *J. Am. Chem. Soc.*, 1978, 100, 5973.
60. K.J. Klabunde, H.F. Efner, T.O. Murdock and R. Ropple, *J. Am. Chem. Soc.*, 1976, 98, 1021.
61. S.C. Davis, S.J. Severson and K.J. Klabunde, *J. Am. Chem. Soc.*, 1981, 103, 3024.
62. K.J. Klabunde and Y. Imizn, *J. Am. Chem. Soc.*, 1984, 106, 2721.
63. R.E. Rosensweig and R. Kaiser, NTIS Rep. No. NASW-1219, NASA Rep. NASA-CR-91684. NASA Office of Adv. Res. and Tech., Washington, D.C., 1967.
64. R.E. Rosensweig, U.S. Patent 3,531,413, 1970.
65. R.E. Rosensweig, U.S. Patent 3,917,538, 1975.
66. S.E. Khalafalla and G.W. Reimers, U.S. Patent 3,764,540, 1973.
67. G.W. Reimers and S.E. Khalafalla, U.S. Patent 3,843,540, 1972.
68. *E.E. Bibik, *Kolloid. Zh.*, 1973, 35, 114. *Chem. Abs.*, 80, 53893b.
69. *E.V. Gulyaikhin, N.I. Plotnikov, A.B. Solodenko, O.F. Purvinskii, B.D. Zhukov and L.A. Shurygina, *Otkrytiya, Izobret., Prom. Obtraztsy, Tovernye Znaki*, 1981, 24, 75. *Chem. Abs.*, 95, P125758h.
70. *N.P. Matusевич, V.K. Rakhuba and V.B. Samoïlov, *ibid*, 1981, 20, 49. *Chem. Abs.*, 95, 196417v.
71. *E.E. Bibik, I.S. Lavrov, N.M. Gribanov and T.M. Kotomina, *ibid*, 1977, 54, 47. *Chem. Abs.*, 87, P145106r.
72. *N. Buske, *E. Ger. Pat.* 114,052, 1975, *Chem. Abs.*, 84, P129765S.
73. *E.E. Bibik and I.S. Lavrov, *Otkrytiya, Izobret., Prom. Obtraztsy, Tovernye Znaki*, 1975, 52, 52. *Chem. Abs.*, 83, P52432a.
74. *M.A. Berlin, E.E. Bibik, V.N. Krygin and V.T. Suprunov, *ibid*, 1982, 28, 102. *Chem. Abs.*, 97, P173809b.

75. *V.A. Silaer, M. Yu. Kozlov, A.P. Sizov and T.B. Speranskaya, *ibid*, 1984, 7, 81. Chem. Abs., 100, 220470b.
76. *M. Nishimura, K. Yamamoto, T. Nagoyoshi and M. Miyazaki, Japan Kokai 76 13,995, 1976. Chem. Abs., 85, P40178a.
77. *J. Shimoizaka, Japan Kokai 76 44,579, 1976. Chem. Abs., 85, 136 75f.
78. *E.E. Bibik, N.M. Griбанov, O.V. Buzanov and V.G. Germashev, Otkrytiya, Izobret., Prom. Obtraztsy, Tovernye Znaki, 1982, 33, 108. Chem. Abs., 95, 230993S.
79. *E.E. Bibik, O.V. Buzanov, N.M. Griбанov and V.G. Germashev, *ibid*, 1982, 38, 11. Chem. Abs., 98, P64531e.
80. *M.A. Berlin, V.A. Antipov, A.M. Tsybulevskii and N.G. Pindyurina, *ibid*. 19 , 8, 76. Chem. Abs., 90, P179279e.
81. *M.P. Matusевич, Probl. Mekh. Magn. Zhidk., 1981, 3. Chem. Abs., 97, 48480m.
82. *J. Shimoizaka, Nippon. Kogyo Kaishi, 1977, 93, 83. Chem. Abs., 88, 162874g.
83. *P. Yu. Grabovskii, T.P. Karbak and D.I. Potz, Otkrytiya, Izobret., Prom. Obtraztsy, Tovernye Znaki, 1984, 7, 81. Chem. Abs., 100, 220471c.
84. N. Buske and H. Sonntag, Colloids and Surfaces, 1984, 72, 195.
85. *J. Shimoizaka, Japan Kokai 76, 44,580, 1976. Chem. Abs., 85, 136276g.
86. A. Welo and O. Baudisch, Phil. Mag., 1927, 3, 396.
87. S.E. Khalafalla and G.W. Reimers, IEEE Trans. Magn., 1980, 16, 178.
88. W.R. Bottenberg and M.S. Chagnon, U.S. Patent 4,315,827, 1982.
89. M.S. Chagnon, U.S. Patent 4,356,098, 1982.
90. *J. Shimoizaka, Japan Kokai, 77, 00,783, 1977: Chem. Abs., 86, P182129e.
91. *N.P. Matusевич, V.K. Rakhuba and V.B. Samoiloв, Otkrytiya, Izobret., Prom. Obtraztsky, Tovernye Znaki, 1982, 20, 49. Chem. Abs., 95, 196417v.

92. K. Kimoto, Y. Kamiya, M. Nomoyama and R. Uyeda, Jap. J. Appl. Phys., 1963, 2, 702.
93. K. Kimoto and I. Nishida, Jap. J. Appl. Phys., 1967, 6, 1047.
94. N. Wada, Jap. J. Appl. Phys., 1967, 6, 553.
95. N. Wada, Jap. J. Appl. Phys., 1968, 7, 1287.
96. A. Tasaki, S. Tomiyama, I. Shuichi, N. Wada and R. Uyeda, Jap. J. Appl. Phys., 1968, 7, 1287.
97. T. Tanaka, and N. Tamagawa, Jap. J. Appl. Phys., 1967, 6, 1096.
98. A. Tasaki, M. Takao and H. Tokunaga, Jap. J. Appl. Phys., 1974, 13, 271.
99. K. Kusaka, N. Wada and A. Tasaki, Jap. J. Appl. Phys., 1969, 8, 599.
100. I. Nakatami and K. Masumoto, Jap. Pat. 60, 162,704, 1985.
101. P.G. Shepherd, J. Popplewell and S.W. Charles, J. Phys. D., 1970, 3, 1985.
102. A. Tasaki, IEEE Trans. Magn., 1983, 19, 1731.
103. E.P. Chock, Jap. J. Appl. Phys., 1970, 9, 1410.
104. T.O. Paine, L.I. Mendlesohn and F.E. Luborsky, Phys. Rev., 1955, 100, 1055.
105. F.E. Luborsky, Phys. Rev., 1958, 109, 40.
106. R.B. Falk and G.D. Hooper, J. Appl. Phys., 1961, 32, 2536.
107. P.G. Shepherd and J. Popplewell, Phil. Mag., 1971, 23, 239.
108. P.G. Shepherd, J. Popplewell and S.W. Charles, J. Phys. D., 1972, 5, 2273.
109. P.L. Windle, J. Popplewell and S.W. Charles, IEEE Trans. Magn. 1975, 11, 1367.
110. S.W. Charles and J. Popplewell, IEEE Trans. Magn., 1976, 12, 795.
111. A.C. Opegard, F.J. Darnell and H.C. Miller, J. Appl. Phys., 1961 32, 184S.

112. S.W. Charles and B. Issari, *J. Magn. Mag. Mat.*, 1986, 54-57, 743.
113. P.H. Hess and P.H. Parker, *J. Appl. Polymer Sci.*, 1966, 10, 1915.
114. J.R. Thomas, *J. Appl. Phys.*, 1966, 37, 2914.
115. O.L. Harle and J.R. Thomas, U.S. Patent 3,228, 882, 1966.
116. J.R. Thomas, U.S. Patent 3,228,881, 1966.
117. T.W. Smith, U.S. Patent, 4,252,673, 1981.
118. T.W. Smith, U.S. Patent, 4,252,672, 1981.
119. E. Papirer, *C.R. Acad. Sci. Paris*, t, 1977, 285, 73.
120. E. Papirer, P. Horny, H. Balard, R. Anthore, C. Petipas and A. Martinet, *J. Colloid. Int. Sci.*, 1983, 94, 207.
121. E. Papirer, P. Horny, H. Balard, R. Anthore, C. Petipas and A. Martinet, *J. Colloid. Int. Sci.*, 1983, 94, 220.
122. T.W. Smith and D. Wychick, *J. Phys. Chem.*, 1980, 84, 1621.
123. C.H. Griffiths, M.P. O'Horo and T.W. Smith, *J. Appl. Phys.*, 1979, 50, 7108.
124. M. Kilner, S.R. Hoon, D.B. Lambrick, J.A. Potton and B.K. Tanner, *IEEE Trans. Mag.* 1984, 20, 1735.
125. T.W. Smith, U.S. Patent 4,252,677, 1981.
126. S.R. Hoon, M. Kilner, G.R. Russell and B.K. Tanner, *J. Magn. Mag. Mat.*, 1983, 39, 107.
127. A.E. Berkowitz and J.L. Walter, U.S. Patent 4,381,244, 1983.
128. A. Berkowitz and J.L. Walter, *J. Magn. Mag. Mat.*, 1983, 39, 75.
129. F.A. Cotton and G. Wilkinson, *Advanced Inorganic Chemistry*, 4th Edition, John Wiley, London, 1980.
130. K.F. Purcell and T.C. Kotz, *Inorganic Chemistry*, Saunders, London, 1977.

131. G.E. Coates, M.L.H. Green and K. Wade, Organometallic Compounds Vol. 2, The Transition Elements, Ed. M.L.H. Green, Butler and Tanner, London, 1960.
132. G. Wilkinson, F.G.A. Stone and E.W. Abel, Comprehensive Organometallic Chemistry, Vol. 5, Pergamon Press, Oxford, 1982.
133. P. Seiler, J.D. Dunitz, Acta Crystallographica, 1980, B36, 2255.
134. I. Winder and P. Pino, Organic Synthesis via Metal Carbonuls, Vol. 1, Interscience, London, 1968.
135. R.B. King, Organometallic Synthesis Vol. 1, Academic Press, New York, 1965.
136. G. Wilkinson, F.G.A. Stone and E.W. Abel, Comprehensive Organometallic Chemistry, Vol. 4, Pergamon Press, Oxford, 1982.
137. S.R. Hoon, D.B. Lambrick and D.M. Paige, J. Phys. E. Sci. Instrum., 1985, 18, 389.
138. P.D. Hooker, Report, Unpublished Work, 1986.
139. C.J. Smithells, Metals Reference Book, 5th Ed. Butterworths, London, 1976.
140. M. Windholz, The Merck Index, 10th Ed. Merck and Co., Rahway, 1983.
141. I. Nakatami, T. Furubayashi, T. Takahashi and H. Hanaoka, to be published in J. Magn. Mag. Mat., 1986.
142. H.M. Randall, R.G. Fowler, N. Fuson and J.R. Dangle, Infra-red Determination of Organic Structures, Van Nostrand, London, 1949.
143. L.J. Bellamy, The Infra-red Spectra of Complex Molecules, John Wiley, London, 1958,
144. C.J. Pouchert, The Aldrich Library of Infrared Spectra, 3rd Ed. Aldrich, 1981.
145. C.W. Chen, Magnetism and Metallurgy of Soft Magnetic Materials, North Holland, Amsterdam, 1977.
146. R.M. Bozorth, Ferromagnetism, Van Nostrand, London, 1955.
147. A.R. Manning, J. Chem. Soc. (A), 1971, 2321.

148. D.J. Patmore and W.A.G. Graham, *Inorg. Chem.*, 1967, 6, 981.
149. T.S. Piper, F.A. Cotton and G. Wilkinson, *J. Inorg. Nucl. Chem.*, 1955, 1, 165.
150. M.J. Mays, R.N.F. Simpson, *J. Chem. Soc.(A)*., 1968, 1444.
151. P. Chini, L. Colloi and M. Peraldo, *Grazz. Chem. Ital.*, 1960, 90, 1005.
152. G. Wilkinson, F.G.A. Stone and E.W. Abel, *Comprehensive Organometallic Chemistry*, Vol. 6, Pergamon Press, Oxford, 1982.
153. R.W. Chantrell, J. Sidhu, P.R. Bissell and P.A. Bates, *J. Appl. Phys.*, 1982, 53, 8341.
154. H.B. Chim, M.B. Smith, R.D. Wilson and R. Ban, *J. Am. Chem. Soc.*, 1974, 96, 5285.
155. J. Ruff, *Inorg. Chem.*, 1968, 7, 1818.
156. S.V. Vonsovskii, *Magnetism*, Vol. 2, John Wiley, London, 1974.
157. J.D. Kleiss, *Phys. Rev.*, 1936, 50, 1178.
158. A.T.T. Hsieh and J. Knight, *J. Organomet. Chem.*, 1971, 26, 125.
159. P. Leech and C. Sykes, *Phil. Mag. Ser. 7*, 1939, 28, 742.
160. F.E. Haworth, *Phys. Rev.*, 1939, 56, 289.
161. G. Longini, P. Chin and A. Cavalieri, *Inorg. Chem.*, 1976, 15, 3025.
162. ASTM X-ray Powder Data File, Philadelphia, 1916.
163. Le Clerc and Michel, *Comp. Rend.*, 1938, 208, 1583.
164. S.C. Davis and K.J. Klabunde, *Chem. Rev.*, 1982, 82, 153.
165. D.K. Shaw, *Introduction to Colloid and Surface Chemistry*, 3rd Ed., Butterworths, London, 1980.
166. N. Wada and M. Ichikawa, *Jap. J. Appl. Phys.*, 1976, 15, 755.

167. H.H. Zeiss, *Organometallic Chemistry*, Reinhold, New York, 1960.
168. J. van Wonergham, S. Mørup, S.W. Charles, S. Wells and J. Villadsen, *Phys. Rev. Letts.*, 1985, 55, 410.
169. J.W. Niemantsverdriet, A.M. van der Kraan, W.L. van Dijk and H.J. van der Baan, *J. Phys. Chem.*, 1980, 84, 3363.
170. R.C. Weast, *CRC Handbook of Chemistry and Physics*, 63rd Ed., CRC Press, Florida, 1982.
171. J.L. Marignier, J. Belloni, M.O. Delcourt and J.P. Chevalier, *Nature*, 1985, 317, 344.
172. I. Nakatami and K. Masumoto, U.S. Patent 4,599,184, 1986.
173. U.R. Evans, *An Introduction to Metallic Corrosion*, Edward Arnold, London, 1963.
174. J. Knight and M.J. Mays, *J. Chem. Soc. (A)*, 1970, 654.
175. A.E. Berkowitz, *Magnetism and Metallurgy*, Vol. I, Academic Press, London, 1969.

* Denotes abstract only available.

